



Argonne National Laboratory is managed by  
The University of Chicago for the U.S. Department of Energy



ANL-05/42

Proceedings of the Workshop on  
Applications of a Very Cold Neutron Source

# Proceedings of the Workshop on Applications of a Very Cold Neutron Source

August 21-24, 2005

prepared by  
Intense Pulsed Neutron Source Division  
Argonne National Laboratory



ANL-05/42

Argonne National Laboratory is managed by  
The University of Chicago for the U.S. Department of Energy

**About Argonne National Laboratory**

Argonne is managed by The University of Chicago for the U.S. Department of Energy under contract W-31-109-Eng-38. The Laboratory's main facility is outside Chicago, at 9700 South Cass Avenue, Argonne, Illinois 60439. For information about Argonne and its pioneering science and technology programs, see [www.anl.gov](http://www.anl.gov).

**Availability of This Report**

This report is available, at no cost, at <http://www.osti.gov/bridge>. It is also available on paper to the U.S. Department of Energy and its contractors, for a processing fee, from:

U.S. Department of Energy  
Office of Scientific and Technical Information  
P.O. Box 62  
Oak Ridge, TN 37831-0062  
phone (865) 576-8401  
fax (865) 576-5728  
[reports@adonis.osti.gov](mailto:reports@adonis.osti.gov)

**Disclaimer**

This report was prepared as an account of work sponsored by an agency of the United States Government. Neither the United States Government nor any agency thereof, nor The University of Chicago, nor any of their employees or officers, makes any warranty, express or implied, or assumes any legal liability or responsibility for the accuracy, completeness, or usefulness of any information, apparatus, product, or process disclosed, or represents that its use would not infringe privately owned rights. Reference herein to any specific commercial product, process, or service by trade name, trademark, manufacturer, or otherwise, does not necessarily constitute or imply its endorsement, recommendation, or favoring by the United States Government or any agency thereof. The views and opinions of document authors expressed herein do not necessarily state or reflect those of the United States Government or any agency thereof, Argonne National Laboratory, or The University of Chicago.

Proceedings Of The  
WORKSHOP ON APPLICATIONS OF  
A VERY COLD NEUTRON SOURCE

Intense Pulsed Neutron Source  
Argonne National Laboratory  
Argonne, Illinois  
August 21-24, 2005

Bradley J. Micklich and John M. Carpenter, Editors

December 21, 2005

ANL-05/42



## IPNS Director's Statement

The idea of convening a workshop to explore potential uses of a very cold (i.e. liquid helium temperature) neutron source was based on the perception that significantly high neutron fluxes of the coldest practical spectrum would have a large impact on emerging science in the US, specifically in nano-science, soft materials, and energy related research. This assumption was confirmed upon my first reading the initial draft of this workshop report. I was immediately struck by the numerous and heretofore unrealized applications of neutron characterizations if very long wavelength neutrons ( $> 10\text{\AA}$ ) were present at fluxes at least two orders of magnitude higher than are currently available internationally. As you read the report, I'm sure you'll agree with the workshop participants that a VCNS possesses exciting possibilities.

A VCN source represents the next "great leap" forward in the field of neutron scattering and materials research. As is always the case, the construction of a neutron facility with significantly improved capabilities is expected to spur developments in optics, moderators, targets and instrumentation and will provide a boon to the understanding and development of new materials. The workshop discussion groups envision breakthroughs in fundamental physics, neutron microscopy, holography, nanoprobes, polarization and chemical contrast. I thank the attendees and the authors of this report for providing this sage vision of future research in the US.

R. G. Teller

## TABLE OF CONTENTS

Executive Summary .....	1
Agenda .....	4
Foreword .....	6
Neutron Sources Working Group .....	8
Instrumentation and Techniques Working Group.....	17
Scientific Applications Working Group .....	35
Conclusions.....	56
Group Photo .....	58
Participants List .....	60
Presentations .....	61

# 1. EXECUTIVE SUMMARY

The Intense Pulsed Neutron Source held a workshop on the scientific prospects of a Very Cold Neutron Source (VCNS) at Argonne National Laboratory on 21-24 August 2005. The workshop, which attracted 39 participants from 12 institutions, was inspired by the prospects to serve the large and growing number of government, academic, and industrial laboratories conducting research on the properties of nanoscale materials. The basis of VCNS is an accelerator/target/moderator system generating a high neutron flux of the coldest practically imaginable spectrum, in an installation providing a large number of beams – a multiple-use very cold neutron scattering facility. The VCNS would characterize materials over large length scales and slow time scales, and complement the Long-Wavelength Target Station (LWTS), a second target station proposed for the Spallation Neutron Source (SNS), the first target station of which is soon to be commissioned at Oak Ridge National Laboratory. A special-purpose installation such as VCNS would better provide for nanoscience and other applications of very cold neutrons than can LWTS, driven from the SNS accelerator system. VCNS would be unique in the world, providing a prolific source of neutrons in the wavelength range greater than 10 Å.

The VCNS would have immediate impact in a wide variety of fields, for example:

- The search for the neutron electric dipole moment and measurement of the neutron lifetime
- Neutron microscopy (at the 50-100 nm scale) of biomolecular systems and nanocomposites with complex surfaces and buried structures
- Holography of hydrogenous minerals and biological materials
- Nanoscale self-organization in geometrically frustrated magnets
- Spectroscopic studies of solar absorption in photoelectrochemical cells
- Structures of biological membranes and devices based on nanodots and nanotubes

The workshop began Monday with some introductory description of the proposed VCNS concept by the workshop organizers. A series of plenary sessions followed, featuring prepared talks on the topics of neutron sources, neutron beam optics, instrumentation, and scientific applications. The talks dealt specifically with approaches to the use of 20-Å neutrons, the peak of the VCNS spectrum. Beginning on Tuesday afternoon, the participants split into three working groups on the areas of neutron sources, instruments and beamline components, and scientific applications. Each group was led by a discussion leader who presented the group's report on Wednesday morning before adjournment.

The neutron source working group affirmed the initial choice of a long-pulse linear accelerator to drive the facility, but accepted the science working group's recommendation that the pulse repetition rate be increased to 5 Hz. The final accelerator parameters are: 1 GeV proton energy, 4 ms pulse width, 5 pulses/second, peak current 75 mA, average beam power (at 5 Hz) 1500 kW. At this power the target must be internally cooled or consist of circulating liquid metal, while edge cooling would be sufficient for

an average power of a few hundred kW. The target material should have high atomic number, preferably lead, since bismuth targets suffer from a buildup of polonium which negatively affects the radiological safety. Detailed calculations of the time-dependent thermal hydraulics will need to be performed to verify that the window and the high-energy region of the target can be adequately cooled. The group was reluctant to depart from the traditional horizontal beam-on-target layout as we have proposed but recognized the significant advantage in having the beam strike the target vertically from above. This would allow the target to be decoupled from the beam lines, providing more open space in the experimental hall. A large amount of experience will be gained in the next few years operating high-power spallation targets at SNS, PSI, and JSNS.

We recognize a strong synergism between the VCNS target/moderator system and the intermediate moderators of UCN sources. Typical UCN sources use a large warm moderator, a cold moderator that operates in the range of 10-20 K, and an ultra-cold moderator operating at 0.5-5 K. It might be that UCN sources are already strong sources of VCNs, but this has not been measured. A similar design philosophy could be followed for VCNS, but the process followed would be different since the principal constraint on the system is not on accelerator beam power but on the amount of heat that can be removed from the few-K moderator. The VCNS moderator is envisioned as a bed of small pellets cooled by liquid helium flowing through spaces between the pellets. This moderator does not need to be a large thermalizing moderator, but could be smaller and thus subject to a lower energy deposition. Experiments are still in progress at several laboratories that would give better information about the optimal material and operating temperature. The lack of neutron scattering kernels for the appropriate materials and temperature complicates attempts to explore the properties of these systems by simulation.

The instrument working group felt that the proposed VCN source would offer excellent opportunities for developing best-in-class instruments for a variety of instrument types. In particular, SANS instruments, reflectometers, high resolution TOF instruments, spin-echo spectrometers, and SESANS techniques should benefit most from being used at a VCN source. In some cases this is because certain properties of long-wavelength neutrons can be exploited in instrument design. In other cases, an existing instrument would function better at VCNS simply because of the colder neutron spectrum.

Neutron optical techniques will work better at longer wavelengths, and the extreme absorption of VCNs for certain isotopes combined with low absorption for other nuclides allows the design of highly precise optical components similar to light optics. Wide-angle VCN beams can be focused with high precision at focal lengths in the meter range. Supermirrors with high  $m$  will allow reflection angles on the order of 10-20 degrees, allowing VCN beams of 1 sterad divergence. Spherical aberrations can be reduced to a large extent. The phase shift of neutrons passing through matter is proportional to wavelength, making VCNs an ideal probe for viewing small contrasts (small variations in density or very thin samples). Likewise, the interaction of neutrons with a gravitational or magnetic field scales with  $\lambda^2$ , so that one can better design instruments exploiting these effects. Optics can be designed to correct for unwanted effects of gravity in long flight

path beamlines. Large-area high resolution detectors commonly used now in x-ray instruments at synchrotron sources could be adapted to neutron science without the need for extensive developments.

The science working group first brainstormed the science case for a VCNS and then collected preliminary thoughts and notes, with additional write-ups and references later supplied by group members. Given the unprecedented high flux of long-wavelength ( $> 20 \text{ \AA}$ ) neutrons anticipated from the VCNS – far superior to the ILL cold source – and the superb performance of advanced optical devices, polarizers, and detectors favoring very cold neutrons, the group was very enthusiastic about the scientific opportunities and possible breakthroughs in many important areas that are unattainable by present neutron sources including the SNS, but realizable by the VCNS.

The group examined the science case under three broad headings. The first was new science to be driven by advanced VCNS instrumentation, including fundamental physics, microscopy, holography, the use of highly focused beams, spin-polarized scatterers, and elastic and inelastic scattering. The second area consisted of special scientific topics, such as materials physics under extreme environments, magnetism, superconductivity, and quantum systems. Finally, the group also examined a number of fields with important applied problems, such as energy sciences, health and biological sciences, the environment, nanostructure of novel materials, and homeland security. In each of these areas, the group felt that not only could current science be improved dramatically by a VCNS, but that a VCNS could make possible entire new fields of research.

A large number of developments related to a VCN source are taking place worldwide on the generation and use of ultra-cold neutrons. We feel that many of the key technical issues can already be adequately addressed, particularly the design of the accelerator system. Some dedicated efforts will be required to obtain critical data such as the neutron scattering kernels necessary to perform more realistic computer simulations of the target/moderator systems and the optimization of instruments, to take advantage of the unique characteristics of a VCNS. The science case is largely expressed in the burgeoning efforts in the field of nanomaterials, but needs to be defined in some detail and refined as a basis for instrument concepts. However, it is clear that the VCNS would enable a whole new field of research and lead to significant advances in nanomaterials, soft matter dynamics, fundamental physics, and applied fields such as energy, environmental, and medical research.

# VCNS WORKSHOP AGENDA

## Sunday, August 21

5:00 – 8:00 VCNS Welcome Reception at the Argonne Guest House

## Monday, August 22

7:30 – 8:30 Registration

8:30 – 9:00 Continental Breakfast

9:00 – 9:30 **Introductory Session**

Jack Carpenter – A Very Cold Neutron Source, VCNS

Brad Micklich – Concepts for a Very Cold Neutron Source at Argonne National Laboratory

9:30 – 10:45 **Source Technology Prepared Talks**

Peter Geltenbort – Ultracold Neutrons (UCN) at the ILL

Yasuhiro Masuda – Spallation Neutron Source for UCN Production in He-II

Manfred Daum – The PSI UCN Source

10:45-11:00 Break

11:00 – 11:05 Welcome – Ray Teller

11:05 – 12:00 **Instrument/Science Prepared Talks**

Chun-Keung Loong – VCNS: A Prelude of Instrument & Scientific Wishes

Ferenc Mezei – Some Instrument Ideas for a Pulsed Very Cold Neutron Source

12:00 – 1:00 Buffet Appetizer Lunch

1:00 – 3:00 **Science Prepared Talks**

Lee Makowski – Neutron Diffraction Studies of Biological Specimens

R. Kent Crawford – Some Considerations for Neutron Scattering at a Very Cold Neutron Source

Jyotsana Lal – Structure and Dynamics in Complex Systems

3:00 – 3:30 Break

3:30 – 5:30 **Instruments Prepared Talks**

Roland Gähler – Novel Instrument Concepts

Gene Ice – Nondispersive-focusing Long wavelength Neutrons

Charles Marjczak – Depth Profile Imaging by Phase Sensitive Neutron Reflectometry With Cold and Very Cold Neutrons

No - Host Dinner

# VCNS WORKSHOP AGENDA

## Tuesday, August 23

8:30 – 9:00 Continental Breakfast

### 9:00 – 10:30 **Source Technology – Neutron Beam Optics-Transport**

Hirohiko Shimizu – Recent Developments on Neutron Optics in Japan

Steven Bennington – Source Design and Optics on the ISIS Second Target Station

Géza Zsigmond – Numerical Study of Optics and Phase Space Transformation of Ultra Cold Neutrons

10:30-10:45 Break

### 10:45 – 12:30 **Science Prepared Talks**

Roger Pynn – Spin Echo Scattering Angle Measurement with Very Cold Neutrons

Gian Felcher – Advantage of Cold Neutrons in Generalized Reflectometry

12:30 – 1:30 Lunch – Deli Buffet

1:00 – 3:15 Breakout Discussions

3:15 – 3:30 Break

3:30 – 5:30 Break Out Discussions

6:30 – 9:00 Reception and Dinner Banquet at the Argonne Guest House

## Wednesday, August 24

8:30 – 9:00 Continental Breakfast

### 9:00 – 10:45 **Break Out Discussions and Write Up Preparations**

(3 groups) Source, Science and Instruments

11:00 – 12:00 Break Out Discussions and Plans for a Future Meeting  
Summary of San Diego Meeting

12:00 – 1:00 Boxed Lunches

1:00 Meeting Adjourned

## 2. FOREWORD

A large and growing number of institutions are conducting research on the properties of matter on the nanoscale. The development and characterization of nanoscale materials is a major research initiative of the US Department of Energy and of government, academic, and industrial laboratories worldwide. Taking note of this, some of us at Argonne have been investigating concepts for a Very Cold Neutron Source (VCNS), with a wavelength distribution peaking at about 20 Å, which would continue the 60-year tradition of slow neutron utilization at Argonne National Laboratory (ANL) beyond Intense Pulsed Neutron Source (IPNS). The VCNS would characterize materials over large length scales and slow time scales and serve as a complement to the Long-Wavelength Target Station proposed for the SNS. A special-purpose installation such as VCNS would better provide for nanoscience and other applications of very cold neutrons than can LWTS, driven from the SNS accelerator system. VCNS would be unique in the world.

The basis of VCNS is a target/moderator system generating a high neutron flux of the coldest practically imaginable spectrum, in an installation providing a large number of beams – a multiple-use very cold neutron scattering facility. There are a number of developments taking place worldwide on the generation and use of ultra-cold neutrons (UCNs), for which the source/moderator technology is closely related to that of VCNS. The science case for VCNS is largely expressed in the burgeoning efforts in the field of nanomaterials, but needs to be defined in some detail and refined as a basis for instrument concepts. However, a great gap remains in our understanding of instruments for carrying out very cold neutron scattering measurements for characterizing nanoscale materials. To address these topics we decided to hold a workshop on neutron sources, instruments, and science for such a facility.

The VCNS workshop met at Argonne on 21-24 August 2005 in the IPNS offices. The workshop attracted 39 participants from 12 institutions. Many participants took advantage of the facilities at the nearby Argonne Guest House, which was also the site of a reception on the evening of 21 August and a banquet on 23 August. After some introductory comments on the proposed VCNS concept by the workshop organizers, a series of plenary sessions featuring prepared talks were held on Monday and Tuesday morning. Beginning on Tuesday afternoon, the participants split into three working groups on the areas of neutron sources, instruments and beamline components, and scientific applications. Group chairs delivered reports on Wednesday morning before adjournment. Lunches and coffee breaks provided the necessary time for informal interaction.

The attendees came well-prepared, on the basis of information provided beforehand, to discuss the capabilities desired in a VCNS, and had clearly devoted time to thinking about scientific applications and instruments that could take advantage of this kind of neutron source. A number of new and interesting ideas came out of the workshop, and inasmuch as this was our intent we feel that the workshop was a rousing success. Progress made, questions raised, and suggestions that emerged encourage us to continue

our development work and to contemplate a follow-on workshop. One of the workshop highlights was a performance of an original musical composition, “The Ballad of Slow Neutron Reflectometry.” Unfortunately we were not able to record this performance for inclusion in the workshop proceedings.

The body of these proceedings contains summary statements of the results of the working groups on Sources, Instrumentation, and Science, and copies of the materials that participants presented.

The organizers extend special thanks to Nicole Green, who served as the workshop secretary throughout planning and execution, and to the other members of the IPNS staff who provided assistance.



### 3. NEUTRON SOURCES WORKING GROUP

Discussion Leader: Manfred Daum

Participants: Steve Bennington, Jack Carpenter, Peter Geltenbort, Erik Iverson, Yoshihisa Iwashita, Chen-Yu Liu, Yasuhiro Masuda, Brad Micklich (scribe)

The Very Cold Neutron Source (VCNS) is intended to provide large numbers of neutrons in the 20-Å range, which would be of interest to emerging scientific fields such as nanotechnology. The target group considered the neutron source to consist of four distinct components: the accelerator (proton beam), the spallation target, the neutron moderator(s), and the beam extraction system. The last of these items will not be dealt with here. Each of these components is itself a complex system that should be optimized in conjunction with the others.

#### 3.1 Accelerator (Proton Beam)

Preliminary neutronics studies of potential VCNS moderators indicated that the resulting neutron pulses would have pulse widths on the order of a few milliseconds for the neutron wavelengths of interest. Thus the incident proton beam should have a pulse width on the same order. As a result, the ANL study group chose a linear accelerator with a pulse repetition rate initially set at 1 pulse/second.

Ferei Mezei had concluded separately, based on a number of factors, that from a scientific point of view the facility should operate at a pulse repetition rate of 3-5 Hz. While more klystron power would be required, the accelerator is substantially unchanged at the higher repetition rates. Local cooling issues at the entrance window and the high-energy end of the target may require the beam radius to be very large. For example, with a 10-cm diameter beam the peak current density is nearly  $1000 \mu\text{A}/\text{cm}^2$ , much larger than the  $20\text{-}30 \mu\text{A}/\text{cm}^2$  for the SINQ and UCN targets at PSI. However, a larger beam radius would reduce the coupling between the target and moderator, which would also reduce the flux per unit beam power. It is therefore important to determine the maximum beam current density at which local cooling becomes a problem. Given the fairly large power in the beam, appropriate consideration should be given to selection and placement of beam diagnostics, since even momentary mis-steering of the beam could have serious facility consequences. The average proton current density at the window of about  $20 \mu\text{A}/\text{cm}^2$  should not be a problem for the target structural integrity, as Gohar [1] indicates that a target window should be capable of operating for a full power year at a power of 5 MW with a proton energy of 600 MeV and a current density of  $40 \mu\text{A}/\text{cm}^2$ .

The resulting linear accelerator parameters follow. Fig. 3.1 shows a schematic of the accelerator cavity design.

Beam parameters:

Energy	1 GeV
Pulse Repetition Rate	5 Hz
Beam width	4 ms
Accelerator RF frequency	325 MHz / 1300 MHz
Peak current	75 mA
Average current	1500 $\mu$ A
Beam average power	1500 kW
Duty cycle	0.02 (2 %)

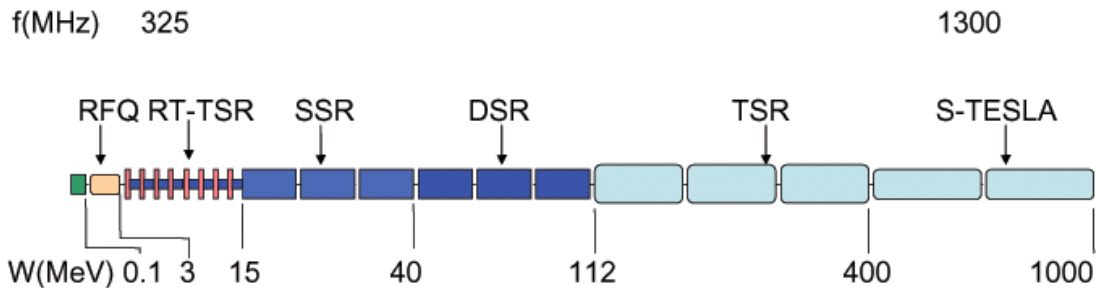


Fig. 3.1. Schematic diagram of VCNS linear accelerator. Structures given with corresponding energy ranges. RFQ: Radio-Frequency Quadrupole; RT-TSR: Room-Temperature Triple Spoke Resonator; SSR: (Superconducting) Single Spoke Resonator; DSR: (Superconducting) Double Spoke Resonator; TSR: (Superconducting) Triple Spoke Resonator; S-TESLA: Superconducting TESLA-type elliptical cavity.

Important points that received considerable discussion were whether the proton beam orientation should be horizontal or vertical and whether the beam direction in a vertical orientation should be up or down. The horizontal orientation makes the placement of the accelerator and shielding easier. Orienting the target vertically with the proton beam incident from below makes maintenance of the target systems much easier because the target handling is decoupled from the beam lines. This arrangement also frees up considerable floor space in the experimental hall for additional neutron beam lines, etc., that could not be accommodated with a more traditional horizontal layout. A vertical beam incident from above would have advantages in the case of a liquid target in that the entrance window would not also have to provide containment for the target material. Vertical layouts also have the advantage of resembling more closely a reactor layout and might more easily allow the inclusion of multiple VCNS sources, each of which might be tailored to the needs of a specific set of instruments.

### 3.2 Spallation Target

Bismuth was selected as the target material in the original VCNS concept because of its high atomic number and low neutron absorption. However, experience has shown that the buildup of radioactive polonium would be a problem that would increase the hazard level of the facility, perhaps to levels that would lead to difficulty in the siting and licensing processes. Lead is another high-Z material that could operate comfortably at this power level. Neutron absorption in lead, though higher than in bismuth, is still small and is not expected to lead to excessively large neutron capture. One interesting idea is the use of radiogenic lead, which is low in the isotope  $^{207}\text{Pb}$ , the isotope with the largest neutron capture cross section. Another benefit to using lead is that the capture gamma problem is not as great as in bismuth. However, repeated melting/cooling of lead is bad for its metallurgical structure.

For the original condition of 1-Hz operation we reasonably expect that the target could be edge cooled, like the TRIUMF Thermal Neutron Facility [2]. However, at higher (3-5 Hz) pulse repetition rates and the same number of protons/pulse, edge cooling is not practical the average power would then be in the range of 1-1.5 MW. It may be necessary to use an externally cooled circulating target of lead, bismuth, or (lead-bismuth eutectic) LBE, such as that being built for the MEGAPIE experiment or other designs proposed for high-power applications. Other options include a traditional plate design and the “cannelloni” target [3] being developed for the UCN source at PSI. This target consists of several hundred tubes of lead clad with Zircaloy, with the tubes filled to about 90%. The heavy water coolant occupies about 40 percent of the target volume. While the relatively high coolant fraction reduces target neutron production efficiency, the heavy water doesn’t absorb many neutrons. The coolant flow rate is about 20 l/s. The design has been well tested, and much experience has been acquired with a design that had the target tubes clad with stainless steel. The target length is about 50 cm for incident protons of energy 600 MeV (at this energy the proton stopping distance in lead is about 26 cm). The target design should extend easily to 1 GeV.

For any of these target options, detailed calculations of the time-dependent thermal hydraulics will need to be performed to verify that the window and the high-energy region of the target can be adequately cooled. In particular, we should determine whether equilibrium thermal-hydraulic conditions are achieved during a pulse. Much information should be available from other long-pulse spallation source projects as well as from other high-power accelerator projects such as the Accelerator Demonstration Test Facility (a subcritical accelerator-driven system for nuclear waste transmutation) and the Accelerator Production of Tritium project.

Even though VCNS would have ~10 times the energy per pulse as SNS, Jack Carpenter indicated that he did not expect cavitation problems if the target were to be liquid. Jack had performed a series of calculations that showed that only first few hundred microseconds of the 4-ms pulse would contribute to development of pressure pulse in the target. Turning on the accelerator pulse over a 200- $\mu\text{s}$  time period might mitigate some of the effects.

### 3.3 Moderator System

The typical UCN source design employs a large warm moderator, a cold moderator (such as for a reactor-based cold neutron source) that operates in the range of 10-20 K, and an ultra-cold moderator at 0.5-5 K. Early VCNS calculations showed that heating of the ultra-cold moderator during the accelerator pulse would be a key (perhaps the key) technical consideration, because of the low heat capacity of moderator materials at low temperatures. The calculations tried to reduce heating in the moderator by maximizing the ratio of cold neutron flux to energy deposited. In order to preserve neutron flux while minimizing gamma heating, thick shielding of heavy metal was used. The results of Masuda [4], however, show that heavy water is a much better warm moderator, while the thickness of a gamma shield is of much less importance.

Figs 3.2 and 3.3 show results from VCNS calculations with large thermalizing moderators of D<sub>2</sub>O, beryllium, and graphite. Since thermal neutron scattering kernels are not available for these materials at the appropriate temperatures, the calculations were performed assuming free-atom scattering from the ultra-cold moderators. These results are compared to the neutron emission from the ILL cold source [5], both on an instantaneous (peak) and a time-averaged basis. The VCNS source, at this level of comparison, looks very encouraging, with a peak long-wavelength flux  $\sim 10^3$  times greater than the ILL cold source, and about 30 times the time-averaged flux at 5 Hz operation.

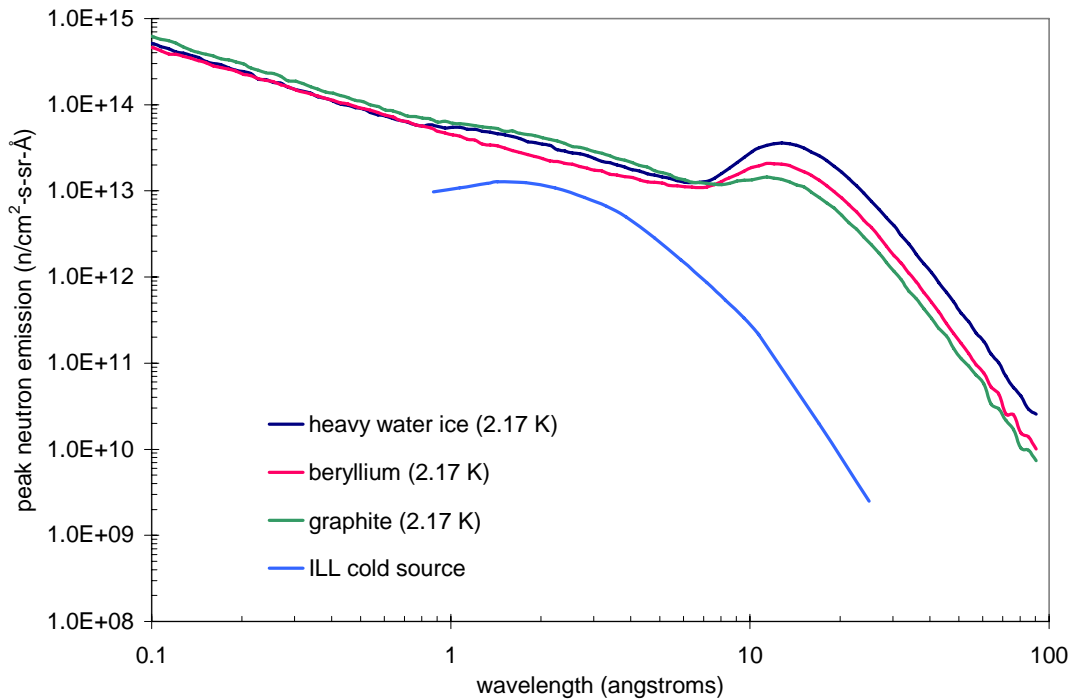


Fig. 3.2. Peak neutron emission from the proposed VCNS compared to the ILL cold source.

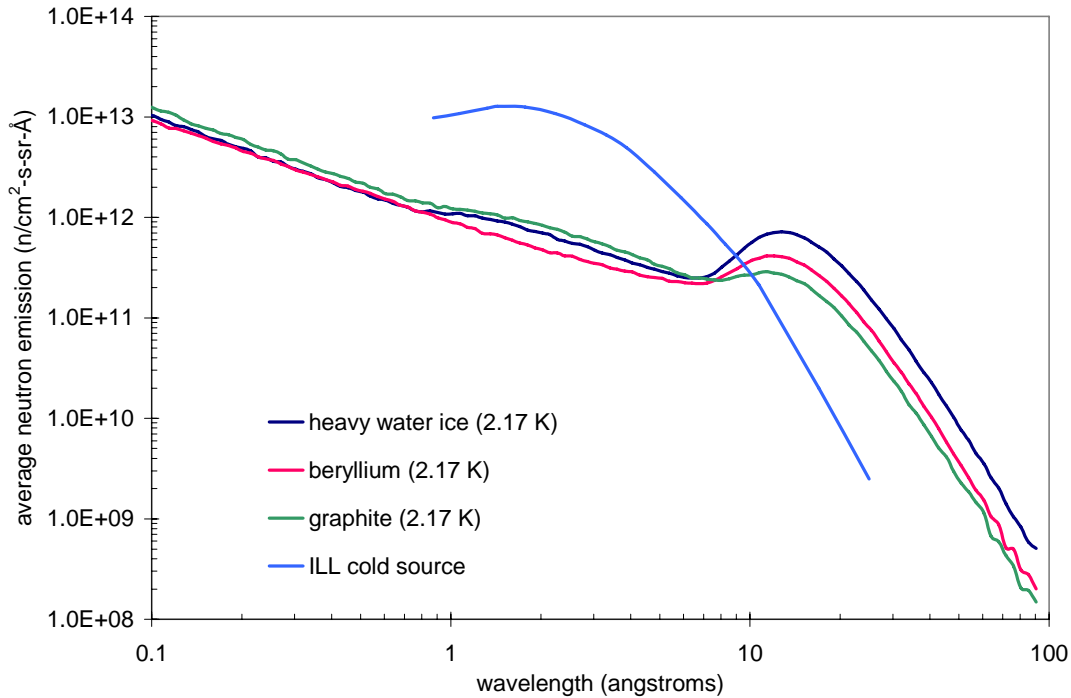


Fig. 3.3. Time-average neutron emission from the proposed VCNS (operating at 5 Hz) compared to the ILL cold source.

The VCNS design proposed an ultra-cold thermalizing moderator composed of solid materials ( $D_2$ ,  $D_2O$ , Be, graphite) in pellet form with liquid helium coolant at about 2 K flowing through the spaces between the pellets. For randomly packed spherical objects the packing fraction is about 64%; this can be increased to about 68% if the objects are slightly aspherical [6]. There are already indications that the heat could be removed by 2-K He on a time-averaged basis, but the temperature rise within the pellet during the pulse might alter the neutron spectrum significantly.  $D_2$  and  $D_2O$  are expected to be better moderators than graphite and beryllium because they have some component of incoherent scattering, while graphite and beryllium have cross sections that fall precipitously for energies below the lowest Bragg edge (about 5 meV in Be and 2 meV in graphite). However, beryllium and graphite have better thermal properties (higher heat capacities). As a result the optimization of flux/heat might actually favor a material such as beryllium that has lower thermalization but can withstand a high power level (perhaps as much as 100 times greater than  $D_2O$ ). Detailed calculations are required to better quantify the effects.

Chris Foster has developed methods to produce pellets of various materials (including deuterium, methane, and ammonia) at cryogenic temperatures. This process could perhaps be improved by not removing pebbles from the base layer, but by instead building up the moderator structure by series of plates, so as to make the average density come out to same as random-packing. The group also noted that there was a difference in structure between household ice and the low-density amorphous (LDA) ice that is formed by vapor deposition. As a result there may be anomalous specific heat behavior in LDA ice at low temperature as an indication of changes in the low-energy modes.

Several experiments have been performed at PNPI in collaboration with PSI, ILL, and LANL and in Japan to measure the UCN and VCN production in  $D_2$  and  $D_2O$  at temperatures of about 10 K [7,8]. Neutron yields as a function of wavelength were measured for temperatures starting at room temperature down to  $\sim 10$  K. The measurements showed that UCN production was significantly higher in  $D_2$  than in  $D_2O$ . A high purity of ortho- $D_2$  is required (greater than 98.6%) to prevent upscattering of ultracold neutrons on para- $D_2$  [9,10]. Measurements of the UCN production as a function of the converter temperature have also been started for other materials such as oxygen and deuterated methane ( $CD_4$ ).

Fig. 3.4 shows that the UCN density in an ultra-cold (inner) solid deuterium moderator does not change much with temperature below 5 K (see also the discussion in [7]). Thus it may not be necessary to operate at temperatures as low as 2 K to achieve a high VCN density. Furthermore, there is not much motivation to reduce the upscatter cross section by going to lower temperatures because the limiting factor in VCN density will become neutron absorption, for which the cross section in ortho- $D_2$  is higher than the upscatter cross section below 5 K (see Fig. 3.5).

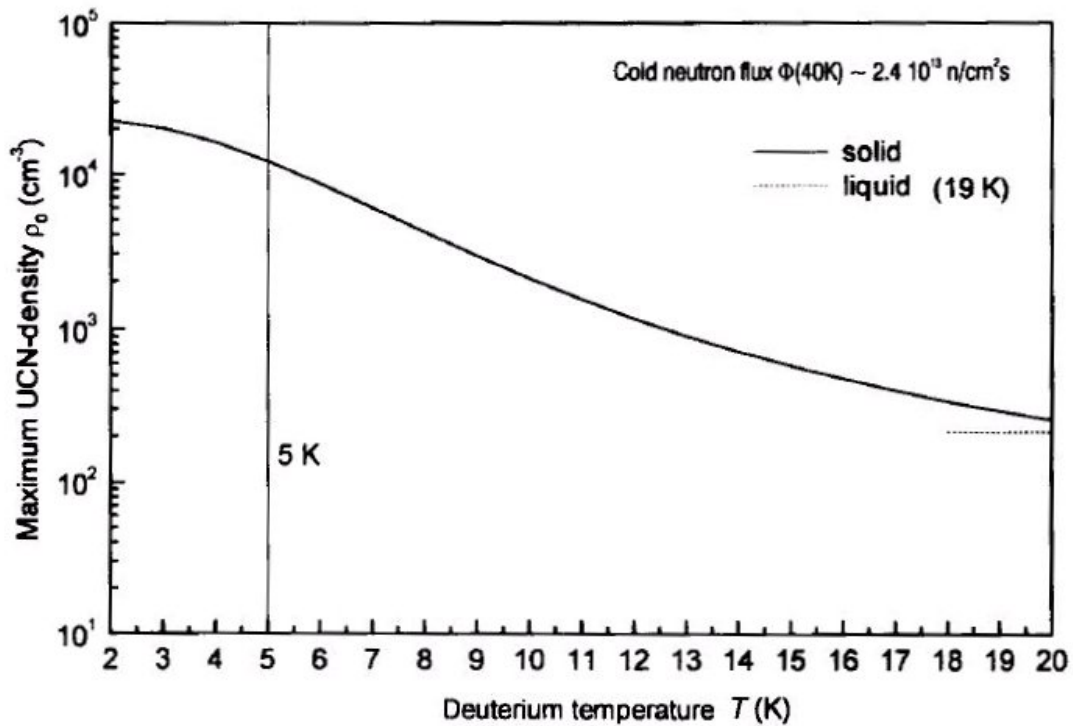


Fig. 3.4. Maximum UCN density in ortho- $D_2$  for a cold neutron flux  $\Phi(40 \text{ K}) \sim 2.4 \cdot 10^{13} \text{ n/cm}^2\text{-s}$  as a function of the  $D_2$  temperature, as calculated from the phonon spectra in  $D_2$ .

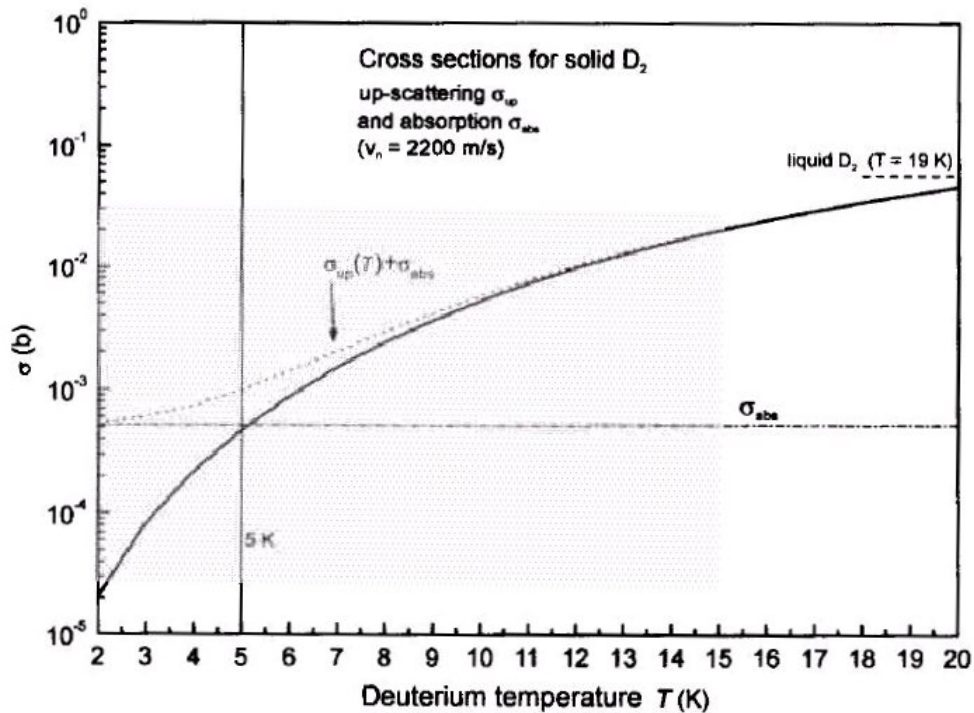


Fig. 3.5. Cross sections for absorption and upscattering of neutrons with  $v = 2200$  m/s on ortho- $D_2$  as a function of the  $D_2$  temperature.

Composite moderators may be useful in combining the properties of different materials. For example, Günter Bauer has suggested mixing  $CD_4$  (deuterated methane) with heavy-water ice, and Masahiko Utsuro has suggested  $CD_4$  in concentrations of up to 10% in solid  $D_2$ . There are also indications that the inclusion of Kr in solid  $CD_4$  can unlock the free-rotor modes that are normally unavailable at temperatures under 20 K, thus providing effective moderation at these temperatures. Experiments on these and other combinations will be performed in the near future. Another type of interesting composite material is carbon nanostructures (tubes, cones) with hydrogenous materials inside. In these the carbon structure lowers the energy of rotational modes, which provides moderation to lower energies, and also conducts heat out of the moderator.

The group also debated whether thermal or super-thermal methods of production would be more efficient. In a superthermal source one wants a small moderator at the coldest temperature so that downscattered neutrons can escape the moderator before they have a chance to upscatter or be absorbed. Using a small moderator volume has the additional advantage of reducing the energy deposited in the lowest-temperature moderator. Only superthermal sources based on solid  $D_2$  (not those based on superfluid He) would be applicable for VCN production. It might be that existing UCN sources are already very good VCN sources, but this has not been measured. For UCN sources (neutron speeds less than 7 m/s), the moderation efficiency is about  $10^{-8}$ , but much better performance will be needed for VCN (neutron speeds  $\sim 190$  m/s) production (perhaps a moderation efficiency of  $10^{-2}$ ).

The design and optimization of a multi-component system such as a VCNS involves choices and tradeoffs between many different parameters. Finding the optimum configuration for the entire system is a daunting task, and any help in automating the process can speed things up considerably. Stuart Ansell of ISIS has written an auto-optimization code package [11] that has been used in the ISIS second target station design and could also find applicability for the design of a VCNS. The code is presently being cleaned up and documented, and should be available in the near future.

Neutron scattering kernels are consistently a weak point in trying to design a cold neutron source on the basis of calculations. Measurements of scattering functions do not exist for materials of interest at the appropriate temperatures. The codes used to generate the scattering kernels in forms suitable for use with transport codes do not always produce good results at the very low temperatures being considered. The formats used in the cross section files are not always adequate to represent the important physics (for example, the ENDF-6 format allows the description of elastic scattering to be either coherent or incoherent, but not both, which means that an accurate description of neutron scattering from solid D<sub>2</sub>O is not possible.) Finally, good benchmark data are required for many potential moderator materials in order to judge how well the simulations using these kernels reproduce well-characterized measurements.

### **3.4 Future Work**

The source discussion group identified a number of areas in which additional work needs to be conducted before detailed estimates of VCNS performance can be completed. It is not necessary for all of the following items to be addressed before better VCNS performance estimates can be given. However, improvements in the following areas will benefit not only the potential VCNS concept, but also all facilities using cold/very cold/ultra cold neutrons.

Additional measurements/calculations/tool development should be undertaken:

- Establish program for calculations and experiments on selected moderator types
- Measurements of neutron scattering functions for candidate materials
- Development of neutron scattering kernels for appropriate materials and temperatures
- Benchmarking measurements of VCN/UCN production
- Determine whether thermal or superthermal production is more efficient
- Complete the documentation for the ISIS auto-optimization code package, suitable for users

We will await high-power target developments in the next few years at ORNL/SNS, at PSI, and at J-PARC, but believe that target and accelerator issues are well in hand.

## References

- [1] M. Y. Gohar, "Characterization of Lead-Bismuth Eutectic Target Material for Accelerator Driven Transmuters," *Jour. Nucl. Mat.* **318**, 185 (2003).
- [2] I. M. Thorson, J. J. Burgerjon, R. E. Blaby, and T. A. Hodges, "TRIUMF Thermal Neutron Facility," Proceedings of the 7th Meeting of the International Collaboration on Advanced Neutron Sources, Chalk River, Ontario, Canada (13-16 Sept. 1983).
- [3] M. Wohlmuther and G. Heidenreich, "Design and Neutronic Performance of the Spallation Target of the Ultra-Cold Neutron Source at PSI," Proceedings of the 17th Meeting of the International Collaboration on Advanced Neutron Sources, Santa Fe, NM, USA (25-29 April 2005).
- [4] Y. Masuda, "He-II Spallation Ultracold Neutron Source," Proceedings of the 17th Meeting of the International Collaboration on Advanced Neutron Sources, Santa Fe, NM, USA (25-29 April 2005).
- [5] P. Ageron, "Cold Neutron Sources at ILL," *Nucl. Instr. Meth.* **A284**, 197 (1989).
- [6] A. Donev et al., "Improving the Density of Jammed Disordered Packings Using Ellipsoids," *Science* **303**, 990 (2004).
- [7] A. Serebrov et al., *Nucl. Inst. and Meth. in Phys. Res.* **A440**, 658 (2000).
- [8] A. Serebrov et al., PNPI preprint 2359 (2000).
- [9] C. L. Morris et al., *Phys. Rev. Lett.* **89**, 272501 (2002).
- [10] F. Atchison et al., *Phys. Rev.* **C 71** 054601 (2005).
- [11] S. Ansell, J. F. Garcia, S. M. Bennington, D. J. Picton, and T. Broome, "Automation Techniques Applied to Systematic Studies of Moderator Coupling," Proceedings of the 6th Meeting of the Collaboration on Advanced Cold Moderators, Jülich, Germany (11-13 Sept 2002).



## 4. INSTRUMENTATION AND TECHNIQUES WORKING GROUP

Discussion Leader: Roland Gähler

Participants: Michael Agamalian, Gene Ice, Yoshihisa Iwashita, Ken Littrell (scribe), Charles Majkrzak, Ferei Mezei, David Mildner, Roger Pynn, Hirohiku Shimizu, Géza Zsigmond

Very cold neutrons (VCNs, with temperatures around 1 – 10 K or wavelengths  $\lambda$  around 14 – 40 Å) are not typically used to explore matter. They are generally considered as the tail of the useful spectrum — if there is no way out, we go for VCNs. This is simply a natural result of the spectral distribution of existing neutron sources: their spectral temperatures are either in the thermal range near 300 K or in the cold range near 30 K so that the phase space density of the Maxwellian distribution of wavelengths decreases as  $1/\lambda^5$ , making their use seemingly unfavorable. However, the basic properties of VCNs make their use appealing if they can be generated in significant quantities:

- The index of refraction  $n$  of neutrons approaches significant deviations from 1 only in the VCN range. The refracting power of a material  $n-1$  ( $\sim \lambda^2$ ) is typically in the range of  $10^{-6}$  for thermal neutrons, but  $10^{-4}$  in the VCN range. While this is small compared to light ( $n-1 \approx 0.5$ ), it already permits the application of a large variety of optical methods for controlling neutron beams and the design of optical instruments similar to those for light. For example, the total angle of reflection from a surface is proportional to  $\lambda$ , the deflection angle in a prism is proportional to  $\lambda^2$ , and the focal length of a focusing lens is proportional to  $1/\lambda^2$ , allowing reasonably useful effects only in the VCN range.
- The index of refraction  $n$  causes a phase shift  $\varphi$  of a neutron wave propagating through matter, with  $\varphi$  proportional to  $\lambda$ . Thus VCNs are favorable whenever small contrasts, i.e., small variations in the density distribution in materials or very thin specimens are to be examined.
- The interaction of neutrons with gravitational and magnetic fields also scales with  $\lambda^2$ , making their effects much more pronounced. This has important consequences for instruments exploiting Larmor precession in magnetic fields, where the precession angle scales with the propagation time through the field.
- VCNs, with their kinetic energies in the sub-meV range, are well-suited for exploring the dynamics of soft matter, as their typical energies of motion are in the same range, thereby enhancing the relative change in energy upon scattering as compared to using thermal or cold neutrons.
- The correlations lengths of beams scale with  $\lambda$  in the lateral direction and with  $\lambda^2/\Delta\lambda$  in longitudinal direction, where  $\Delta\lambda$  is the  $\lambda$ -bandwidth of the beam. The longitudinal correlation length prepared in NSE instruments is proportional to  $\lambda^3$ ; and the lateral correlation length in SESANS is proportional to  $\lambda^2$ .

- Their wavelength makes VCNs very powerful for the exploration of the structure of the nanometer-scaled world. Larger complexes in biology will be a main target for new VCN instruments.
- The extreme absorption of VCNs for certain isotopes (6 Mbarn for  $^{157}\text{Gd}$ ) combined with the very low absorption for elements like Si, Al, and O (around or less than 1 barn at 20 Å) allow the design of highly precise optical components similar to light optics. Near-perfect null-scattering highly-absorbing mixtures can be made.

It is very attractive to exploit the properties of VCNs in neutron science if the intensity problem can be solved. The Liouville theorem, a fundamental law of physics, allows an enhancement of the phase space density of VCNs only if a colder source may be used; the best match of a source temperature to the VCN spectrum is in the range of  $T = 2 - 4$  K. The intensity at long wavelengths and in the peak of the spectrum scales with  $T^{-3/2}$  so that we may expect a gain between one and two orders in phase space density (or in source brilliance) by going from 30 K to 2 – 4 K.

In order to estimate the gains for various types of instruments, we have assumed an order of magnitude gain in VCN production efficiency at 20 Å, which means equal brilliance at 0.5 MW accelerator power compared to the ILL. (As a reminder from the ESS project, a rule of thumb is that a 5-MW spallation source with a coupled, cold moderator will produce the same cold neutron flux as the ILL). Assuming 0.3 MW source power with this gain and a factor of 8 for pulse structure utility, we estimate gains in experimental efficiency of 5 for SANS and NSE compared to present, best-in-class instruments at ILL. Similarly, we expect a gain of 30 for quasielastic and low-energy TOF-INS.

A source with a repetition rate in the range of 1 to 5 Hz and an accelerator pulse width of a few ms is well-adapted to the use of VCNs in a pulsed mode for many instruments.

We consider the following existing instrument types as the ones that can benefit most from being used at a VCN source:

- long-baseline SANS instruments,
- reflectometers (for both horizontal and vertical geometry),
- high-resolution TOF instruments
- spin-echo spectrometers
- SESANS techniques.

These instruments, optimized for VCNs, will allow a matching or a certain overlap with optical methods in many cases.  $Q$ -resolutions around  $10^{-3} \text{ \AA}^{-1}$  are appropriate for most applications in the soft matter range. The gain factors for inelastic instruments like TOF-INS and NSE scale with  $\lambda^2$ ; however, for elastic instruments like reflectometers and SANS instruments, gain factors generally are independent from  $\lambda$ , as long as the wavelength distribution follows the  $1/\lambda^5$  tail of a cold spectrum.

For pulsed VCN sources, the following gains can be assumed for resolution and intensity:

	resolution at fixed geometry	Intensity at fixed resolution
SANS	$\lambda^{-1}$	$\lambda^0$
Reflectometry	$\lambda^{-1}$	$\lambda^2$
TOF-INS	$\lambda^{-3}$	$\lambda^2$
NSE	$\lambda^{-3}$	$\lambda^2-\lambda^4$

How do existing instruments benefit from going colder?

- a. Pushing flux and resolution simultaneously on SANS, NSE, TOF-INS
  - i. 300 kW,  $\leq 5$  Hz, 5 for SANS and NSE (intensity at 20 Å at ILL, utility scales as same-wavelength flux) up to 30 for TOF-INS with repetition-rate multiplication
  - ii. ILL 3× better than SNS at long wavelengths, TOF-INS at SNS benefits from high peak flux (SNS 23 kJ/pulse at 30 Hz)—5 gain without, 25 gain with rep rate multiplication in the low-resolution limit; gains 1–5 in the high resolution limit.
- b. Having larger dynamic range on SESAME

The consequences for tomography or indirect-geometry INS instruments based on artificial crystals are not that obvious and should be studied further.

We consider the following emerging techniques to be especially promising for the future use of VCNs:

- a. The large-area high-resolution detectors commonly used now in X-ray instruments at synchrotron sources should be adapted to neutron science. Note that the number of photons from an absorbed neutron is about 10 – 100 times higher than from X-rays in the 10–100 keV range. Detectors of 1 m<sup>2</sup> with resolutions in the 200 μm range are possible without the need of main in-house developments. The advent of CCDs with parallel readout, working already as prototypes, will allow near ideal detectors for the VCN instruments in mind. We propose to fund research which targets the development of these detectors. These detectors work without any windows in vacuum, thus avoiding small angle scattering, which is crucial for windows of high strength materials.
- b. In environments of higher  $\gamma$  radiation levels, scintillators coupled to photomultipliers can be used. By pulse shape analysis,  $\gamma$ - and neutron events can be sorted out with high efficiency. Those methods should be improved as well. The thin thickness of scintillators required for VCNs (typically 0.1 mm for 90%

absorption at 20 Å) will further reduce  $\gamma$  interaction probability and also energy deposition in the scintillator.

- c. Pulsed magnetic optics promise wide applications in the VCN range. The potential energy of neutrons in magnetic fields of Tesla range ( $E_{pot} = 6.8 \times 10^{-8}$  eV/T) allows focussing of wide angle VCN beams with high precision at focal lengths in the meter range and virtually no losses. SANS techniques may specifically benefit from those techniques and we strongly recommend the continuation of those developments.
- d. The advent of supermirrors with high  $m$  (at present more than 60% reflectivity at  $m = 5$ ; supermirrors with  $m = 10$  are envisaged) will allow reflection angles in the 10–20 degree range. This allows VCN beams of 1 sterad divergence by super mirror trumpets. Further, it allows focusing optics at much higher reflection angles than at present, thus reducing spherical aberrations to a large extent.
- e. With the slower repetition rates and stronger interactions for the same strength of field, dynamical optics such as pulsed magnetic lenses, time-varying apertures such as the gravity focuser at LQD and LANSE, and the tail-cutter artificial-lattice Bragg mirror on the LANSCE protein diffractometer become more practical.

In addition to hardware developments, developments in data-handling and interpreting like the following need to be supported if a VCN source is to meet its full potential:

- Coupling of data analysis to molecular dynamics simulations.
- Soft matter visualisation tools such as push me/pull me protein database (PDB) models linked to scattering curves.
- Information reliability checks.
- Corrections for multiple scattering.
- Inelastic corrections on elastic instruments.

Of course, these lists are far from exhaustive. Other more speculative techniques that may benefit from the use of VCNs are correlation spectroscopy with waveguides, VCN interferometry, VCN tomography, and neutron microscopy. Funding should be provided to explore these and other possibilities.

The use of a VCN source will help to overcome flux limitations in two ways:

- Optics work better.
- New source design allows different TMR choices and engineering optimisations — different engineering limitations.

The proposed VCN source will offer excellent opportunities for developing best-in-class instruments for a variety of instrument types. Due to the length and energy scales probed by VCNs — and, consequently, the kinds of instruments that benefit most — this source would be ideally suited for soft-matter research and for nanoscience, beautifully complementing the capabilities of existing sources, which are at their best for atomic-scale structures and the corresponding energies.

#### 4.1 SANS at the VCNS

Traditional small-angle neutron scattering (or SANS) is a perfect candidate for a flagship instrument at the very cold neutron source. The length scales that it probes, 1–1000 nm (and beyond), correspond to the length scales that are characteristic of polymer blends, proteins, micelles, membrane thicknesses, grain sizes in metallic alloys, and nanostructures or nanomaterials. Consequently, SANS is one of the most productive and oversubscribed techniques at every neutron scattering user facility. The intensity of 6–25 Å neutrons at the VCNS makes it particularly well-suited for SANS.

The parameter that is measured in a SANS experiment is the intensity as a function of the momentum transfer

$$Q = \frac{4\pi}{\lambda} \sin\left(\frac{\theta}{2}\right),$$

where  $\lambda$  is the neutron wavelength and  $\theta$  is the angle through which the neutron has been scattered. The typical SANS instrument at present is a long-baseline "pinhole camera"; in this type of instrument the beam is collimated by two apertures, one at the sample position and another with twice the diameter located at the same distance from the first as is the detector. This geometry simultaneously optimizes flux on sample and resolution (in the classical sense of ability to distinguish features at nearby values of  $Q$ ) for fixed wavelength and total instrument length. What is usually referred to as resolution in the SANS community and is typically considered a measure of the quality of the instrument is  $Q_{min}$ , the minimum value of  $Q$  that is reliably accessible. For an optimized pinhole instrument, the radius of the beam spot at the detector is four times the radius of the sample aperture. Therefore,

$$Q_{min} = \frac{8\pi r_s}{\lambda_{max} L_f},$$

where  $r_s$  is the sample aperture radius,  $L_f$  is the final flight path, and  $\lambda_{max}$  is the maximum wavelength used. Another important parameter is the maximum value of  $Q$  that can be measured. This is given by

$$Q_{max} = \frac{2\pi r_{max}}{\lambda_{min} L_f},$$

where  $r_{max}$  is the distance from the center of the scattering pattern to the farthest useable detector pixel and  $\lambda_{min}$  is the minimum wavelength used. Of course, at a reactor instrument,  $\lambda_{min} = \lambda_{max}$ , since only a single wavelength is used; instruments at these

sources require multiple measurements using different wavelengths and flight path lengths to span the full  $Q$  range of interest.

At present, the "gold standard" for SANS instruments is the D22 instrument at the ILL in France. This instrument is generally considered by the SANS community to be the best in class, producing high-quality data in the shortest time over the region of interest. To span the full range of  $Q$  with D22, a total of three measurements are needed: one with 18 Å neutrons and an 18 m flight path, and two with 7.5 Å neutrons at 8 m and 1.4 m, respectively. Typically, most of the time will be consumed on the long-wavelength run while the detector will have to be masked on the short-wavelength, short-camera run to prevent saturation. Thus, to a first approximation, the length of the experiment is determined by the time required for adequate statistics on the long-wavelength run.

On this basis, the VCNS will offer enormous opportunities for SANS. From the simulated spectra provided in the source section of this report, we can expect a gain in source brilliance at 20 Å of a factor of 10–20 (depending on the model chosen) over the ILL cold source, the brightest cold source in the world. At 7 Å, the VCNS will still be producing at least half as many neutrons. Therefore, D22 would take data approximately 10 times faster if it were simply moved unmodified and run as a monochromatic, steady-state SANS instrument at the VCNS.

This only tells part of the story. For a pulsed source, a broad range of wavelengths are simultaneously available for use. The wavelength band useable is related to the total length of the instrument  $L$  and the source pulsing frequency  $f$  as follows:

$$\lambda_{max} - \lambda_{min} = \frac{3955.4}{Lf}.$$

Here, the wavelengths are assumed to be in Angstroms, lengths in meters, and frequency in Hertz. Assuming a 20 m final flight path instrument with a 10 m exclusion zone before the collimation for a total flight path of 50 m and a 5 Hz source frequency, the instrument will be able to use a band of 6–22 Å simultaneously. On a related note, the typical relative wavelength band used for a monochromatic measurement on a reactor source is of order 10%. At a pulsed source, the single-measurement wavelength band is related to the wavelength, source pulse length  $t_p$ , and the total length of the instrument by

$$\frac{\Delta\lambda}{\lambda} = \frac{3955.4t_p}{L\lambda},$$

where  $t_p$  is in seconds. Thus if the source pulse length is assumed to be the same as the proton pulse length of 4 ms, the relative wavelength band ranges from 5.3% at 6 Å down to 1.4% at 22 Å. Since these are smaller than 10%, no additional pulse conditioning is necessary to match the reactor resolution, and running using time binning for wavelength selection will actually produce higher resolution. The use of time binning is equivalent to performing multiple measurements on a steady-state instrument; this is what gives rise to the time-of-flight advantage. Assuming that the additional time channels add on average half as much information as the first, the time-of-flight gain is

$$G_{tof} = \frac{\lambda_{max} - \lambda_{min}}{\lambda_{max} + \lambda_{min}} \left( \frac{\Delta\lambda}{\lambda} \right)^{-1},$$

where  $(\Delta\lambda/\lambda)$  is the steady-state wavelength resolution, leading to  $G_{tof} = 5$  for the situation described. This is a reasonable estimate as at the endpoints only a single time-channel will contribute but at the center of the range all contribute equally. Thus, the total gain would be about 10 at extreme low  $Q$ , unity at extreme high  $Q$ , and as high as 50 or more in between.

The following table summarizes a comparison of the accessible ranges for an instrument with a 0.5 m detector radius and 0.005 m sample aperture radius and a variety of final flight paths using a time-of-flight wavelength range of 7–20 Å and fixed wavelengths of 7.5 and 18 Å. In practice, it may be better to use multiple detectors with different resolutions at different final flight paths as is done currently at all pulsed sources rather than a single moveable detector.

$L_f$ (m)	$Q_{min}$ (Å <sup>-1</sup> ) 7–20 Å	$Q_{max}$ (Å <sup>-1</sup> ) 7–20 Å	$Q_{min}$ (Å <sup>-1</sup> ) 18 Å	$Q_{max}$ (Å <sup>-1</sup> ) 18 Å	$Q_{min}$ (Å <sup>-1</sup> ) 7.5 Å	$Q_{max}$ (Å <sup>-1</sup> ) 7.5 Å
20	0.00032	0.022	0.00035	0.0087	0.00084	0.021
10	0.00063	0.045	0.00070	0.017	0.0017	0.042
5	0.0013	0.090	0.0014	0.035	0.0034	0.084
2.5	0.0025	0.18	0.0028	0.070	0.0067	0.17

One issue that is a concern for a long-baseline time-of-flight SANS instrument is gravity. As the wavelength of the neutrons increases, they drop farther over a given distance. At a reactor source this is not an issue because the beamstop (and perhaps the detector) can be lowered to match the beam center at the wavelength used. For time-of-flight instruments there are also tested solutions: the height of the sample aperture can be varied in time with the source frequency or a material or magnetic prism can be used to redirect the beam back to the center of the detector. Since the effects of magnetic or material optics and gravity have the same wavelength dependence, this correction will be wavelength independent.

One final comment is that the concept instrument described here is unnecessarily conservative in its design. It is possible to decouple the minimum  $Q$  from the size of the sample aperture by using multiple confocal apertures like crossed, focusing Soller collimators or true, focusing optics such as material or magnetic lenses or focusing mirrors. As noted elsewhere in this document, all of these methods work better at longer wavelengths and, in the case of magnetic optics, it becomes reasonable to have them actively tuned to match the wavelength in time with the pulse frequency.

## 4.2 Spin-echo Spectroscopy at VCNS

The spin-echo method, originated by Ferenc Mezei, is a unique method for measuring energy transfers in the Fourier time domain. It allows measurements of quasielastic scattering energy transfers with extremely precise resolution AND without the severe losses in intensity that follow from precise definition of incident and scattered neutron energies. Fig. 4.1 illustrates the layout of a spin-echo spectrometer. The figure represents the polarizers as  $^3\text{He}$  filters.

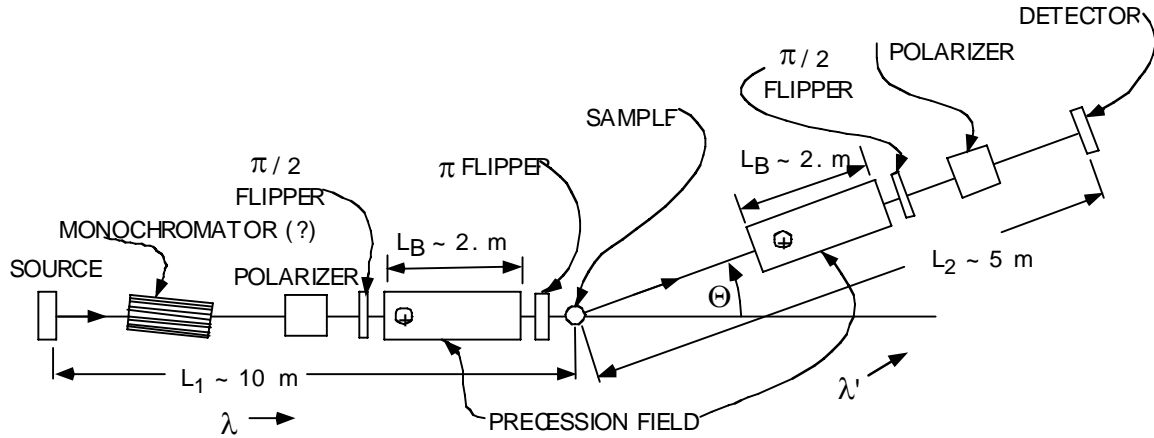


Fig. 4.1. Conceptual arrangement of components of a spin-echo spectrometer.

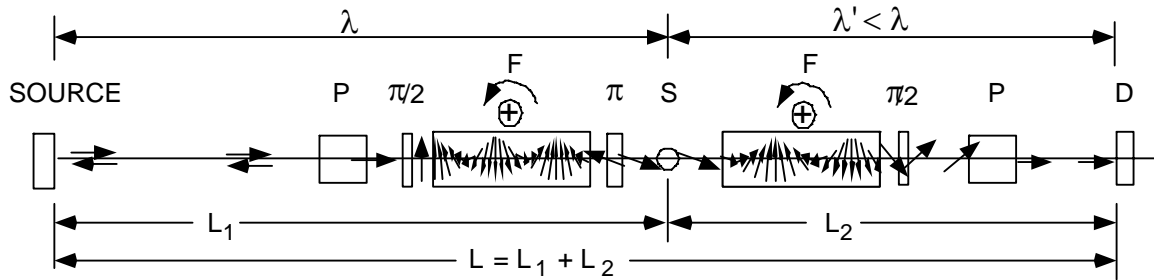


Fig. 4.2. Spins of neutrons passing through a spin-echo spectrometer.

Fig. 4.2 illustrates how the neutron spins behave in passing through a spin-echo spectrometer. The first polarizer selects neutrons from the source polarized in the longitudinal direction. The  $\pi/2$  flipper turns the spins in the horizontal plane. The spins rotate in the precession field  $B$  (up in the Fig.) by an angle  $\Phi_1 = \gamma_L B L_B / v$ , in which  $\gamma_L \sim 2.913$  kHz/Gauss is the Larmor constant, and  $v = (h/m)/\lambda$ ; in units of common practice,  $(h/m) = 3955.4$  Å-m/sec and  $h = 4.136 \times 10^{-12}$  meV-sec. The  $\pi$  flipper reverses the spins, and the neutrons scatter from the sample, changing their wavelength to  $\lambda'$ . The flipped neutrons enter the second precession field, directed parallel to the first precession field, where they rotate in the same sense, partially unwinding the initial rotation. The second

$\pi/2$  flipper rotates the spin in the same sense as the first one and would restore the original spin direction if the scattering were elastic. Fig. 4.2 shows the case for  $\lambda' < \lambda$ , that is, when neutrons gain energy in scattering, but severely under-represents the number of rotations in the precession fields. The net rotation is  $\Delta\Phi = \Phi_1 - \Phi_2 = \gamma_L B L_B (1/v - 1/v') = \gamma_L B L_B (m/h)(\lambda - \lambda')$ . The second  $\pi/2$  flipper turns the spin by  $\pi/2$  in the direction opposite to that of the first flipper. The second polarizer transmits a fraction of the neutrons according to the projection of the spin vector upon the polarizing direction (longitudinal in this illustration)  $\cos \Delta\Phi$  (shorter arrows in the figure). The polarization of the transmitted beam incident on the detector is  $P(\lambda, \lambda') = P_o(\lambda)S(Q, \omega) \cos \Delta\Phi$ , where  $P_o(\lambda)$  is the polarization of the incident beam after the first polarizer. The instrument encodes the wavelength difference that occurs upon scattering onto the precession phase difference.

The energy gained in inelastic scattering is  $\hbar\omega = (1/2)m (v'^2 - v^2)$ , which for quasielastic scattering is approximately  $\hbar\omega \sim (h^2/m)(\lambda - \lambda')/\lambda^3$ . Thus  $\Delta\Phi = \gamma_L B L_B (1/2\pi) (m/h)^2 \lambda^3 \omega$ .

Because the detector integrates over all scattered neutron energies, the polarization of the beam is the average over all scattered neutron wavelengths; that is, for given initial wavelength, the average over all energy transfers  $\hbar\omega$ , recalling that the range of energy transfers in quasielastic scattering is intrinsically very narrow, is

$$P(\tau; \Theta, \lambda, B) = P_o(\lambda) \int S(Q, \omega) \cos(\Delta\Phi) d\omega.$$

Meanwhile, the wave vector change is  $Q = 4\pi \sin(\Theta/2)/\lambda$ . Because  $S(Q, \omega)$  is real,  $P(\tau; \Theta, \lambda, B)$  measures the real part of the intermediate scattering function  $\text{Re}[\chi(Q, \tau)] = \text{Re}[\int S(Q, \omega) \exp(i\omega\tau) d\omega]$ , a function for which models already exist for many classes of systems. The spin-echo spectrometer measures  $\chi(Q, \tau)$  as a function of  $\tau$ .

The factor  $\tau = \gamma_L B L_B (1/2\pi) (m/h)^2 \lambda^3$  has the dimensions of time: it is the ‘‘Fourier time.’’ The maximum value of the Fourier time,  $\tau_{\max}$ , is the measure of the energy transfer resolution accessed in spin-echo spectroscopy, usually approximated as  $\delta\epsilon \sim 0.2 h / \tau_{\max}$ . For a practical case,  $L_B = 2$  m,  $\lambda = 5$  Å,  $B_{\max} = 6000$  gauss,  $\tau_{\max} = 4.44$  nsec, and  $\delta\epsilon \sim 0.186$   $\mu\text{eV}$ .

In the reactor implementation of spin-echo spectrometers, the incident beam is approximately monochromatic: usually a rotating drum monochromator selects a band  $\Delta\lambda/\lambda \sim 10\%$  around a chosen wavelength  $\lambda \sim 5$  Å. The field strength and the incident wavelength are varied to scan a range of Fourier times and the wavelength and the scattering angle varied to scan a range of  $Q$ s. In a time-of-flight implementation, the wavelength is related to the time of arrival  $t = L/v$ , where  $L = L_1 + L_2$ , so for each  $t$ ,  $\lambda = (h/m) t/L$  and measurements use a wide range of times, thus wavelengths, Fourier times and wave vectors. Operating with different field strengths would increase the range of  $\tau$ s. There has to date been no pulsed-source implementation of a spin-echo spectrometer, although reactor instruments have been successfully operated in a time-of-flight mode.

With VCNS operating at 5 Hz, the  $L = 15$  m instrument illustrated previously above could routinely access all wavelengths up to about 50 Å without overlap, increasing  $\tau_{max}$  to about 4.44  $\mu\text{sec}$  and decreasing  $\delta\epsilon$  to about 0.186 neV. If the minimum wavelength utilized were 4 Å, then, with a 1000-gauss  $B$ -field, for that wavelength the smallest Fourier time accessed would be  $\tau_{min} = 0.38$  nsec. With the VCNS 4.0-ms-long source pulse for all wavelengths, the wavelength resolution for defining the nominal wavelength would be 2% for 50-Å neutrons, and 27% for 4-Å neutrons; it might be necessary to shape the pulse of the shorter-wavelength neutrons using a chopper in this instrument. One can imagine operating the 15-meter instrument in the second time frame with neutrons in the 50–100 Å wavelength band — then the maximum Fourier time would be 35  $\mu\text{sec}$ .

These calculations, based on round-number but representative parameter assumptions, may be slightly optimistic. In reality, use of very long wavelength neutrons, which droop under gravity, may require introducing gravity compensating wedges to compensate.

VCNS with such a spin-echo instrument would provide striking improvements in the capabilities for this spectroscopy.

### 4.3 Neutron Resonance Spin Echo (NRSE) and Modulated Intensity by Zero Effort (MIEZE) for VCN

NRSE is a technique in which the static coils from a classical NSE are replaced by so-called simulated fields. A simulated field consists of two or more phase-locked RF-spinflippers running at the same frequency. The advantage of this technique is, beside its being relatively cheap and easy to install, that the room between the coils can be used to install additional neutron optics. It is also easier to incline the simulated fields in respect to the neutron beam. Apart from that all characteristics of NSE apply.

The MIEZE technique (see Fig. 4.3) is a version of NRSE, where the second field is not simulated completely. Therefore the echo signal is focused at a fixed distance from the coils and is time dependent. To measure the MISANS (modulated intensity small angle neutron scattering, a hybrid spectrometer using a MIEZE and a SANS at the same time) signal a fast detector (scintillator) has to be placed at the focusing distance. The advantage of this technique is, that all neutron optic components can be installed before the sample and therefore that huge detectors can be used. Furthermore the neutron beam is polarized at the sample position.

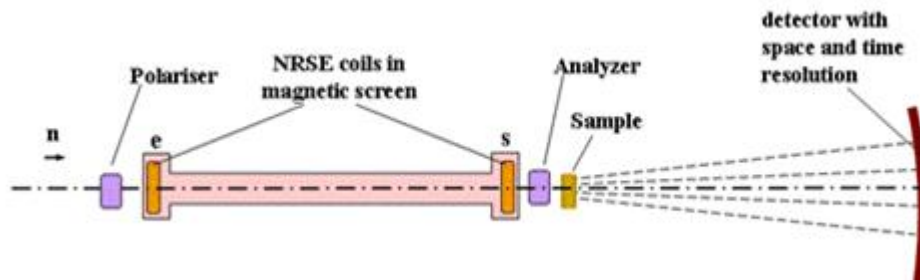


Fig. 4.3. Sketch of a MIEZE device in a small angle setup.

Both of these techniques are easily adapted to a pulsed source since only the current of the RF-flippers has to be matched to the arriving wavelength while all other parameters of the spectrometer are wavelength-independent. Fig. 4.4 shows the results of a test measurement at the polarized reflectometer POSY I at IPNS in which the detector senses the direct beam (no sample). In the presence of inelastic (quasi-elastic) scattering from the sample, the signal at the detector would be washed out as the velocity of the neutrons is smeared by the interaction with the sample. The result is a drop in the contrast in the sine-shaped intensity oscillations in analogy to the drop in polarization in a conventional NSE experiment.

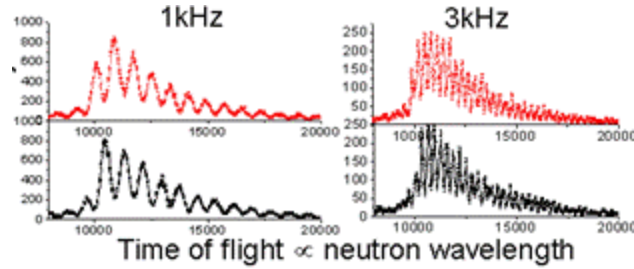


Fig. 4.4. Test measurement of a MIEZE signal at a IPNS at low resolution.

Because longer wavelengths enhance the small-angle resolution towards a lower  $q$ -minimum and the dynamic time scale for bigger objects increases exponentially (depending on the measured system), a MISANS type spectrometer would be well adapted to the VCNS since the energy resolution goes with  $\lambda^3$  and is therefore matched with the needs dictated by the sample. The energy resolution would span 4 decades, without changing the instrument setup while using the whole neutron bandwidth in every pulse. Scientists at the IPNS are continuing the development of the MISANS concept.

#### 4.4 Spin-Echo Small-Angle Scattering at VCNS

The spin-echo method adapts to small-angle diffraction measurements, in a technique that Theo Rekveldt has developed in recent years. It allows measurement of long-range density-density correlations without the severe losses in intensity that follow from precise definition of incident wavelengths and scattering angles. Figures 4.5 and 4.6 illustrate the layout of a spin-echo small-angle diffractometer. The figures represent the polarizers as  $^3\text{He}$  filters.

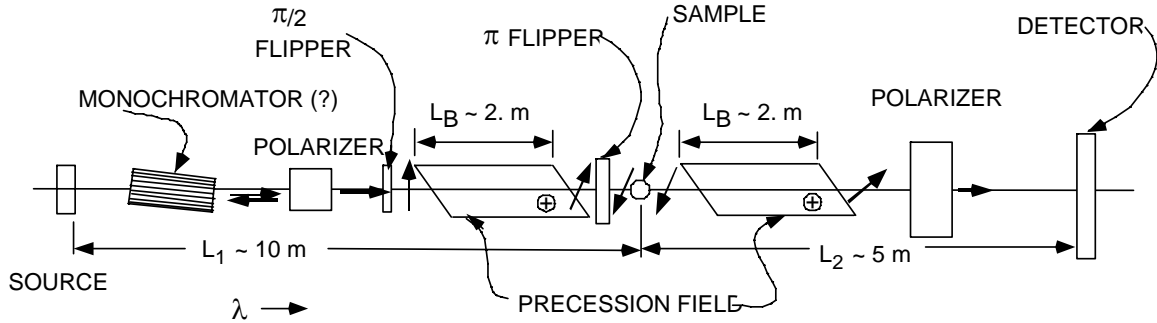


Fig. 4.5. Conceptual arrangement of a spin-echo SANS instrument.

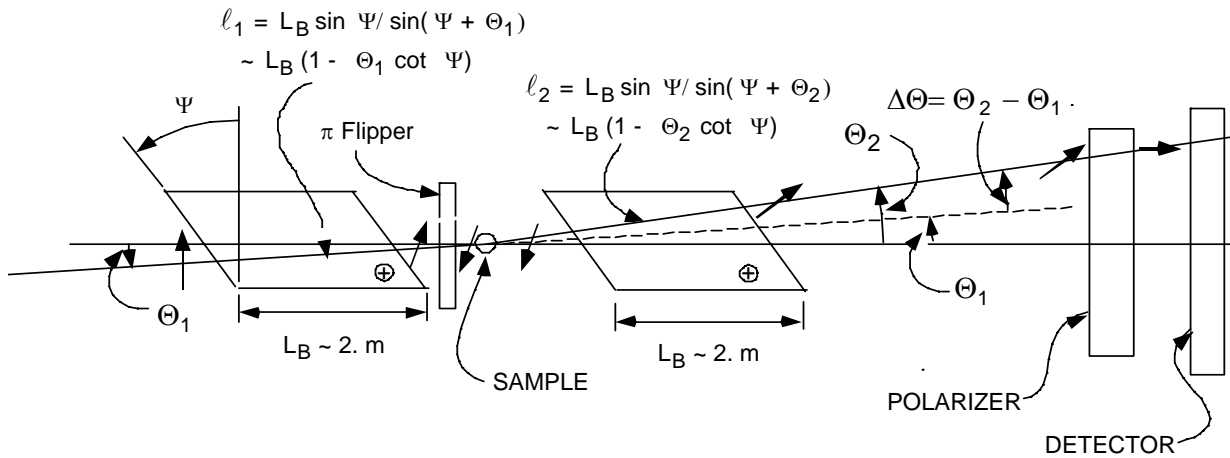


Fig. 4.6. Spins in a spin-echo SANS instrument. The angles of the neutron trajectories are exaggerated.

The first polarizer selects neutrons from the source polarized in the longitudinal direction. The  $\pi/2$  flipper turns the spins in the horizontal plane. Neutrons entering the first precession field at angle  $\Theta_1$  travel a distance  $\ell_1 = L_B(1 - \Theta_1 \cot \Psi)$ . The spins rotate in the precession field  $\mathbf{B}$  (up in the Fig.) by an angle  $\Phi_1 = \gamma_L B \ell_1 / v$ , in which  $\gamma_L \sim 2.913$  kHz/Gauss is the Larmor constant, and  $v = (h/m)\lambda$ ; in units of common practice,

$(h/m) = 3955.4 \text{ \AA-m/sec}$  and  $h = 4.136 \times 10^{-12} \text{ meV-sec}$ . The  $\pi$  flipper reverses the spins, and the neutrons scatter from the sample, changing their direction to  $\Theta_2$ . The flipped neutrons enter the second precession field, directed parallel to the first precession field, where they travel a distance  $\ell_2 = L_B(1 - \Theta_2 \cot \Psi)$  rotating in the same sense, partially unwinding the initial rotation. The second precession field rotates the spin in the same sense as the first one and would restore the original spin direction if the scattering were without change in direction. The net rotation is  $\Delta\Phi = \Phi_1 - \Phi_2 = \gamma_L B L_B (\Theta_2 - \Theta_1) \cot \Psi / v = \gamma_L B L_B \Delta\Theta \cot \Psi (m/h)\lambda$ . The second polarizer transmits a fraction of the neutrons according to the projection of the spin vector upon the polarizing direction (longitudinal in this illustration)  $\cos \Delta\Phi$  (shorter arrows in the Fig.). The polarization of the transmitted beam incident on the detector is  $P(r; \lambda, B, \Psi) = P_o(\lambda)S(Q) \cos \Delta\Phi$ , where  $P_o(\lambda)$  is the polarization of the incident beam after the first polarizer. The instrument encodes the change in angle that occurs upon scattering onto the precession phase difference. However, this occurs in only one dimension, so the instrument measures a slit-smearred result as in Kratky cameras.

Because the detector integrates over all scattered neutron directions, the polarization of the beam is the average over all scattered neutron wavelengths; that is, for given initial wavelength, the average over all angles  $\Theta_1$  and  $\Theta_2$ , recalling that the range of wave vectors in small angle scattering is intrinsically very narrow, is

$$P(r; \lambda, B, \Psi) = P_o(\lambda) \int S(Q) \cos(\Delta\Phi) d(\Delta\Theta).$$

In terms of  $Q = 2\pi \Delta\Theta/\lambda$ ,  $\Delta\Phi = \gamma_L B L_B (m/h)(1/2\pi) \cot \Psi \lambda^2 Q = r Q$ , where  $r = \gamma_L B L_B (m/h)(1/2\pi) \cot \Psi \lambda^2$  is the ‘‘Fourier length,’’

$$P(r; \lambda, B, \Psi) = P_o(\lambda) (\lambda/2\pi) \int S(Q) \cos(Qr) dQ.$$

The result is related to the pair correlation function  $\rho(r) - \rho_o$  by

$$(2\pi/\lambda)(1/P_o(\lambda)) \partial P(r; \lambda, B, \Psi) / \partial r = \int Q S(Q) \sin(Qr) dQ = 4\pi r (\rho(r) - \rho_o).$$

To scan a range of  $r$ s requires scanning a range of field strengths  $B$  and/or a range of wavelengths  $\lambda$ . In the reactor implementation a drum monochromator selects a band of wavelengths  $\Delta\lambda/\lambda \sim 10\%$ , and  $r$  varies with  $B$  for each wavelength. In the time-of-flight version,  $r$  varies with wavelength at fixed  $B$ , and a different range of  $r$ s follows for different  $B$ s.

In terms of round number, representative parameters,  $B_{max} = 6000$  gauss,  $L_B = 2$  m,  $\lambda = 4 \text{ \AA}$ ,  $\Psi = 30^\circ$ , the maximum Fourier length is  $r_{max} = 3.90 \times 10^4 \text{ \AA}$ . The corresponding  $Q$ -resolution, calculated as  $\Delta Q = 2\pi/r_{max} = 1.6 \times 10^{-4} \text{ \AA}^{-1}$ . With 50- $\text{\AA}$  neutrons, with the same field and geometric parameters,  $r_{max} = 6.1 \times 10^6 \text{ \AA} = 610 \text{ \mu m}$ .

With the VCNS 4-msec-long source pulse for all wavelengths and a 15-m-long total flight path, the wavelength resolution for defining the nominal wavelength would be 2%

for 50-Å neutrons, and 27% for 4-Å neutrons. It might be necessary to shape the pulse of the shorter-wavelength neutrons using a chopper in this instrument. One can imagine operating the 15-meter instrument in the second time frame with neutrons in the 50–100 Å wavelength band; then the maximum Fourier length would be about 2400 μm. In reality, use of very long wavelength neutrons, which fall significantly under gravity, may require introducing gravity-canceling wedges to compensate the droop.

VCNS with such a spin-echo SANS instrument would provide striking improvements in the capabilities for examining materials at very long length scales. There are numerous variations on this theme, described in the reference [1].

#### 4.5 Double-Chopper Cold Neutron Spectroscopy at VCNS

At present, this kind of instrument exists only at reactor sources, but it is actually quite well suited to a pulsed source: In these instruments the flux on sample is proportional to the peak source flux, not the time-averaged flux. Thus, ISIS has chosen an instrument of this class, LET, as one of its day-one flagship instruments for TS2 and the SNS has approved another, CNCS. The LET instrument is expected to perform at a comparable level to the recently-upgraded IN5 spectrometer at the ILL in Grenoble. As Fig. 2 in the source section shows, all of the proposed TMR choices for the VCNS have a peak flux about 5 times greater than that of the ILL cold source in the thermal range increasing to two orders of magnitude greater in the VCN range. Thus, at an incident 80 meV, the high-energy cutoff for this type of instrument at reactors due to the diminishing component of thermal neutrons as energy increases, an IN5-type instrument would perform about 5 times faster at the VCNS, while at an incident energy of 1 meV it would perform about 50 times faster. Of course, the gains will only increase as the incident energy decreases. These estimates do not take into account the gains from the innovations in beamline optics being introduced in LET such as dual-aperture choppers with guide trumpets or the possibility of using repetition-rate multiplication. The former are estimated to contribute an additional, multiplicative gain of 2–5 over an IN5-type instrument; the utility of the latter is doubtful because of the low duty cycle. Thus, a DCS direct-geometry instrument for quasielastic scattering is a very promising instrument for a source like the VCNS.

#### 4.6 Gravity-Effects Cancellation in Transport of Very Cold Neutrons

Neutrons fall in the Earth's gravitational field exactly like other massive bodies, accelerated downward at the rate of gravitational acceleration,  $g$ . In the context of neutron beam transport, usually in an initially horizontal beam, neutrons with an initial horizontal speed  $v_x$  accelerate to a vertical component of velocity  $v_y = gt$  fall a distance  $\epsilon = 1/2 gt^2$  in time  $t$ , where  $t = L/v_x$ , where  $L$  is the horizontal distance traveled. In the present discussion,  $v_y \ll v_x$ . Thus, in terms of the wavelength  $\lambda = h/mv$ , ( $h/m = 3955$ . Å-m/sec,  $g = 9.8$  m/sec<sup>2</sup>)

$$v_y = gL/v_x = (m/h)gL\lambda$$

and

$$\varepsilon = \frac{1}{2} gL^2 / v_x^2 = \frac{1}{2} (m/h)^2 gL^2 \lambda^2 .$$

For  $L = 20$  m and  $\lambda = 20$  Å,  $\varepsilon = 5$  cm, a considerable distance. After flying a horizontal distance  $L$ , the neutron trajectory droops by an angle  $\alpha$ , measured from the horizontal. For the same condition as above,  $\alpha = 0.29^\circ$ . For 40-Å neutrons,  $\varepsilon = 20$  cm, and  $\alpha = 1.2^\circ$ ,

$$\alpha \approx \tan(\alpha) = \frac{v_y}{v_x} = (m/h)^2 gL \lambda^2 .$$

The angle of a neutron trajectory can be turned by a prism in the same way as a light beam (albeit through a relatively small angle). A prism with an interior angle  $A$  deflects a beam by an angle  $\Delta$ , given by [1]

$$\Delta = 2(n-1)\tan(A/2),$$

where  $n$  is the index of refraction for neutrons:

$$n = 1 - (1/2\pi)\rho b \lambda^2 .$$

Here,  $\rho$  is the number density of scatterers in the prism material, and  $b$  is the coherent scattering length per atom (in a polyatomic material,  $b$  is the total scattering length per unit and  $\rho$  is the number density of scattering units.) Therefore,

$$\Delta = -(1/\pi)\tan(A/2)\rho b \lambda^2 .$$

The droop angle and the prism deviation are both proportional to  $\lambda^2$ , thus it is possible to cancel the droop at distance  $L$  for all wavelengths by passing the beam through a prism such that  $\Delta = -\alpha$ , or

$$\tan(A/2) = \frac{\pi g}{\rho b} (m/h)^2 L ,$$

returning the beam to horizontal. The result is independent of the neutron wavelength and, to first order, independent of the angle of incidence on the prism. This angle may be very large and impractical if  $L$  is large or  $\rho b$  is small. For  $\text{MgF}_2$ ,  $\rho b = 5 \times 10^{14} \text{ m}^{-2}$ , so for  $L = 20$  m, the angle must be

$$\tan(A/2) = 7.9 ; A = 165^\circ .$$

This is a rather large included angle, but is practical in some circumstances, in particular for VCNs. Multiple prisms with a smaller included angle may also be used in series for the same effect.

E. M. Forgan and R. Cubitt [2] have worked out and demonstrated a scheme based on this idea for correcting gravity droop in a small angle diffractometer (the case is slightly more complicated than that of our simple example). They carried out their demonstration

in the D22 the fixed-wavelength SANS instrument at ILL, with 20-Å neutrons and initial and final flight path lengths of about 20 m, using a quartz prism.

This method would be particularly well suited to time-of-flight diffractometers, which have fixed flight path lengths, but has not yet been implemented on a time-of-flight SANS instrument.

## 4.7 Guides with Very Cold Neutrons

We illustrate the high effectiveness of guide tubes used with Very Cold Neutrons.

### 4.7.1 Straight Guides

For a fully illuminated guide, the gain (that is, the ratio of the number of neutrons emerging from the exit of the guide to the number that would flow without internal reflections) for a one-dimensional single-channel parallel-sided straight guide (neglecting the effect of gravity) is

$$\begin{aligned} G_{1-D}(\lambda) &= 1 + (\theta_c / \psi_o)^2 ; \theta_c \leq \psi_o \\ &= 2(\theta_c / \psi_o) ; \theta_c \geq \psi_o \\ \psi_o &= W / L ; \theta_c = m\gamma\lambda ; \gamma = 0.0017 \text{ radians} / \text{Å} ; m \geq 1.0. \end{aligned}$$

The gain for a 2-dimensional rectangular guide is

$$G_{2-D}(\lambda) = (G_{1-D}(\lambda, W_H)) \times (G_{1-D}(\lambda, W_V)).$$

Fig. 4.7 illustrates the gain for a straight guide of length  $L = 5$  m (roughly speaking, the thickness of the primary shield of the source,) horizontal width  $W_H = 2$  cm, and vertical height  $W_V = 10$  cm, as a function of wavelength. Gains in conventional circumstances, factors of a 10 ~ 100 for several-Å neutrons and current critical-angle multipliers  $m \sim 3$ , become factors 100 ~ 1000 for 10 ~ 30-Å VCNs. Gravitational droop would reduce the gains for longest wavelengths, but vertical curvature could compensate this at one wavelength and nearby.

### 4.7.2 Curved Guides

Curved guides act as band-pass filters. The gain of a curved guide is the product of the gain for a straight guide multiplied by the factor  $T(\lambda)$

$$\begin{aligned} T(\lambda) &= (2/3)K^2 ; K < 1 \\ &= (2/3)K^2 [1 - (1 - 1/K^2)^{3/2}] ; K > 1 , \end{aligned}$$

where  $K = \lambda / \lambda^*$ , and  $\lambda^*$  is the “critical wavelength” of the curved guide,

$$\lambda^* = (1/m\gamma)[2W/R]^{1/2} ,$$

and  $R$  is the radius of curvature (horizontal) of the guide. Taking  $\lambda^* = 5 \text{ \AA}$  and the dimensions of the straight guide as above with horizontal width 2 cm requires  $R = 22.2 \text{ m}$ . Fig. 4.7 shows the gain of the straight guide and of the curved guide. In the horizontal plane the emerging direction of the guide is  $12.9^\circ$  and the offset from the straight path is 56 cm.

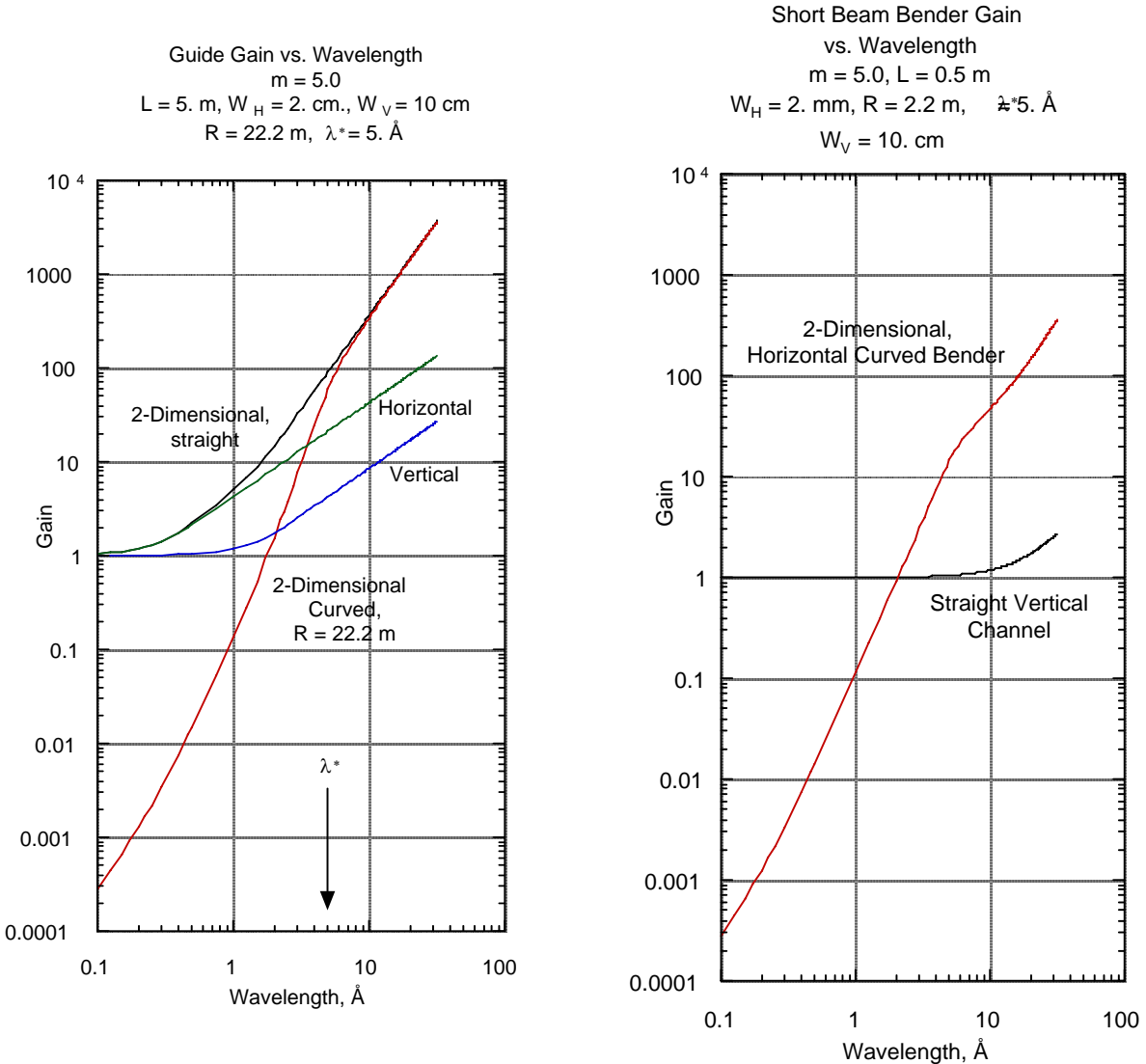


Fig. 4.7. Guide gains in the VCN wavelength range. Left,  $L = 5 \text{ m}$ ; right,  $L = 0.5 \text{ m}$ .

### 4.7.3 Compact Benders

Stacks of short, curved guides with tall, narrow channels, known as “compact benders,” already in common use, function to divert neutron beams away from the straight-through fast and short-wavelength neutrons that pass through the guide walls. The governing equations show that, as long as the ratios of width  $W_H$  and radius of curvature  $R$  and the

length  $L$  are preserved, short guides with narrow channels have the same gains in the sense defined above as do longer guides with wider channels. (Of course, the entrance area of the narrower channels is smaller than that of the wider channels, so the throughput of each channel is proportionately smaller.) Therefore, the gain calculations above apply equally well in the horizontal plane to each channel of compact benders, say for 1/10 the dimensions,  $W = 2$  mm,  $R = 2.2$  m,  $L = 0.5$  m. In the vertical plane, benders are taller in relation to the length. The Fig. shows the gain for a vertical single channel with  $W_V = 10$  cm,  $L = 0.5$  m used with the short, curved, narrow horizontal channel. In the horizontal plane the emerging direction is  $12.9^\circ$  and the offset from the straight path is 5.6 cm.

#### Reference

- [1] M. Theo Rekveldt, W. G. Bouwman, W. H. Kraan, O. Uea, S. V. Grigoriev, K. Halbicht, and T. Keller, ‘Elastic Neutron Scattering Measurements Using Larmor Precession of Polarized Neutrons,’ 87–99 in *Neutron Spin Echo Spectroscopy*, Eds. F. Mezei, C. Pappas, and T. Gutberlet, Lecture Notes in Physics, Springer-Verlag (2003).
- [2] E. M. Forgan and R. Cubitt, ‘Cancellation of Gravity for Slow Neutrons in Small Angle Scattering Experiments.’ *Neutron News*, **9**, 25–31 (1998).



## 5. SCIENTIFIC APPLICATIONS WORKING GROUP

Discussion Leader: Colin Carlile

Participants: Masa Arai, Steve Bennington, Peter Geltenbort, Alexander Kolesnikov, Jyotsana Lal, Chun Loong (scribe), Jim Rhyne, Jim Richardson, Stephan Rosenkranz, Art Schultz, Mike Snow

The Group first brainstormed the scientific case for a VCNS in an afternoon breakout session (Aug 23), and then collected preliminary thoughts and notes in the next day's summary session. Afterward, additional write-ups and references were supplied by group members via emails. This report represents a compilation of the collected contributions.

Given the unprecedented high flux of long wavelength ( $>20 \text{ \AA}$ ) neutrons anticipated from the VCNS – a time-averaged flux level on the order of 30 times and a peak flux on the order of 1000 times that from the present ILL cold source -- and the superb performance of advanced optical devices, polarizers, and detectors favoring very cold neutrons, the Group is very enthusiastic about the scientific opportunities and possible breakthroughs in many important areas that are unattainable by the present neutron sources including the SNS but realizable by the VCNS.

The Group has chosen to cut through the subject under three headings:

- 5.1 New science to be driven by advanced VCN instrumentation
- 5.2 Special scientific areas
- 5.3 Special applied topics

However, as experimental practice using very cold neutrons awaits further development, the scope of scientific deliverables is yet uncharted. The contents of this report need to be refined and strengthened through consultation with the communities of various disciplines and perhaps by pursuing additional pilot R&D programs.

### 5.1 New Science to be Driven by Advanced VCN Instrumentation

#### 5.1.1 *Fundamental Physics*

##### Search for the neutron electric dipole moment (EDM) and measurement of the neutron lifetime using magnetic trapping in superfluid helium

These proposed experiments are unique in using ultracold neutrons that are created in superfluid helium by downscattering the 9- $\text{\AA}$  neutrons within the moderating vessel itself as opposed to using external extraction of UCN. Both experiments have recently been proposed for SNS in the first call for letters of intent. A VCNS of the power proposed should have significantly higher fluxes of 9- $\text{\AA}$  and colder neutrons than from cold sources of conventional reactors and spallation sources, whose spectra typically peak at 3-4  $\text{\AA}$ . Since phase space goes as  $k^3$ , this can be a big effect. The start date for the neutron EDM experiment at SNS is approximately 2010 and is projected to run for about 5 years or so. The current upper limit on the neutron EDM is still several orders of magnitude larger

than the size predicted in the Standard Model of particle physics. Neutron EDM measurements can be expected to continue for a long time with increasing sophistication at least until a nonzero effect is seen. The VCNS's new capability could make possible a productive extension of the EDM experiment after the SNS measurement. The longer-term potential for the superfluid helium UCN lifetime experiment is less clear but also potentially interesting at a VCN source. The neutron lifetime experiment has competition from other techniques such as room temperature magnetic storage. The scientific motivation depends on the long-term need for higher precision as input into Big Bang Nucleosynthesis calculations of the  $^4\text{He}$  abundance of the universe and as a test of weak interaction theory.

#### High precision neutron beta decay measurements

A number of research groups are pursuing neutron beta decay measurements to achieve sufficient accuracy for: (a) measurements of the Standard Model parameter  $V_{ud}$  for testing the concept of weak interaction universality (i.e., do all quarks really feel the same weak interaction as predicted by theory?) and (b) exploration of alternative models to the standard one. A very cold neutron beamline from a high-flux spallation source with low repetition rate can in principle allow more flexibility to attain high signal-to-noise ratio in the decay measurement since the slower neutrons spend more time in the apparatus and the lower repetition rate reduces the background. The combination of VCNS's brightness, tailored source spectrum, and potential for the use of focusing optics could yield an order of magnitude or more increase in sensitivity for a decay apparatus. The SNS now has received several letters of intent for neutron decay measurements, for example. However, the longer-term activity in the neutron beta decay field with respect to the VCNS timetable is hard to predict since research priorities may shift significantly depending on what the Large Hadron Collision (LHC) discovers about the theory of the weak interaction.

#### Weak neutron-nucleus interactions

Experiments to search for the weak interactions between neutrons and simple nuclei like H, D, and  $^4\text{He}$  are in progress at LANSCE and NIST and have been proposed for the SNS. Whether or not these studies will be of interest on the VCNS timetable is not clear. It may be useful to note an advantage of a VCNS for such measurements: systematic effects due to Bragg scattering which have plagued past measurements of parity-odd neutron spin rotation are eliminated at a VCNS since most neutrons are beyond the Bragg cutoff for solids of potential interest. If a vertical cold neutron beam can be arranged allowing a view of the gammas from neutron-proton capture one could also attempt to measure the circular polarization of unpolarized n-p capture due to the weak interaction. This experiment is one of the few ways to measure the  $\Delta I=2$  component of the nucleon-nucleon weak interaction.

#### *5.1.2 Microscopy*

The well-known advantage of neutron microscopy is its unique chemical contrasting and sensitivity, owing to the large change in the neutron-optical properties over different isotopes of elements as the wavelength increases toward the very cold neutron regime. Ultimately, toward the limiting energies typically  $\sim 10^{-7}$  eV corresponding to ultracold

neutrons, total reflection at high incident angles or exponentially decaying transmission is realized. The resolution of neutron microscopy, assuming the availability of new lenses, zone plates, focusing devices, etc., for using very cold neutrons, may vary from micrometers to nanometers. Previous research in this field in the '80s and early '90s has subsided mainly due to the lack of sufficient flux to test and improve design concepts of devices and components [1]. We believe that the advent of the VCNS will revive this field. By leveraging the incident spectrum over the entire very-cold to ultracold region with unprecedented brightness from the VCNS and by developing new optical devices and adapting techniques known to other microscopies such as the phase-contrast schemes, the research community can bring forth new microscopic imaging capabilities useful for studies of biomolecular systems and nanocomposites with complex surface and buried structures.

### *5.1.3 Holography*

The advantage of neutron holography as compared to others using visible light, electrons and x-rays is its relatively larger penetration depth into the bulk of materials (true even for very cold neutrons) and the irregular atomic number-dependence of the scattering cross section. The loss of phase information is a common shortcoming for diffraction techniques including using neutrons. Holography enables the rendering of a 3D structure yet retaining the phase information thereby providing a more complete measurement. As required by all holographic techniques, coherency in terms of phase stability and reproducibility of the reference and scattered waves is a big challenge for neutron holography. This problem has been overcome by employing the so-called “inside-source” or “inside detector” techniques. The former requires a point-like source of spherical neutron waves within the sample and the latter requires gamma-ray emission from lightly doped neutron-absorbing isotopes to act as point-like detectors also inside the sample.

When using the inside-source method, the large incoherent scattering from hydrogen atoms, either readily present in most biological and mineralogical specimens or purposely embedded into samples, serves as the point-source scatterer. Any system that contains a single hydrogen atom per unit cell can be studied; the incoherent scattering from the hydrogen provides the spherical reference signal which scatters from the other atoms in the lattice and creates an interference pattern with the unscattered reference signal to produce a pattern which can be used to reconstruct the 3D structure around the hydrogen atom without invoking a specific model.

Holography of single-crystal samples with atomic-scale resolution has been demonstrated recently. The reconstruction of the holographic images relies on sophisticated computer data processing during which intensities from Bragg peaks or Debye-Scherrer rings have to be removed carefully. For very cold neutrons, this hindrance may be removed as the neutron wavelengths are beyond the Bragg cut-off. However, spatial resolution will be reduced as compared to using thermal neutrons. This may not be a serious drawback because for large structures of biological assemblies and nanocomposites, atomic resolution of holographic images often is not necessary. One challenge is to maintain at least identical point symmetry for all the hydrogen atoms in the sample, which is a stringent condition to be met for complex materials.

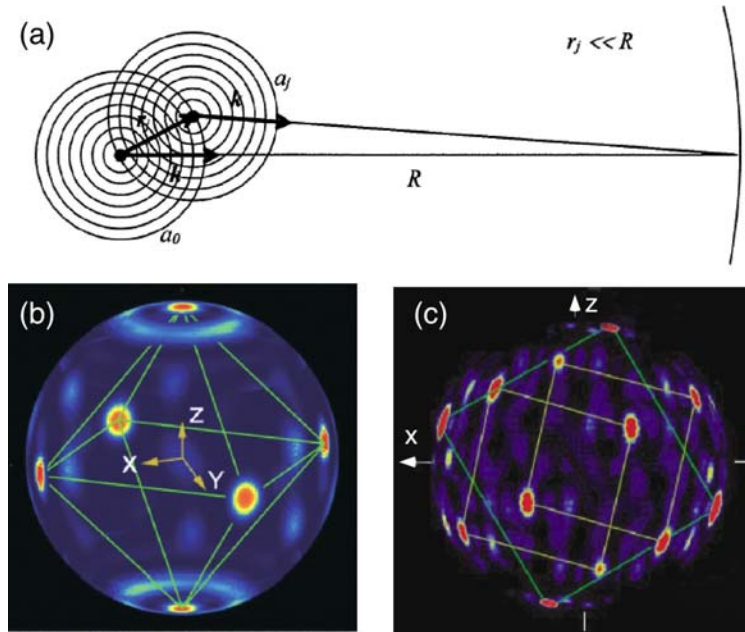


Fig. 5.1. (a) The inside-source or inside-detector technique of holography. The hologram is formed by the inference between waves scattering by neighboring atoms and the unscattered waves, after Faigel & Tegze. [2] (b) The restored holographic image of the 3-D octahedron of Pd atoms (red spots) surrounding a hydrogen atom at the center (not shown), after Cser *et al.* [3] (c) A holographic illustration of the first neighboring Pb atoms (red spots) surrounding a Cd atom (yellow spot), after Cser *et al.* [4].

#### 5.1.4 Highly Focused Beams for Extreme Sample Environment

Currently, *in situ* neutron experiments can routinely be carried out at pressures up to  $\sim 30$  GPa, temperatures up to  $\sim 1500^\circ\text{C}$ , and magnetic fields of  $\sim 17\text{T}$ . Ancillary equipment enabling higher pressures/temperatures/magnetic fields such as diamond anvil cells, magnetic-induction or laser heating/melting under containerless levitation, and small-bore high-power pulsed magnets exist but they restrict the beam aperture down to mm or sub-mm size. Very few neutron experiments have been carried out because the neutron beam, masked or collimated down to such sizes using methods presently known for thermal and cold neutrons, will reduce the flux by 1000 times or more, thereby rendering the studies impractical. Such difficulty will be significantly alleviated for very cold neutrons. Owing to the much slower speeds of very cold neutrons, manipulation of their trajectories and spin direction is inherently easier. Recent progress in neutron optics has indicated that a large ( $\sim\text{cm}$ ) beam of very cold neutrons can be focused down to mm size *without undue sacrifice of the intensity*. Likewise, a new generation of very efficient, focusable polarizers and detectors are achievable. Therefore, these advantages, unique to very cold neutrons in conjunction with the anticipated  $\sim 1000$ -fold increase of source flux of the VCNS (Fig. 5.2), will permit myriad experiments on sub-mg samples under extreme environments to be performed routinely, a majority of which, such as *inelastic* scattering, are truly unthinkable for today's sources including the SNS.

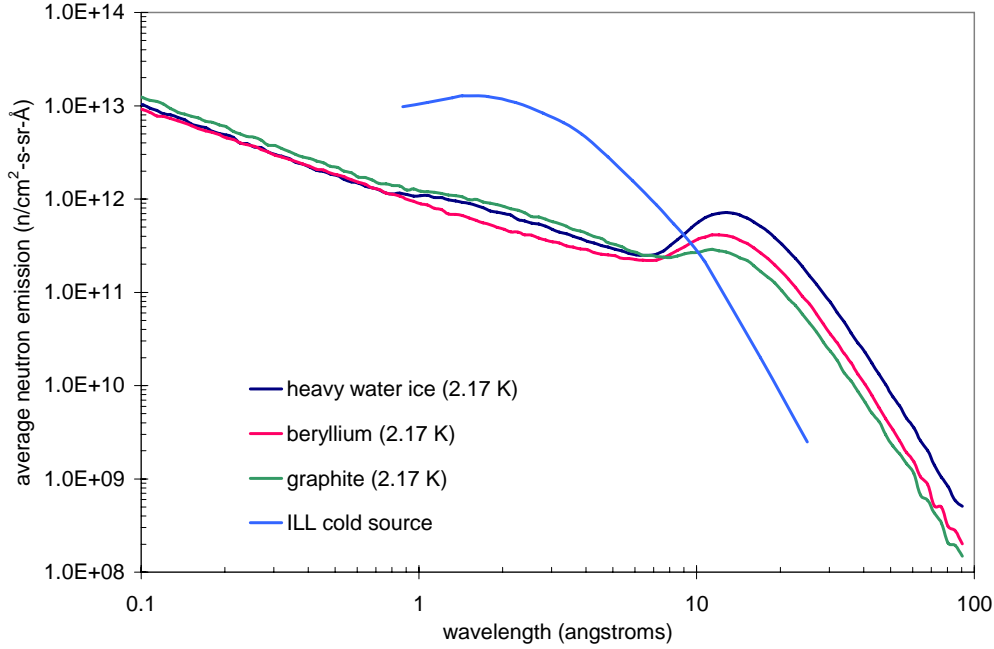


Fig. 5.2 The expected time-average neutron flux of the VCNS as compared to the ILL cold source.

### 5.1.5 Spin-Polarized Scatterers and Chemical Contrasts

#### Tuning of scattering cross sections of polarized targets at very cold neutron energies

The coherent scattering length of polarized neutrons scattered from spin-polarized hydrogen atoms is  $b_H = [-0.374 \pm 1.456 P_H] \times 10^{-12}$  cm, where  $-1 \leq P_H \leq 1$  is the polarization of the proton spins and the + and – signs correspond to the complete neutron polarization parallel and anti-parallel to the applied magnetic field  $\mathbf{B}$ , respectively. Therefore, the value of  $b_H$  can be varied over a wide range between -1.83 and +1.082 in units of  $10^{-12}$  cm by tuning the ratio of  $B/T$  (where  $T$  is the temperature of the polarized target). High magnetic field and low temperature are required – typically for a  $B/T$  ratio of higher than 1000 T/K - in order to achieve a large contrast between the coherent scattering lengths of the + and – neutron polarization. Similarly, the coherent scattering length of other spin-polarized nuclei such as D and  $^{14}\text{N}$  can be varied but the experimental requirement may be stringent.

The incoherent scattering cross section of hydrogen atoms also depends on the polarization of the neutrons ( $p$ ) and the protons ( $P$ ), namely,

$$\sigma_{inc} = 106.56 \left( \frac{3}{4} - \frac{pP}{2} - \frac{P^2}{4} \right) \times 10^{-24} \text{ cm}^2. \quad \text{Therefore, the incoherent scattering can be}$$

completely switched off when  $p = P = 1$ . Fig. 5.3 shows the proton spin-polarization dependence of the coherent and incoherent scattering of H and D. This high-field ( $>10$  T), low-temperature ( $<1\text{K}$ ), and high neutron-polarization conditions are much easier to attain for very cold neutrons, with an option of using a focusable beam to match the sample size. *Only the VCNS can produce a high enough flux of very cold neutrons on*

a suite of beamlines for different kinds of elastic- and inelastic-scattering instruments. The ability of tuning the scattering cross sections of spin-polarized targets is unique to neutrons and very important for research in condensed soft matter, particularly biological systems.

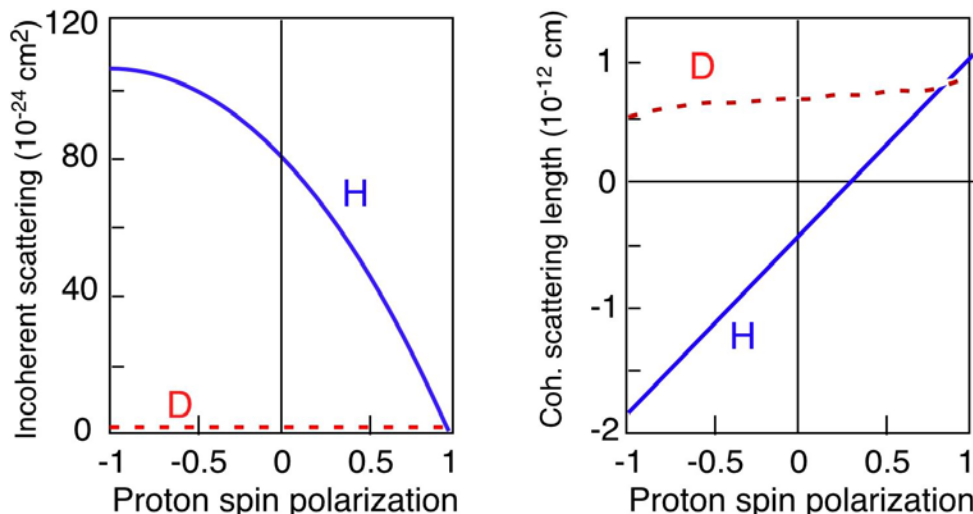


Fig. 5.3. The incoherent and coherent scattering of H and D as a function of the proton spin polarization of the atoms, after Stuhrmann [5].

#### Enhanced chemical contrast for very cold neutron energies

For very cold neutrons, i.e., with increasing wavelengths from 20 to 200 Å, the removal (e.g., scattering plus absorption) cross-section may vary by several orders of magnitude depending on the target nucleus or isotope. Such very large chemical contrast in scattering will be important for studying complex nanosystems where most interesting interactions occur at the interfaces among the nanoparticles or nanolaminates and the embedded environment. Catalysis, corrosion, fuel cells, clay and zeolite chemistry, biological pathways in microorganisms, nanoelectronic devices and sensors of various kinds are a few examples. Neutron scattering studies of complex phenomena at the interfaces of these nanosystems are difficult mainly because scattering from the interior of the particles or the substrate often overshadow the targeted signals from the interfaces. Additionally, functional low-dimensional devices often cannot be deposited on atomically flat substrates for neutron reflectivity measurements. Using very cold neutrons, the difference in the scattering cross sections among atoms (e.g., between H and Si) becomes larger, and the absorption between adsorbed molecules at the interfaces and the substrate (e.g., CD<sub>4</sub> versus Ni) differs significantly. Therefore, arguably, very cold neutrons offer the much-needed enhanced chemical contrast and surface-sensitivity for studying nanomaterials.

Grieger *et al.* [6] have measured the total cross-section of methane as a function of neutron energy and temperature as shown in Fig. 5.4. What is remarkable is that the cross-section at low energies (200 μeV or 20 Å) and low temperatures (300 mK) tends to 160 barns per proton. All proton spins are aligned and spin incoherence has been eliminated yet the famed cross-section of the proton not only remains but also rises by a factor 2! This cross-section is then purely coherent.

If this method can be generalized to other materials in a more or less routine manner then it would open up many new scientific opportunities, most notably in single-crystal diffraction of biological materials and both powder and single-crystal studies of hydrogen-containing organic chemicals without the need for deuteration. The increased scattering power per molecular unit (a factor of 32 in the case of methane) would allow either the lower limit for the size of single crystals which can be studied with neutrons to be reduced by a factor of 10 — perhaps to around  $0.1 \text{ mm}^3$  — or a significant reduction in the data acquisition time for a given data quality. This application is to be further explored at ILL (Carlile, Forsyth & Wills) but it should be emphasized that to be fully effective the neutron energy needs to be low to eliminate fully incoherent scattering and measurements must be made with a well-polarized beam. It would seem to be well suited to a VCNS source.

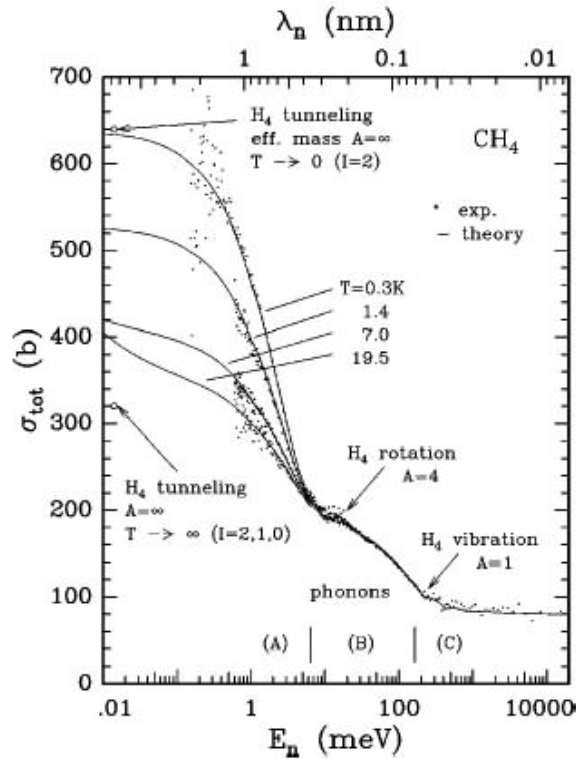


Fig. 5.4. The dependence of the total neutron scattering cross section of solid methane II as a function of incident neutron energy and temperature.

Roughly speaking, traditional neutron-scattering experiments are classified into small-angle scattering, high/wide-angle diffraction/spectroscopy, and grazing-angle reflection/scattering, etc., each of which adapts a certain favored sample geometry, for characterization of the normal-to-plane microstructure, structure/dynamics at interatomic distances, normal-to-plane layer/in-plane structure, respectively. Using very cold neutrons, the scattering angles are substantial even at a  $Q$  normally regarded as in the domain of small-angle scattering (e.g.,  $Q=0.088 \text{ \AA}^{-1}$  with  $100\text{-\AA}$  neutrons at  $90^\circ$  scattering). Therefore, very cold neutron scattering enables new possibilities of varying the magnitude and direction of the scattering vector relative to the intrinsic sample geometry (e.g., aligned filament direction, magnetic anisotropy, strain in polymeric or

inorganic composites, mutual orientation between nanoparticles, etc.). In conjunction with the strongly enhanced chemical contrast and focusability and polarizability of the intense beam, VCNS instruments are very useful to probe the structural and dynamic properties of functional nanomaterials.

Due to the very large change of scattering/absorbing power of very cold neutrons across a nanostructure, unlike the case for thermal and cold neutrons, the Born approximation, which ignores the rescattering (multiple scattering) of the neutron wave by the scatterer, can no longer be applicable. Instead, the Schrödinger equation for the entire neutron-scatterer system has to be treated properly. The formulation of a general theory of scattering relevant to very-cold and ultracold neutrons has been attempted recently [7].

### *5.1.6 Elastic Scattering*

#### Single crystals, large oriented structures and powders

Diffraction using very cold neutrons expands the realm of diffraction for structural characterization to larger  $d$ -spacings and correlation lengths of 10-100 nm. This is very important for a variety of systems: from protein crystals to biological membranes, from polymeric liquid crystals to filamentous viruses, and from vortex lattices in superconductors to nanoparticle assemblies. In addition to accessibility to large  $d$ -spacings, using very cold neutrons permits the detection of  $d$  values at higher angles – roughly an order-of-magnitude increase compared to thermal neutron diffraction. Thus, in principle, sophisticated optics and polarization devices as well as high-resolution detectors can be placed at larger angles to facilitate instrumentation design and better background control. For example, Makowski and coworkers have used neutron fiber diffraction combined with selectively deuterated amino acids to characterize the protein coat of a filamentous bacteriophage. These low-resolution ( $\sim 5$ -15 Å) analyses are currently difficult due to poor signal-to-noise and could possibly be improved using high-flux, long-wavelength neutrons at backscattering angles. Other important materials for study are amyloid fibrils associated with Alzheimer's disease and DNA complexes with proteins such as chromatin.

In the case of complex systems such as biological membranes and devices based on nanodots or nanotubes, single-crystal samples exhibiting a high degree of long-range order are difficult to achieve. Often only ordering of the basic building blocks or functional groups over a 1-10 nm length scale is preserved. Neutron diffraction measurements of the long  $d$ -spacing features, made possible by using very cold neutrons and particularly on H/D-contrasted or proton-polarized samples, provide the much-needed information. We surmise, for example, that the previous low-resolution ( $\sim 5$ -10 Å) structure of detergents in crystals of membrane proteins using variable H<sub>2</sub>O/D<sub>2</sub>O contrast matching performed by Timmins and coworkers [9] can be extended to a new level of detailed investigation.

#### Small-angle scattering and reflectometry

Limited flux of long-wavelength neutrons currently poses severe constraints on data collection in the smallest  $Q$  values for small-angle neutron scattering and in the large  $k_z$  region for reflectivity measurements. This in turn restricts the determination of size distribution and large structures such as the make-up of membranes with protein,

microtubules, actin, intermediate filaments, and DNA, and the resolution of multiplexing layer structures such as those in lipid bilayers and biosensors. The availability of high fluxes of very cold neutrons from the VCNS will help push the current  $Q_{\min}$  and  $k_{z\text{-max}}$  to values at least comparable to the state-of-art SANS instruments and reflectometers at the current sources including SNS. More importantly, the emerging technique of spin-echo small-angle scattering (SESANS), combining very cold neutrons with novel time-of-flight spin-precession analysis at low-angles, will likely extend the  $Q_{\min}$  to an unprecedented value of  $\sim 1 \times 10^{-5} \text{ \AA}^{-1}$ .

Another area of improvement in reflectometry is to leverage the increased critical angle for attaining better  $k_z$  resolution. In soft matter thin films, standing waves occur when incident waves interfere with waves reflected from the substrate. Multiple internal reflections lead to enhanced intensity at resonant wave vectors below the  $k_{zc}$  for total reflection. At these resonant wave vectors the enhanced neutron intensity incoherently scattered by, say, hydrogen, causes a marked decrease in the reflectivity. The positions of resonant dips provide an aid in fitting the reflectivity data by restricting the possible scattering length density profiles. This phenomenon may find application in the study of in-plane correlations by enhancing off-specular scattering.

### 5.1.7 Inelastic Scattering

The coverage of neutron spectroscopic investigations of various material systems across different disciplines is often illustrated in the so-called (Q-E) or (r-t) plots, where the neutron wavevector-energy transfer is related reciprocally to the length-time scale of dynamic correlation by Fourier transforms. Fig. 5.5 compares the domain of neutron spectroscopy with those of other techniques. We note that in spite of continuing progress over the last century achieved by the spectroscopy community, substantial gaps, particularly in the region of low energy and long time scale over 4 decades of distances, still exist today. This implies our experimental tools for investigation of slow (longer than  $10^{-8}$  s) dynamics over the 1-100 nm length scale, indispensably useful for studying biological systems and nanocomposites, are incomplete. *We believe that the VCNS can significantly improve this situation by extending the time-length scale to tens of microseconds and micrometer and thus enabling new and exciting science for the 21<sup>st</sup> century.*

Within the domain of neutron inelastic scattering, Fig. 5.5 shows the contributions from backscattering, chopper, and spin-echo spectrometers. The inverse-geometry instruments including the backscattering spectrometer usually rely on the use of crystal analyzers for final energy selection. They are not effective in using very cold neutrons in either employing energy-analyzing crystals or improving the energy resolution. However, both the spin-echo and direct-geometry multi-chopper spectrometers will benefit a great deal by using very cold neutrons. It can be shown that, in the case of the neutron spin-echo spectrometer, the resolution ( $\Delta E$  or  $\Delta Q$ ) and observed intensity depend on  $\lambda^{-3}$  and  $\lambda^{-4}$  to  $\lambda^{-2}$ , respectively, where  $\lambda$  is the neutron wavelength. Therefore, the  $\sim 1000$ -fold increase in fluxes of very cold neutrons from the VCNS will permit highly efficient operation while improving the energy resolution. More importantly, the spin-echo technique uses exclusively polarized neutrons and novel spin precession devices. The fact that very cold neutrons are employed makes the spin-echo operation more efficient.

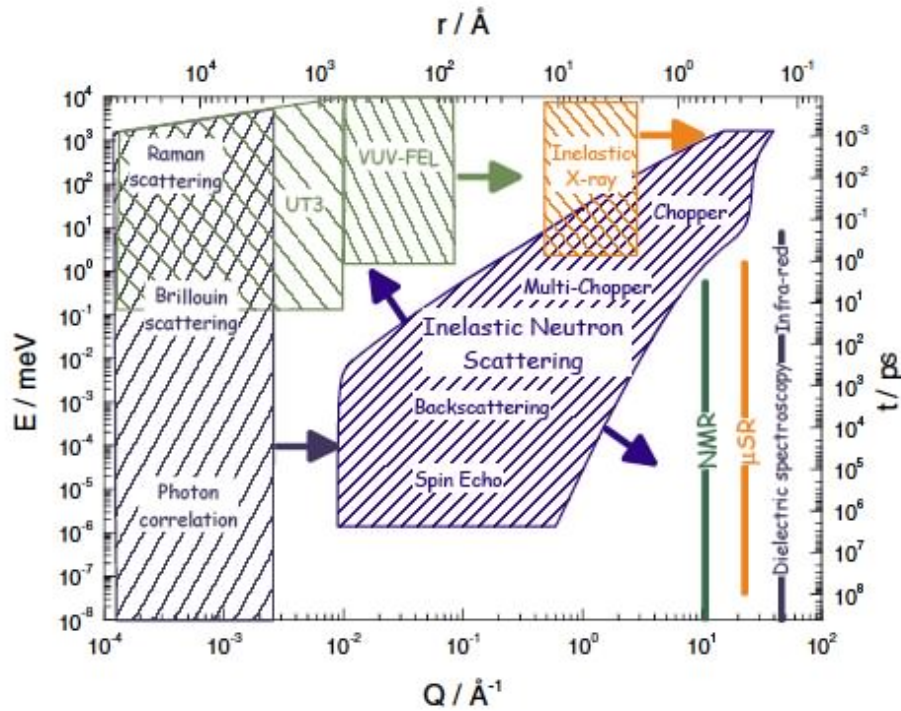


Fig. 5.5 The domains over the (Q-E) or (r-t) space of neutron and other spectroscopic techniques, after Boue *et al.* [10].

Perhaps the most exciting and welcoming advancement from using very cold neutrons is the multi-chopper spectrometer because the resolution and the intensity improve according to  $\lambda^{-3}$  and  $\lambda^2$  (smaller  $\Delta E$  corresponds to higher resolution). Furthermore, a multi-chopper system commands the versatility in optimization of the time-of-flight data collection (e.g., by repetition rate multiplication) and in tailoring the pulse shape of the neutrons for resolution consideration.

Finally, although the mainstream of very cold neutron spectroscopy is to study relaxation or diffusion processes of sub-ns or longer time scale and to resolve fine energy structures in tunneling and magnetic excitations, i.e., quasielastic scattering and inelastic scattering in the sub-meV region, one should not neglect the option of upscattering thereby accessing a much wider dynamic range (up to tens of meV). Normally, inelastic scattering in this energy range is better carried out by downscattering of thermal neutrons. However, since focusing thermal neutrons is formidably difficult, the intensity loss resulting from using a sub-mm-size beam on very small samples under extreme environments (see Section 5.1.4) will probably prohibit any inelastic-scattering measurement in the foreseeable future even for the most powerful sources like SNS. Therefore, upscattering from very cold neutrons on a VCNS chopper spectrometer will allow the realistic practice of inelastic scattering on samples under extreme pressure, temperature, and magnetic-field conditions. It should be possible to measure the low energy density-of-states from which, in conjunction with modeling, information concerning the Gruneisen parameters, specific heat, and other useful thermodynamic properties can be extracted. It will also be possible to analyze the quasielastic spectra to relate diffusion processes to viscosity and mass transport behavior.

## 5.2. Special scientific topics

### 5.2.1 Material Physics Under Extreme Environments

The ability to focus very cold neutrons means that it is possible to use high-pressure cells. If we are able to focus to a spot size of a fraction of a mm (say 100  $\mu\text{m}$ ) then it will be possible to use diamond anvil cells which reach pressures up to 100 GPa (see Sec. 5.1.4). Work on dynamics is potentially more interesting, and can be done in neutron energy gain. (See Sec. 5.1.7.)

#### Silicate melts and glasses at high pressure and high temperature

Silicate magmas are a well-known manifestation of volcanic activity. Today, it is likely that most magmatism is a relatively shallow phenomenon, occurring at depths up to  $\sim 100$  km below mid-ocean ridge-spreading centers and at subduction zones. Understanding the melt density and rheology requires determining the structure and compression mechanisms by *in-situ* studies at pressures up to  $\sim 30$  GPa and  $T \sim 1500^\circ\text{C}$ . These are conditions that are achievable with existing high-pressure cells adapted for neutron scattering. The geological magmas are also similar to commercial glass composition, so it is of scientific and commercial interest to compare and contrast the structural nature and compression mechanisms within glasses and liquids, compressed to pressures within this range. In particular, it is important to study the role of coordination changes in glass-forming ions ( $\text{Al}^{3+}$ ,  $\text{Si}^{4+}$ ,  $\text{Ge}^{4+}$ ) in determining both the melt and glass density, and the viscous relaxation. This is best achieved by a combination of neutron and X-ray structure determination, combined with spectroscopic methods such as Raman and NMR and inelastic neutron scattering.

In future studies the pressure range should be extended to at least  $P \sim 100$  GPa. High-pressure properties of silicate melts likely played a fundamental role in shaping the physical and chemical evolution of the planet. Magma ascent and emplacement, as well as crystal nucleation, growth, and segregation, are controlled by pressure-dependent melt densities and transport phenomena. Magmatic buoyancy forces are determined by the density contrast between melts and crystalline minerals. In the pressure range of the Earth's mantle, silicate melts display higher compressibilities than their crystalline counterparts, as a result of the diversity in compression mechanisms. As a consequence of this, magma buoyancy forces generally decrease with increasing pressure and can even invert. It has been postulated that gravitationally stable magma oceans could have existed at depth at some stage in its history, profoundly influencing its thermal and chemical evolution.

#### Structural physics at high pressures

Fundamental ices like  $\text{H}_2\text{O}$ ,  $\text{NH}_3$ ,  $\text{CH}_4$  are important model systems for understanding H bonding and molecular dissociation. There has been a large amount of high-profile work on dissociation in these systems, and particularly the development of symmetric bonds at pressures sufficiently high to force the proton to the centre of the inter-molecular bonds. This has been demonstrated in ice itself (Goncharov et al. Science 1996) and hydrogen halides (Katoh et al. Phys Rev B 2000), where it is accompanied by complex excitation physics. The very high P and T behavior of simple ices is also important for the modeling of the outer planets and their satellites. For example, Cavazzoni et al. (Science

1999) have predicted that the protons in  $\text{NH}_3$  will dissociate above about 1500 K and 60 GPa to create a superionic solid state. A key problem in relation to centering in ice is the detailed nature of the ice VII phase, which centers to ice X above about 70 GPa. Evidence at lower pressures suggests the centering may be made complex by site disordering of the oxygen atoms, and there is also some evidence for incommensurate modulation of the structure. The complex, orientationally-ordered structures of methane above 5 GPa are still unknown, and it is an intriguing question as to what the ultimate, very high density methane structure will be. And the full H-bonding structures of  $\text{NH}_3$ ,  $\text{H}_2\text{S}$  and the hydrogen halides – where strong H-bonding can be induced under pressure – need to be determined above 10 GPa, and followed up into the range of centering and dissociation.

Diatomic molecules are important model molecular systems, with a range of fascinating behavior. Oxygen is the only insulating magnetic element. There is much interest in its  $\epsilon$  phase in the 10-25 GPa range, and how this evolves to higher pressures, and there are intriguing proposals for dimer or chain structures (Gorelli et al. Phys Rev Lett 1999; Neaton and Ashcroft, Phys Rev Lett 2002). There is also much yet to determine about the magnetic behavior and structure in the range from intermediate up to very high pressures. Recent work has identified a new  $\eta$  phase, adjacent to the melting line between 10 and 20 GPa, which appears to have an orientationally disordered structure (Santoro et al. Phys Rev Lett 2004). Nitrogen is as rich. Several complex phases have yet to be characterized structurally, and some fascinating recent work has found a polymeric form at very high pressures, above 100 GPa (Eremets et al. Nature Materials 2004). Perhaps most interest of all attaches to hydrogen where there is a wealth of exotic physics but almost nothing is yet known in detail about the structure. A recent breakthrough has been a successful diffraction study of the broken symmetry phase above 25 GPa (Goncharenko and Loubeyre, Nature 2005), but only to low resolution. Full structural studies are now needed.

### High Field Magnetism

The same arguments used for high pressure also apply to other extreme environments. The ability to focus the beam makes it possible to push the limits on high field research. The current state of the art is 17 T – but the use of small bore pulsed field magnets could push this beyond 45 T with pulse rates on the order of 1 Hz. Again 20 Å neutrons are not ideal for structural studies, even of magnetic systems. However, the emergent behavior that is seen in strongly correlated systems, i.e., spin stripes, frustration, etc., can have structures on these length scales. Inelastic experiments are more interesting. Indeed the energy scale associated with a high magnetic field is commensurate with these low energies.

### *5.2.2 Magnetism*

#### Molecular Magnets

Molecular magnetism is a new and exciting area of condensed matter research. The interest in molecular magnets stems from, among other things, their uses developing and exploring concepts of quantum magnetism in the simpler environment of zero-dimensions and with a small number of interacting spins compared to higher dimensional

objects with infinite interacting spins normally investigated in condensed matter physics. Despite their apparent simplicity, the Hilbert space of these systems is in many cases still too large for exact solutions of the energy levels, hence approximations are required to develop theories, moreover, these theories can be readily tested using neutron scattering experiments.

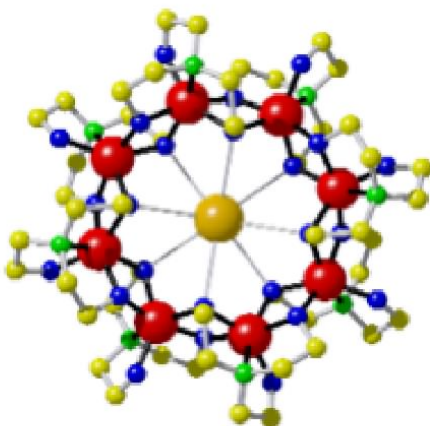


Fig. 5.6 The iron-ring structure of a  $[\text{CsFe}_8\{\text{N}(\text{CH}_2\text{CH}_2\text{O})_3\}_8]^+$  molecular magnet.

Molecular magnets are magnetic objects on the nanoscale that consist of highly symmetric clusters of magnetic ions that interact with each other. Current nanomagnets contain between 2 and 30 transition metal magnetic ions and come in a variety of shapes. The original molecular magnets were the ferric wheels where the iron ions formed rings and interacted magnetically with nearest neighbors. These were synthesized in the 1990s. The eight-iron wheel  $[\text{CsFe}_8\{\text{N}(\text{CH}_2\text{CH}_2\text{O})_3\}_8]^+$  or  $\{\text{CsFe}_8\}$  is shown in Fig. 5.6. More complex wheel-type structures are now available such as the hexadecameric and tetradecameric clusters or the cubane-type  $[\text{Cr}_8\text{O}_4(\text{C}_6\text{H}_5\text{COO})_{16}]_4\text{-CH}_3\text{CN}=\{\text{Cr}_8\}$  where the 8  $\text{Cr}^{3+}$  ions can be mapped onto the vertices of a cube and interact with each other via two ferromagnetic and two antiferromagnetic exchange constants creating a highly frustrated and entangled system. Other more complex shapes are continually being developed.

Not all energy levels are available to neutron scattering; transitions must involve a change in angular momentum of the system of one unit. However, the ground state of the system can be varied by tuning the magnetic field - a technique that allows many more energy levels to be measured. The saturation field for molecular magnets (the field where all the moments point in the same direction) can be as high as 100 T (e.g. for  $\{\text{Cr}_8\}$   $B_{\text{sat}} = 27$  T and for  $\{\text{V}_6\}$   $B_{\text{sat}} \sim 100$  T), but even with fields of 25 T there are many systems to be explored. Along with high magnetic fields, there is a need for low temperatures so that the magnet can be measured in its ground state, which given that these levels are typically of the order of a few tens of  $\mu\text{eV}$ , requires temperatures in the mK region. Therefore a combination of mK temperatures and high magnetic fields

would allow a complete measurement of a range of molecular magnets providing the opportunity for new physical ideas to be explored experimentally (See Sec. 5.1.4.)

### Magnetic nanocrystals

Chemically synthesized nanocrystals have great potential for magnetic storage and permanent magnet applications. The ideal particles should have well-defined saturation magnetization and coercivity. One way to control this down to a single-particle level is to engineer a core-shell structure of magnetically soft and hard components. Because of the strong exchange-coupling between the two components, magnetic moments in both the core and shell are coupled, and at the interface the spins are expected to align parallel to each other in order to relieve interfacial spin frustration. These types of spin magnets possess a wide and tall hysteresis loop so that the stored energy is high, yielding ultra-strong magnetic composite materials. Polarized-neutron small-angle scattering can help identify the spin structure of each of the components and their mutual interactions. Very cold neutrons are useful for the reasons stated in Sec. 5.1.6.

### Magnetic fluctuations and excitations

Many systems and topics of high scientific and technological interest exhibit dynamics in the energy range that requires high-resolution inelastic scattering using very cold neutrons, (see Sec. 5.1.7). Examples include frustrated systems, which often exhibit unusual low temperature ground states with macroscopic degeneracy and slow, glassy like dynamics, e.g., geometrically frustrated magnet  $\text{Dy}_2\text{Ti}_2\text{O}_7$ . Other examples include quantum critical behavior and generally, complex materials in which disorder and the associated nanoscale self-organization determines physical properties, where disorder may be induced by competing interactions or incompatibility of local and global symmetry constraints. Many other systems with varying types of disorder such as rotational disorder in molecular solids and intercalation compounds, adsorption in microporous frameworks, and quasicrystals are also candidates for inelastic scattering studies.

### *5.2.3 Superconductivity*

Neutron scattering continues to make vital contributions to our understanding of high-temperature superconductivity. Studies in applied magnetic fields of the interplay between magnetism and superconductivity have been particularly revealing. One experiment that is crucial to our understanding of high- $T_c$  materials is the complete suppression of superconductivity by an applied magnetic field. This would be unique in revealing directly the nature of the electron liquid from which the superconducting state emerges. However, upper critical fields required to suppress superconductivity in hole-doped high- $T_c$  materials are greater than 25 T. As a consequence, an investigation of the magnetism in the high field phase has not so far been possible. To date, neutron scattering experiments can be done with fields of up to 15 T, and already these have revealed interesting phenomena in high- $T_c$  materials. Another research area in high- $T_c$  superconductors that has not so far been explored using neutron scattering is the effects of hydrostatic pressure. Pressure has been shown to substantially increase the superconducting transition temperature of cuprate superconductors raising it, for example, from 135 K to 164 K at 23 GPa in  $\text{HgBa}_2\text{Ca}_2\text{Cu}_3\text{O}_{8+\delta}$ . A pressure of 80 GPa, would not only allow exploration of the high pressure effects that have currently been

investigated by other techniques, but also would make available pressures much greater than are currently used in condensed matter opening up whole new areas of the high- $T_c$  phase diagram.

#### *5.2.4 Quantum Systems*

##### Model Quantum Magnets and Bose-Einstein Condensation

Model quantum magnets provide a laboratory in which to develop and test fundamental theories of the physics of quantum phase transitions. One recent example is the study of the Ising ferromagnet, widely regarded because of its simplicity to be the “fruit fly” of this field. Instead of the expected behavior of completely softening to zero at the quantum critical point, the magnetic excitation spectrum retained a finite frequency due to the hyperfine coupling with the nuclei. This dramatically revealed the sensitivity of quantum critical systems to coupling to secondary degrees of freedom, which, in limiting the maximum coherence length that can be achieved, was also shown to have implications for any solid-state realizations of a quantum computer. Another important recent example is the remarkable observation of Bose-Einstein condensation in a magnetic system. These examples serve to illustrate not only the wider implications of the study of quantum phase transitions in model magnets, but also how progress in this field is limited by the availability of both appropriate neutron instrumentation and sample environment.

##### First-order phase transitions

First-order phase transitions taking place in various helium systems down to absolute zero can be very interesting objects to study macroscopic quantum nucleation. At zero temperature the formation of nuclei of a new stable phase cannot occur via a thermal activation mechanism, and the phase transition should be described by a quantum effect related to a complicated tunneling motion through a potential barrier separating the initial metastable state from the final stable one. High-resolution inelastic scattering using very cold neutrons is essential to resolve the tunneling energy structure (see Sec. 5.1.7).

##### Resonant interaction of two-level systems

There is still a specific interest in the problem of two-level-systems (TLS) inherent in amorphous materials. The standard model of isolated TLS relaxing via phonons is not valid at very low temperatures. A special feature of these materials is the dipole-dipole interaction between TLSs. The concept of resonant interacting pairs of TLSs as a new kind of elementary excitation has recently been proposed [11]. This model can be a key to understanding unusual relaxation properties of glasses.

High-resolution high-intensity neutron spectroscopy at low energies can be very helpful for understanding this phenomenon, (see Sec. 5.1.7).

## 5.3 Special applied topics

### 5.3.1. Energy science

#### Hydrogen production through nanoscale-enhanced photocleavage of water

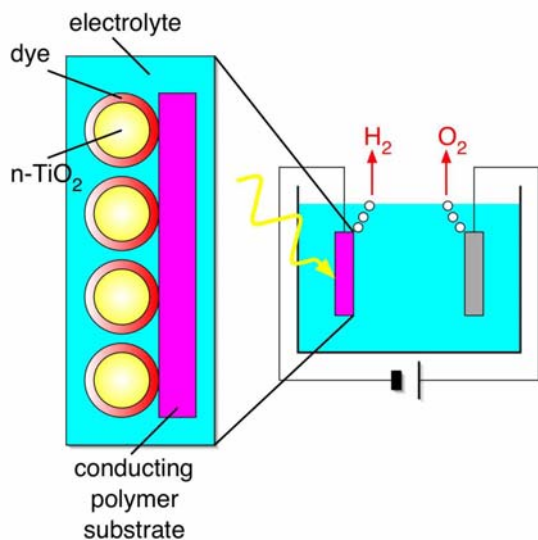


Fig. 5.7. A PEC producing hydrogen by photocleavage of water.

A photoelectrochemical cell (PEC), as shown schematically in Fig. 5.7, based on renewable and inexhaustible sources, provides an energy efficient, environmentally benign process that will meet DOE's goals for the hydrogen economy. A key component of the PEC will be semiconducting nanoparticles coated with light-absorbing dyes to enhance the production of electron-hole pairs that will electrolyze water molecules. As explained in Sec. 5.1.5 and 5.1.7, *in-situ*, concurrent quasielastic-scattering, small-to-wide angle diffraction and hydrogen-induced neutron prompt gamma-ray measurements using the VCNS are highly desirable for the characterization and optimization of absorption of the solar spectrum and to tune the band-gap for efficient electron-hole pair production. Quantum-mechanical calculations coupled with molecular-dynamics simulations employing reliable interatomic potentials will guide the design and optimization of the PEC.

#### Harvesting hydrogen from purple membrane: a light-driven protein-based proton pump

Purple membrane (PM) from *Halobacterium halobium* contains bacteriorhodopsin (bR), which functions as a light-driven proton pump. bR is a transmembrane protein consisting of 7  $\alpha$ -helices which span the lipid bilayer, (see Fig. 5.8). The chromophoric group of bR consists of the retinylidene. This inner group of amino acids catalyzes the all-trans / 13-cis-retinal isomerization at room temperature. Proton transport starts with the release of a proton from the extra-cellular side and ends with a proton uptake from the cytoplasmic side. A light-driven bio-based hydrogen generator is perceived if the protons are collected and allowed to recombine to form hydrogen gas through electron gain from the surrounding medium (mainly water). Since the proton migration and H<sub>2</sub>-formation processes are poorly understood, control of the proton transport so that specific steps of the photocycle can be switched off or altered for hydrogen there remain many challenges. This includes overexpression of the bR gene to produce gram quantities of bR,

molecular-level trapping by increasing Asp/Glu residues to enhance protonation-deprotonation, and entrapment of  $H^+$  ions for conversion to  $H_2$  gas. VCNS small-angle scattering and inelastic scattering instruments will be highly effective for investigating the structure and dynamics of bR in the purple membrane, (see Secs. 5.1.5 and 5.1.7).

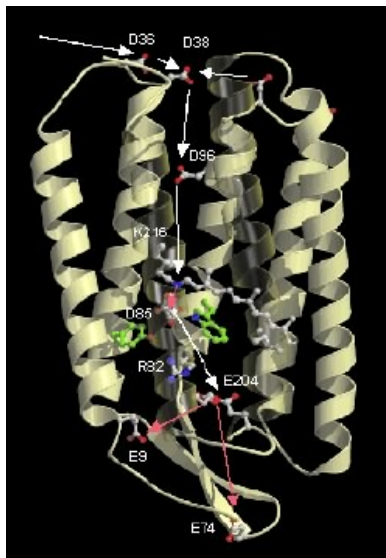


Fig. 5.8. Bacteriorhodopsin (bR), showing the 7  $\alpha$ -helices and the central proton pathway.

Purple membrane exists naturally and abundantly in the ocean so supply is virtually unlimited and cost is low. It is remarkably robust and durable and remains functional up to  $120^{\circ}C$  and under extreme pH conditions. It is capable of pumping  $\sim 100$  protons / sec / molecule using sun light, therefore, an ideal energy source for a hydrogen economy.

#### Utilization of methane from gas clathrate as an energy source

It has been estimated that most of the world's methane is stored as methane hydrate clathrate on the ocean floors and under the ice caps [12]. It is of major interest to develop methods to harvest the methane and possibly at the same time sequester carbon dioxide in the form of a gas hydrate. *In-situ* high-resolution quasielastic scattering of gas clathrate under applied pressure will elucidate the stability of the clathrates and the diffusion dynamics of the methane molecules.

#### *5.3.2 Health and Biological Science*

Studies of the structure and stability of vesicles, liposomes and colloidosomes, emulsion droplets, and foams are important areas of research in food, cosmetics, petroleum industry, and in the design of better drug delivery systems.

Gene therapy has the potential to treat many different diseases, even those previously thought impossible to cure. Investigations into new methods of delivering genes to the body are aiding in the search for cures to inherited diseases and AIDS. The goal of gene therapy is to optimize the delivery of foreign DNA into the nucleus of the cell. Gene therapy is a method of correcting genetic defects via transfection, replacing missing or

defective genes with a healthy, foreign piece of DNA in the nucleus. There are two general methods of transfection: physical and carrier. The physical method involves placing the foreign DNA into cells with a small needle. The method is useful in experimental research, but not very practical for clinical purposes since it requires cells to be treated individually. We could use virus as the carrier, but this method has several drawbacks. Currently, the use of synthetic carriers like liposomes and polymers are starting to be explored as foreign DNA carriers. SANS can be used to study structures of liposome-gene and polymer-gene systems. When they are dissolved in water, neutron reflectivity can be used to look at what happens to these systems as they approach surfaces of artificial cell membranes.

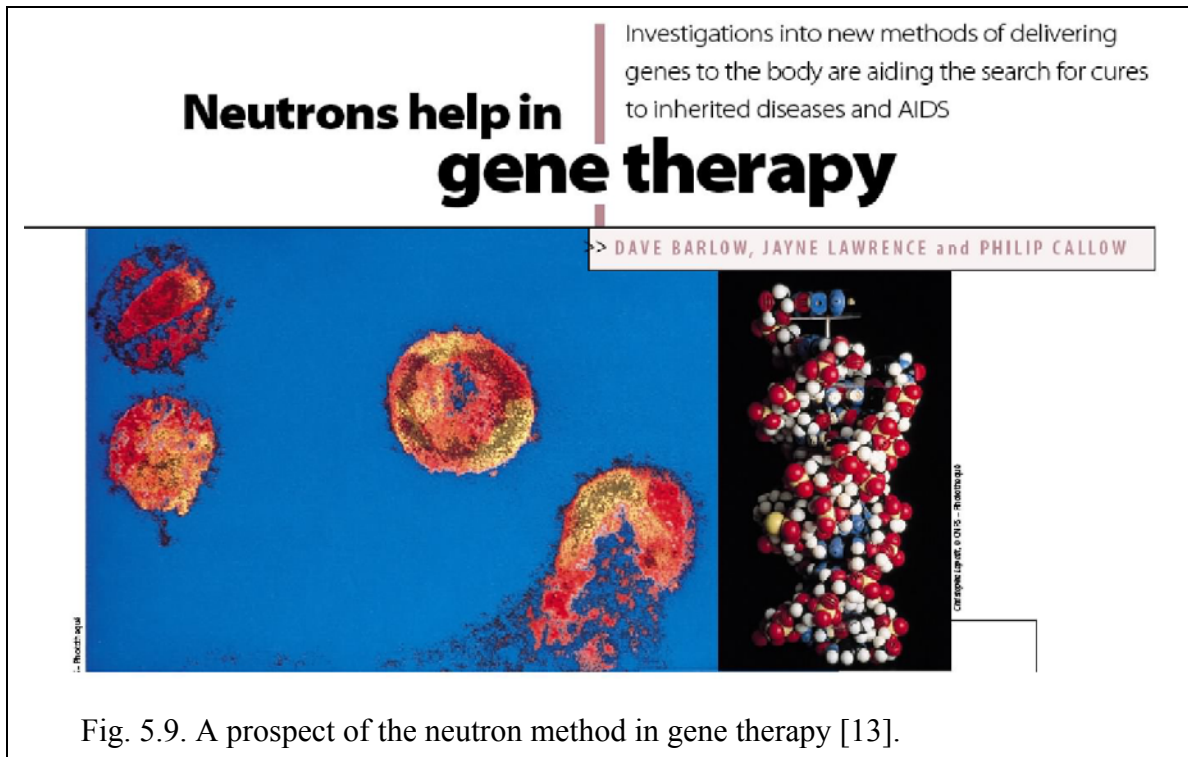


Fig. 5.9. A prospect of the neutron method in gene therapy [13].

### 5.3.3 Environment

#### Enriching of soils

The interactions of clays with organic polymers have attracted the interest of soil scientists for a long time. This is prompted by the biostability of “humus” which for the most part is a mixture of polyanions, referred to as humic substances. The clay-humus interaction in soil plays an important role in many soil processes, such as mineral cycling, weathering, and profile development and aggregate stabilization. Studies of adsorption of polymers and bio-macromolecules on clays by contrast variation techniques using SANS can help understand the mechanism of how polymers attach to clays. The improved contrast and lower  $Q_{\min}$  in future VCNS instruments will be useful for such studies.

### Fundamental studies of nanoparticle formation in air pollution

Soot and smoke are major air pollutants emitted from combustion engines or fires. SANS has been used successfully by B. Wyslouzil's group at NIST to understand the underlying mechanism of soot formation, leading to the development of useful models for engine design and optimization. They try to understand how combustion flame conditions in laboratory flames affect the properties of soot in the flame and validate fundamental models of soot formation. The same group has also investigated nanodroplet aerosols, another air pollutant, using SANS patterns to study their size distribution and structure. Extending the  $Q_{\min}$  to lower values in future VCNS instruments will be useful for such studies.

### Corrosion science

Corrosion costs hundreds of billions of dollars per year in the US economy. At the outset, corrosion occurs at the nanometer scale – the buildup of “foreign” molecules at the interface in an otherwise “pure” environment. The foreign molecules diffuse and the corresponding evolving entity “grows and spreads”, eventually to form a colony that leads to macroscopic corrosion. We need first a fundamental understanding of such initial reaction, i.e., the elemental make-up, atomic/molecular diffusion/migration, localized redox reaction, etc. Only after we understand these critical initial steps can industries begin to research the detection of the colonies and preemptive actions to prevent corrosion. The culprit of the pre-corrosive entities usually contains hydrogen (e.g., water molecules, bacteria), oxygen, carbon and nitrogen (e.g., redox) that exhibit strong neutron scattering cross sections. As explained in Sec. 5.1.5, very cold neutrons are sensitive to the interfaces of the nanoparticles (e.g., grain boundaries and gas-solid and liquid-solid surfaces). Low-Q scattering using very cold neutrons will shed light on the structural organization, and quasielastic and inelastic scattering can determine the nature of diffusion dynamics of the pre-corrosive entities over the 1-100 nm and  $10^{-6}$ - $10^{-13}$  sec time-length scale.

### Cultural heritage and pollution control

The scientific opportunities in the realm of cultural heritage are largely unexplored, but relate to the potential to utilize the uniquely high flux of very cold neutrons to non-destructively expose antiquities for the purpose of age characterization, etc.

Diffraction studies of gases may in fact be feasible with this source. If so, there could be a number of applications in studies related to pollution.

#### *5.3.4 Nanostructure and Atomic/Molecular Dynamics of Novel Materials*

### Functional materials

Many of the materials that are currently of great interest are those with potentially useful properties such as thermoelectric materials or materials with negative thermal expansion, ionic conductors, polymer electrolytes, catalysts, and superconductors or materials with potentially interesting nano-scale structure such as carbon nanotubes. These are all complex materials whose function depends on vibration or atomic motion in the 0-20 meV range.

The development of computational methods that can calculate the excitations in these complex materials is driving the need for detailed measurements of the excitations in these materials. With a large number of atoms per unit cell these materials have complex and overlapping dispersion surfaces that are only weakly scattering. To be able to map these requires an instrument that combines high neutron intensity in the correct energy range, and excellent momentum and energy resolution.

#### Thermo-electric materials

The skutterudites and clathrate structured thermoelectric materials rely on a strong local vibration to scatter the sound modes in the materials to turn them into thermal glasses, whilst leaving the electrical conductivity unaffected. Most of these new classes of thermo-electric materials have open structures that can be filled with heavy atoms, usually rare earths [14].

#### Nano-structured materials

Complex nano-structured materials such as the polymorphs of carbon often have low energy vibrations associated with nanoscale structure. For example, in nanotubes the inter-tube vibrations depend critically on the larger scale structure of the material and intra-tube vibrations are dependent on the diameter and chirality of the tubes. These materials are often available only in small quantities so that the ability to spatially focus the beam becomes crucial.

#### Fast ion conductors and hydrogen storage

The diffusive motion of hydrogen in materials is central to a large range of important technologies, such as fuel cells, batteries, and hydrogen storage materials. These technologies are set to gain critical importance over the next number of years as concerns over global warming grow and fossil fuel stocks decline. Quasielastic, and inelastic-scattering data in conjunction with molecular dynamics and *ab-initio* calculations are key techniques for understanding the location and diffusion motion of hydrogen in these materials. Much of the current work in this field is focused on improving the stability of these materials under normal operating conditions. The ability to do parametric studies and studies under realistic conditions will be crucial in understanding the mechanisms of breakdown in these materials. Instruments at VCNS will facilitate these studies.

#### Catalysts and nano-porous materials

The chemical changes that occur at interfaces during heterogeneous catalysis using zeolites (for example) are both technologically relevant and a challenge to experimental and theoretical techniques. The vibrational spectroscopy of adsorbates is mostly confined to the lower frequency intra-molecular and external modes of the adsorbate; it is in this region that the surface-adsorbate complex has its modes. Neutron scattering provides direct information about the strength and nature of these interactions; the amplitude weighting of the neutron intensities makes the interpretation of the results and the comparison to calculation straightforward.

Very cold neutrons are well matched to the length and time scale of the diffusive and rotational motions of the adsorbates in catalysts such as the zeolites.

### 5.3.5 Homeland Security

A VCNS may enable the following:

- Design of nanodevices for technological applications
- Direct investigation of structure and shape
- Imaging of spin densities, magnetic domains
- Investigation and characterization of viruses, then allowing development of antidotes
- Development of new materials with improved properties, e.g., bullet-proof vests based on spiderweb technology
- Improved energy efficiency for homeland security purposes

### References

- [1] See, for example, A. I. Frank, *Sov. Phys. Usp.* **30** (1987) 110.
- [2] G. Faigel and M. Tegze, *Rep. Prog. Phys.* **62** (1999) 355.
- [3] L. Cser *et al.*, *Appl. Phys. Lett.* **85** (2004) 1149.
- [4] L. Cser *et al.* *Phys. Rev. Lett.* **89** (2002) 175504.
- [5] H. B. Stuhrmann, in *Structure and Dynamics of Biomolecules* (Ed. E. Fanchon *et al.*, Oxford U. Press, New York, 2000) p. 391.
- [6] H. B. Stuhrmann, in *Structure and Dynamics of Biomolecules* (Ed. E. Fanchon *et al.*, Oxford U. Press, New York, 2000) p. 391.
- [7] A. L. Barabanov and S. T. Belyaev, *Eur. Phys. J. B* **15** (2000) 59.
- [8] W. Stark *et al.*, *J. Molecular Biology* **199**, (1988) 171.
- [9] E. Pebay-Peyroula *et al.*, *Structure* **3**, (1995) 1051.
- [10] F. Boue *et al.* in *The ESS Project, V. II.* (The European Spallation Source Project, 2002) p. 5-1.
- [11] A.L. Burin, *et al.*, *JETP Letters*, **80** (2004) 513.
- [12] C.A. Koh, *Chem. Soc. Rev.* **31** (2002) 157.
- [13] From The ILL Report on Neutrons and Life 2001.
- [14] B. C. Sales *et al.*, *Phys. Rev. B* **61**, (2000) 2475.

## 6. CONCLUSIONS

Attendees at the Workshop on Applications of a Very Cold Neutron Source took part in the program with enthusiasm, and the discussions following the presentations produced significant conclusions regarding work to follow.

### Sources

The discussion group dealing with Source questions confirmed the close relationship between the technology proposed for the VCNS and that of UCN sources, especially spallation driven ones. Collaborations in the shared aspects of the parallel developments will form and surely be fruitful. All UCN and VCN developments suffer severely from the lack of knowledge of the scattering properties of candidate moderators at relevant temperatures and in suitable form for computer simulations, performance evaluations, and optimizations. Joint efforts have already sprung up among participants in the Source discussion group; these activities will require several years and more than a few person-years of effort.

A comparison emerged of the provisionally estimated VCN source intensity with what is today's best, the ILL L-D<sub>2</sub> cold source, which shows a peak flux of VCNs on the order of  $10^3$  times and a time-average flux on the order of 30 times that of the ILL source. This is in part a result of discussions in the Instrumentation group to the effect that the appropriate pulsing frequency should be 5 Hz rather than the initially assumed 1 Hz, a suggestion that we immediately adopted for VCNS.

### Instrumentation

The Instrumentation discussion group provided a number of guidelines for future work on VCN scattering instrumentation, although they could describe only a few specific instruments. They tabulated, however, the wavelength dependence of numerous categories of optical devices, namely beam focusing devices and guides, which are strongly favorable for VCNs compared to the shorter-wavelength cold and thermal neutrons familiar in current practice. Spin-echo and spin modulation methods came to the fore as the basis for use in the long-pulse mode. There is a clear and widely felt need for innovation of instruments capitalizing on VCN optics and in adaptation of methods to long-pulse sources. Although very bright people have proposed a lot of brilliant ideas, there is as yet very little practical experience in this area. The process of instrument innovation must go forward in parallel with source optimization and in close coordination with the needs dictated by scientific applications.

### Science

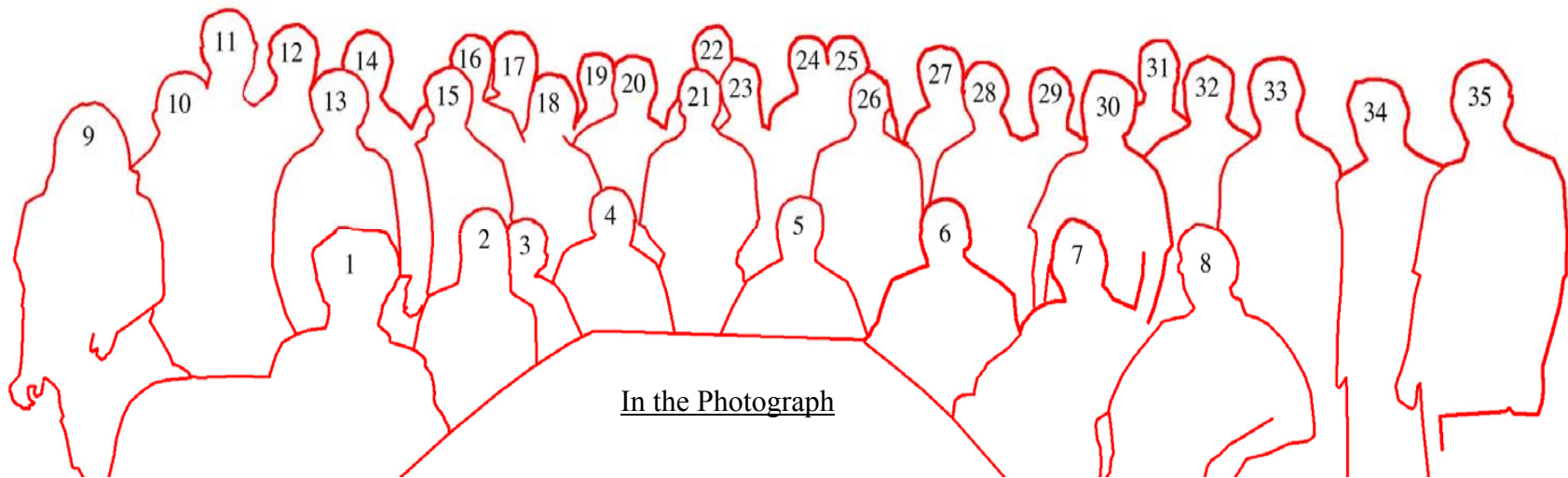
The Science discussion group produced an impressive array of possibilities for performing entirely new types of research, based on opportunities that VCNS provides for studies of large-scale structures and hierarchical structures exhibiting large ranges of scales of ordering, in high-resolution studies of slow motions, in magnetism, and in

fundamental neutron physics. The science case provides a motivating basis, which must guide the development of instrument concepts in close coordination. The case itself needs critical refinement and expansion as scientists recognize further opportunities.

This first Workshop confirmed the exciting scientific potential for a VCN source, refined the needs for ongoing work, spawned a number of development collaborations, and strongly suggests the need for follow-on workshops to extend the knowledge of the prospects for a VCNS. The most important near term work required is to obtain scattering functions for very cold moderator materials and to implement them in source evaluation calculations.

## Group Photo





1. Roland Gähler  
 2. Nicole Green  
 3. Michael Agamalian  
 4. John M. Carpenter  
 5. Yoshihisa Iwashita  
 6. Jim Rhyne  
 7. Colin Carlile  
 8. David Price  
 9. Jyotsana Lal  
 10. Peter Geltenbort  
 11. Markus Bleuel  
 12. Bradley Micklich  
 13. Yasuhiro Masuda  
 14. Manfred Daum  
 15. Géza Zsigmond  
 16. James Richardson  
 17. Erik Iverson  
 18. Chen-Yu Liu  
 19. Alexander Kolesnikov

20. Ferei Mezei  
 21. Steve Bennington  
 22. Stefan Rosenkranz  
 23. Gian Felcher  
 24. Ken Littrell  
 25. Roger Pynn  
 26. Chris Benmore  
 27. Paul Sokol  
 28. Arthur Schultz  
 29. Kent Crawford  
 30. Hirohiko Shimizu  
 31. Gene Ice  
 32. Paul Brod  
 33. David Mildner  
 34. Masatoshi Arai  
 35. Charles Majkrzak

Agamalian, Michael 3  
 Arai, Masatoshi 34  
 Benmore, Chris 26  
 Bennington, Steve 21  
 Bleuel, Markus 11  
 Brod, Paul 32  
 Carpenter, John M. 4  
 Carlile, Colin 7  
 Crawford, Kent 29  
 Daum, Manfred 14  
 Felcher, Gian 23  
 Gähler, Roland 1  
 Geltenbort, Peter 10  
 Green, Nicole 2  
 Ice, Gene 31  
 Iverson, Erik 17  
 Iwashita, Yoshihisa 5  
 Kolesnikov, Alexander 19  
 Lal, Jyotsana 9

Littrell, Ken 24  
 Liu, Chen-Yu 18  
 Majkrzak, Charles 35  
 Masuda, Yasuhiro 13  
 Mezei, Ferei 20  
 Micklich, Bradley 12  
 Mildner, David 33  
 Price, David 8  
 Pynn, Roger 25  
 Rhyne, Jim 6  
 Richardson, James 16  
 Rosenkranz, Stefan 22  
 Schultz, Arthur 28  
 Shimizu, Hirohiko 30  
 Sokol, Paul 27  
 Zsigmond, Géza 15

**Very Cold Neutron Source Workshop**  
ANL-IPNS / August 21-24, 2005

**Participant List**

M. Agamalian, ORNL	C-Y Liu, IU
M. Arai, KEK	C-K Loong, ANL-IPNS
C. Benmore, ANL-IPNS	C. Majkrzak, NIST
S. Bennington, ISIS	L. Makowski, ANL-BIO
P. Brod, ANL-IPNS	Y. Masuda, KEK
C. Carlile, ILL-ISIS	F. Mezei, HMI
J. Carpenter, ANL-IPNS	B. Micklich, ANL-IPNS
K. Crawford, ORNL	D. Mildner, NIST
M. Daum, PSI	R. Osborn, ANL-MSD
G. Felcher, ANL-MSD	D. Price, HFIR
R. Gähler, ILL	R. Pynn, LANL
P. Geltenbort, ILL	S. Rosenkranz, ANL-MSD
G. Ice, ORNL	J. Rhyne, LANL-LANSCE
E. Iverson, ORNL	A. Schultz, ANL-IPNS
Y. Iwashita, ICR	H. Shimizu, RIKEN
J. Jorgensen, ANL-IPNS	S. Sinha, UCSD
A. Kolesnikov, ANL-IPNS	P. Sokol, IU
J. Lal, ANL-IPNS	R. Teller, ANL-IPNS
K. Littrell, ANL-IPNS	T. Worlton, ANL-IPNS
	G. Zsigmond, PSI

**Very Cold Neutron Source Workshop**  
ANL-IPNS / August 21-24, 2005

**Presentations**



**John M. Carpenter**

**Argonne National Laboratory**

**A Very Cold Neutron Source, VCNS**

A Very Cold Neutron Source, VCNS



Workshop on Applications of a  
Very Cold Neutron Source

Argonne National Laboratory  
22-24 August 2005

We have convened this Workshop and we are all here to determine whether there is enough in the VCNS technical concept and enough prospect for scientific applications to justify further inquiry into VCNS.

### VCNS: Motivation

The practical motivation for this study is to establish the prospects for a neutron source providing intense pulsed beams with spectra as cold as is realistic.

The philosophical motivation is to continue Argonne's long tradition in the development and use of neutron sources and techniques.

The scientific motivation is to serve applications in nanoscience, biology, and technology.

The vision is that of a facility at Argonne National Laboratory providing unique neutron scattering capabilities to the international community toward the end of the next decade.

### VCNS: Preliminary Considerations

- "As cold as is realistic" means 2-4 K, that is, a moderator at the temperature of liquid helium. Multi-kW L-He refrigerators exist at many installations, for example in the L-He-cooled cold sections of high-power particle accelerators.
- Preliminary studies lead to bismuth as target material and as fast-neutron shield, and to a 2-to-4 K pebble-bed of D<sub>2</sub>O ice (but maybe solid D<sub>2</sub>, Be, or CD<sub>4</sub>) moderator cooled by flowing L-He.
- The response time of a 2-K D<sub>2</sub>O moderator, about 4 msec, indicates a "long-pulse" operating mode. Long-wavelength (~ 20 Å) neutrons require long interpulse intervals, therefore a low pulsing frequency.
- We assume a 300 kW proton beam, 4-msec pulse width and 1-Hz pulsing frequency, indicating a linac accelerator driver.

### For Reference

The energy of 2.2 K neutrons is 190  $\mu\text{eV}$ ;  
The wavelength is 20.8  $\text{\AA}$ ;  
The speed is 190. m/sec.

### VCNS: Safe Observations

- Production of large quantities of mm-scale, solid pellets ( $\text{CO}_2$ ,  $\text{CH}_4$ ,  $\text{NH}_3$ ,  $\text{D}_2$ , ...) is an established technology (CAF, Inc, Oak Ridge). The same technology should be applicable to  $\text{D}_2\text{O}$ , which would produce low-density amorphous (LDA) ice.
- Target technology presents no challenges and has already been demonstrated at comparable scale. (200 kW at TTNF at TRIUMF, Vancouver, ~ 1990)
- A prolific source of Very Cold Neutrons (wavelengths  $\sim 20 \text{\AA}$ , energies  $\sim 100 \mu\text{eV}$ ) will serve applications in studies of large structures and slow motions.
- Ongoing activities in developing Ultra Cold Neutron (UCN) facilities are relevant and will be helpful.

### VCNS: Challenges

- Neutronic simulations require scattering kernels that don't exist for the temperatures of interest—developing these kernels requires considerable effort.
- Data on low-temperature thermal conductivities and specific heats of candidate moderator materials are sparse, yet essential to evaluating static and dynamic effects of moderator heating.
- Heat transfer calculations for L-He cooling is a special field, e.g. in superconducting accelerator components.

### VCNS: Challenges, more

- There is little or no experience with neutron scattering instruments suitable for the expected scientific applications and for use of very cold neutrons in the long-pulse mode.
- Instruments are likely to rest heavily on neutron optical devices, all of which work better at long than at short wavelengths. Gravity will play a significant role. VCNS will be an LPSS.
- Instrument concepts need to be developed and demonstrated. We intend to convene a pair of workshops, a "one-two punch." If sufficient interest in the science emerges from this workshop, we will convene another at a later time.
- No prototype of VCNS has existed or yet exists on which to demonstrate the moderator or the instrument concepts. LENS may serve in this essential role, as might a modification of IPNS.

### VCNS: Design Challenges

- The main problem to be overcome in the design is to reduce the nuclear heating (neutron and  $\gamma$ ) in the moderator medium while maintaining a high neutron flux in the moderator. The fundamental constraints are the low heat transport rates and low heat capacities of cryogenic materials.
- We have already reasonable assurance that the heat can be carried away in a time-average sense from the moderating material (tentatively,  $\text{D}_2\text{O}$  ice or Be metal) by flowing L-He.
- A new aspect of the problem is that the instantaneous heating of the moderating medium can raise the temperature during the pulse to unacceptable levels.



### VCNS: Design Approach

- Because nuclear heating (fast n and  $\gamma$  from the source) decreases exponentially with distance from the source region, while neutrons, in the absence of absorption, are preserved in slowing-down, we expect to find a large radius at which the heating is acceptable and the cold neutron flux is as large as possible.
- The source power in this approach is an adjustable parameter.
- This is a departure from convention in neutron facility design, but has some similarities to the thermal columns of the "Atoms for Peace" reactors of the 1950s.

### VCNS: Optimization

- The parameter to be optimized is the ratio of cold neutron flux to nuclear heating in the moderator. This ratio improves with distance from the source, but at the sacrifice of the ratio of cold neutron flux to source power.
- Moderator heating at large distances from the source is predominantly due to capture gamma rays that originate in the shielding material.
- Optimizable parameters are the distance of the moderator from the source, the choice and layering of shielding materials, and the source power and pulsing frequency. The tool is MCNPX.

### What We Hope To Do

- Uncover scientific applications for VCNS
- Develop instrument ideas for VCNS that serve the science
- Compile a proceedings of this Workshop (see 1973 model)
- Apply for funding to carry on
- Extend technical studies of the source and instruments

### Requests to the participants

- Prepared talks, please leave Powerpoint overheads with Nicole Green
- We will name discussion leaders and ANL assistants—
- Leaders please prepare brief summary presentations
- Please write up notes of discussions, ready in ~ 3 weeks.

### Radiogenic Lead

- All natural lead (204,206,207,208) is either "primordial" (i.e. produced directly in the supernova 4.56 Gy ago), or "radiogenic," i.e. the stable products of the three natural actinide decay chains. The Th-232 chain gives Pb-208; the U-238 chain gives Pb-206; the U-235 chain gives Pb-207. Lead-204 is only primordial.
- Different U and Th mines produce different isotopic ratios of lead as byproduct, which are advantageously depleted in the neutron-capturing isotopes  $^{204}\text{Pb}$  and  $^{207}\text{Pb}$ .
- For example, years ago, two varieties of radiogenic lead were feedstocks for ORNL calutron production of isotope-separated reference lead materials. The table that follows compares the 2200-m/sec capture cross sections and the resonance capture integrals of the isotopes and example mixtures.

### VCNS: Gamma Rays, Radiogenic Lead

Gamma rays generated in the shielding dominate the heat production in the moderator. Radiogenic lead is available in isotopic compositions that reduce the capture rate in the shield.

A	$\sigma_\gamma$ , mb	I, mb	Primordial Lead Standard Composition			Radiogenic Lead High-206 Lead			Radiogenic Lead High-208 Lead		
			f, %	f $\sigma_\gamma$	f I	f, %	f $\sigma_\gamma$	f I	f, %	f $\sigma_\gamma$	f I
204	661.	1700.	1.4	9.2	24.	0.2	1.32	3.4	.024	.16	.41
206	30.5	200.	24.1	7.4	48.	87.8	26.8	176.	25.6	7.81	51.2
207	709.	400.	22.1	156.	88.	8.9	63.1	35.6	1.78	12.6	7.1
208	0.5	2.0	52.4	0.26	1.0	3.3	.017	.065	72.6	.36	1.45
Averages			$\sigma_\gamma$	I		$\sigma_\gamma$	I		$\sigma_\gamma$	I	
			173.	161.		91.2	218.		20.9	73.2	

Bismuth (monoisotopic),  $\sigma_\gamma = 34$ . Mb, I = 190 mb, is much superior to standard lead. However, the "high-208" radiogenic lead is better still.

The average gamma energies emitted per capture are 5408, 6714, and 4663 keV for the three varieties of Pb, and 4604 keV for Bi.



# Brad Micklich

## Argonne National Laboratory

### Concepts for a Very-Cold Neutron Source at Argonne National Laboratory



*Concepts for a Very-Cold Neutron Source at Argonne National Laboratory*

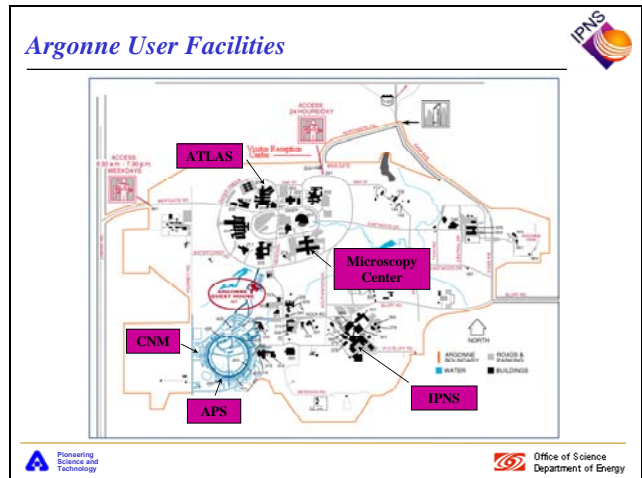
**Dr. Bradley J. Micklich**  
Radiation Physicist, IPNS

Very-Cold Neutron Source Workshop  
22 August 2005

Argonne National Laboratory

A U.S. Department of Energy  
Office of Science Laboratory  
Operated by The University of Chicago

*Argonne User Facilities*

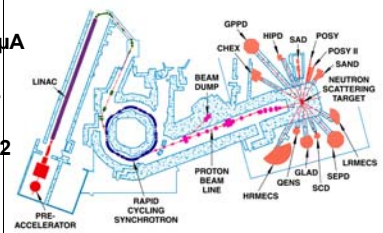


IPNS

Office of Science  
Department of Energy

*IPNS Operating Parameters*

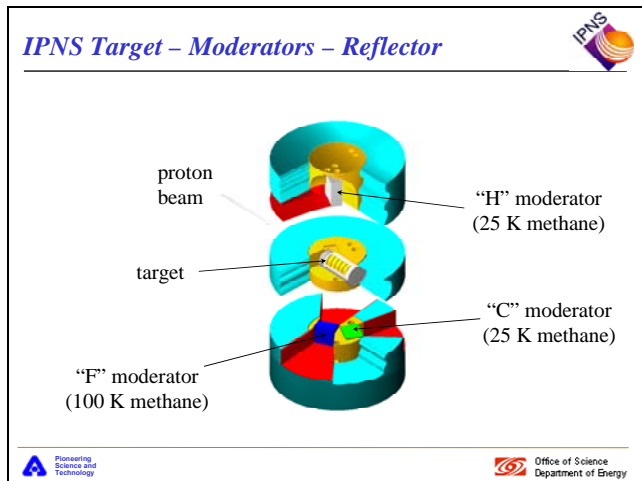
- Neutrons are produced through spallation/fission by 450-MeV protons striking a depleted uranium target
- Yield is about 14 neutrons/proton
- Proton beam pulsed at 30 Hz
- Pulse width 70 ns
- Average current 15  $\mu\text{A}$
- Neutron energy resolved by time-of-flight
- 13 instruments on 12 beam lines



IPNS

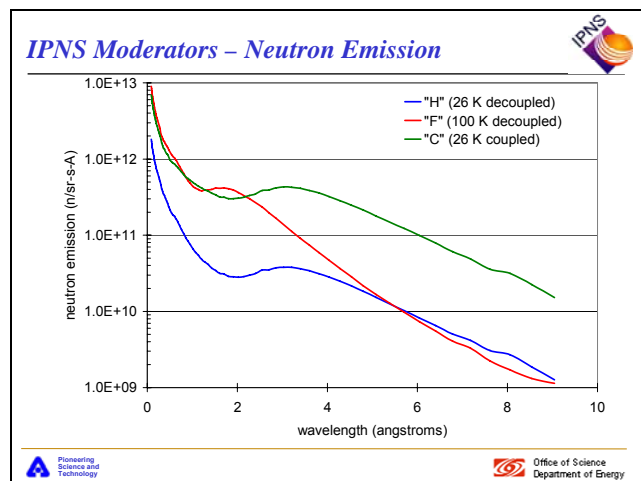
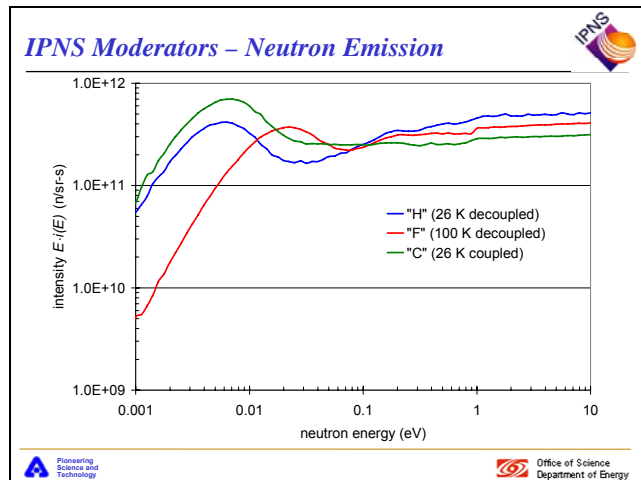
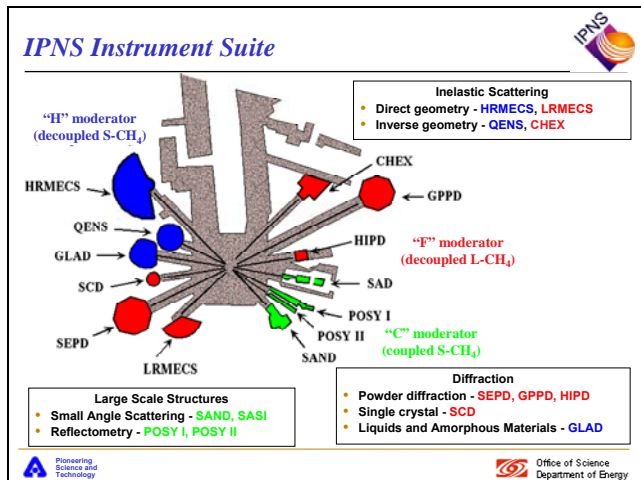
Office of Science  
Department of Energy

*IPNS Target – Moderators – Reflector*



IPNS

Office of Science  
Department of Energy



- ### A Very Cold Neutron Source at Argonne
- Motivation - establish the prospects for a neutron source providing intense pulsed beams with spectra "as cold as is realistic".
  - The philosophical motivation is to continue Argonne's long tradition in the development and use of neutron sources and techniques.
  - The scientific motivation is to serve applications in nanoscience, biology, and technology.
  - The vision is that of a facility at Argonne National Laboratory providing unique neutron scattering capabilities to the international community toward the end of the next decade.

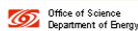
- ### VCNS – Preliminary Considerations
- "As cold as is realistic" means 2-4 K, that is, a moderator at the temperature of liquid helium.
  - Helium exhibits superfluid properties beneath the  $\lambda$  point (2.186 K).
  - For reference
    - The energy of 2.2 K neutrons is 190  $\mu$ eV
    - The wavelength is 20.8 Å
    - The speed is 190 m/sec
  - A prolific source of very cold neutrons (wavelengths  $\sim$  20 Å, energies  $\sim$  100  $\mu$ eV) could serve applications in studies of large structures and slow motions.

- ### VCNS – Safe Observations
- Accelerator development can be done in collaboration with the high-energy physics community.
  - Target technology presents no challenges and has already been demonstrated at comparable scale (200 kW at TTNF at TRIUMF, Vancouver,  $\sim$  1990).
  - Production of large quantities of mm-scale, solid pellets (CO<sub>2</sub>, CH<sub>4</sub>, NH<sub>3</sub>, D<sub>2</sub>, ...) is an established technology (CAF, Inc, Oak Ridge). The same technology should be applicable to D<sub>2</sub>O, which would produce low-density amorphous (LDA) ice.
  - Much use can be made of collaborations or interaction with relevant activities elsewhere.

## VCNS – Challenges



- Neutronic simulations require scattering kernels that don't exist for the temperatures of interest - developing these kernels requires considerable effort.
- Low-temperature scattering data have been generated for many materials at IKE-Stuttgart, including:
  - Solid p-H<sub>2</sub> at 5, 6, and 13 K
  - Solid o-D<sub>2</sub> at 5, 6, 13, and 17 K
  - Beryllium at 2 K, 25 K
  - Liquid helium at 1 K
  - Light water ice at 4, 20, 30, 77, 113, 165, 218, 248, 258, and 273 K
  - Solid methane at 22 K
  - Aluminum at 20, 100, and 293.6 K
- We are working to obtain the existing scattering kernels and to learn to process kernels for ourselves.



## VCNS – Challenges



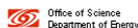
- Data on low-temperature thermal conductivities and specific heats of candidate moderator materials are sparse, yet essential to evaluating static and dynamic effects of moderator heating.
- Heat transfer calculations for L-He cooling is a special field, e.g. in superconducting accelerator components. We are working with a specialist in this field, Steve Van Sciver (Florida State University).
- We have already reasonable assurance that the heat can be carried away in a time-average sense from the moderating material (tentatively, D<sub>2</sub>O ice) by flowing liquid He.



## VCNS – More Challenges



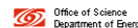
- Scientific applications need to be identified.
- There is little or no experience with neutron scattering instruments suitable for the expected scientific applications and for use of very cold neutrons in the long-pulse mode.
- Instruments are likely to rest heavily on neutron optical devices, all of which work better at long than at short wavelengths. Gravity will play a significant role.
- Instrument concepts need to be developed and demonstrated.
- No prototype of VCNS has existed or yet exists on which to demonstrate the moderator or the instrument concepts. LENS (Indiana Univ.) may serve in this essential role, as might a modification of IPNS.



## VCNS Design Approach



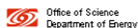
- Because nuclear heating (fast n and  $\gamma$  from the source) decreases exponentially with distance from the source region, while neutrons, in the absence of absorption, are preserved in slowing-down, we expect to find a large radius at which the heating is acceptable and the cold neutron flux is as large as possible.
- The source power in this approach is an adjustable parameter, which is a departure from convention in neutron facility design.
- The parameter to be optimized is the ratio of cold neutron flux to nuclear heating in the moderator. This ratio improves with distance from the source, but at the sacrifice of ratio of cold neutron flux to source power.



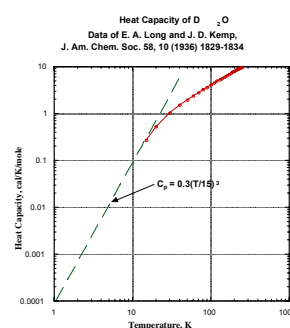
## VCNS – Design Challenges



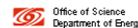
- The main problem to be overcome in the design is to reduce the nuclear heating (neutron and  $\gamma$ ) in the moderator medium while maintaining a high neutron flux in the moderator. The fundamental constraints are the low heat transport rates and low heat capacities of cryogenic materials.
- A new aspect of the problem is that the instantaneous heating of the moderating medium can raise the temperature during the pulse to unacceptable levels (300 kJ/pulse vs. 3400 J/pulse for present IPNS).



## Heat Capacity of D<sub>2</sub>O



The figure shows the data of Long and Kemp, presumably D<sub>2</sub>O ice Ih (frozen from the liquid), which extend to temperatures just low enough to justify extrapolation to the lower temperatures of interest to us. Because the low-temperature limit of the Debye expression for the lattice specific heat of insulators indicates that  $C_p$  is proportional to  $T^3$ , we have extrapolated accordingly as the figure shows. (1 cal/mole = 0.2088 joules/gm)



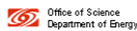
## Heat Capacities of D<sub>2</sub>O and Be – Heating



- If a short power pulse deposits heat  $\Delta Q$  per gram in the moderator, initially at temperature  $T_1$ , the material heats up immediately to a temperature  $T_2$  such that  $\Delta H(T_2, T_1) = \Delta Q$ , where  $\Delta H$  is the difference in enthalpy between temperatures  $T_2$  and  $T_1$ ,

$$\Delta H(T_1, T_2) = \int_{T_1}^{T_2} C(T) dT = 4.64 \times 10^{-6} (T_2^4 - T_1^4)$$

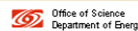
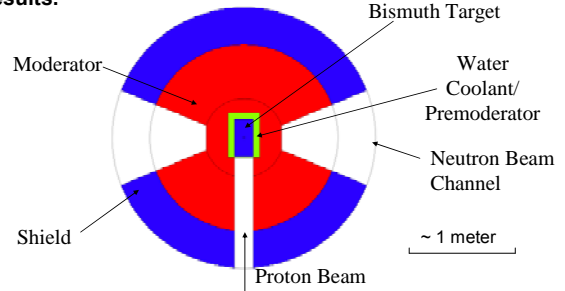
- If we say  $T_1 = 2$  K and insist that  $T_2$  remain less than 4 K, then  $\Delta H = 1.14 \times 10^{-6}$  J/gm and  $\Delta Q$  must be  $\Delta Q < \Delta H = 1.14 \times 10^{-6}$  J/gm, a very conservative assumption that represents our goal.
- By contrast, the specific heat of beryllium (a metal) is  $C(T) = 2.5 \times 10^{-5}$  T J/gm-K, so  $\Delta H(T_2, T_1) = 1.5 \times 10^{-4}$  J/gm.
- Beryllium may provide a needed heat capacity advantage over D<sub>2</sub>O, although D<sub>2</sub>O and D<sub>2</sub> are, we expect, better moderators.



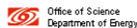
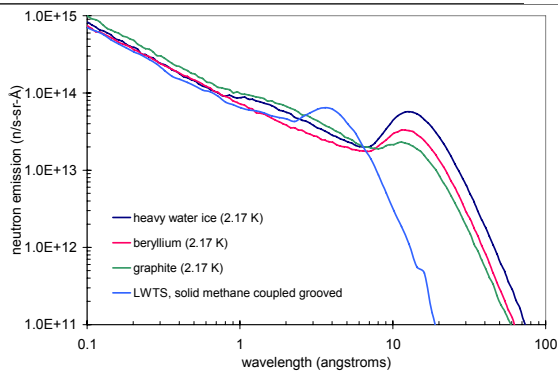
## VCNS – Preliminary Studies



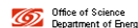
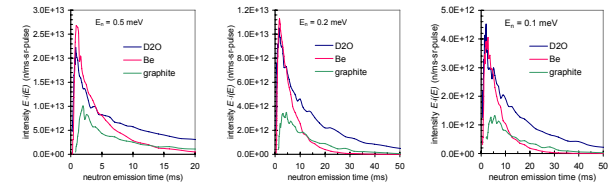
- Calculations with simple models using free-atom scattering treatments were used to generate some early results.



## VCNS – Preliminary Studies



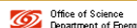
## VCNS – Preliminary Studies



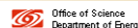
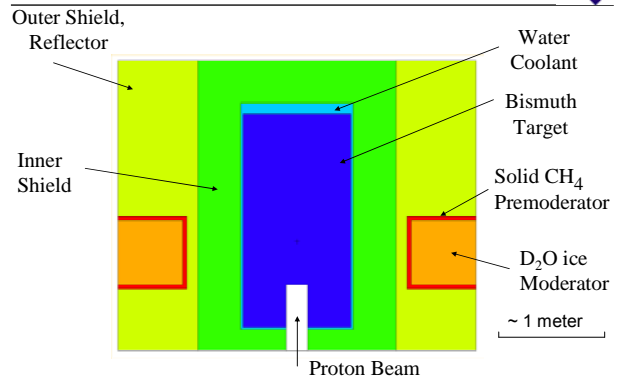
## VCNS – Accelerator Concepts

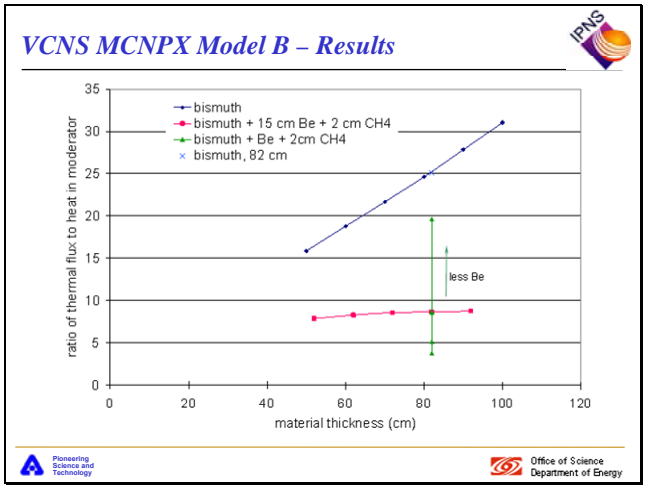


- The response time of a 2-K D<sub>2</sub>O moderator, about 4 msec, indicates a “long-pulse” operating mode.
- Long-wavelength (~ 20 Å) neutrons require long interpulse intervals, therefore a low pulsing frequency.
- Conceptual design of a VCNS accelerator system
  - Pulse length 4 msec, pulsing frequency 1 Hz
  - 1-GeV proton linac
  - Instantaneous current 75 mA
  - 300 kW time-average beam power
- The linac components are ones common in modern high-power proton linac technology.
- The VCNS will complement the capabilities of the SNS in the very cold neutron regime. The SNS accelerator system is not capable of driving the conceived VCNS.



## VCNS Model B (Cylindrically Symmetric)



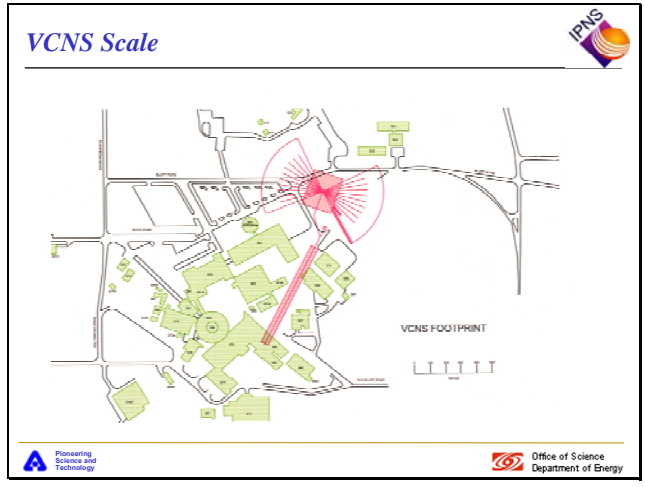
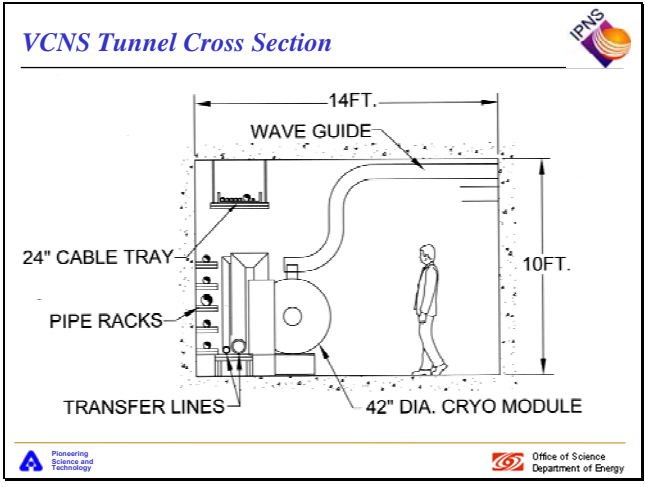


- ### VCNS – Summary Remarks
- Efforts to date have largely been devoted to scoping studies on the target/moderator system neutronics, and to working out a feasible design for the VCNS accelerator system.
  - The neutronics analysis and optimization requires much more work and innovation.
  - The science case needs development both to show that there is scientific interest in such a facility and to provide motivation and purpose for neutron scattering instrument concept development.
  - Serious progress will require feasibility demonstration in a prototype.

### Basic Cavity Types in VCNS Linac

CAVITY TYPES	Frequency MHz	# OF CAVITIES	Ein MeV	Eout MeV
Room Temperature Triple Spoke	325	20	3	15
Superconducting Single Spoke	325	30	15	40
Superconducting Double Spoke	325	30	40	112
Superconducting Triple Spoke	325	44	112	400
Superconducting Elliptical 0.81 $\beta$	1300	48	400	1044

- ### VCNS Accelerator System
- The accelerator and target systems and the experiment area could fit into available space near Argonne's 362 building, which could house the operations scientific staff.
  - A very preliminary estimate of the cost of the installation is \$500-600 M for the accelerator systems, \$100 M for the target systems and the experimental area.





# Peter Geltenbort

## ILL (Institute Laue Langevin)

### UltraCold Neutrons (UCN) at the ILL

**UltraCold Neutrons (UCN) at the ILL**

UCN  
PF2 - THE running source  
cryoEDM  
micro-D<sub>2</sub> source  
ultracold nanoparticles

Thanks to the beautiful slides of  
J. Bazin, A. Frey, P. Bühler, P. Harris, V. Meslot, G. N. P. Pellegrini, G. Plonka, M. Van der Grinten,  
& Volker D. W. H. Hönl

P. Geltenbort Workshop "Very Cold Neutron Source" Aronne Nat. Lab. August 22 - 24, 2005 1

**Properties of UCN**

$E_{kin} (\sim 5 \text{ ms}^{-1}) = 100 \text{ neV} (10^{-7} \text{ eV})$   
 $\lambda_{UCN} \sim 1000 \text{ \AA}$

Interaction with matter:  
 UCN see a *Fermi-Potential*  $E_F$   
 $E_F \sim 10^{-7} \text{ eV}$  for many materials, e.g.

- beryllium 252 neV
- stainless steel 200 neV

**UCN are totally reflected from suitable materials at *any* angle of incidence, hence **storable!****

Long storage and observation times possible (up to several minutes!)

High precision measurements of the properties of the free neutron (lifetime, electric dipole moment, gravitational levels, ...)

UCN are furthermore storable by gravity and/or magnetic fields

Fermi potential	$\sim 10^{-7} \text{ eV}$
Gravity $\Delta E = m_n g \Delta h$	$\sim 10^{-7} \text{ eV} / \text{Meter}$
Magnetic field $\Delta E = \mu_n B$	$\sim 10^{-7} \text{ eV} / \text{Tesla}$

P. Geltenbort Workshop "Very Cold Neutron Source" Aronne Nat. Lab. August 22 - 24, 2005 2

**ILL - Reactor**

**Neutron sources at ILL**

Fuel (chain reaction):  $^{235}\text{U}(n_{th}, f) \rightarrow$  fission neutrons

Moderator: D<sub>2</sub>O at 300K  $\rightarrow$  thermal neutrons

Hot source: 10 dm<sup>3</sup> of graphite at 2400 K

Cold source (horizontal): 6 dm<sup>3</sup> of liquid D<sub>2</sub> at 25 K  
 Cold source (vertical): 20 dm<sup>3</sup> of liquid D<sub>2</sub> at 25 K

Ultracold Neutrons    Cold Neutrons    Reactor Neutrons

Temperature (K)    10<sup>-4</sup>    10<sup>1</sup>    10<sup>3</sup>

Energy (eV)    10<sup>-7</sup>    10<sup>-3</sup>    10<sup>-1</sup>

Velocity (m/s)    5    800    2200

P. Geltenbort (C. Vetter) Workshop "Very Cold Neutron Source" Aronne Nat. Lab. August 22 - 24, 2005 3

**ILL : a neutron factory and a user facility**

**ILL : a powerful neutron source**

HCS    Hot Source  
VCS

thermal neutrons, hot neutrons, cold neutrons

HCS: Horizontal Cold Source  
VCS: Vertical Cold Source  
P. Geltenbort (C. Vetter) Workshop "Very Cold Neutron Source" Aronne Nat. Lab. August 22 - 24, 2005 4

## The UCN/VCN facility PF2

Neutron turbine  
A. Steyerl (TUM - 1985)

Vertical guide tube

Cold source

Reactor core

P. Geltenbort Workshop "Very Cold Neutron Source" Argonne Nat. Lab., August 22 - 24, 2005 5

## Vertical cold source at the ILL

P. Geltenbort Workshop "Very Cold Neutron Source" Argonne Nat. Lab., August 22 - 24, 2005 6

## Generating Ultracold Neutrons (UCN)

"Steyerl turbine"  
Doppler shifting device

Very cold neutrons

Blades

Turbine wheel

$p = 10^{-5}$  mbar

VCN exit port

0.46m

Scanning guide and detector

UCN exit ports

Ultracold neutrons

P. Geltenbort Workshop "Very Cold Neutron Source" Argonne Nat. Lab., August 22 - 24, 2005 7

## The PF2 beam facility

PF2: Physique Fondamentale 2  
2<sup>nd</sup> installation for fundamental physics

4 positions for Ultracold Neutrons (UCN)

- MAM
- EDM
- UCN

$v = 5 \text{ ms}^{-1}$   
 $\rho = \sim 50 \text{ cm}^{-3}$  (at the experiment)

- TES

1 position for Very Cold Neutrons (VCN)

- VCN beam  $v = 50 \text{ ms}^{-1}$   
 $\phi = 10^8 \text{ cm}^{-2} \text{ s}^{-1}$

P. Geltenbort Workshop "Very Cold Neutron Source" Argonne Nat. Lab., August 22 - 24, 2005 8

## UCN facilities

### Status and Future

More UCN facilities in the future

- PSI (CH) see M. Daum's talk
- Mainz / Munich (D)
- LANL, NCSU, SNS, ANL, ... (USA)
- RCNP (Japan) see Y. Masuda's talk
- ILL (F)
- ...

P. Geltenbort Workshop "Very Cold Neutron Source" Argonne Nat. Lab., August 22 - 24, 2005 9

## The build up of slow neutrons

Down scattering  
(weakly dependent on moderator temperature)

Up scattering  
(strongly dependent on moderator temperature)

UCN phase space

UCN Beta-decay

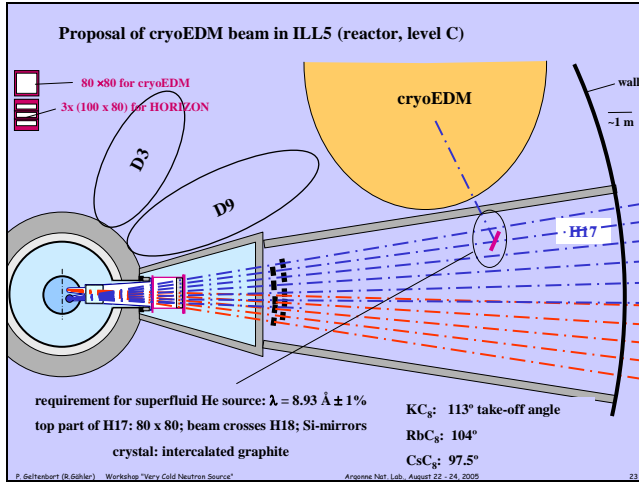
UCN capture by nuclei

UCN used in the experiment

Mike Pendlebury University of Sussex  
Argonne Nat. Lab., August 22 - 24, 2005 10







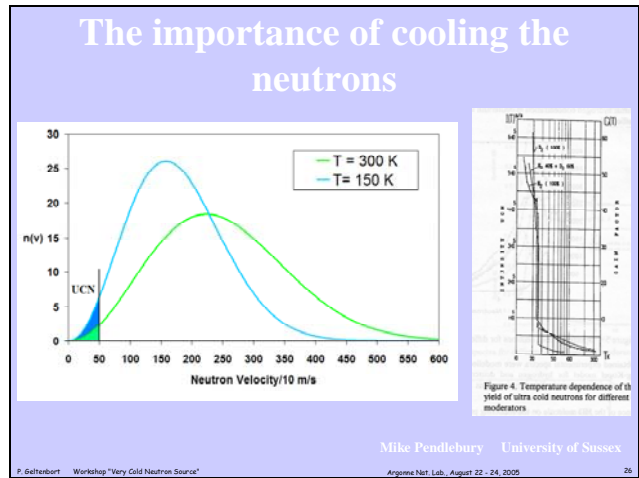
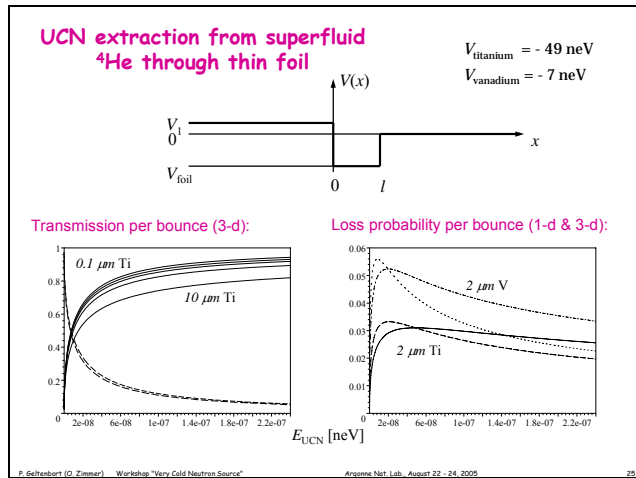
### Superthermische UCN-Produktion an MEPHISTO

Gemessene UCN-Erzeugungsrate im <sup>4</sup>He:  
 $0.91 \pm 0.13 \text{ cm}^{-2}\text{s}^{-1}$   
für kalten Neutronenfluß  
 $\phi = 2.6 \times 10^7 \text{ cm}^{-2}\text{s}^{-1}\text{\AA}^{-1}$  bei 9 \AA

C.A. Baker et al., PLA 308 (2003) 67

S. Mironov  
J. Peters  
P. Schmidt-Wellenburg  
H.-F. Wirth

P. Geltenbort (G. Zimmer) Workshop "Very Cold Neutron Source" Argonne Nat. Lab., August 22 - 24, 2005 24



### How are UCN produced?

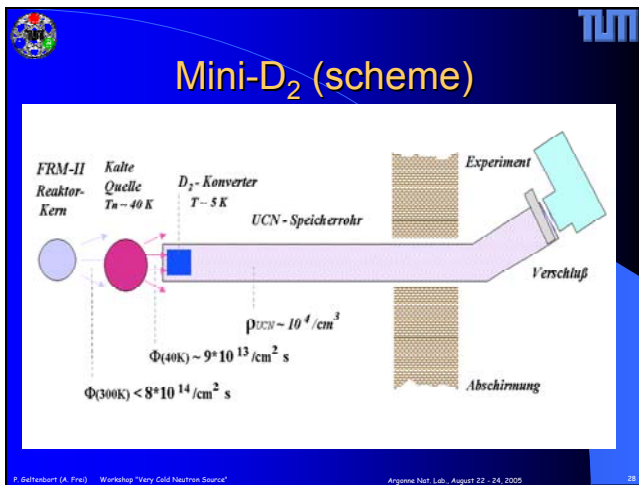
By downscattering of higher-energy neutrons

We need a moderator material

- high inelastic scattering cross section
- low absorption cross section
- very low temperature (no heating)

UCN

P. Geltenbort (A. Frey) Workshop "Very Cold Neutron Source" Argonne Nat. Lab., August 22 - 24, 2005 27



## Mini-D<sub>2</sub> at SR4

Cold source  
SR4 beam tube  
In-pile cryostat  
UCN-storage tube

UCN storage tube equilibrium :

- absorption and up-scattering in the converter
- losses wall collisions
- decay
- escape through holes

P. Geltenbort (A. Fre) Workshop "Very Cold Neutron Source" Argonne Nat. Lab., August 22 - 24, 2005 29

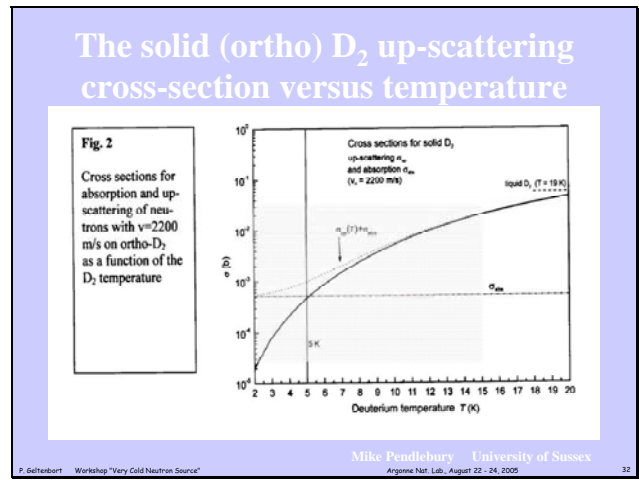
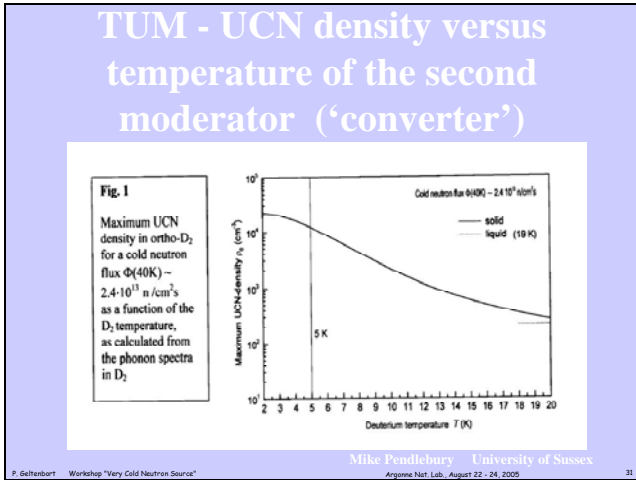
## The converter

Materials

- Solid D<sub>2</sub>
- Al6061
- Zirkaloy-4

In-pile cryostat  
300 K cooling channels  
5 K cooling ch.  
UCN-storage tube  
Solid D<sub>2</sub> converter  
25 K cooling ch.

P. Geltenbort (A. Fre) Workshop "Very Cold Neutron Source" Argonne Nat. Lab., August 22 - 24, 2005 30



## Safety aspects

1. Reactor is source of high neutron and gamma flux
2. UCN device will be located inside the biological shield of FRM-II
3. Deuterium is a dangerous (explosive) material
4. Other experimental facilities are planned to work on FRM-II

We must guarantee

low level of radiation dose

Decoupling of UCN from FRM-II

**Double-wall concept of barriers**

P. Geltenbort (A. Fre) Workshop "Very Cold Neutron Source" Argonne Nat. Lab., August 22 - 24, 2005 33

## The TRIGA Mainz setup

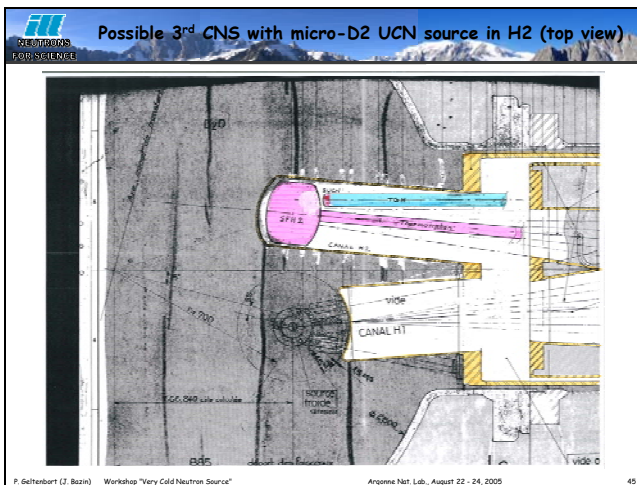
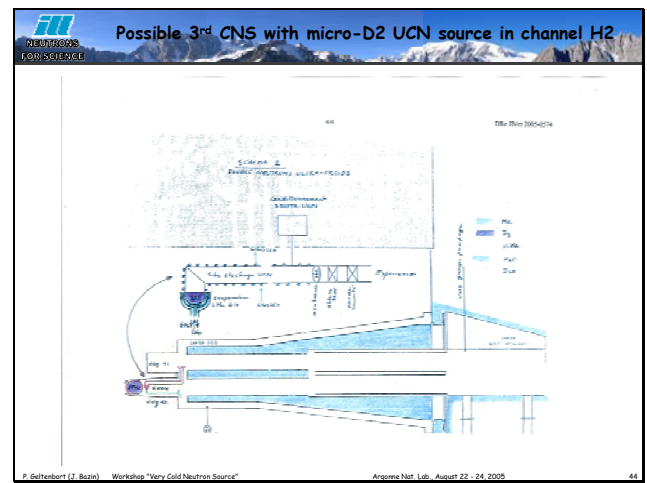
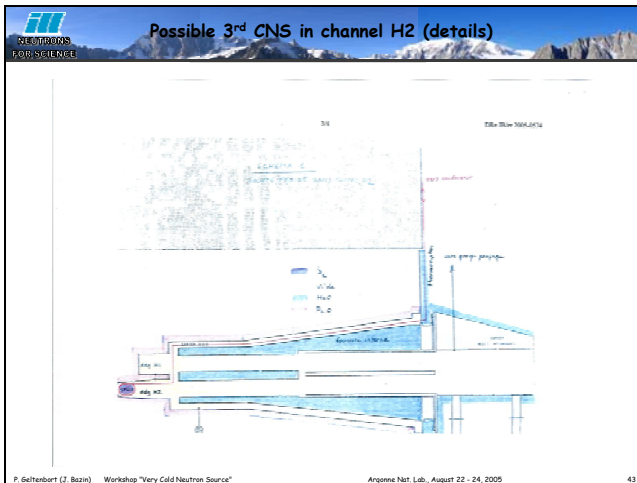
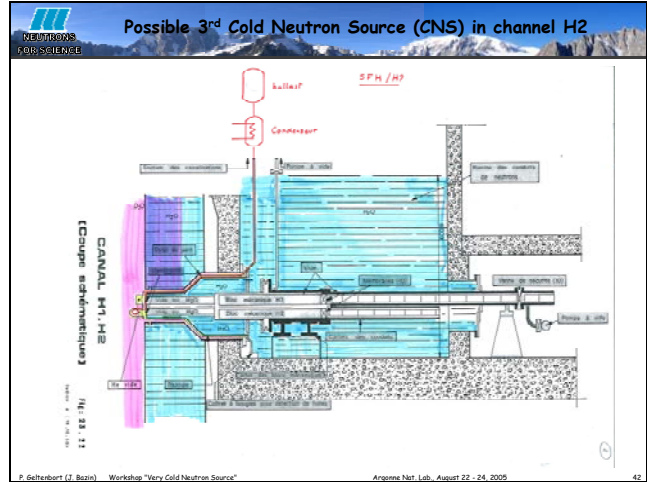
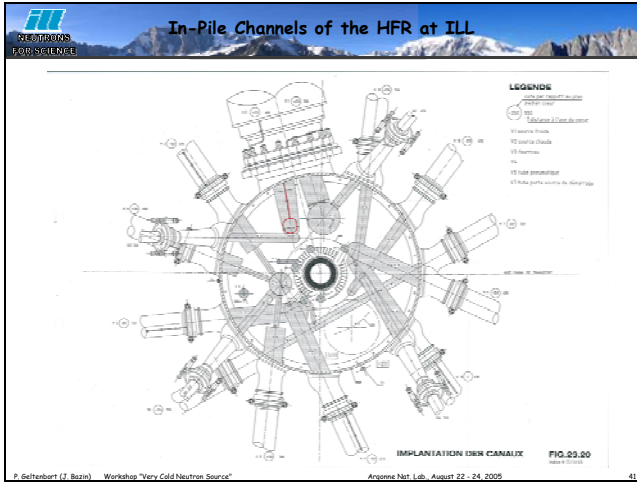
Neutron valve  
Test cryostat  
Neutron storage volume  
Reactor channel  
UCN guide tube  
Deuterium converter in in-pile cryostat

$\sim 1$  UCN/cm<sup>3</sup>

pulsed neutrons

P. Geltenbort (A. Fre) Workshop "Very Cold Neutron Source" Argonne Nat. Lab., August 22 - 24, 2005 34





**ULTRACOLD NANOPARTICLES**

NUCLEI Theory

**Interaction of Neutrons with Nanoparticles**

V. V. Nesvizhevsky<sup>\*</sup>  
*Institute Laue-Langevin, Grenoble, France*  
 Received February 13, 2001; in final form, October 5, 2001

**Abstract**—Two hypotheses concerning interaction of neutrons with nanoparticles and having applications in the physics of ultracold neutrons (UCN) are considered. In 1997, it was found that, upon reflection from sample surface or spectrometer walls, UCN change their energy by about  $10^{-7}$  eV with a probability of  $10^{-7}$ – $10^{-8}$  per collision. The nature of this phenomenon is not clear at present. Probably, it is due to the inelastic coherent scattering of UCN on nanoparticles or nanostructures weakly attached at surface, in a state of Brownian thermal motion. An analysis of experimental data on the basis of this model allows one to estimate the mass of such nanoparticles and nanostructures at  $10^7$  au. The proposed hypothesis indicates a method for studying the dynamics of nanoparticles and nanostructures and, accordingly, their interactions with the surface or with one another, this method being selective in their sizes. In all experiments with UCN, the trap-wall temperature was much higher than a temperature of about 1 mK, which corresponds to the UCN energy. Therefore, UCN increased their energy. The surface density of weakly attached nanoparticles was low. If, however, the nanoparticles temperature is lower than the neutron temperature and if the nanoparticles density is high, the problem of interaction of neutrons with nanoparticles is inverted. In this case, the neutrons of initial velocity below  $10^6$  m/s can cool down, under certain conditions, owing to their scattering on ultracold-heavy-water, deuterium, and oxygen nanoparticles to their temperature of about 1 mK, with the result that the UCN density increases by many orders of magnitude. © 2002 MAIR "Nauka/Interpedita".

ILL Research Proposal 3-07-194\*

## Thermalization of neutrons in gels of ultracold nanoparticles Measurement of the total cross sections

V. Nesvizhevsky et al.

A progress in maximum UCN density could be possible using the recently proposed method of neutron thermalization in gels of ultracold nanoparticles. It consists in the equilibrium cooling of very cold neutron (VCN) owing to their many collisions with ultracold nanoparticles made from low-absorbing materials ( $D_2O$ ,  $D_2$ ,  $O_2$  etc) down to the temperature of these nanoparticles of  $\sim 1$  mK during the diffusion motion of these neutrons in a macroscopically large ensemble of nanoparticles. Simplified model of free nanoparticles provides promising estimations. We therefore initiate a program of detailed study of feasibility of production of UCN using this principle. It consists of two steps. At the first stage, we will investigate the elastic and inelastic neutron interaction in a broad energy range with small samples of such gels of different chemical composition, size, structure etc at the temperature of  $\sim 1$  K. The second step consists in studies of the thermalization process itself. We ask for the beam time at PF1B and PF2 beam positions in order to carry out first measurements of the total cross sections with new experimental equipment developed for the first part of our program.

\* Experiment performed in July 2005 at PF2/VQN; very preliminary results seem to agree with theory

P. Eitelhart Workshop "Very Cold Neutron Source" Arbonne Nat. Lab. August 22 - 24, 2005 47

I hope I could convince you that **ultracold neutrons** are and will be a fancy and powerful tool for **fundamental physics studies** at the ILL




**Thank you, merci beaucoup and besten Dank for your attention!**

P. Eitelhart Workshop "Very Cold Neutron Source" Arbonne Nat. Lab. August 22 - 24, 2005 48



# Yasuhiro Masuda

## KEK (High Energy Accelerator Research Organization)

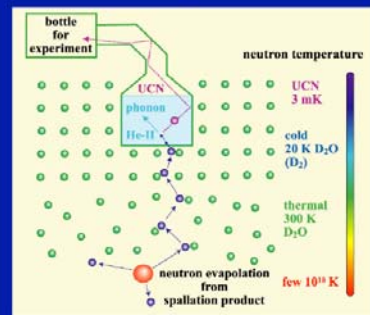
### Spallation Neutron Source for UCN Production in He-II

#### Spallation neutron source for UCN production in He-II

Target and moderator for spallation UCN production

Y. Masuda (IPNS, KEK)  
IPNS, ANL, Aug. 22\_24

#### Our UCN production



#### UCN density in He-II

$$\rho_{\text{ucn}} = \int_0^{E_c} \sigma(k_i \rightarrow k_{\text{ucn}}) N_{\text{He}} \Phi_p \tau dE$$

$\sigma$ : Born approximation  
 $d^2\sigma/dQd\omega$   
 $= k_f/k_i a^2 S(Q,\omega)$

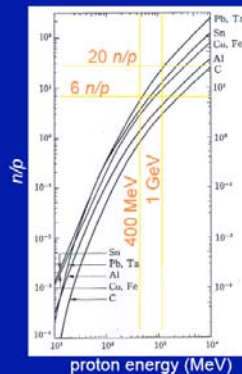
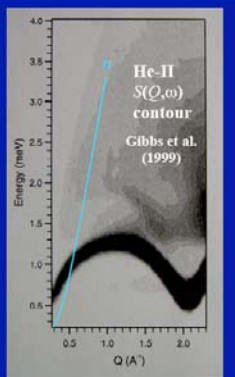
$\Phi_p$ : proton beam power

$\tau$ : phonon up-scattering rate in He-II

$\tau = 570 \text{ s at } T = 0.3 \text{ K}$

$1/\tau \propto T^2$

Golub et al. (1983)



#### Neutron production rate

Proton energy and target mass dependence

$$N_n \propto E_p^n$$

$n > 1$  for  $E_p < 1 \text{ GeV}$   
 $n = 1$  for  $E_p > 1 \text{ GeV}$

K. Tesch, Radiat. Protec. Dosim. 11 (1985)185

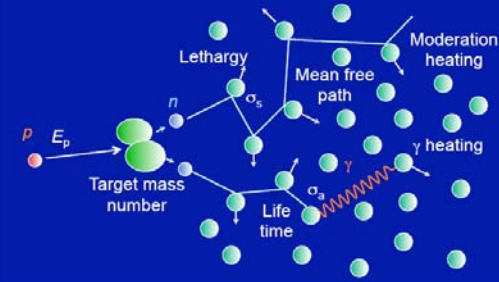
## Spallation has advantage in low $\gamma$ heating

Good for cryogenic apparatus

	Spallation	reactor
Power for $\Phi_n = 10^{14}/\text{cm}^2\text{s}$	5 MW	60 MW
$n/\gamma$ ratio	12	1
Number of neutrons / particle energy	10 n / 600 MeV	2 n / 200 MeV <i>n</i> is used for chain reaction

## Neutron source parameters

$n$  production, moderation, diffusion, dwelling time, and heating



## Moderator for UCN

High  $\Phi_n$  (1 meV) in a superfluid helium (10 l)

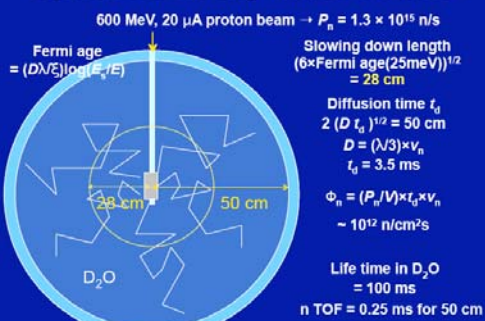
high lethargy and short mean free path  
low absorption

low  $\gamma$  heating in 0.5 K helium

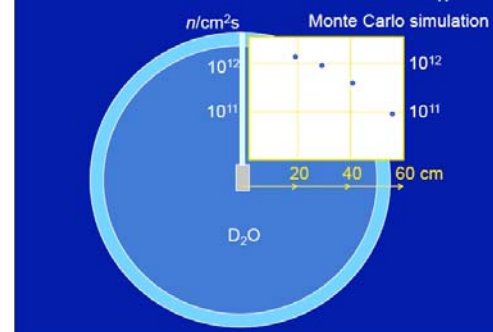
## Moderator material

	H <sub>2</sub> O	D <sub>2</sub> O	D <sub>2</sub>	Be	C	Pb
Lethargy	0.95	<u>0.57</u>	0.75	0.21	0.16	0.01
$\xi = -\text{ave}(\ln(E_i/E_f))$ $= 2/(M/m + 2/3)$						
<i>m</i> : neutron mass, <i>M</i> : target nucleus mass						
Mean free path (cm)	0.29	<u>2.2</u>	6.0	1.2	2.6	2.7
$\lambda = 1/(N\sigma_s)$						
Density <i>N</i> (10 <sup>23</sup> /cm <sup>3</sup> )	0.34	0.33	0.25	1.24	0.80	0.33
Scattering $\sigma_s$ (b)	103	13.6	6.8	7.0	4.8	11.3
Life time (ms)	0.21	<u>100</u>	177	3.46	13	0.81
$\tau_n = 1/(N\sigma_a v)$						
Absorption $\sigma_a$ (mb)	665	1.23	1.04	7.6	3.53	171
$\gamma$ heating						

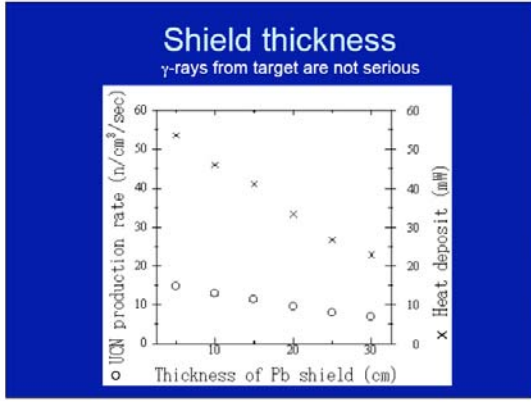
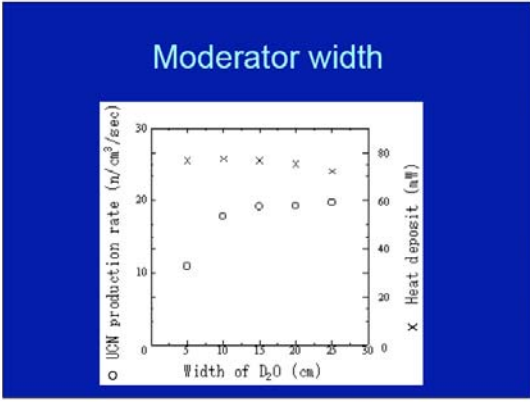
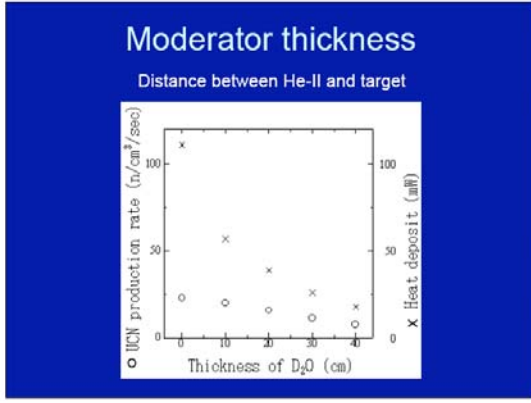
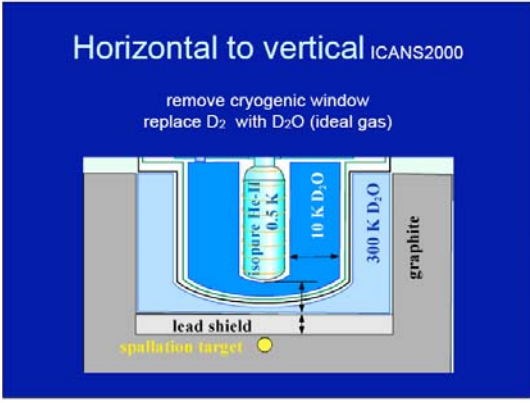
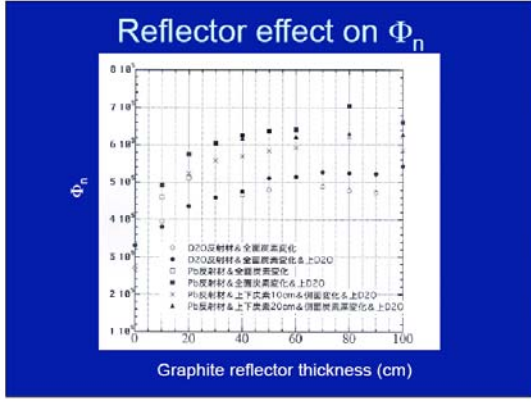
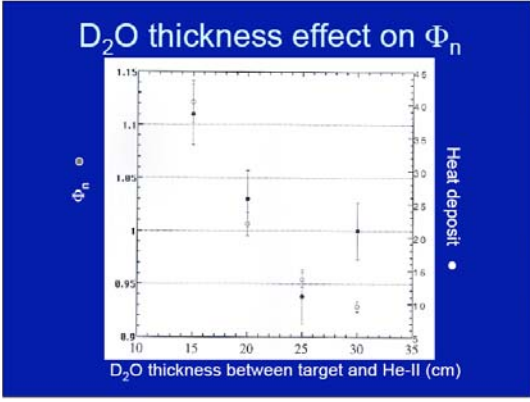
## Spherical heavy water source

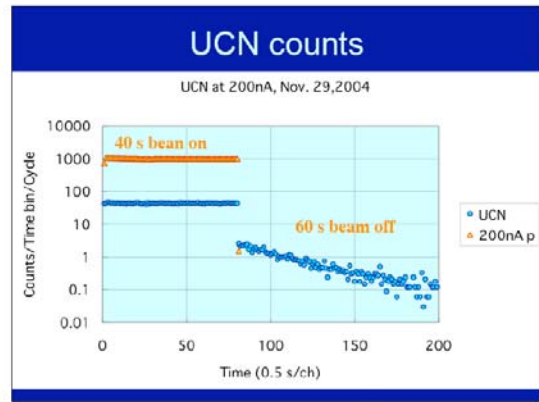
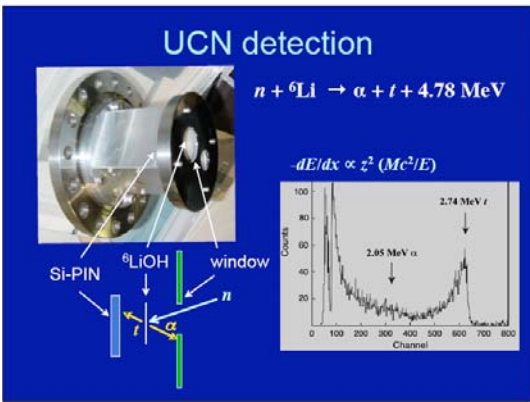
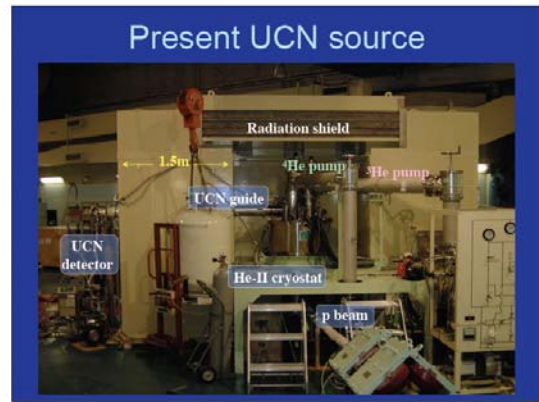
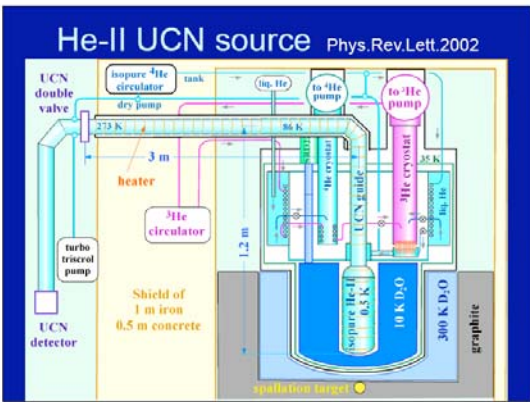
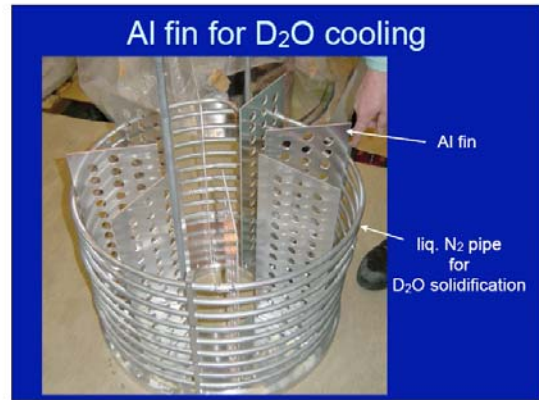
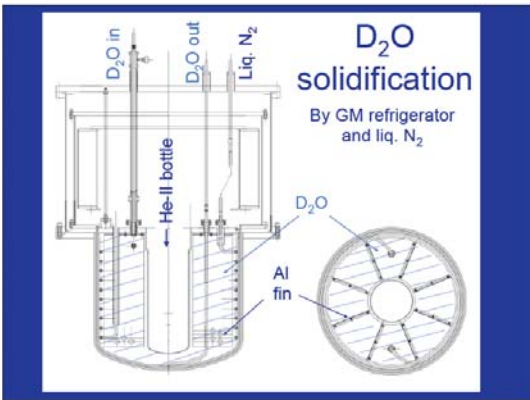


## Radial distribution of $\Phi_n$

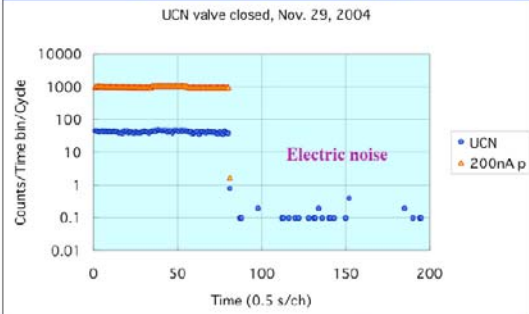








## UCN valve closed



## Point of moderator

$n/\gamma$  :

$\alpha_\gamma$  should be small

The distance from the target should be short.  
 $\gamma$  ray from the target is not problem.

Neutron temperature : compressing phase space

The neutron temperature may be around 80 K.

$D_2O$  is frozen at 273 K.

Almost all the neutrons are elastically scattered  
 in 10-K  $D_2O$  just like in polyethylene.

The neutron temperature will be lowered  
 in 20-K  $D_2$  or 4-K  $D_2$ .

## UCN density

Present:  $\rho = 1.4$  UCN/cm<sup>3</sup> at  $E_c < 100$  neV  
 in the experimental volume of 10 l (+ He-II + guide = 43 l)

p beam power  $\times 10$  (160W  $\rightarrow$  1.6 kW),  
 Graphite reflector  $\times 2$   
 Storage time  $\tau \times 10$  (14 s (1.2K)  $\rightarrow$  150 s (0.5 K))  
 $\rho = 280$  UCN/cm<sup>3</sup>

## World competition

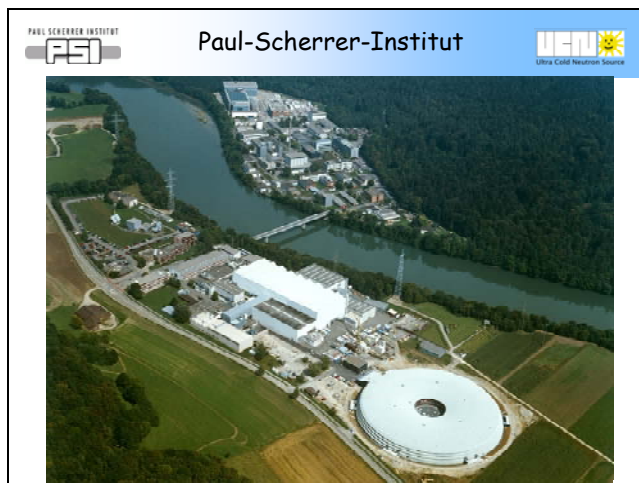
	2005	future	PSI*	Los Alamos*
	He-II in 20K $D_2O$	He-II in 20K $D_2$	SD <sub>2</sub>	SD <sub>2</sub>
$E_p$ (MeV)	400	500	600	800
$I_p$ ( $\mu$ A)	4	60	2000	100
on/off (s)	150/450	150/450	8/800	0.4/10
$E_p \times I_p$ av (kW)	0.4	7.5	12	3.2
$\tau$ (s)	150	150	888	2.6
$E_c$ (neV)	100	190	250	250
$\rho$ (UCN/cm <sup>3</sup> )	280	$3 \times 10^5$	$3 \times 10^3$	120
( $E_c = 100$ neV)	280	$1 \times 10^5$	750	30

\* ICANS-XVI, April 2005

**Manfred Daum**

**Paul Scherrer Institute**

**The PSI UCN Source**



PAUL SCHERRER INSTITUT  
PSI  
The PSI UCN source  
UCM  
Ultra Cold Neutron Source

PNPI  
Petersburg  
Nuclear  
Physics  
Institute

NEUTRONS  
FOR SCIENCE

**Status August 2004:**

- 1) Introduction
- 2) Source principle
- 3) Solid deuterium containment
- 4) Solid deuterium
- 5) Diamond-like carbon
- 6) Conclusions

A collection of logos including the Paul Scherrer Institute (PSI) logo, the Petersburg Nuclear Physics Institute (PNPI) logo, the Neutrons for Science logo, and a historical document with a coat of arms.

PAUL SCHERRER INSTITUT PSI Ultra Cold Neutron Source

## The PSI UCN source

**Status August 2005:**

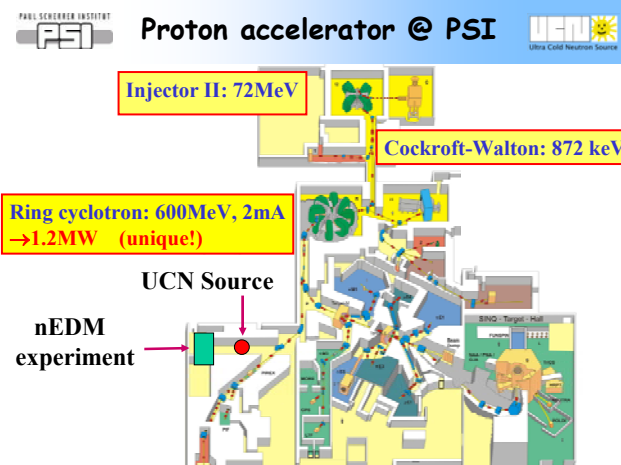
- 1) Introduction
- 2) Source principle
- 3) Solid deuterium containment
- 4) Solid deuterium
- 5) Diamond-like carbon
- 6) Conclusions

PNPI contributions (1998 – 2004) are gratefully acknowledged



PAUL SCHERRER INSTITUT PSI Ultra Cold Neutron Source

## Proton accelerator @ PSI



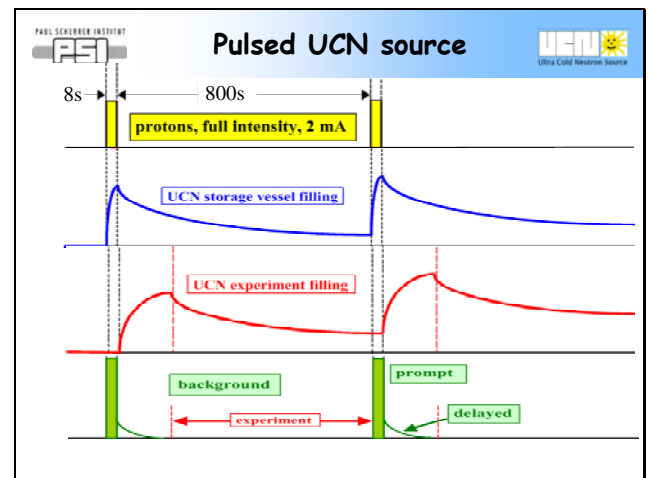
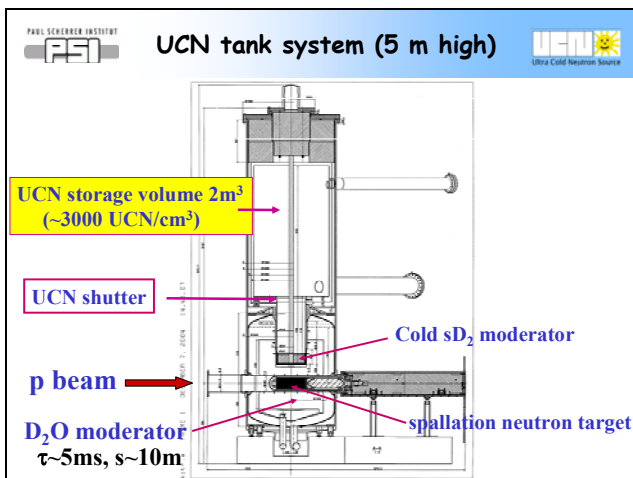
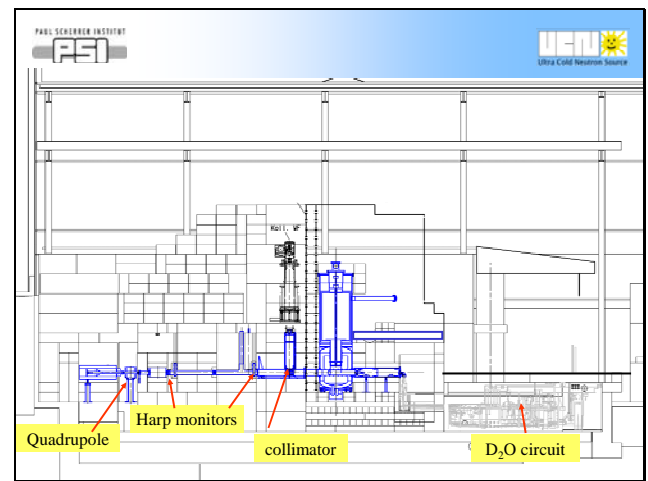
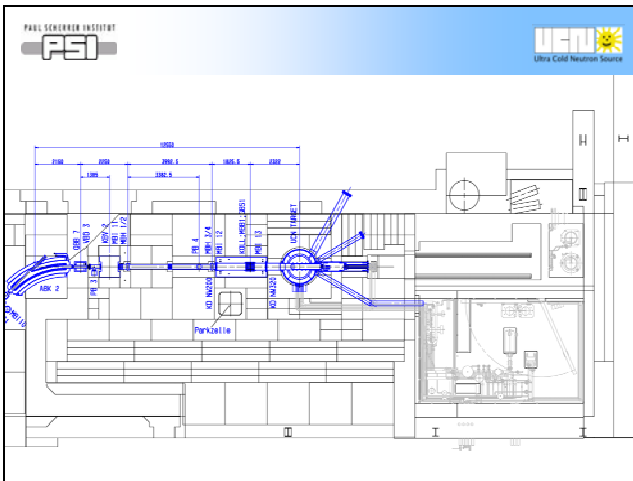
Injector II: 72MeV

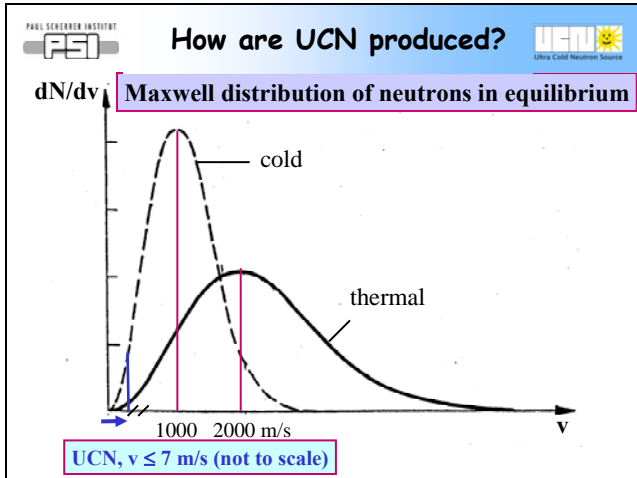
Cockroft-Walton: 872 keV

Ring cyclotron: 600MeV, 2mA  
→ 1.2MW (unique!)

UCN Source

nEDM experiment





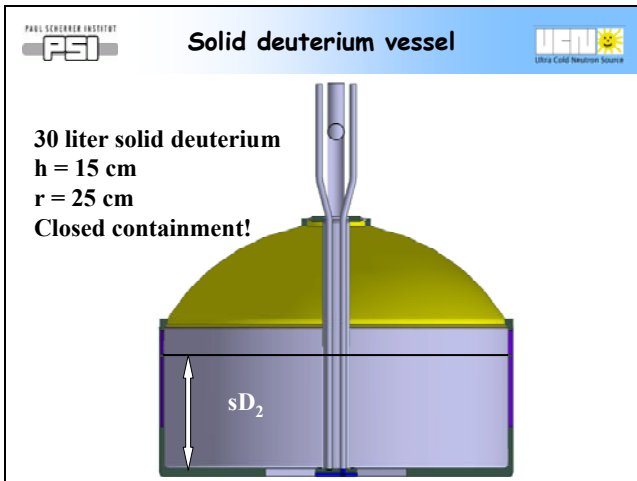
PAUL SCHERRER INSTITUT PSI Ultra Cold Neutron Source

### UCN densities @ PSI

At PSI UCN source in  $D_2O$ :  
 $\rightarrow \rho(UCN) = 8 \text{ UCN cm}^{-3}$  at  $T = 300\text{K}$

Measured gain factor at  $T = 5 \text{ K}$ : 1200  
 $\rightarrow \rho(UCN) = 9'600 \text{ UCN cm}^{-3}$  at  $T = 5\text{K}$

After extraction losses:  $\rho(UCN) \approx 3'000 \text{ UCN cm}^{-3}$   
 (confirmed by own experiments at PSI SINQ)  
 Remember at ILL:  $\rho(UCN) \approx 40 \text{ UCN cm}^{-3}$



PAUL SCHERRER INSTITUT PSI Ultra Cold Neutron Source

### UCN Transmission in Materials

Probability for a reaction:  $\omega \cdot \sigma$   
 $\omega$  : area density of scatter centers in the foil  
 $\sigma$  : absorption cross section of one scatter center

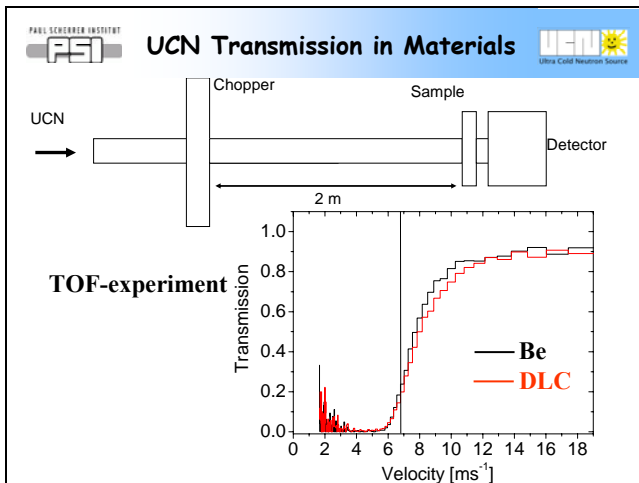
$\omega = L [\text{Mol}^{-1}] \cdot l [\text{cm}] \cdot \rho [\text{g/cm}^3] / A [\text{g/Mol}]$   
 $L$ : Avogadro's number  
 $l$ : foil thickness in cm  
 $\rho$ : density  
 $A$ : Atomic weight

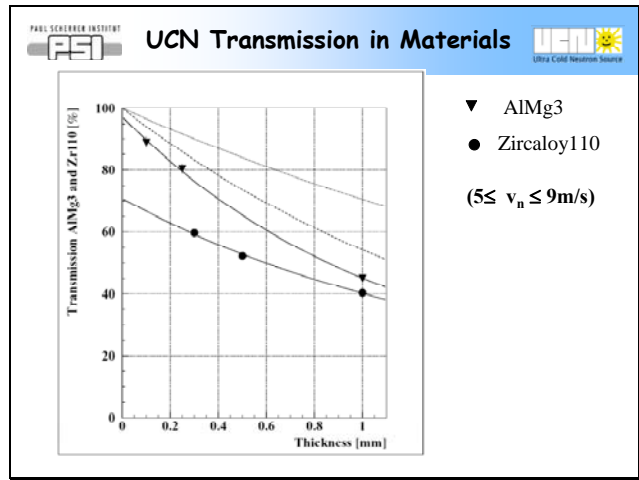
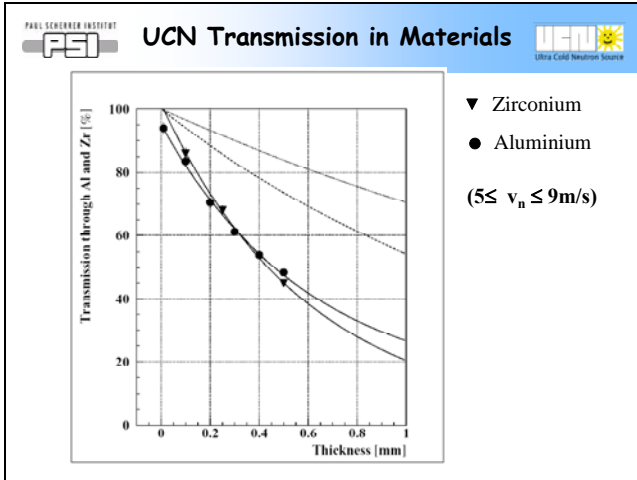
PAUL SCHERRER INSTITUT PSI Ultra Cold Neutron Source

### UCN Transmission in Materials

Probability for a reaction:  $\omega \cdot \sigma = L \cdot l \cdot \rho / A \cdot \sigma$

$\sigma_{Al} = 230 \text{ mbarn};$	$\sigma_{Zr} = 181 \text{ mbarn}$
$A_{Al} = 27;$	$A_{Zr} = 91;$
$\rho_{Al} = 2.7 \text{ g/cm}^3;$	$\rho_{Zr} = 6.5 \text{ g/cm}^3;$

$$\frac{(\omega \cdot \sigma)_{Al}}{(\omega \cdot \sigma)_{Zr}} \approx 1.8$$


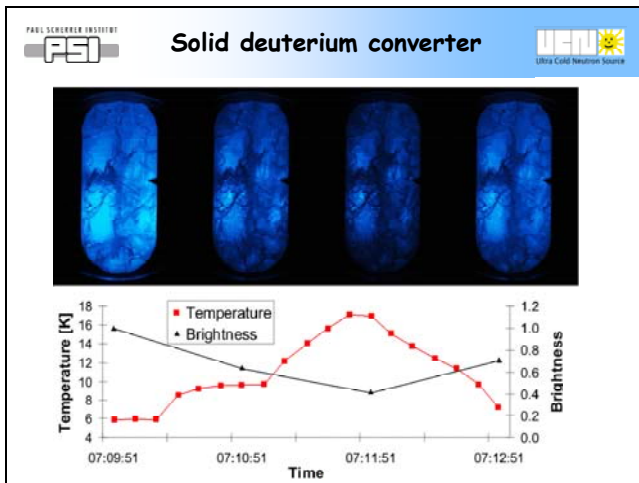
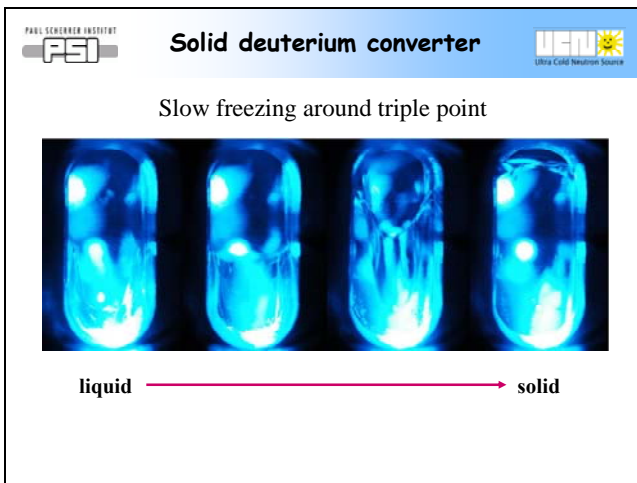
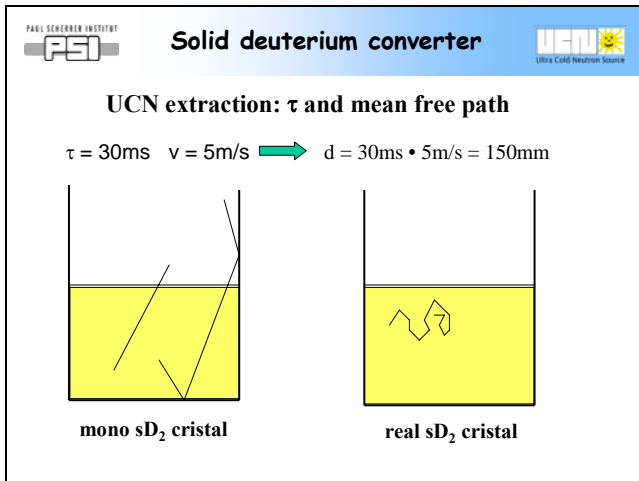


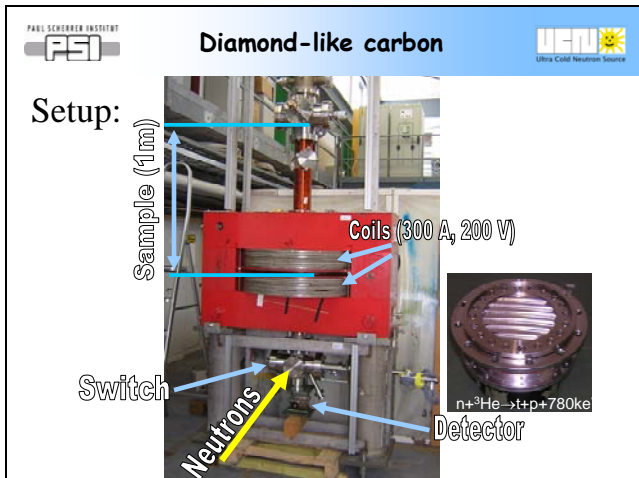
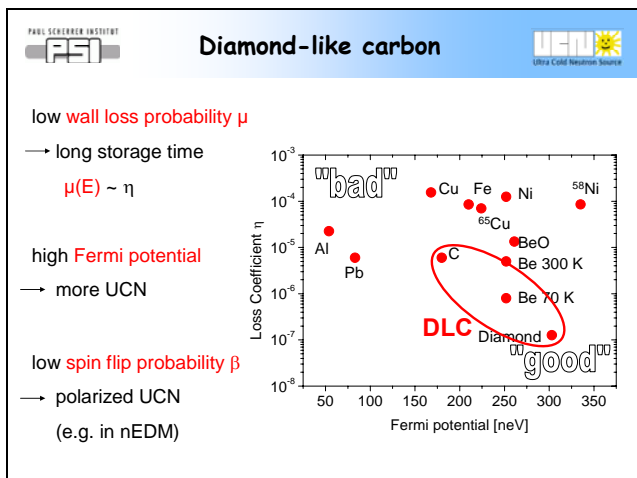
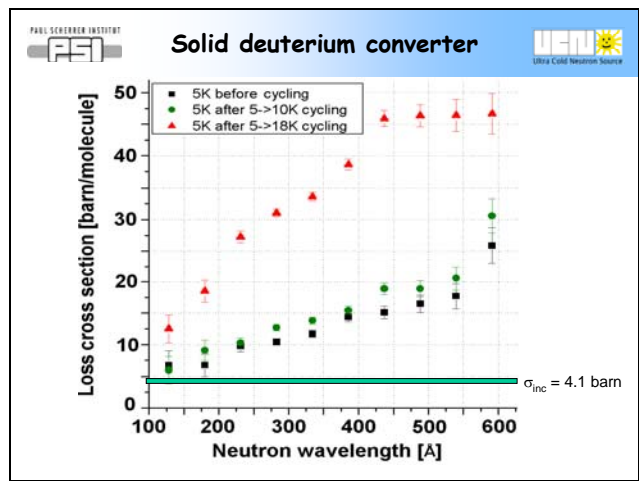
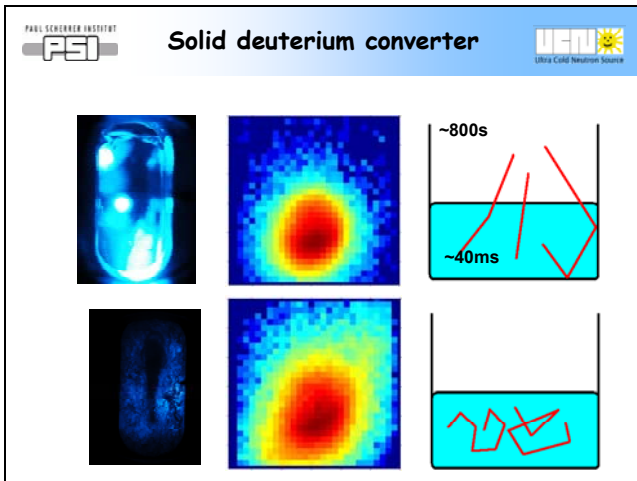
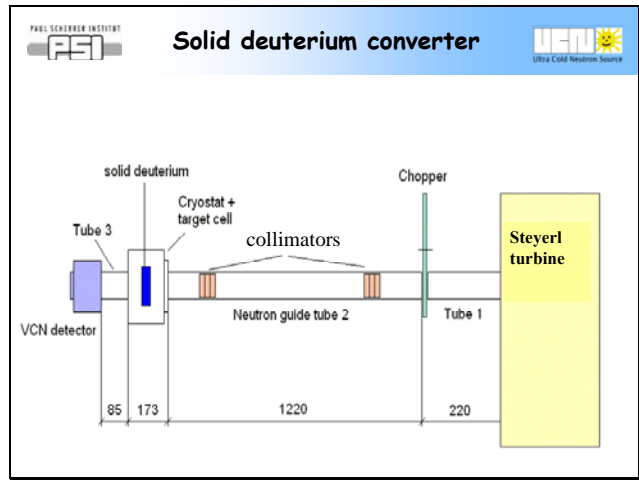
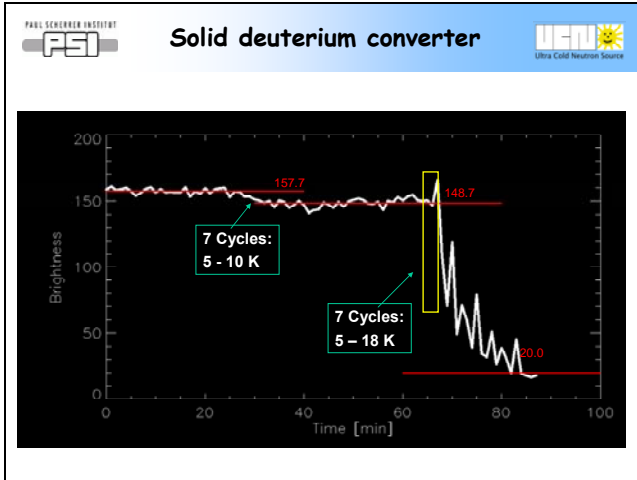
PSI PAUL SCHERRER INSTITUT Ultra Cold Neutron Source

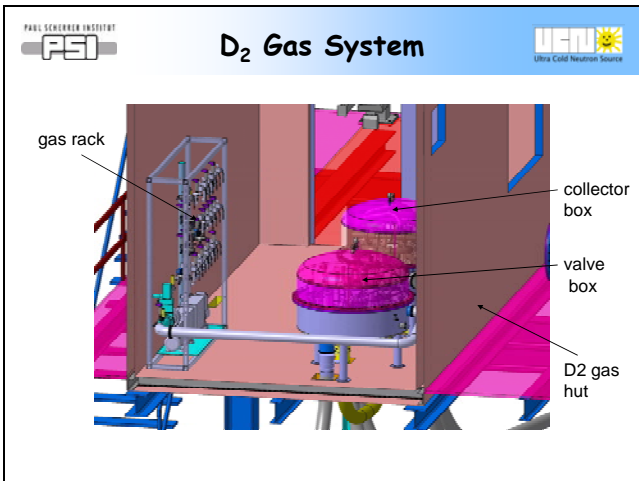
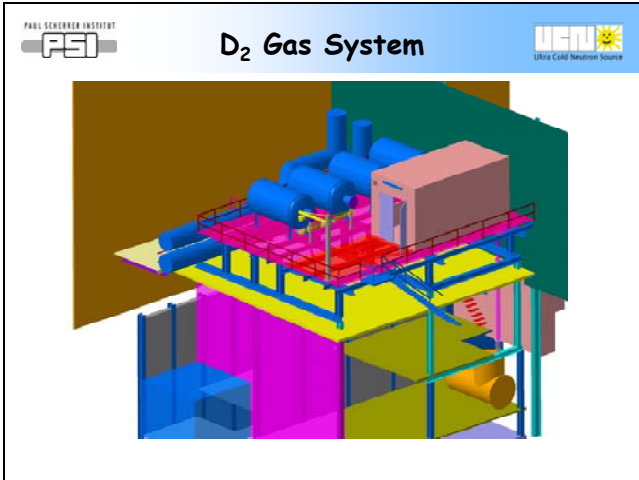
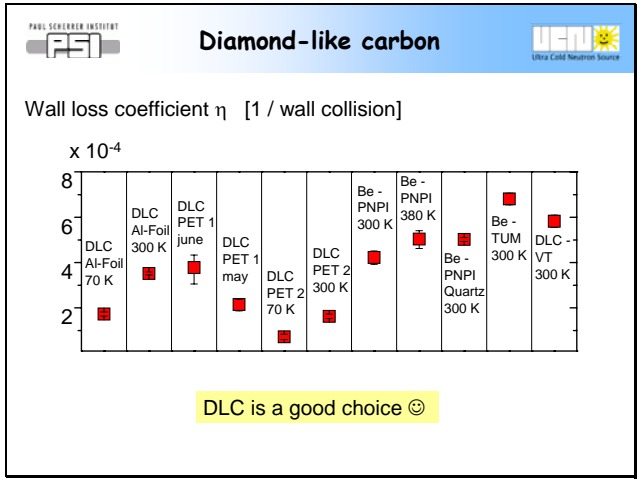
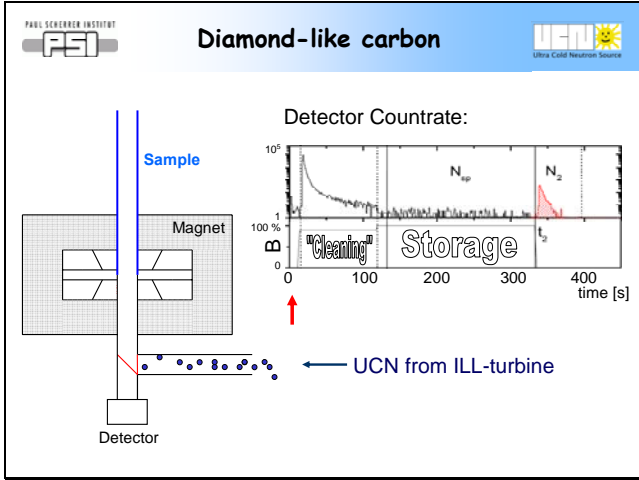
### UCN Transmission in Materials

**Conclusions:**

- ☺ AlMg3 seems to be an excellent (better!) choice.
- ➔ Investigate mechanical properties of AlMg3 for source vessel.
- ➔ Measure with AlMg3 of correct thickness (~0.5mm) and from various producers under various conditions.
- ♥ Higher transmission and less (political) stress!







PAUL SCHERRER INSTITUT  
PSI  
Ultra Cold Neutron Source

## D<sub>2</sub> Gas Hut

PAUL SCHERRER INSTITUT  
PSI  
Ultra Cold Neutron Source

## Isolation Vacuum System

vacuum system  
already integrated  
in containment

PAUL SCHERRER INSTITUT  
PSI  
Ultra Cold Neutron Source

## Proton beam to PSI UCN

January 2005

February 9, 2005

PAUL SCHERRER INSTITUT  
PSI  
Ultra Cold Neutron Source

## Shielding around UCN source

PAUL SCHERRER INSTITUT  
PSI  
Ultra Cold Neutron Source

## Per astra ad astra

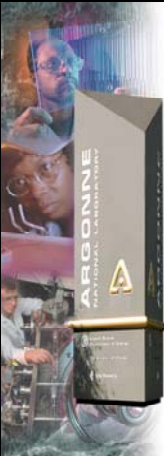
On the way to the top!



# Chun-Keung Loong

## Argonne National Laboratory

### VCNS: A Prelude of Instrument & Scientific Wishes



**VCNS: A Prelude of Instrument & Scientific Wishes**

Chun Loong [ckloong@anl.gov](mailto:ckloong@anl.gov)  
Intense Pulsed Neutron Source Division

The Very Cold Neutron Source Workshop  
August 22-24, 2005, Argonne

**Argonne National Laboratory**

A U.S. Department of Energy  
Office of Science Laboratory  
Operated by The University of Chicago

**VCNS**

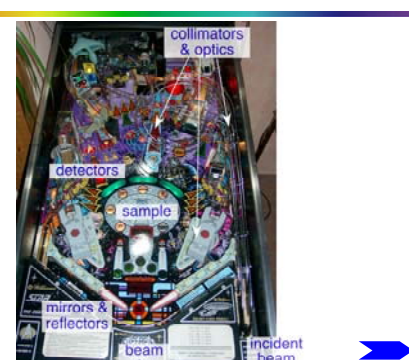
NEVER BEFORE HAD WE

- A machine dedicated to generate VCN fluxes peaked at  $\sim 190 \mu\text{eV}$  ( $\lambda=20.8 \text{ \AA}$ ) with a pulse width of 4 ms at 1-Hz pulsing rate, and
- A beamline and instrument suite optimized for time-of-flight scattering experiments aiming at a wide scope of scientific studies.

Interaction	Strength ( $\mu\text{eV}$ )
Nuclear	$0.157 \rho_{\text{g/cc}} a_{\text{m}} / A_{\text{amu}}$
Magnetic	$\pm 0.0603 B_{\text{T}}$
Gravitational	$0.1025 h_{\text{m}}$

The Very Cold Neutron Source Workshop, August 22-24, 2005, Argonne

**A VCN Instrument**



collimators & optics

detectors

sample

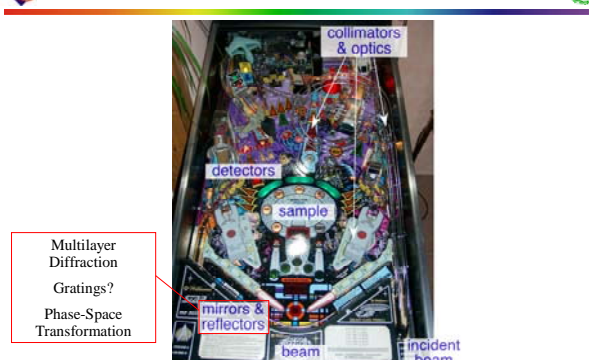
mirrors & reflectors

beam stop

incident beam

The Very Cold Neutron Source Workshop, August 22-24, 2005, Argonne

**Instrument Components - Phase-Space Manipulator**



collimators & optics

detectors

sample

mirrors & reflectors

beam stop

incident beam

Multilayer Diffraction

Gratings?

Phase-Space Transformation

The Very Cold Neutron Source Workshop, August 22-24, 2005, Argonne

### Instrument Components - Detectors

Beam Monitors & Position-Sensitive Detectors  
Micro-Strip Gas-filled?  
Scintillator-Type?

The Very Cold Neutron Source Workshop, August 22-24, 2005, Argonne

### Instrument Components - Optics

Choppers  
Collimators  
Focusing Lens  
Polarizers  
Supermirrors  
Spin Flippers & Analyzers

The Very Cold Neutron Source Workshop, August 22-24, 2005, Argonne

### Instrument Components - Sample

Thin Windows  
Thin Sample Geometry  
Sample Environments - Cryostats, Furnaces, xyz-Magnets,...

The Very Cold Neutron Source Workshop, August 22-24, 2005, Argonne

### Beamlines & Instruments

Very CN falls between CN (techniques reasonably developed) and Ultra CN (novel & rather for special-purposes)

Approaching from CN side =>

- Small-Angle Diffractometers
- Reflectometers
- Spin-Echo Spectrometers
- Inelastic-Scattering Spectrometers (Direct & Inverse Geometry)

Approaching from the UCN side =>?

The Very Cold Neutron Source Workshop, August 22-24, 2005, Argonne

### VCN: Challenges and Opportunities

**Severe multiple scattering:**  
=> to seek theoretical treatment, e.g., Barabanov & Belyaev; to learn from electron scatterers,...

**Enhanced interfacial sensitivity in complex, large structures:**  
=> Nanocomposites, biological systems, devices, catalysts, energy research related to hydrogen economy,...

**Higher (Q,E) resolution in spectroscopy:**  
=> Slow dynamics related to biological functions, highly-spaced energy structures of quasi-particle excitations, tunneling spectra,...

The Very Cold Neutron Source Workshop, August 22-24, 2005, Argonne

### VCN: Challenges and Opportunities (2)

SANS with lower  $Q_{im}$   
features due to extended-length sub-structure?

QENS connecting to NMR

Collective excitations  
carbon nanotubes  
AF spin ladder  
quantum liquid  
D/GM

Bio & nano assemblies  
Spintronics, devices, ...  
Polymer & protein dynamics  
Phonons, magnons, ...  
Molecular magnets, ...

Reflectivity with enhanced capability  
Incident  
Specular  
Off-specular  
Diffraction

Magnetic tunneling spectrum  
Intensity  
 $T=13.8K$

The Very Cold Neutron Source Workshop, August 22-24, 2005, Argonne

# Ferenc Mezei

## Los Alamos National Laboratory

### Some Instrument Ideas for a Pulsed Very Cold Neutron Source

Argonne, August 22, 2005

Some Instrument Ideas for a Pulsed Very Cold Neutron Source

F. Mezei  
Los Alamos National Laboratory & HMI, Berlin

---

August 22, 2005VCNS Workshop, F. MezeiPage 1

**Very Cold Neutron Source vs Cold Neutron Source**

- spectral temperature  $T_{\text{eff}} \sim T_{\text{cold}}/10$
- typical wavelength range: shifts from 6 - 10 Å to 20 - 30 Å
- optimal repetition rate shifts from 15 - 20 Hz to ~ 5 - 6 Hz

---

August 22, 2005VCNS Workshop, F. MezeiPage 2

**Wavelength scaling: on the long wavelength slope of a Maxwellian spectrum**

	Resolution for fixed geometry ( $\delta q$ or $\delta \omega$ )	Intensity for fixed resolution ( $\delta \Omega_{\text{in}} \delta \Omega_{\text{out}} \delta \lambda$ f c)
SANS	$\lambda^{-1}$	$\lambda^0$
Reflection	$\lambda^{-1}$	$\lambda^{-2}$
TOF inelastic	$\lambda^{-3}$	$\lambda^2$
NSE	$\lambda^{-3}$	$\lambda^{-4} - \lambda^{-2}$

---

August 22, 2005VCNS Workshop, F. MezeiPage 3

**WCNS provides long pulses ( $\geq 4$  ms)**

- Equal  $\lambda$  resolution to cold coupled moderators at shifted wavelength needs ~ 2.5 ms → **pulse shaping required**
- Optimal TOF spectrometer pulse repetition rate on sample: 25 - 40 Hz → **Repetition Rate Multiplication required**

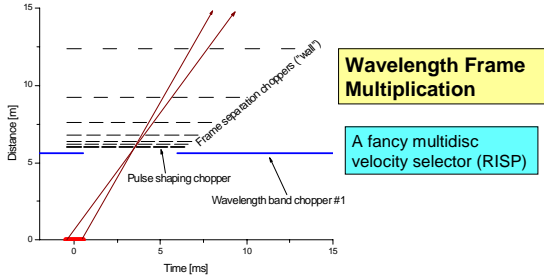
Proposed & developing LPSS techniques can be useful.

---

August 22, 2005VCNS Workshop, F. MezeiPage 4

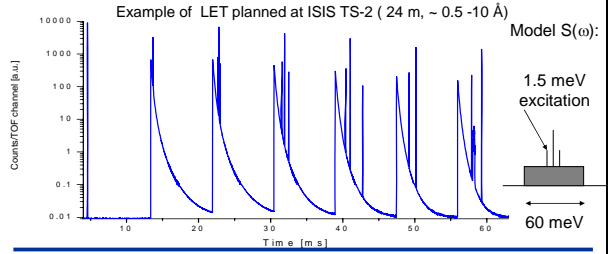
**Pulse shaping for elastic scattering is easier to implement for extended pulse length**

Multiplexing chopper system: reduced number of frame separation choppers (~ 4 for 4 ms, instead of ~ 8 for 1.5 ms pulses)



**Repetition Rate Multiplication provides for TOF spectroscopy**

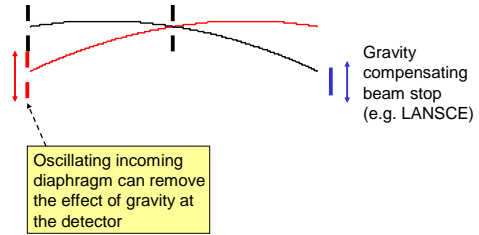
- a) Pulse shaping to achieve very high resolutions (~ 0.2  $\mu\text{eV}$  at primary pulse length ~ 100  $\mu\text{s}$ )
- b) ~ 5 times enhanced intensity



**Gravity:**

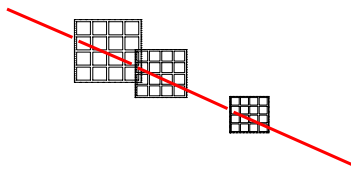
For 20 Å the drop is 1.25 cm over 10 m:  
 a manageable concern for SANS  
 OK for guides

Gravity: direct beam center position is a function of wavelength (variation typically 1 - 5 cm)



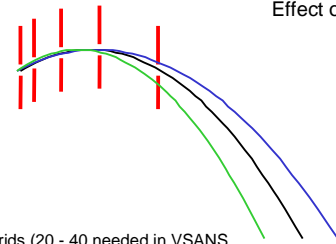
**Development for ESS / CW cold source application**

multiple beam focussed on the same spot on detector for enhanced intensity for 1-2 mm size pinholes)



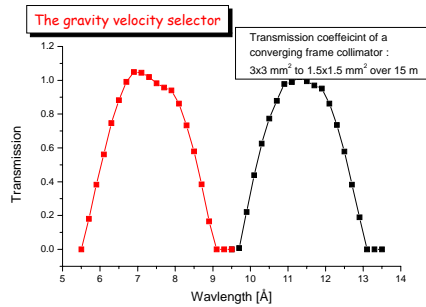
Based on established pin hole approach: **enabled by** modern high precision manufacturing (ESS, being built at HMI)  
 Gravity effects enhanced for cold neutrons: similar to VSNS with ordinary size pin holes

Effect of gravity:

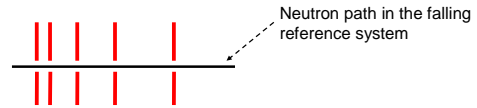


The grids (20 - 40 needed in VSANS with cold neutrons, less for VCNS) can be adjusted to the parabolic neutron paths in a **(narrow) wavelength range**

Converging grid collimator is a good and cheap **velocity selector** for continuous source VSANS (HMI project)



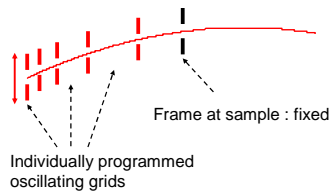
**Solution for broad band pulsed source applications:**  
**"Relativistic collimator":** neutron weightlessness in accelerating (free falling) collimator



Oscillatory motion of collimator electronically driven to impose **constant acceleration g** for part of the 60 ms frame

40 ms free fall per pulse period means < 2 mm amplitude of oscillation

Alternative gravity compensating approach:  
 individually controlled oscillating grids to keep beam at sample and direct beam spot on detector fixed for all wavelengths



### Partial summary

Very cold neutrons (VCN) with  $E \sim 0.1 - 0.2$  meV are available today with low intensity at cold sources and used to a limited extent. Assuming established instrumentation approaches:

- a) The use of VCN is particularly advantageous in inelastic spectroscopy both to enhance intensity at constant resolution (TOF) and to extend resolution limits (TOF & NSE). Here enhanced VCN flux will open up **new opportunities**.
- b) Enhanced flux will make the use of VCN **advantageous** in SANS where there is no clear advantage for VCN at existing sources. Instrumentation concepts developed for Long Pulse Spallation Sources (pulse shaping, repetition rate multiplication,...) are crucial for instrument design at a pulsed VCN source.



# Lee Makowski

## Argonne National Laboratory

### Neutron Diffraction Studies of Biological Specimens

#### Neutron diffraction studies of biological specimens

Lee Makowski

#### Advantages and Disadvantages

- Advantages
  - H/D Contrast Difference
  - H<sub>2</sub>O/D<sub>2</sub>O Exchange
    - solvent accessible space
    - distribution of protein; nucleic acid; lipids
  - Specific isotopic labeling (crystals/non-crystalline)
  - Localization of protons (crystallographically)
- Disadvantages
  - Low contrast
  - Need for large specimens
  - Inelastic H scattering

#### Example

- Studies of filamentous bacteriophages M13 and Pf1
- Helical assembly of coat proteins
- Carried out at HFBR in late 80's; early 90's
- 100% D<sub>2</sub>O
- Isotopically labeled proteins
- Magnetically oriented specimens

#### Pf1 Bacteriophage

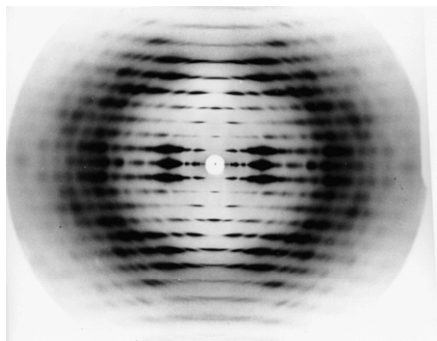
**1.8 microns long**  
**~65 Å diameter**  
**(proportions of a 10 foot pencil)**

**~5000 copies of a small**  
**(46 residue) protein**  
**(~4500 mw)**

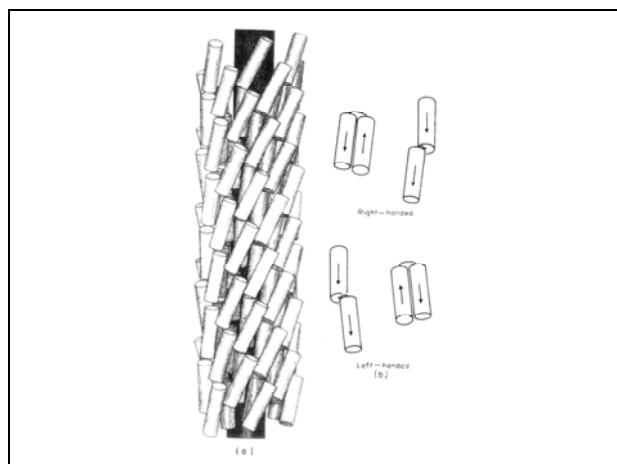
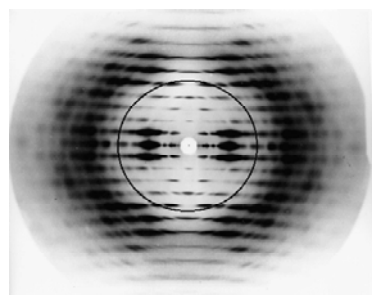
M13 (close relative)



## Fiber Diffraction from Non-crystalline Specimens



## 7 A data is just the start...



## Neutron Diffraction of Specifically Deuterated Pf1

Deuterated at:

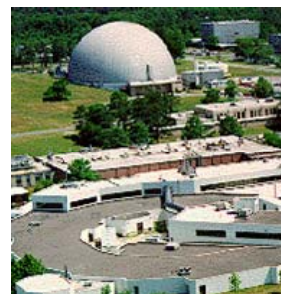
met (2)

val (5)

tyr (2)

ile (6)

to aid in model building



### Specimen Preparation:

Virus grown with deuterated amino acids to incorporate into virus particle  
valine; tyrosine; methionine; isoleucine

Specimens in 100% D<sub>2</sub>O

Liquid crystals of the virus prepared in 0.5 cm optical path quartz  
spectrophotometer cells in 2% acrylamide

Oriented in a 6.3 T magnetic field

UV irradiated while in the magnetic field to polymerize the acrylamide

Specimens removed from magnetic field did not disorient

### Data Collection

Used HFBR; protein crystallography beam line (Benno Schoenborn)

2d detector set with beam at one corner (to collect one quadrant)

Collected data from water for several hours to determine distribution of detector  
sensitivity

$\lambda = 1.615$  angstroms

Collected each specimen for 24 hours

native virus (no specific deuteration)

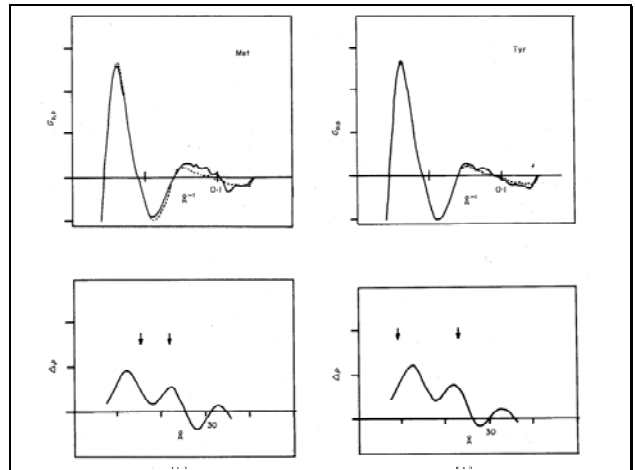
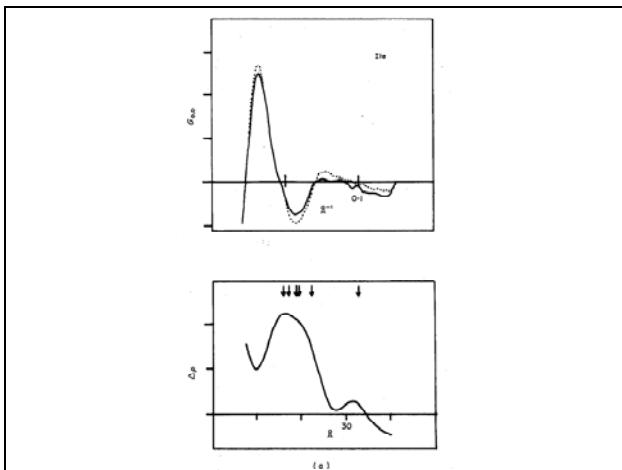
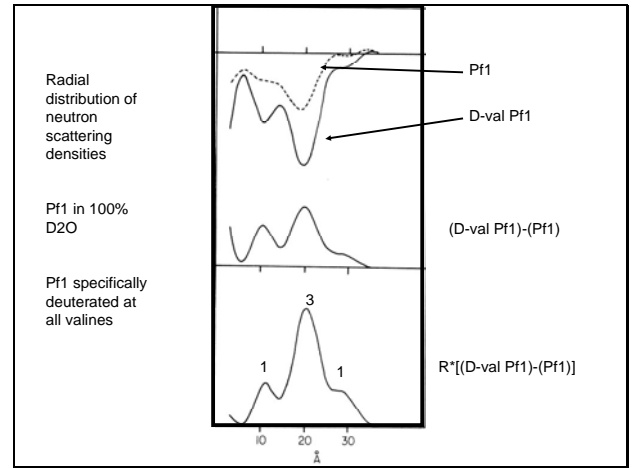
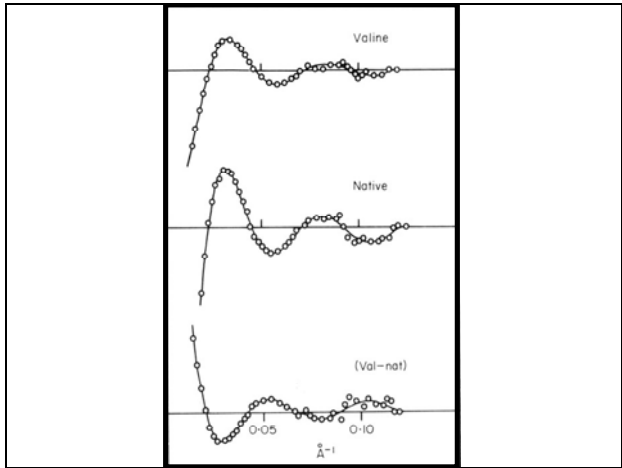
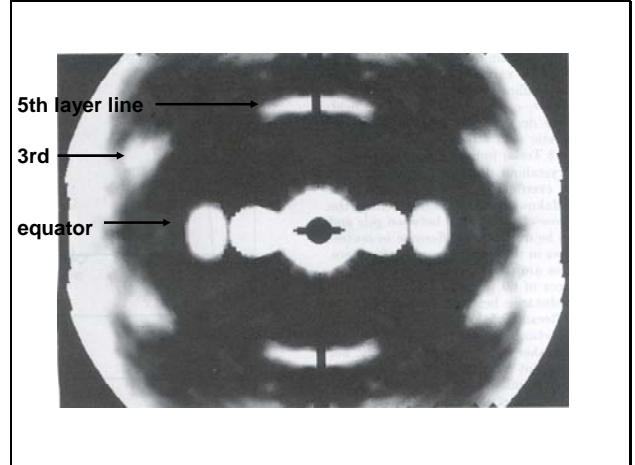
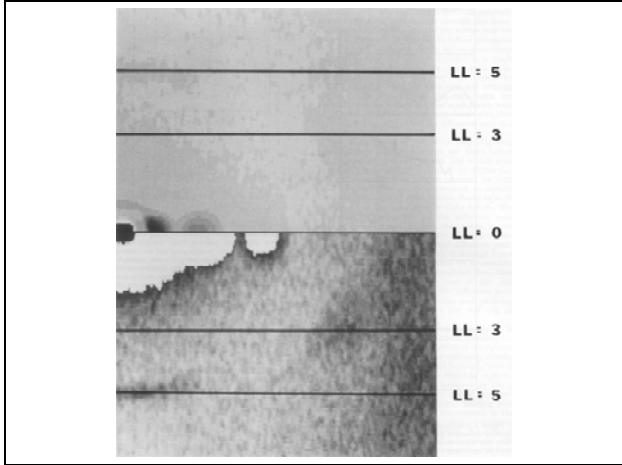
virus specifically deuterated at all valine; methionine; isoleucine; tyrosine

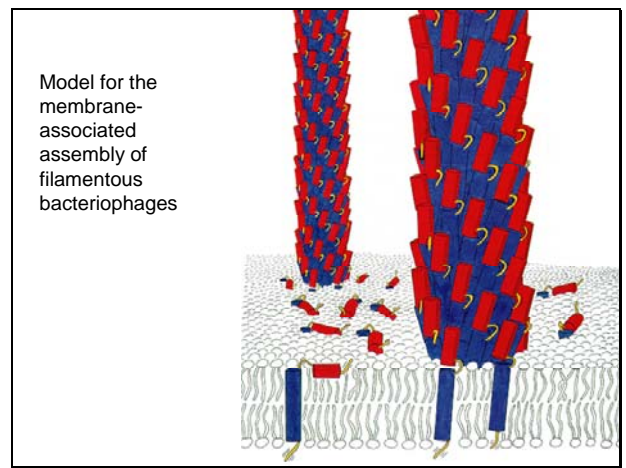
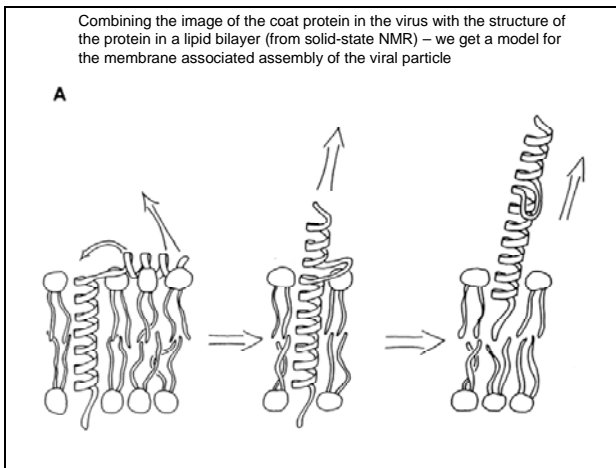
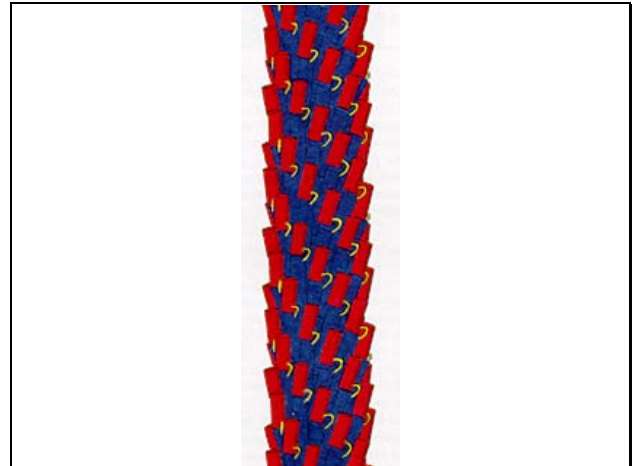
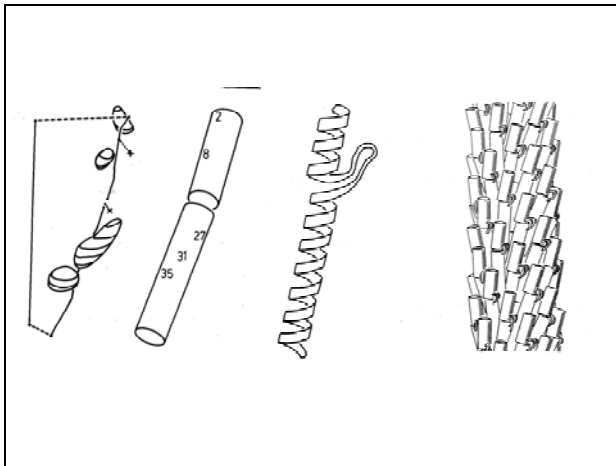
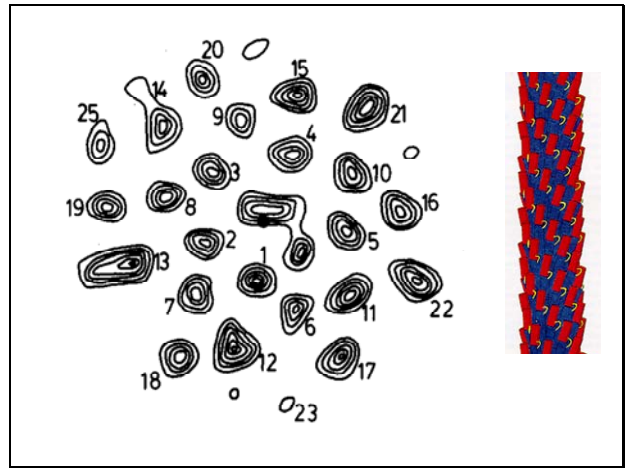
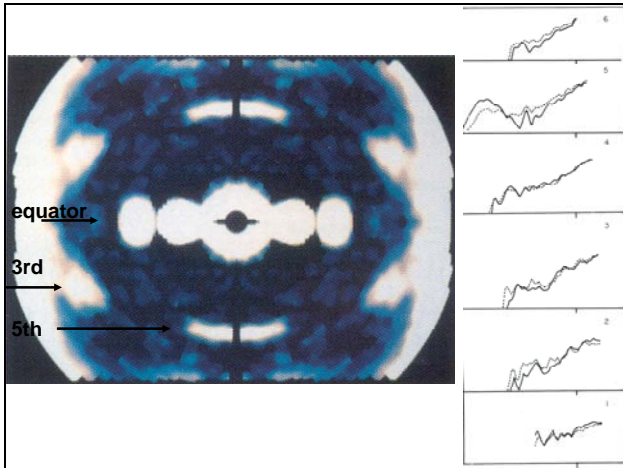
### Data Processing

Corrected detector data for sensitivity distribution

Averaged the data onto a polar coordinate system in reciprocal space

Carried out angular deconvolution to separate the contributions from different layer lines





# R. Kent Crawford

## Oak Ridge National Laboratory

### Some Considerations for Neutron Scattering at a Very Cold Neutron Source

Very Cold Neutron Source Workshop Aug 2005 

**Some Considerations for  
Neutron Scattering at a Very Cold Neutron  
Source**

**R. Kent Crawford**  
*Instrument Systems Group Leader*  
**SNS**

---

OAK RIDGE NATIONAL LABORATORY  
U. S. DEPARTMENT OF ENERGY

1 

Overview 

- Current and proposed capabilities at SNS
- Gaps in scientific capabilities
- Instrumentation opportunities and challenges

---

OAK RIDGE NATIONAL LABORATORY  
U. S. DEPARTMENT OF ENERGY

2 

The Spallation Neutron Source 




---

OAK RIDGE NATIONAL LABORATORY  
U. S. DEPARTMENT OF ENERGY

3 

SNS High Power Target Station (HPTS) 

Current Planned Power	1.4 MW
Power After Upgrade	>2 MW
Frequency	60 Hz
Moderators	
• Poisoned decoupled ambient water	8 beams
• Poisoned decoupled supercritical hydrogen (~22 K)	8 beams
• Coupled supercritical hydrogen (~22 K)	8 beams

Whole moderator face, coupled hydrogen moderator @ 1.4 MW  
 -- Flux at moderator face (n/sr/sec/Å) [from [http://www.sns.gov/users/instrument\\_systems/components/data/moderator/HPTS-scl/sourcefiles/source\\_scl21a\\_td\\_05\\_1.dta](http://www.sns.gov/users/instrument_systems/components/data/moderator/HPTS-scl/sourcefiles/source_scl21a_td_05_1.dta)]

10 Å	20 Å	40 Å
$2.5 \times 10^{12}$	$1.1 \times 10^{11}$	$2.0 \times 10^9$

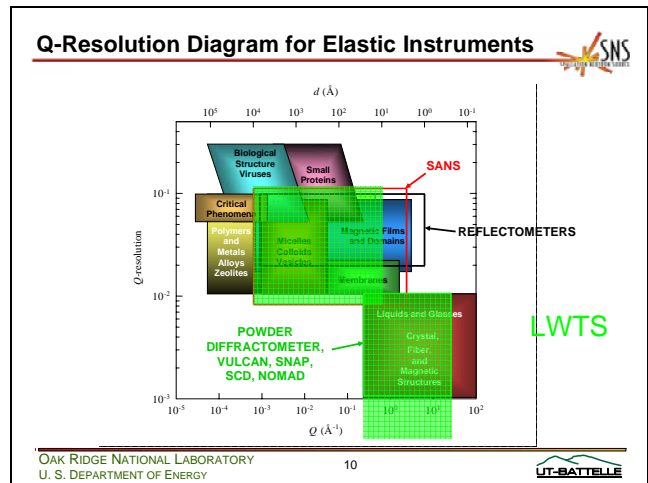
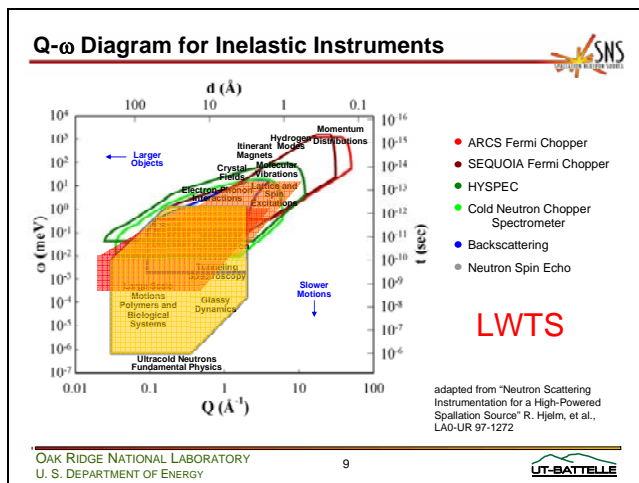
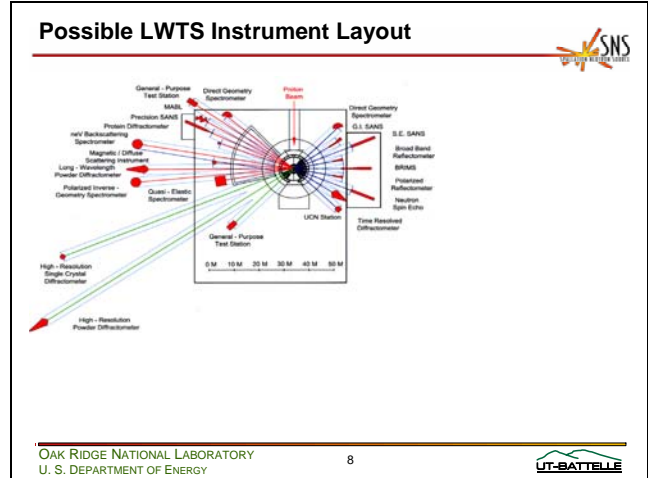
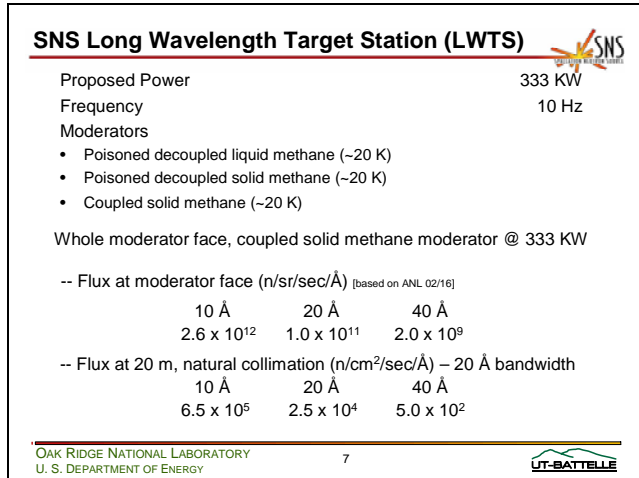
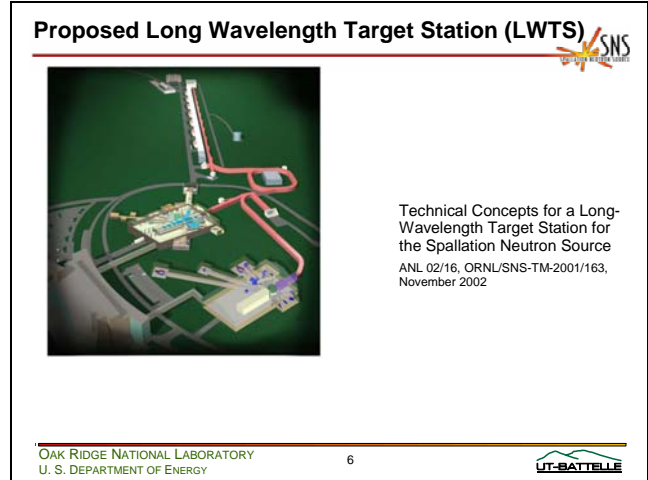
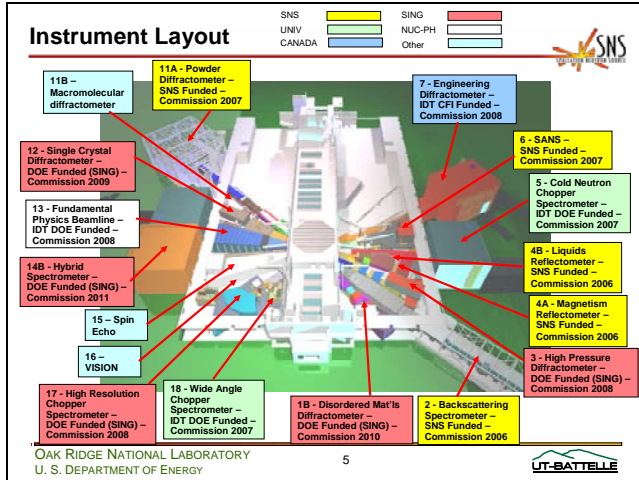
-- Flux at 20 m, natural collimation (n/cm<sup>2</sup>/sec/Å) – 3.3 Å bandwidth

10 Å	20 Å	40 Å
$6.3 \times 10^5$	$2.8 \times 10^4$	$5.0 \times 10^2$

---

OAK RIDGE NATIONAL LABORATORY  
U. S. DEPARTMENT OF ENERGY

4 



## Summary of SNS-HPTS and SNS-LWTS



- Both cover very broad range of science, using neutrons out to moderately long wavelengths.
  - SNS-HPTS to be completed next spring
  - SNS-HPTS currently funded for construction of 15 instruments
  - SNS-LWTS feasibility study only at this time
- SNS-LWTS calculated performance significantly exceeds SNS-HPTS performance at long wavelengths, even though SNS-LWTS uses much less beam power.
  - Efficient neutronics arrangement
  - Advanced moderator concepts

## Areas not fully covered



- Larger objects
  - Critical phenomena
  - Polymers
  - Biological structures
  - Complex structures (e.g., rocks)
  - Nanoscale materials
- Slower motions
  - Polymers
  - Biological systems

## Potential VCNS Strengths

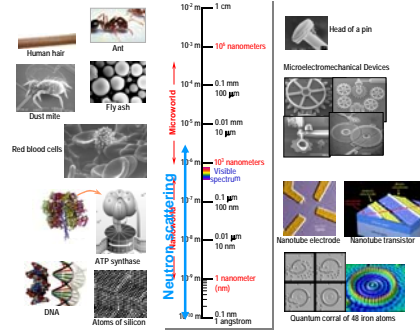


- High peak flux at long wavelengths ( $\sim 10 - 40 \text{ \AA} ?$ )
- High time-averaged flux at long wavelengths
- Very broad wavelength range
- Time structure of source
- New types of instruments

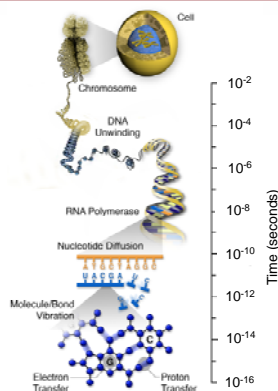
## Neutrons probe a broad range of length scales



Nanoscale science and technology presents extraordinary opportunities



## Neutrons probe a broad range of time scales



## Large structures and long times suggest -



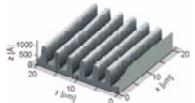
Nanoscience

Need broad range of distances  
and times to get the full picture

## Magnetic Nanostructures



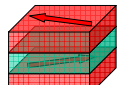
>10's of micron to micron ( $10^{-4}$  –  $10^{-6}$  m) – **Domains**  
Large Lateral Magnetic Domains in Co/CoO



Micron to Submicron ( $10^{-6}$  –  $10^{-8}$  m) – **Lithography**  
Off-Specular Scattering of Patterned Arrays



Submicron to Nano ( $10^{-7}$  –  $10^{-9}$  m) – **Self-Assembly**  
SANS Measurement of Self-Assembled Nanoparticles



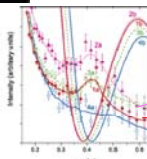
Nano to Angstrom ( $10^{-9}$  –  $10^{-10}$  m) – **Interfaces**  
Specular Reflection from magnetic multilayers

## Chemistry in Confined Geometries

### Water confined in nanotubes



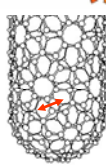
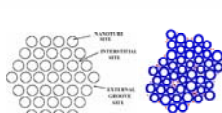
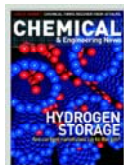
Derived from a combination of Neutron Diffraction and Inelastic Neutron Scattering



D<sub>2</sub>O in nanotube  
dry nanotube  
H<sub>2</sub>O in nanotube

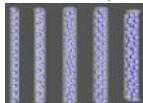
A. I. Kolesnikov et al.: Phys. Rev. Lett. **93** (2004) 035503

## Hydrogen Storage in Nanotubes and Zeolites



- Experiments are intensity limited
- Impossible experiments
  - Parametric Studies
    - Guest-Host Interactions
      - Low Concentration
      - High Pressures
    - Other adsorption sites
      - D<sub>2</sub>, CO<sub>2</sub>, ...
    - New Phases
    - New Effects
      - Tube diameters
      - Wall Rigidity

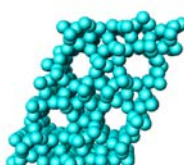
Encapsulated Hydrogen behaves differently



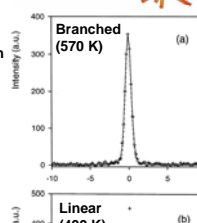
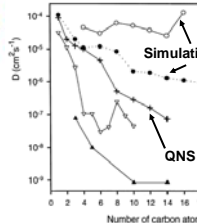
At SNS:  
Backscattering  
Vision

P. Sokol  
Chunlong

## Diffusion in Zeolites – Quasielastic Neutron Scattering (QNS)



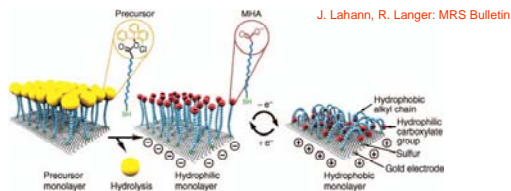
View down the 5.5 Å diameter channels of ZSM-5



- Alkane diffusion in zeolites studied by QNS using the backscattering spectrometer IN-16 at the ILL – H. Jobic, J. of Molecular Catalysis A-158 (2000) 135-142.
- Long n-alkanes diffuse slower than shorter ones with no plateau effect as predicted by simulation methods.
- On the microscopic length scale of these measurements, branched alkanes (CH(CH<sub>3</sub>)<sub>2</sub> – 570 K) diffuse much more slowly than n-alkanes (CH<sub>3</sub>(CH<sub>2</sub>)<sub>6</sub>CH<sub>3</sub> – 400 K)

## Biomimetics – functional surfaces

### Dynamically Controlled Surface Properties (T, pH, Light, V, etc.)



### Applications:

- Biosensors
- Microfluidic devices (valves, reservoirs)
- Structural templates for tissue engineering
- Drug delivery
- Study of cell/cell and cell/protein interactions

## Instrumentation Challenges

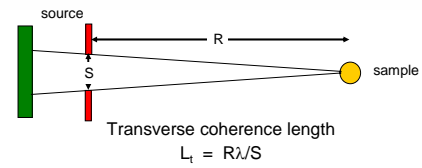
- Windows
  - Absorption can be a problem  $1/e$  distance in Al =  $718 (1.8/\lambda)$  mm = 65 mm @ 20 Å
- Detectors
  - Need very thin windows in many cases
- Gravity
  - Wavelength-dependent deflection of neutrons
  - 20 Å neutron drops ~5 cm in 20 m

## - and Opportunities

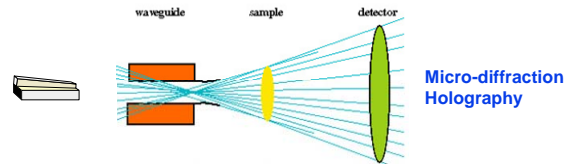


- New component possibilities
  - Efficient semiconductor detectors
  - Many options for focusing
- New types of instrumentation
  - Coherent beams?

## Coherent Beams



### Phase contrast microscopy



## Summary



- VCNS needs to provide capabilities not provided elsewhere
- Many opportunities in nanoscience and other areas
- Exciting new possibilities in instrumentation and in source development



Jyotsana Lal

Argonne National Laboratory

Structure and Dynamics in Complex Systems

**ARGONNE**  
NATIONAL LABORATORY

Jyotsana Lal  
Argonne National Laboratory  
Structure and Dynamics in Complex Systems

Presented at:  
Workshop On Applications of a Very Cold Neutron Source  
August 21-24, 2005  
Argonne National Laboratory  
Argonne, IL

The information presented here has been created by the University of Chicago as Operator of Argonne National Laboratory ("Argonne") under Contract No. W-31-109-ENG-38 with the U.S. Department of Energy. The U.S. Government retains the right and certain other rights in this material. All other rights, including copyright, are reserved by the University of Chicago. Information on this material is available in the public domain, and permission is granted to reproduce, prepare derivative works, distribute copies to the public, and perform publicly and display publicly, in whole or in part.

THE UNIVERSITY OF CHICAGO  
Office of Science

Argonne National Laboratory is managed by  
The University of Chicago for the U.S. Department of Energy

### Very Cold Neutrons

Energy (E) scales: MeV (10<sup>6</sup> eV), 1 eV, meV (10<sup>-3</sup> eV), μeV (10<sup>-6</sup> eV), neV (10<sup>-9</sup> eV)

Temperature (T) scales: 10<sup>6</sup> K, 10<sup>3</sup> K, 10<sup>2</sup> K, 1000 K, 10<sup>2</sup> K, 1 K, 0.1 K, 0.01 K, 1 mK, 100 μK, 10 nK

Wavelength (λ) scales: 100 fm, 0.1 Å, 1 Å, 10 Å, 100 Å, 1000 Å, 1 μm

Neutron types and characteristics:

- fast neutron: nuclear reaction
- epithermal neutron
- thermal neutron: room temperature, λ=1.8 Å, v=2200 m/s
- cold neutron
- very cold neutron
- ultracold neutron: total reflection, λ=570 Å, v=7 m/s

300 kW proton beam, 4-msec pulse width and 1-Hz pulsing frequency

The energy of 2.2K neutrons is 190 μeV, the wavelength is 20.8 Å, speed is 190 m/s

Will serve applications in studies of large structures and slow motions.

### (Modulated Intensity Small Angle Neutron Scattering)

## A Hybrid Instrument-MISANS

Diagram labels: n, e, L<sub>1</sub>, L<sub>2</sub>, L<sub>s</sub>, polarizer, NRSE coils in magnetic screen, vacuum tube, sample, scintillation detector with space and time resolution, analyzer.

Intensity varies sinusoidally with a frequency up to 2MHz. Its contrast is a measure of the quasielastic scattering.

$$L_2 = L_1 \omega_e / (\omega_s - \omega_e)$$

$$\tau_{MIEZE} = 4(\omega_s - \omega_e) \frac{\hbar L_s}{m v^3}$$

M. Bleuel & R. Gähler

### Exploring the static and dynamic phase space

Phase space plot showing Frequency (Hz) and Energy (eV) on the y-axis (log scale from 10<sup>-14</sup> to 10<sup>16</sup>) and Wavelength (Å) and Wavevector (Å<sup>-1</sup>) on the x-axis (log scale from 10<sup>-7</sup> to 10<sup>1</sup>).

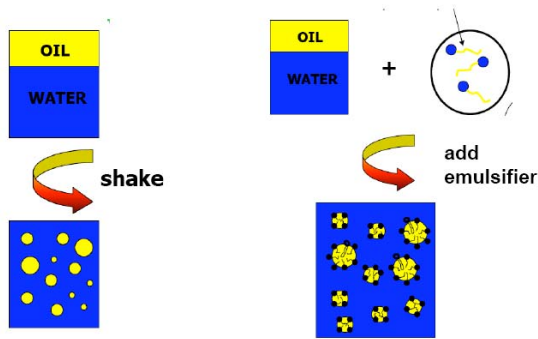
Regions identified: Raman Scattering, Brillouin Scattering, Laser PCS, X-Ray PCS, Inelastic X-Ray Scattering, Inelastic Neutron Scattering, MISANS.

Instrument details at a VCN source-MISANS: Has high energy resolution (sub-neV); measures relaxation times in (~500) nanoseconds at small angles 10<sup>-1</sup> to 10<sup>-4</sup> Å<sup>-1</sup>.

Unique Features:

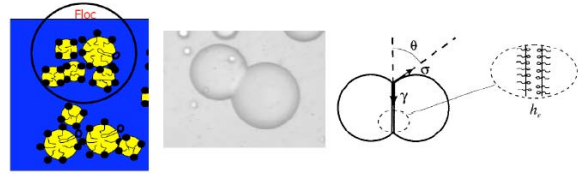
- Unique capability to measure structure and slow dynamical processes in condensed matter systems measuring directly S(q,t).
- Has polarized beam at sample - easier to measure magnetic & hydrogen containing samples.
- Capitalizing on H/D contrast unique to neutron scattering.

### Vesicles and large colloidal particles, emulsions droplets and foams



### Foculation & Ostwald ripening

Attractive Van der waals forces between droplets become larger than repulsive (electrostatic or steric).



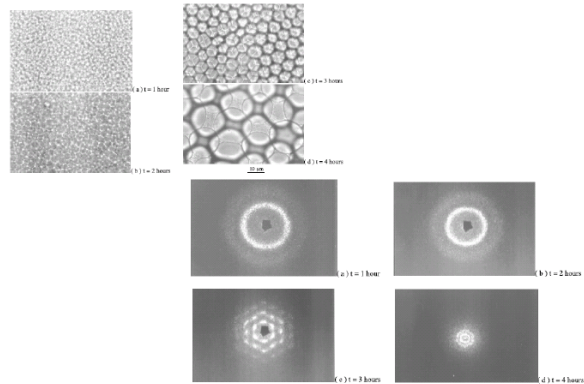
Big droplets eat smaller one. The pressure in small droplets is larger than large ones. So oil droplets coalesce to big ones where stress is lower.

Finally film rupture and droplet fusion takes place-phase separation

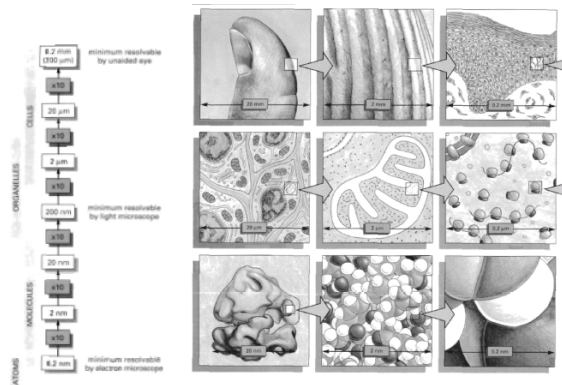
### Applications of coalescence phenomena

1. Major problem in Petroleum Industry-dehydration of crudes (water in oil emulsions).
2. Food industry-stability must remain over many months.
3. Cosmetic Industry-creams and emulsion must remain stable
4. In biology-adhesion and budding of cells.
5. Drug delivery -vesicles or liposomes must remain stable as they circulate in the bloodstream

### Droplet Size evolution at Various times



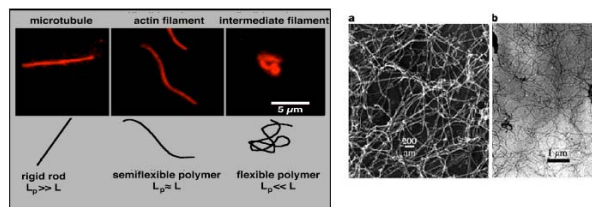
### The sizes of cells & their component parts



### Polymer networks in cell biology

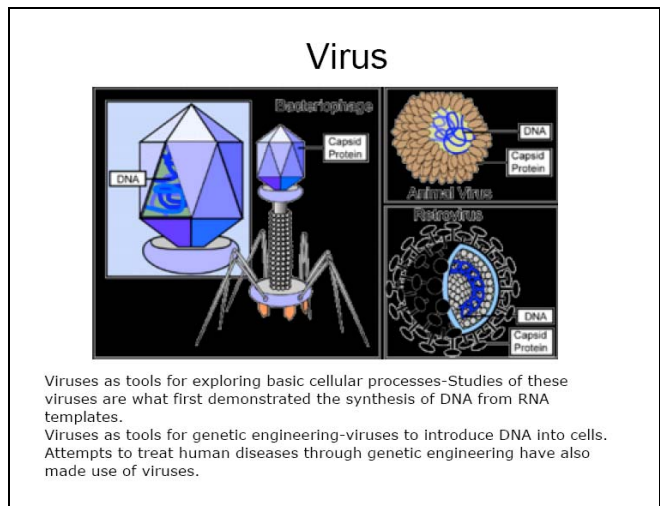
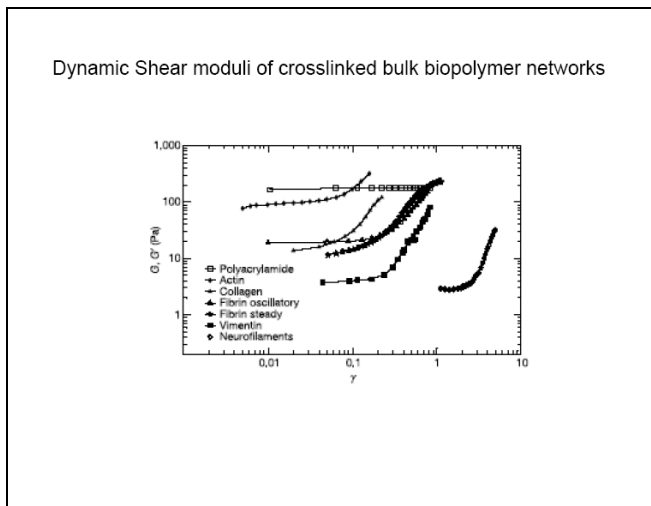
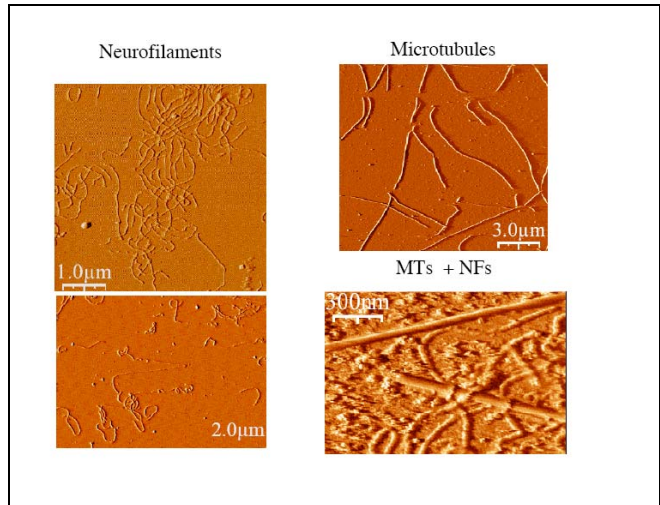
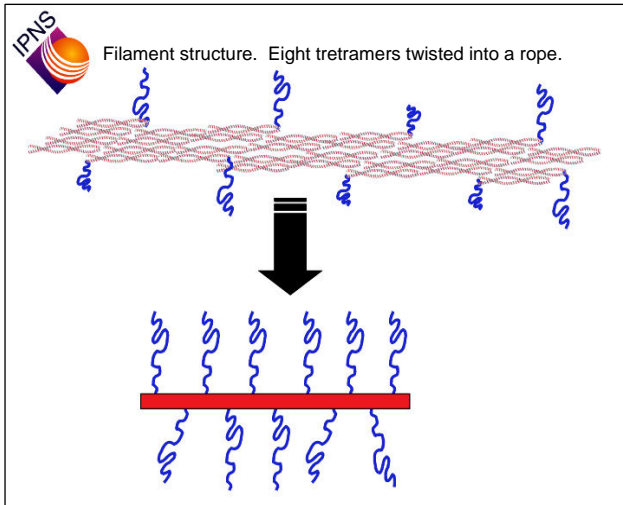
Networks of filamentous polymers are a common feature of cells and biological tissues.

Biological polymers, especially those derived from the cytoskeleton, attractive materials by which to test theories of polymer physics



Example of cytoskeletal filaments

Neurofilament and fibrin protofibril networks



Gene therapy is a method of correcting genetic defects via transfection, replacing the missing or defective genes with a healthy, foreign piece of DNA into the nucleus.

To optimize the delivery of foreign DNA into the nucleus of cells in gene therapy

There are two general methods of transfection: physical and carrier.

Goal-To better understand the interactions between the positively charged lipid DNA complexes and the cell wall & the various organelles within the cell.

### neutron optical devices

- all of which work better at long than at short wavelengths.

$$n = \frac{k_n}{k} = 1 - \frac{\chi^2}{2\pi} Nb$$

as  $n$  will differ more from 1. This leads to, for example better focusing with cold neutron with multiple biconcave  $MgF_2$  & magnetic lenses

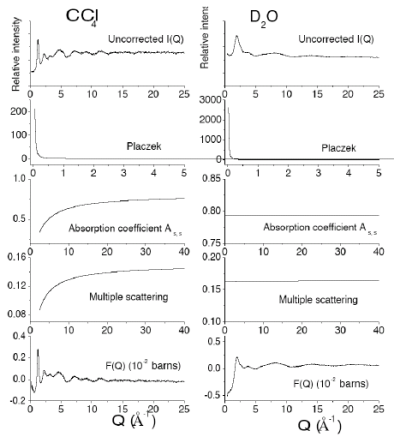
- As  $\lambda$  increases can use Bragg optics from artificial structures such as multilayers or diffraction gratings at grazing incidence (diffract from periodicity of layers instead of atoms)
- Phase definition is better

K. Littrell

In the low energy limit - where neutron velocity is slow compared to atomic collisions

Gravity will play a significant role

C. Benmore



Elegant way of using multiple scattering - maybe analogue of diffuse wave spectroscopy (DWS) with laser light scattering which makes use of the multiple scattering process rather than avoiding it.

Measures temporal autocorrelation of the intensity fluctuations of scattered light in either transmission or reflection.

Roland Gähler

Institut Laue Langevin

Novel Instrument Concepts

Novel Instrument Concepts

R. Gähler, ILL Grenoble

- 1) MIEZE, Bunching and its applications
- 2) SANS-Tomography / USANS / Micro-SANS

Argonne, 08/2005      INSTITUT MAX VON LAUE - PAUL LANGEVIN      R. Gähler

How to bunch the highway traffic from Paris to Grenoble?

Assume: Random start time  $t_0$  and speed  $v_0$ ,  
no change of  $v_0$  on the way (except an optional tiny change at S)

Paris      Dijon      Grenoble

Checkpoint E      Checkpoint S      'Detector'

Aerial view near Paris and all along the way  
except very close to Grenoble!

Aerial view at Grenoble

Argonne, 08/2005      INSTITUT MAX VON LAUE - PAUL LANGEVIN      R. Gähler

How to bunch the highway traffic from Paris to Grenoble?

- 1) Choose a certain frequency at Grenoble:  $\langle T_D \rangle = 1 \text{ s}$        $\omega_D = 2\pi \text{ Hz}$ ;
- 2) Put clocks at checkpoints E (S) and choose their frequencies  $\omega_E$  ( $\omega_S$ ) according to the equations:
 
$$\omega_D = \omega_S - \omega_E; \quad \omega_E L_1 = \omega_D L_2 \quad \left. \vphantom{\omega_D = \omega_S - \omega_E} \right\} \begin{array}{l} \omega_E = 1.3 \cdot 2\pi \text{ Hz}; \quad T_E = 1/1.3 \text{ s} \\ \omega_S = 2.3 \cdot 2\pi \text{ Hz}; \quad T_S = 1/2.3 \text{ s} \end{array}$$
- 3) Measure the phase  $\phi_E = \omega_E \cdot t_E$  ( $\phi_S = \omega_S \cdot t_S$ ) for each car passing the checkpoints;

Paris      Dijon      Grenoble

Checkpoint E      Checkpoint S      'Detector' D

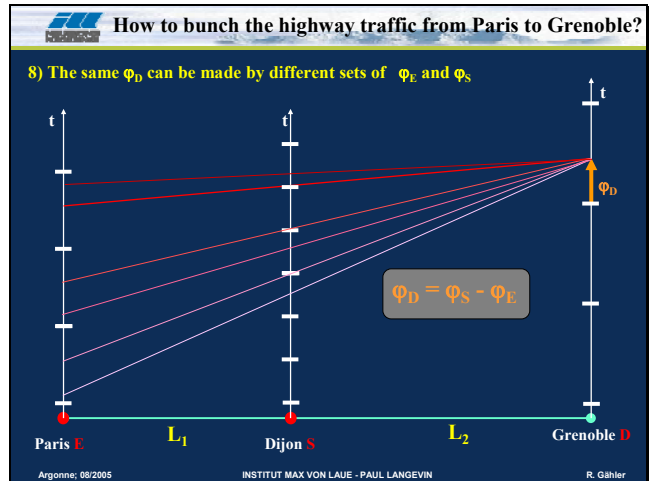
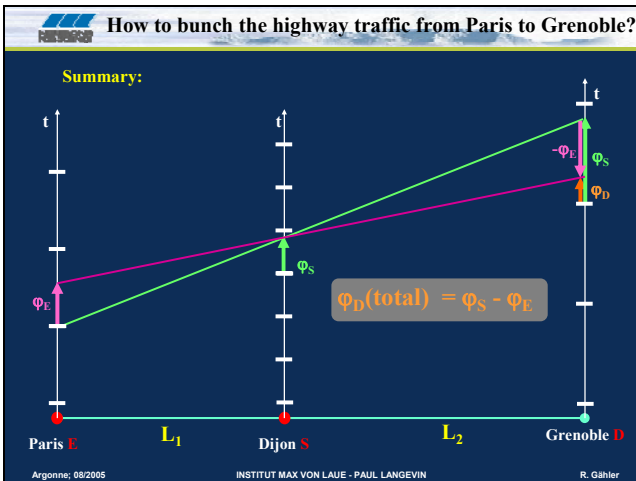
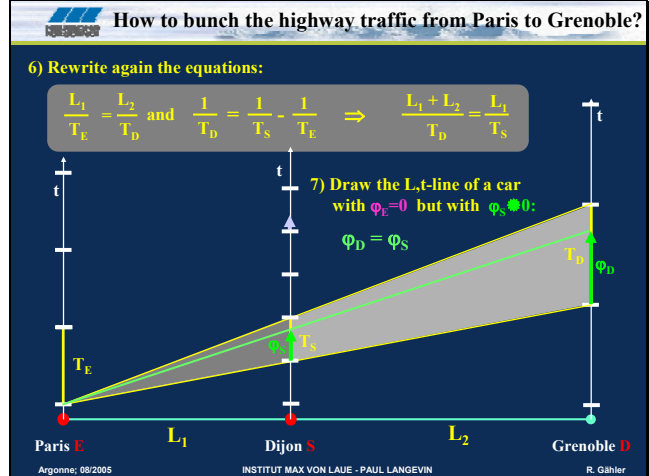
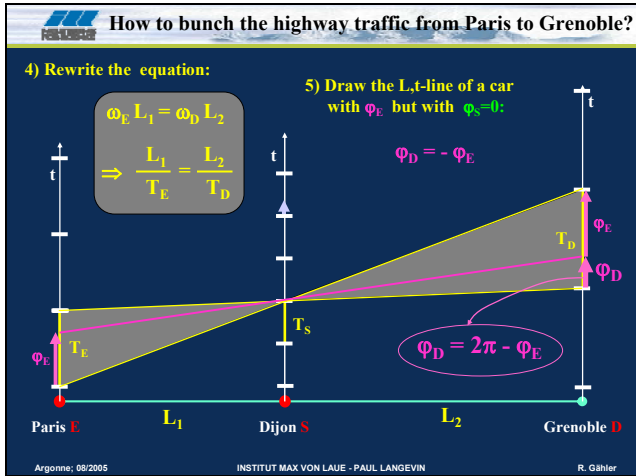
Argonne, 08/2005      INSTITUT MAX VON LAUE - PAUL LANGEVIN      R. Gähler

How to bunch the highway traffic from Paris to Grenoble?

- 4) Draw a space/time diagram, sub-divide all 3 time axes in periods (white bars) of their proper frequencies and mark the phases  $\phi_E$  and  $\phi_S$  when a car passes. Put phase flags on the passing cars.

Paris E      Dijon S      Grenoble D

Argonne, 08/2005      INSTITUT MAX VON LAUE - PAUL LANGEVIN      R. Gähler



### How to bunch the highway traffic from Paris to Grenoble?

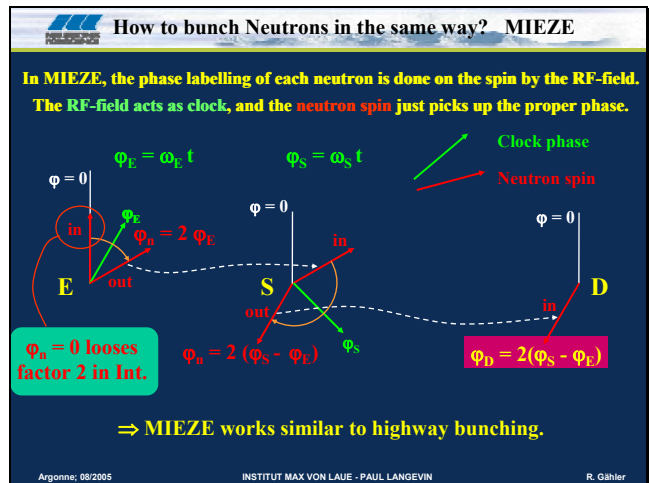
9) After passing the checkpoint S at Dijon, we set on each car the phase flag to  $\varphi_S - \varphi_E$  and this is its phase at Grenoble.  $\varphi_D = \varphi_S - \varphi_E$

If you do nothing anymore, the phase flags on the cars arriving in Grenoble will be periodic with period  $1s$ .

10) Two possibilities to achieve a time structure at Grenoble:

- Keep only cars with  $\varphi_D \approx N \cdot 2\pi$  and skip those with  $\varphi_D \approx (2N+1) \cdot \pi$ ; The position of this action between Dijon and Grenoble is arbitrary!
- Speed up (a tiny bit) those with  $\varphi_D$  and slow down those with  $\varphi_D$ , such that both overlap at Grenoble. **Bunching!**  
 $\Delta v = \{0.25s/4h\} = \{10^{-4}\}$ ; if you do it close after Dijon;  
 Attention: Bunching is dispersive!

Argonne, 08/2005 INSTITUT MAX VON LAUE - PAUL LANGEVIN R. Gähler



**Three possible scenarios:**

**A: Do nothing downstream of S:**  
Spins at D will rotate with  $\Phi_D = 2(\Phi_S - \Phi_E)$ ;  $\Phi_D$ : [0 – 10 MHz]

**B: Place polarizer downstream of S:**  
Intensity will oscillate with  $\omega_D = 2(\omega_S - \omega_E)$ ;  $\omega_D$ : [0 – 10 MHz]

**C: Place buncher downstream of S:** typical value  
Intensity will oscillate with  $\omega_D = 2(\omega_S - \omega_E)$ ;  $\omega_D$ : [0.1 – 10 MHz]  
but with twice the intensity compared to B.

This is a very efficient system to create time structures, which otherwise cannot be created for very cold neutrons.

Argonne, 08/2005 INSTITUT MAX VON LAUE - PAUL LANGEVIN R. Gähler

**2) Sketch of the quantum mechanical picture of bunching**

Bunching relies on the longitudinal Stern-Gerlach effect  
⇒ There is no classical explanation!

Argonne, 08/2005 INSTITUT MAX VON LAUE - PAUL LANGEVIN R. Gähler

**MIEZE with bunching; no analyser anymore!**

buncher: (one or several high-field-RF-flippers)  
No phase locking to  $\omega_S, \omega_E$ !

Argonne, 08/2005 INSTITUT MAX VON LAUE - PAUL LANGEVIN R. Gähler

**Quantum-mechanical view of bunching; no classical view exists!**

The variation of  $\Delta k = k_1 - k_2$  due to  $\omega_r$  is not cancelled by the MIEZE condition and leads to an extra phase difference  $d\phi$  between both waves at the detector.

$$\Psi_{out} = \left[ \begin{matrix} e^{i(\theta+\phi)} - e^{-i(\theta+\phi)} \\ e^{i(\theta-\phi)} + e^{-i(\theta-\phi)} \end{matrix} \right] e^{-i\Phi_0} \Psi_{in} \Rightarrow \begin{matrix} \sin(\theta+d\phi) \\ \cos(\theta-d\phi) \end{matrix}$$

$\theta = (\omega_S - \omega_E)t = \omega_D t$

This determines  $\omega_B$ .

$$d\phi = \sqrt{\frac{m}{8\hbar}} \omega_D \omega_0 L_2 \frac{1}{\omega_0^{3/2}} = \frac{\pi}{4}$$

$k_1 - k_2$  depends on  $\omega_B$ !

Bunching more easy for slow neutrons

Argonne, 08/2005 INSTITUT MAX VON LAUE - PAUL LANGEVIN R. Gähler

**3) Applications of MIEZE (with bunching)**

- A. MISANS (SANS with high energy resolution) [ANL: Bleuel / La]
- B. SPAN-like NRSE spectrometer with very high resolution [NIST: proposal]
- C. Increase of energy resolution in TOF ⊖
- D. Decay time in n-induced reactions (time resolution: ms – μs) ⊖
- E. Spin-dependent reactions and phenomena ⊖
- F. Lock-in techniques for n-scattering? ✖
- G. Multi - MIEZE setups (?) ⊖
- H. Time interferometry ('Mach-Zehnder in time') ✖

Argonne, 08/2005 INSTITUT MAX VON LAUE - PAUL LANGEVIN R. Gähler

**High resolution spinecho for quasielastic scattering (NIST proposal)**

up to 180 analyzing units  
length of each unit ≈ 4m

Argonne, 08/2005 INSTITUT MAX VON LAUE - PAUL LANGEVIN R. Gähler

### Increase of energy resolution in TOF

Resolution of TOF:  
Example INS at 6 Å at max. chopper speed:  
 $6\text{Å} \cdot 2.2\text{ meV}$ ;  $t_f = 6.1\text{ms}$ ;  $\Delta t_f = 55\mu\text{s}$  for  $l=4\text{ m}$  and  $\Delta E = 40\mu\text{eV}$

**MIEZE**

A MIEZE/Bunching system at  $\omega_b = 200\text{ kHz}$  (typ. value) in front of the spectrometer can modulate the elastic line (or inelastic line) with  $5\mu\text{s}$  resolution.

- Tolerable path length differences:  $\Delta l \approx 2\text{mm!}$
- Works on inelastic lines as well, as  $\Delta v/v \approx 0.01$ ;
- Sacrifices only a factor 2+6 in count rate;
- Measures  $S(q,t)$  for small  $q$  and  $S(q,\omega)$  for larger  $q$ .

Argonne, 08/2005      INSTITUT MAX VON LAUE - PAUL LANGEVIN      R. Gähler

### Decay times in n-induced reactions (time resolution $T_d$ : ms - $\mu\text{s}$ )

How to measure decay times in n-induced reactions?

Here, coincidence methods can be problematic

Argonne, 08/2005      INSTITUT MAX VON LAUE - PAUL LANGEVIN      R. Gähler

### Decay time in n-induced reactions (time resolution $T_d$ : ms - ns)

**Solution: In beam irradiation by an intensity-modulated beam**

rate equation:  $dN/dt = -\lambda N + A(\cos\omega t + 1)$  [rate of change = - decay rate + production rate]

**Solution:**  
 $N(t) = C e^{-\lambda t} + A/\lambda + A \frac{\omega \sin \omega t + \lambda \cos \omega t}{\lambda^2 + \omega^2} = A \left[ 1/\lambda + \sqrt{\lambda^2 + \omega^2} \frac{\sin(\omega t + \varphi)}{\lambda^2 + \omega^2} \right]$ ;  $\varphi = \arctan \lambda/\omega$ ;

dies out rapidly      constant level

$\omega = 0.2\lambda$   
 $\omega = \lambda$   
 $\omega = 5\lambda$

$\lambda = \ln 2/T_d$ ;  $\omega = 2\pi/T_m$ ;  
 $\lambda = \omega \Rightarrow T_m/T_d = 9.06$

$T_m$ : {1s - 0.1μs}  
 $\Rightarrow T_d$ : {0.1s - 10ns}

Argonne, 08/2005      INSTITUT MAX VON LAUE - PAUL LANGEVIN      R. Gähler

### Spin-dependent reactions and phenomena

- Measurements of asymmetries in  $\beta$ -decay
- Spin dependent nuclear reactions
- Parity violation experiments

Most of these effects are subtle and require difference measurements: "spin↑ - spin↓"

- By omitting the analyser in MIEZE, the spin direction will rotate in zero field in any plane with any frequency from 0 Hz -10 MHz;
- The frequency of rotation  $\omega_b$  does not occur in the electronics;  $\omega_b = \omega_s - \omega_E$ ;
- This rotation zone is far downstream from the last beam component;
- The rotation zone can be moved in beam direction;
- For a beam of  $\Delta v/v$ , the length of the rotation zone is  $l_0 \approx \frac{v^2}{\Delta v} \frac{2\pi}{\omega_b}$ ;  $l_0$  (typ) {mm - m};

Argonne, 08/2005      INSTITUT MAX VON LAUE - PAUL LANGEVIN      R. Gähler

### Multi-MIEZE with different detection planes

Transmission functions  $T_1$  and  $T_2$  are independent from each other.  
 $\Rightarrow$  At both planes, the intensities show sinusoidal modulation.

This effect could be used in TOF and MISANS, to match energy resolution to  $q$ :  
For small  $q$  and small  $\omega$ , a higher  $N$  may be chosen than for large  $q$ .

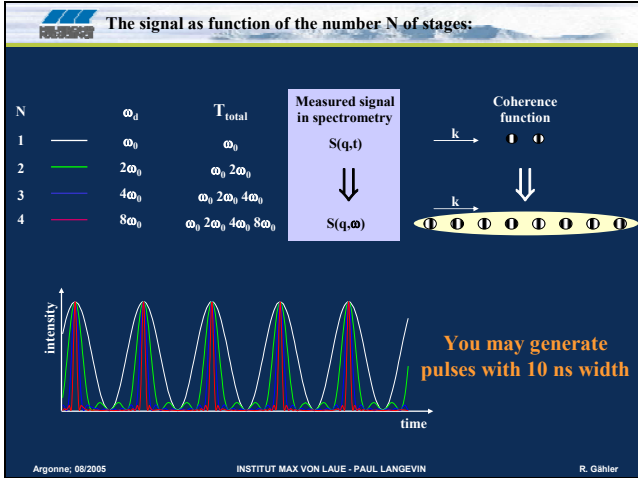
Argonne, 08/2005      INSTITUT MAX VON LAUE - PAUL LANGEVIN      R. Gähler

### Multi-MIEZE with common detection plane

Transmission function:  $T_1 \times T_2 \times T_3 = T_{\text{total}}$

Common plane of detection for all stages

Argonne, 08/2005      INSTITUT MAX VON LAUE - PAUL LANGEVIN      R. Gähler



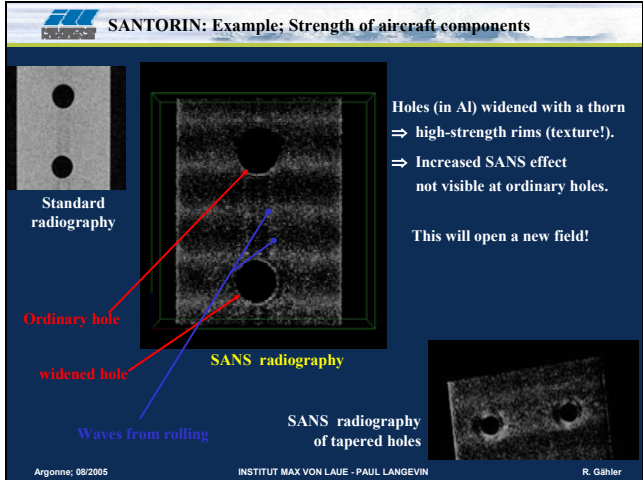
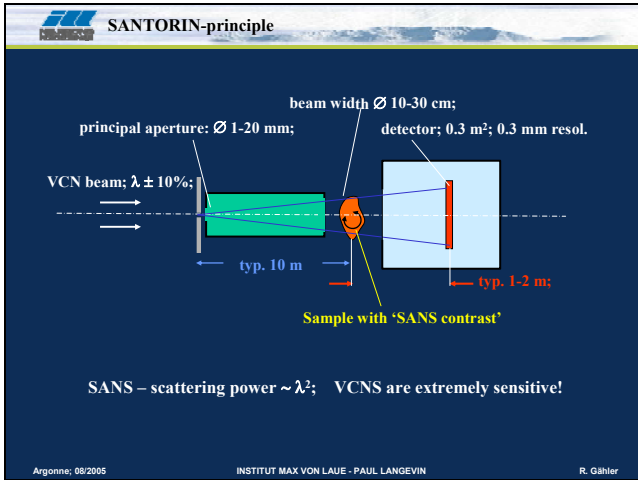
**SANTORIN - SANS-TOMOGRAPHY**

Small ANgle TOMographic and Radiographic Imaging with Neutrons

3D mapping of nano-structured materials;;

Standard Tomography uses absorption for contrast;  
SANTORIN uses SANS for contrast;  
Application: high tech materials;

Argonne, 08/2005      INSTITUT MAX VON LAUE - PAUL LANGEVIN      R. Gähler



**USANS option SAMBA**

**SAMBA: Small Angle Multi Beam Analysis**

There is need to examine nano- and microstructured materials for larger correlation lengths!

Examples:

- Nanotube-clustering in glue
- Micro-structure of tires
- Bubbles in Vicor glass
- Oil in Sediments
- Hardening of concrete
- Structure of marble

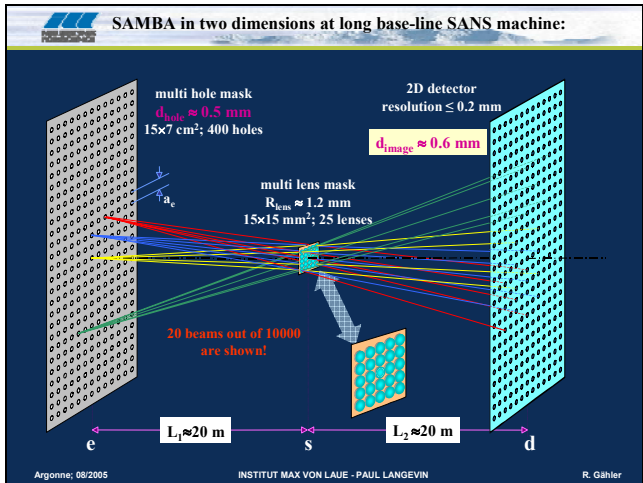
Aim: Extend beam correlation length  $l_c$  by factor 10 in 2 dimensions at standard SANS machines:  $l_c = 1000 \text{ \AA} \Rightarrow l_c = 1 \mu\text{m}$

Consequence for standard SANS:  $I \Rightarrow 10^{-4} I_0$  (too low!)

SAMBA uses up to  $10^4$  narrow beams with  $l_c = 1 \mu\text{m}$

Only moderate loss in intensity but sacrifice in q-range

Argonne, 08/2005      INSTITUT MAX VON LAUE - PAUL LANGEVIN      R. Gähler



**SAMBA: Multi lens and image quality**

\*Pin holes at pulsed sources  
gravity correction: only necessary at contin. Source;  
At pulsed sources to be corrected electronically

Multi lens\* + prisms

2 lenses R = 2.28 mm  
mean spherical aberration: 0.12 mm;

Mean image width including all aberrations: 0.6 mm after 40 m flight path;  
SAMBA – optics best made for VCNs!

Argonne, 08/2005      INSTITUT MAX VON LAUE - PAUL LANGEVIN      R. Gähler

**SANS (with standard q-resolution) for 50 μm samples;**

For sufficient contrast along 50μm, VCNs are needed;

multi hole mask  
 $\varnothing_{\text{hole}} \approx 0.1\text{-}1\text{ mm}$   
15x15 cm<sup>2</sup>; 900 holes

2D detector  
resolution  $\leq 0.1\text{ mm}$   
 $\varnothing_{\text{image}} \approx 0.12\text{ mm}$

900 micro guides feeding the 900 holes

Single hole mask  
 $\varnothing 50\ \mu\text{m}$

B-10  
Gd-157

$L_1 \approx 1\text{ m}$        $L_2 \approx 1\text{ m}$

Kumakhov lens

$$I = 900 I_0 \left[ \frac{50}{10000} \right]^2 = 0.02 I_0;$$

$I_0$  for standard SANS

Argonne, 08/2005      INSTITUT MAX VON LAUE - PAUL LANGEVIN      R. Gähler

**off the shelf camera system**

BRUKER ADVANCED X-RAY SOLUTIONS      BRUKER SCINUS

neutron?

resolution:  
73 μ on Ø 300 mm

CCD: 62 × 62 mm  
15μ; 4096 4096

Argonne, 08/2005      INSTITUT MAX VON LAUE - PAUL LANGEVIN      R. Gähler

**Main messages:**

- Beams with high frequency time structures can be generated with high efficiency.
- There seem to be lots of new applications for such beams.
- Super-MIEZE/bunching machines demand high tech;
- New SANS techniques demand high contrast sensitivity
- SANS with VCNs require new methods to increase countrates

Argonne, 08/2005      INSTITUT MAX VON LAUE - PAUL LANGEVIN      R. Gähler

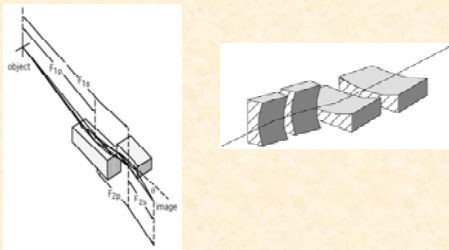
# Gene Ice

## Oak Ridge National Laboratory

### Nondispersive-focusing Long-wavelength Neutrons

#### Nondispersive-focusing long-wavelength neutrons

Gene Ice  
Oak Ridge National Laboratory



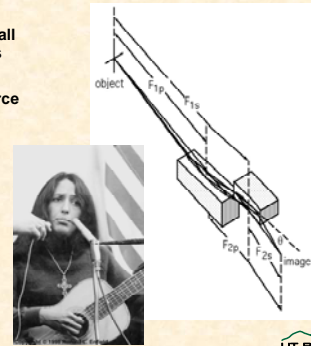
OAK RIDGE NATIONAL LABORATORY  
U. S. DEPARTMENT OF ENERGY



1

#### Genius of Kirkpatrick-Baez mirrors - simple surface focusing at glancing angles

- Aberrations typically small compared to alternatives
- Often work near the source theoretical limit
- "Easily" manufactured elliptical surfaces



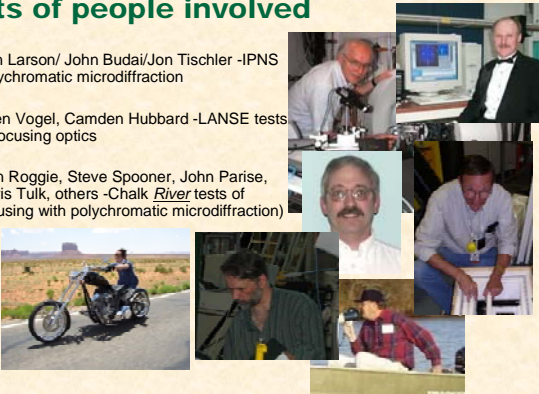
OAK RIDGE NATIONAL LABORATORY  
U. S. DEPARTMENT OF ENERGY



2

#### Lots of people involved

- Ben Larson/ John Budai/Jon Tischler -IPNS polychromatic microdiffraction
- Sven Vogel, Camden Hubbard -LANSE tests of focusing optics
- Ron Roggie, Steve Spooner, John Parise, Chris Tulk, others -Chalk River tests of focusing with polychromatic microdiffraction)



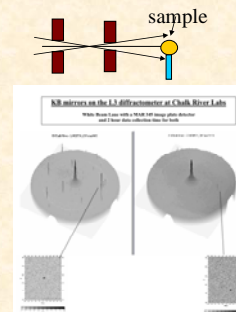
OAK RIDGE NATIONAL LABORATORY  
U. S. DEPARTMENT OF ENERGY



3

#### Neutron KB supermirrors provide vastly greater intensity in small beams

- Focus at the sample allows larger divergence
- Near source-limited brilliance within useable emittance
- Nondispersive allows for efficient use of full spectrum
- *Much* better signal and signal-to-noise for small samples



**Prototype already extends to small sample volumes**

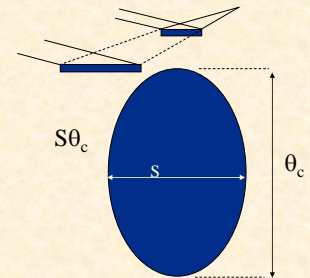
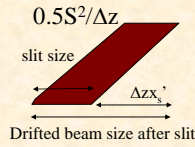
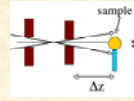
X-ray/neutron focusing same challenge: *collect maximum convergence*

- Nondispersive hard x-ray nanobeams LDRD
  - 70 nm
  - Sophisticated fabrication methods
  - Goal- 1 nm!
- Polychromatic neutron microdiffraction LDRD 25-100  $\mu\text{m}$ 
  - Why haven't these optics been used before?



Long wavelength motivated: Luke Daemen LANSCE

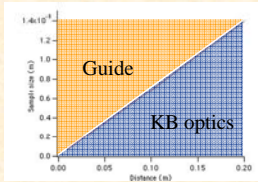
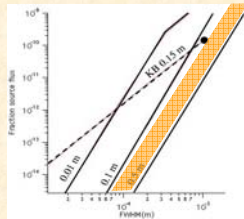
Focusing systems pass large *phase space emittance* for small beams



- *Relative advantage depends sample-optics distance  $\Delta z, S, \lambda$*

Comparison to beam guide +slit finds cross over

- Ray tracing find fraction of source collected by various designs
- $\lambda \sim 0.1 \text{ nm}; S/\Delta Z < 0.007$  KB preferred



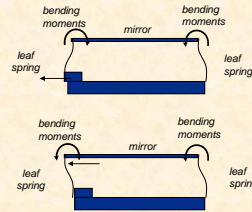
Not unusual!  $\Delta Z \sim 250\text{mm}-500\text{mm} \rightarrow 3 \text{ mm}$  samples

Focusing importance grows with  $\lambda$ !

$\lambda \sim 2 \text{ nm}; S/\Delta Z < 0.14$  KB preferred

Prototype system to measure and demonstrate KB capabilities

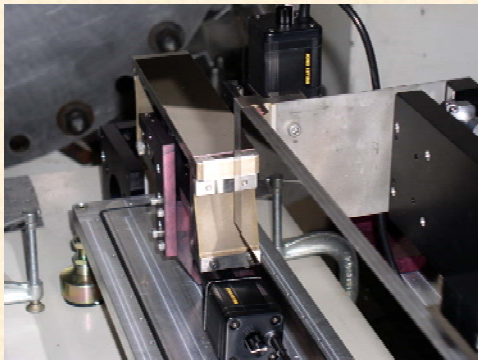
- X-ray community mirror bending experience can be exploited
- Prototype system cost  $\sim \$40\text{K}$ , including 3 sets of mirrors
- System calibrated - visible light



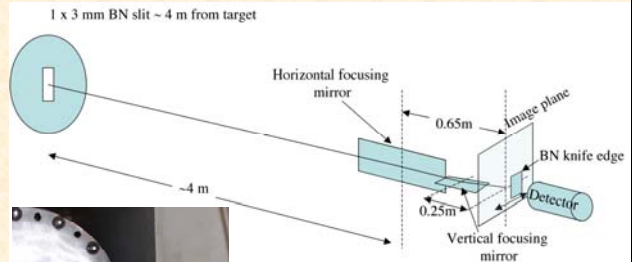
Combined bending moments give elliptical mirror figure ( $R \sim 100 \text{ m}$ )

Fused quartz substrate coated with M3 multilayers.

Closeup of M3 mirrors shows bending mechanism



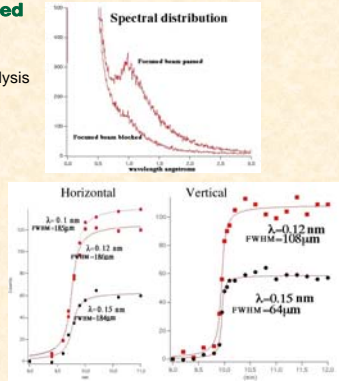
First neutron test on Flight Path 5 LANSCE



- Theoretical size- $122 \times 152 \mu\text{m}$
- Measured-  $105 \pm 33 \mu\text{m} \times 188 \pm 2 \mu\text{m}$
- No observable gravitational dispersion  $\lambda \sim 0.8-1.5 \text{ \AA}$

**The focal properties at different wavelengths was automatically measured**

- Background complicated analysis
- No measurable dispersion
- Spot size
  - $105 \pm 33 \mu\text{m} \times 188 \pm 2 \mu\text{m}$
  - Geometrical
  - $122 \times 152 \mu\text{m}$



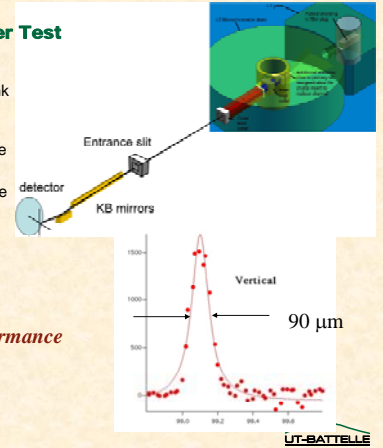
OAK RIDGE NATIONAL LABORATORY  
U. S. DEPARTMENT OF ENERGY



11

**Integrated Chalk River Test**

- Deflecting mirror in mono tank suppresses background
- Upstream slits provide source
- Image plate allows microLaue
- Focus spot  $89 \times 90 \mu\text{m}$



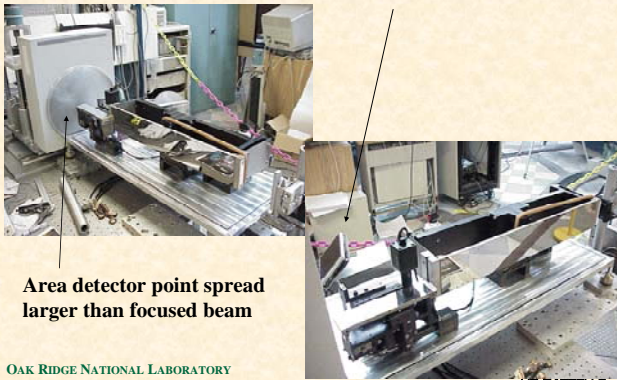
*Near theoretical performance*

OAK RIDGE NATIONAL LABORATORY  
U. S. DEPARTMENT OF ENERGY



12

**Mirrors quickly aligned with real-time camera**



**Area detector point spread larger than focused beam**

OAK RIDGE NATIONAL LABORATORY  
U. S. DEPARTMENT OF ENERGY



13

**Gain estimated**

- A little tricky because area detector saturated
- Estimate using area detector profile and line profiles with proper FWHM
- "Gain" measured ~20
  - Estimated ~100-180
  - "Theory" focused ~150
  - "Theory" small beam ~100



Area detector-point-spread function ~300 μm

Measured beam size ~ 90 μm

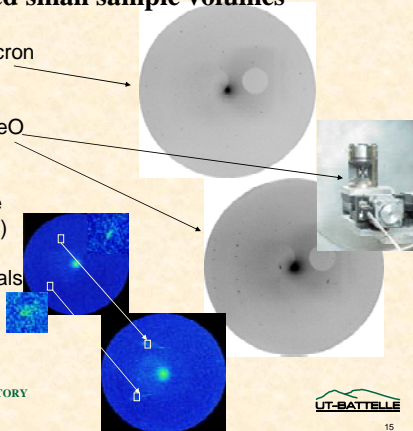
OAK RIDGE NATIONAL LABORATORY  
U. S. DEPARTMENT OF ENERGY



14

**Small beam used small sample volumes**

- 300 x 300 x 700 micron Forsterite-40 spots
- 200 x 500 micron FeO under pressure
- Deformed Cu single crystal (3D resolution)
- Quasi-elastic materials



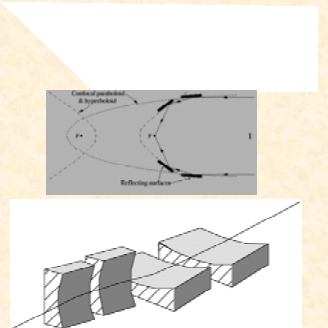
OAK RIDGE NATIONAL LABORATORY  
U. S. DEPARTMENT OF ENERGY



15

**Other KB options under-explored**

- Nested mirrors-2.5 x performance
- AKB Combines Wolter Optics and KB approach- imaging?
- KBA Crossed Paired Sagittal focusing- larger divergence?
- DKBTM Deflections extend divergence collected



OAK RIDGE NATIONAL LABORATORY  
U. S. DEPARTMENT OF ENERGY



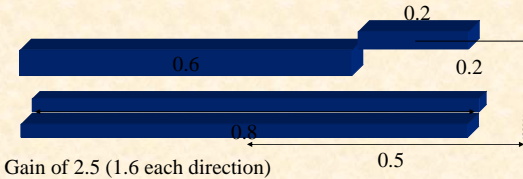
16

### Nested mirrors (monolithic?) increase divergence

- Mirror to focal ratio 1.6 (instead of 1.0)
- Primary mirror closer to image

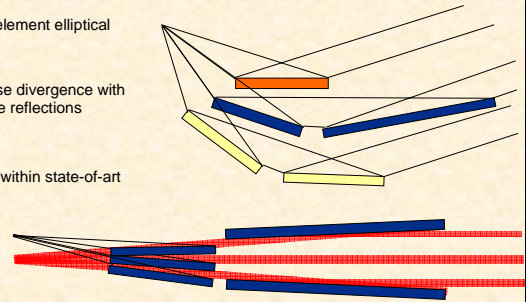
$$\Delta Z_{\text{break even}} = 8\text{mm}; 100 \mu\text{m}$$

Note: mirrors **do not** need to be within 8 mm



### "Deflected" KB™ can collect larger divergence

- Basic element elliptical mirror
- Increase divergence with multiple reflections
- Optics within state-of-art



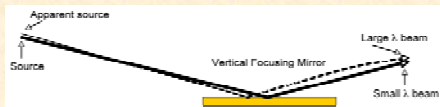
2D Focusing complicated but possible

### What about *long* wavelengths?

Two problems:

1. Central ray dispersion
2. Change in scattering angle

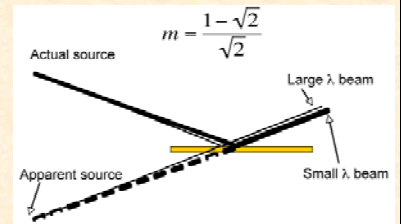
$$\Delta y_{\text{total}} \sim \frac{gF_1^2}{2v^2} M(1-M)$$



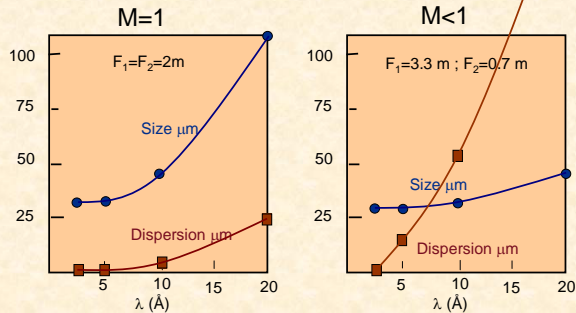
Negligible for  $\lambda \sim 0.1 \text{ nm}$ ; serious for  $\lambda \sim 1 \text{ nm}$

### What tricks can one use? $\Delta y_{\text{total}} \sim \frac{gF_1^2}{2v^2} M(1-M)$

- $M \sim 1$
- $M$  small
- $F_1$  small
- Reflections

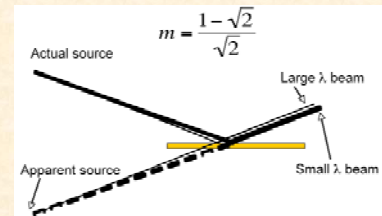


### Neither solution is ideal for $\lambda \sim 20 \text{ \AA}$ !



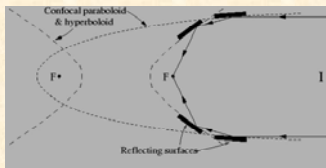
### Multiple reflections maintain source point

- Large source divergence ensures mirror coverage
- Good focus without dispersion
- Should allow for nearly ideal focusing at  $\lambda \sim 20 \text{ \AA}$



Very long wavelengths allow large angle optics!

- Turn beam
- Wolter optics practical
- Backreflection etc.



OAK RIDGE NATIONAL LABORATORY  
U. S. DEPARTMENT OF ENERGY



23

## Summary

- KB mirrors work near the theoretical limit
- Focusing increasingly important with large  $\lambda$ .
- More advanced systems in development
- Can be extended to 20 Å
- At larger  $\lambda$ , alternatives become possible



OAK RIDGE NATIONAL LABORATORY  
U. S. DEPARTMENT OF ENERGY



24

## Ballad of slow neutron focusing

Neutrons fall on their path in space  
Hard to focus- in just one place  
Slow ones fall a little more  
If it was easy -it would be a bore

Mirrors reflect nondispersively  
But it takes some tricks- you've heard from me  
To help slow neutrons focus just in one place  
Centered on the sample space

Mag near 1 or mag small too  
Extend the  $\lambda$ -we can do  
Neutrons fall on their path through time  
To waste even one would be a crime

Mirrors have the symmetry  
To flip neutron paths through gravity  
We can use this trick- to focus beams  
With better resolution than by other means

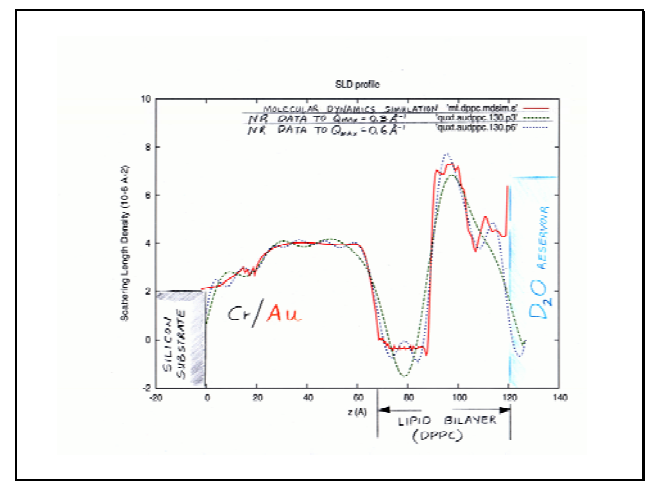
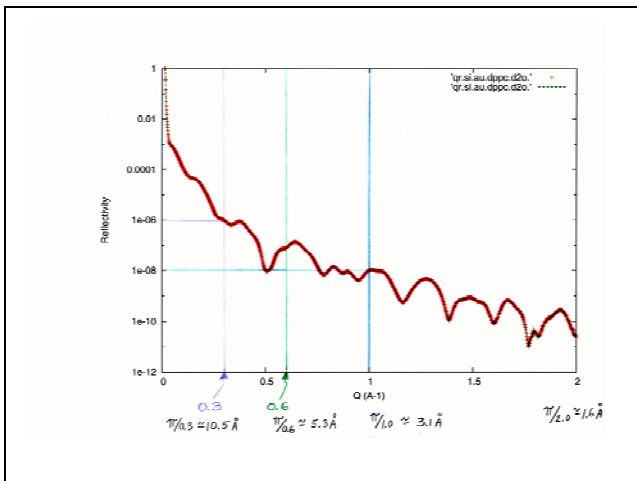
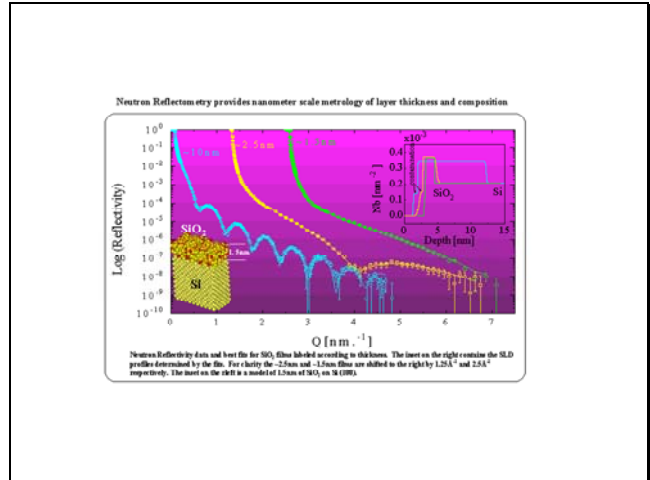
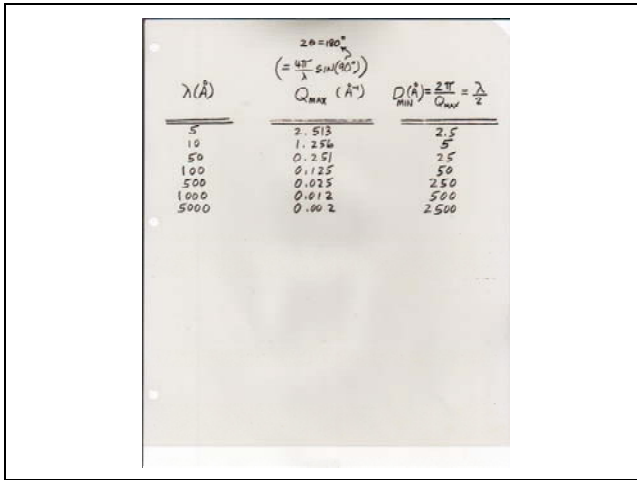
OAK RIDGE NATIONAL LABORATORY  
U. S. DEPARTMENT OF ENERGY



25







**Supported Lipid Bilayers**  
A model system to mimic the structure and dynamics of cell membranes.

**Proteins in Lipid Bilayers**

- Difficult to characterize by traditional x-ray crystallography.
- Play a crucial role in cell function
  - regulate ion and nutrient transport
  - engage in binding, signalling and cell recognition
  - participate in cell fusion events.

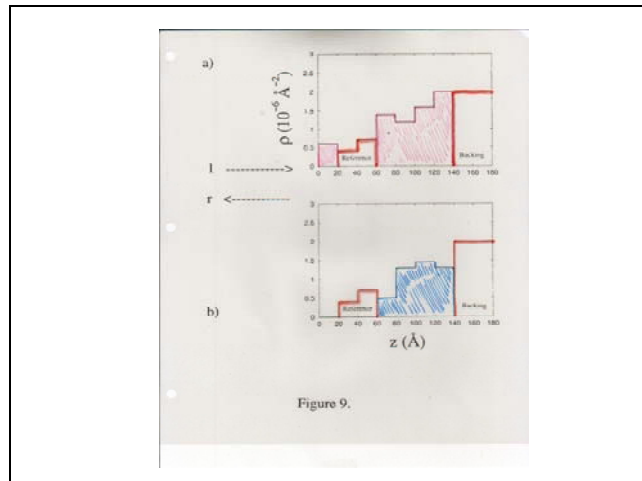
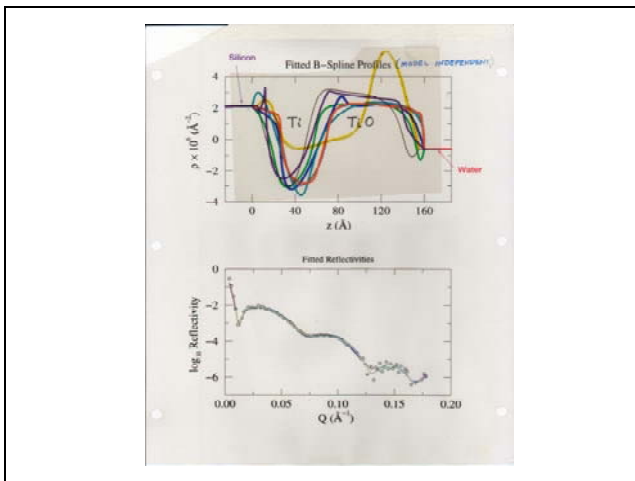
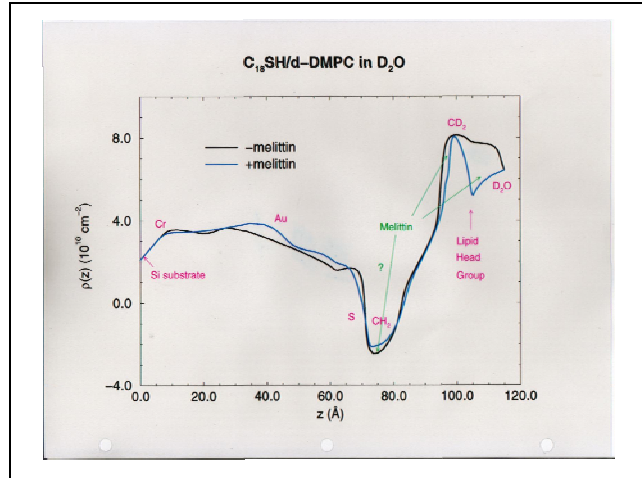
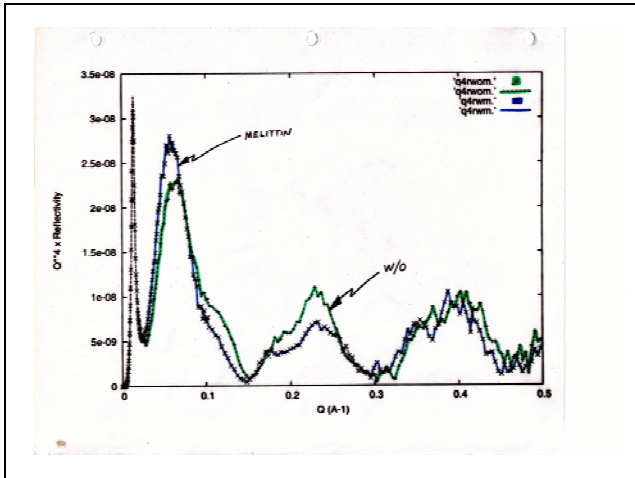
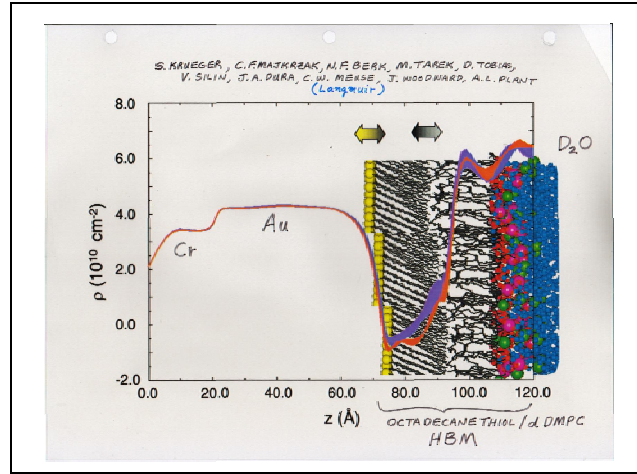
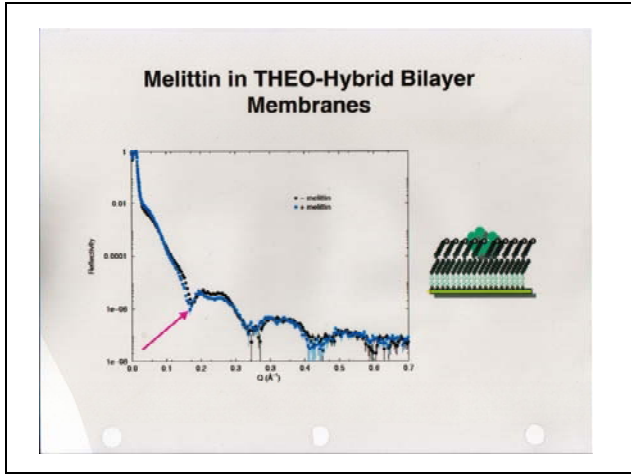
**Biosensors (Anne Plant & coworkers)**

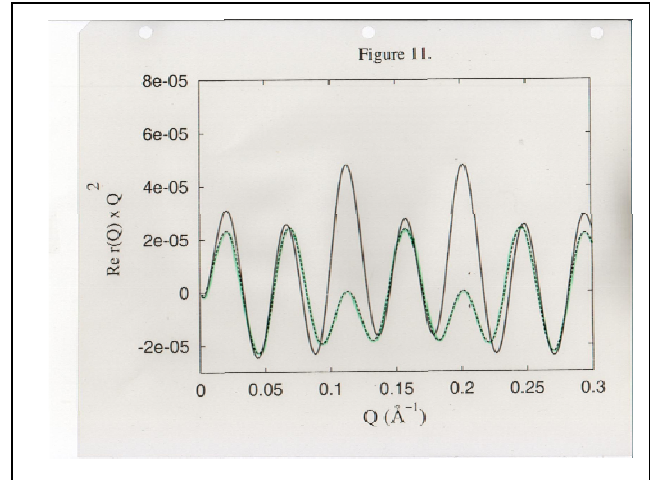
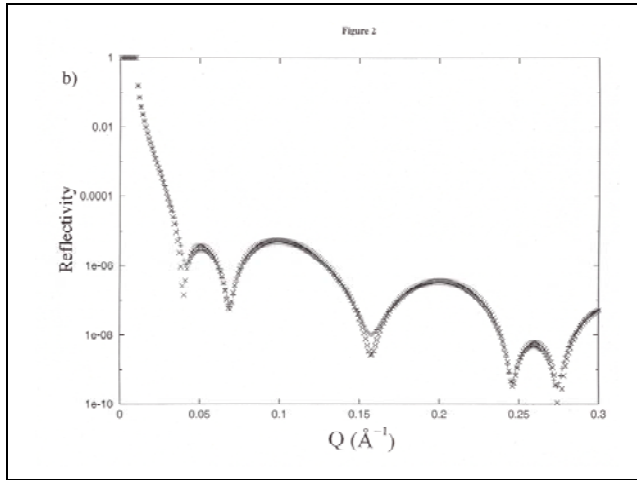
**Melittin in Hybrid Bilayer Membranes**

S. Krueger, A. Plant, et al., NIST (Langmuir)

- pore-forming toxin
- used as model membrane peptide
- active in IBMs

- depth of penetration into bilayer  
 - nature of pore (water-filled?)  
 - conformational changes  
 - random or ordered distribution?  
 - influence on surrounding lipids (location, conformation)





**Inverting reflectivity**

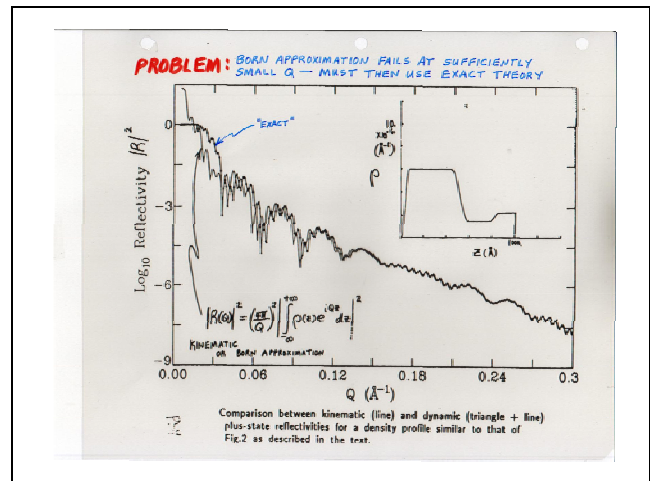
**Phase determination**  
 C.P. Makrakis and N.F. Berk, Phys. Rev. B 52, 11027 (1995).  
 V.-O. de Haan, et al., Phys. Rev. B 52, 11020 (1995).  
 H. Loh, H.R. Lippert and G. Reiter, this conference.

**Approximate Inversion**  
 H. Loh, Phys. Rev. B 48, 1 (1993).

**Exact Inversion**  
 H. Loh, H.R. Lippert, et al., Phys. Lett. A 179, 347 (1992).

**Exact Inversion**  
 S.K. Sinha, et al., Surface X-Ray and Neutron Scattering, 85 (Springer, 1992).  
 C.P. Makrakis, N.F. Berk, et al., SPIE Proc. 1738, 392 (1992).

NIST



**FOURIER TRANSFORM OF THE COMPLEX REFLECTION AMPLITUDE**

$$\mathcal{R}(z) = \frac{1}{2\pi} \int_{-\infty}^{\infty} r(k_x) e^{ik_x z} dk_x$$

**GELFAND LENTMAN MARCHEUKO INTEGRAL EQUATION**

$$K(z, \gamma) + \mathcal{R}(z, \gamma) + \int_{-\infty}^{\infty} K(z, x) \mathcal{R}(x, \gamma) dx = 0$$

**SCATTERING LENGTH DENSITY**

$$\rho(z) = 2 \frac{d \mathcal{R}(z, z)}{dz}$$

**GIVEN THE COMPLEX REFLECTION AMPLITUDE, THE SCATTERING LENGTH DENSITY  $\rho$  CAN BE OBTAINED FROM AN EXACT, FIRST PRINCIPLE INVERSION FOR A REAL POTENTIAL OF FINITE EXTENT AND THE SOLUTION IS UNIQUE!**

**NO FITTING, NO ADJUSTABLE PARAMETERS**

**FORMALISM ALLOWS A COMPOSITE POTENTIAL TO BE EXPRESSED AS A PRODUCT:**

$$\begin{pmatrix} A & B \\ C & D \end{pmatrix} = \begin{pmatrix} a & b \\ c & d \end{pmatrix} \begin{pmatrix} w & x \\ y & z \end{pmatrix}$$

**COMPOSITE WAVELENGTHS REFERENCE (1, 2, 3)**

**IR(Q)² = |R₁(Q)|², |R₂(Q)|², and |R₃(Q)|²**

$$\Sigma_i = z \left[ \frac{1 + |R_i|^2}{1 - |R_i|^2} \right] = A_i^2 + B_i^2 + C_i^2 + D_i^2$$

**A₁² = a²w² + b²x² + 2abwx**  
**C₁² = c²w² + d²x² + 2cdwx**  
**B₁² = a²z² + b²z² + 2abz²**  
**D₁² = c²z² + d²z² + 2cdz²**

**(INDEPENDENT AT EACH Q)**

**REF ABR REF**

$$\Sigma_i = (w² + z²)² + (b² + d²)² + 2(wb + zd)²$$

**SOLVE FOR WAVELENGTHS a, b, AND z TO GET**

$$R_{\text{composite}} = \frac{(a-b)z - 2i y}{2 + B + d}$$

**a = a²c²**  
**b = b²d²**  
**y = ab + cd**

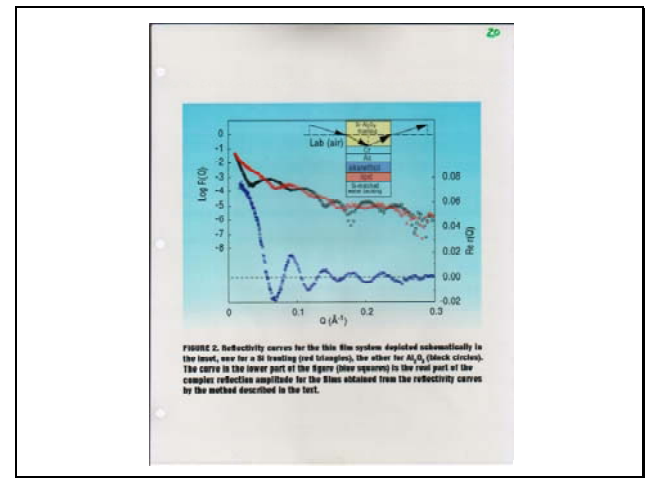
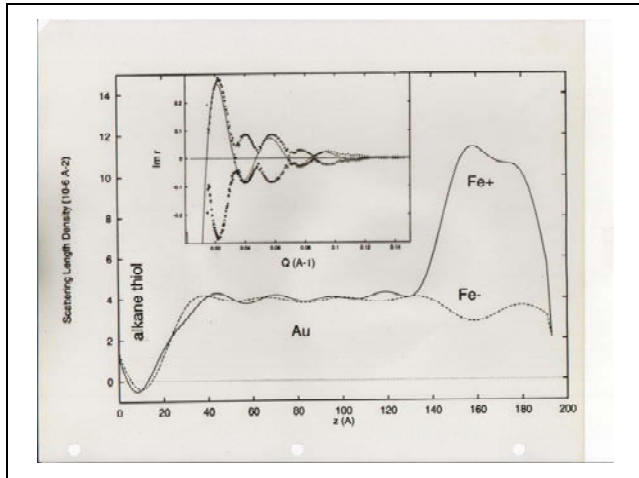
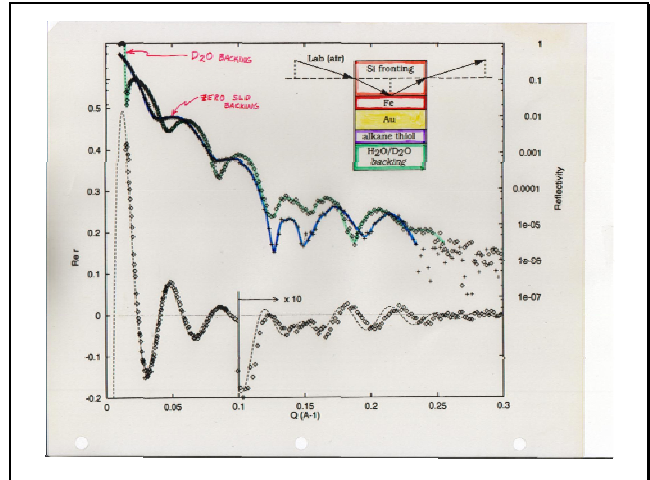
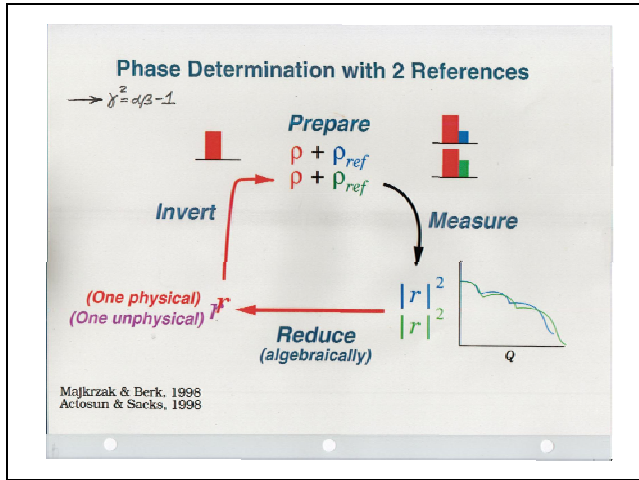
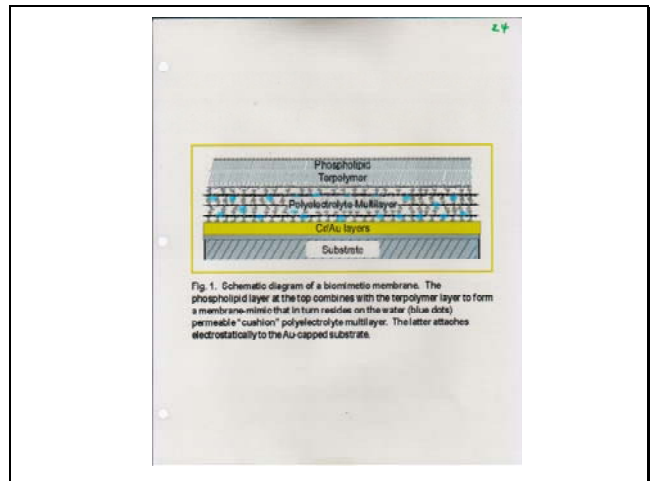
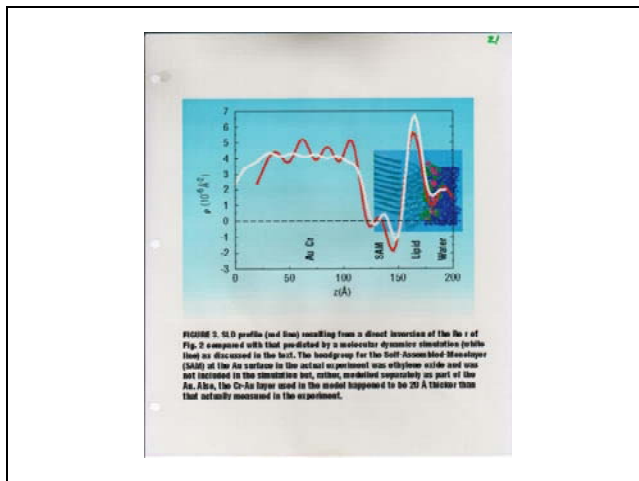
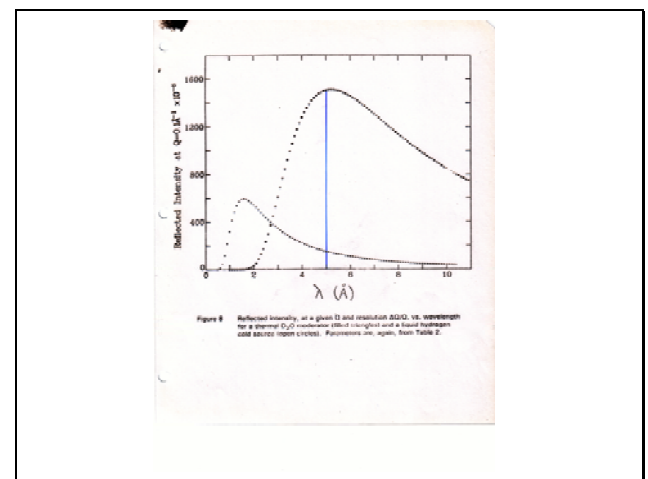
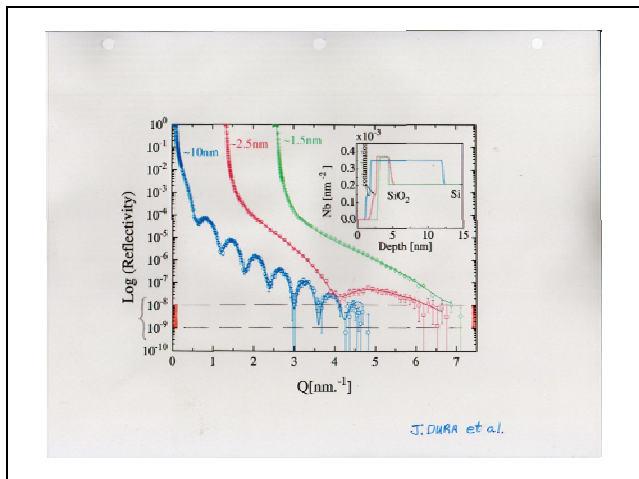
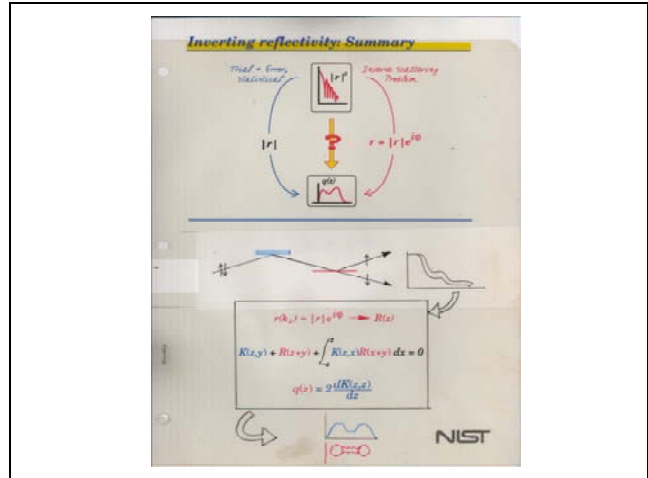
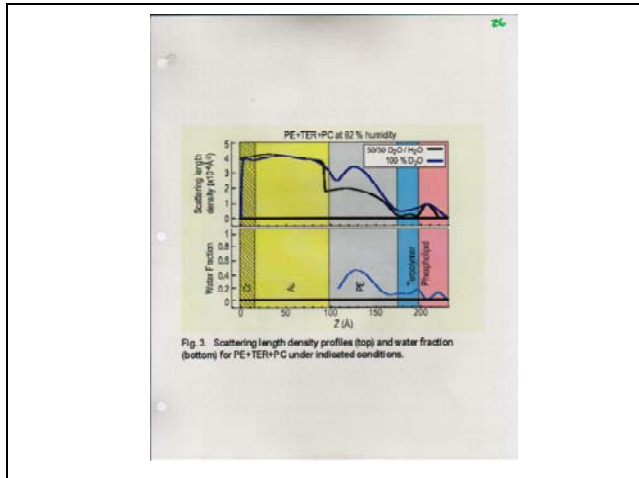


FIGURE 2. Reflectivity curves for the thin film system depicted schematically in the inset, one for a Si fronting (red triangles), the other for Au (black circles). The curve in the lower part of the figure (lower squares) in the red part of the complex reflectance amplitude for the films extracted from the reflectivity curves by the method described in the text.





Neutron Reflectometry as Optical Imaging

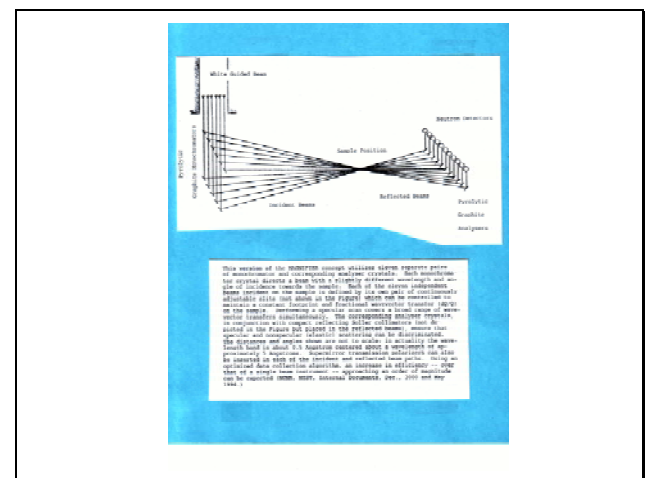
W. L. BROWN, J. DWAR, and J. S. HODGSON

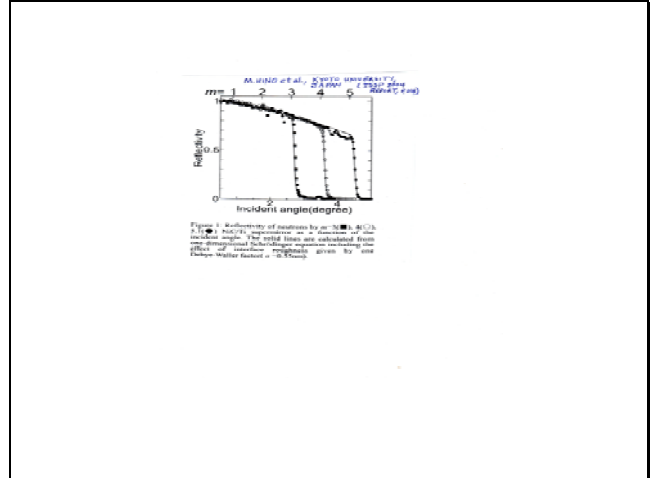
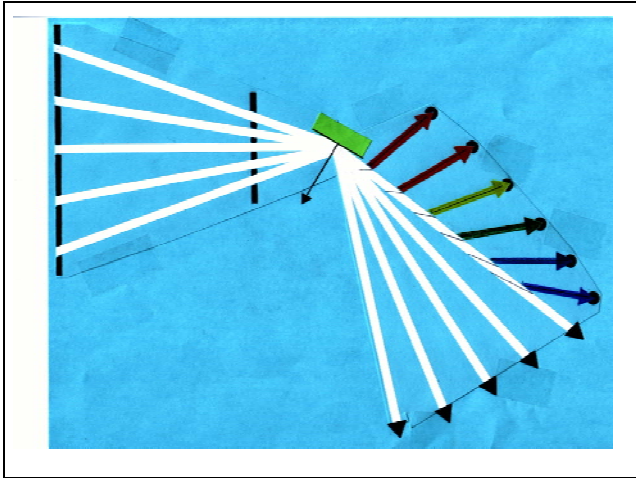
Lawrence Livermore National Laboratory, Livermore, California

Abstract

Introduction

Conclusion





### Conclusions

In phase-sensitive specular neutron reflectivity measurements, the possibilities for doing what is the equivalent of one-dimensional real space imaging with subnanometer resolution are significantly expanded by:

- \* Increasing source intensity (e.g., x 10);
- \* Broadening the wavelength band (e.g., x 10);
- \* Widening beam angular divergence (e.g., x 10);
- \* Optimizing sample geometry.



# Hirohiko Shimizu

## RIKEN

### Recent Developments on Neutron Optics in Japan

**Recent Developments on Neutron Optics in Japan**

**Hirohiko M. SHIMIZU (清水裕彦)**  
**RIKEN (理化学研究所)**

Date(2005/08/23) by(H.M.Shimizu) @ Argonne  
page 1  
中性子光学素子の開発と応用  
Neutron Optics (NOP)

### Refractive Optics

Refractive optics works more effectively at longer wavelengths.

#### Compound Refractive Optics

$$n = \frac{\sin \theta}{\sin \theta'} = \sqrt{1 - \frac{bN_0^2 \lambda^2}{2\pi}} \approx 1 - \frac{bN_0^2 \lambda^2}{4\pi}$$

b: bound coherent scattering length  
N: number density of nuclei  
λ: neutron wavelength

$$\sin \theta' = \sin \theta \cos \alpha = \sqrt{\cos^2(\theta + \alpha) - \frac{bN_0^2 \lambda^2}{2\pi}}$$

$$\sin \theta' - \sin \theta = -\frac{\alpha}{2} \frac{\sin \theta}{\cos(\theta + \alpha)}$$

$\Delta \theta \propto \lambda^2$

#### Magnetic Optics

Equation of Motion

$$d^2 \vec{r} / dt^2 = \mp \alpha \nabla |\vec{B}|$$

$\alpha = 5.77 \text{ m}^2 \text{ s}^{-2} \text{ T}^{-1}$

$\vec{B} = C_z \rho^2$

$\omega^2 = \sin^2 \theta \rho^2 \alpha^2$      $\theta = \omega t$

$$\frac{d^2 X}{dt^2} = \mp \alpha X (X^2 + Y^2)^{-1/2}$$

$$\frac{d^2 Y}{dt^2} = \mp \alpha Y (X^2 + Y^2)^{-1/2}$$

**normalized time:**  
 $\theta = \omega(z/v_z) \propto \lambda$

**focal length  $\propto \lambda^2$**   
if total path length is sufficiently longer than the magnet length.

Date(2005/08/23) by(H.M.Shimizu) @ Argonne  
page 2  
中性子光学素子の開発と応用  
Neutron Optics (NOP)

### Observation of Large Scale Slow Dynamics of Soft-matters

**Method:**  
Small Angle Neutron Scattering  
Neutron Spin Echo

**Devices:**  
Refractive Optics  
Imaging Detector  
Sample Nuclear Polarization

Date(2005/08/23) by(H.M.Shimizu) @ Argonne  
page 3  
中性子光学素子の開発と応用  
Neutron Optics (NOP)

### Optics in Small Angle Neutron Scattering

#### Pin-hole Geometry (P-SANS)

#### Focusing to Sample

more neutrons for large Q-region

#### Focusing to Detector (F-SANS)

fine spot image for small Q-region without losing neutrons

Date(2005/08/23) by(H.M.Shimizu) @ Argonne  
page 4  
中性子光学素子の開発と応用  
Neutron Optics (NOP)

## Focusing Optics

### Reflective Optics

**High-Q<sub>c</sub> Supermirror**

M.Hino et al. (Kyoto Univ.)

### Curved Supermirror

K.Ikeda et al. (RIKEN)

### Biconcave

### Fresnel-shape

T.Adachi et al. (RIKEN)

### Coaxial Double Biconcave

T.Adachi et al. (RIKEN)

### Microprism

T.Shinohara et al. (RIKEN)

**Refractive optics has large effective aperture.**

Date(2005/08/23) by(H.M.Shimizu) @ Argonne  
page 6
中性子光学素子の開発と応用  
Neutron Optics (NOP)

## Magnetic Optics

no material on the beam path

### a refractive optics without parasitic scattering

Superconducting Electromagnet

Large Aperture  
T.Oku et al. (JAERI)

Extended Halbach Permanent magnet

Compact  
Maintenance Free  
T.Oke et al. (JAERI)

Pulsed Electromagnet

Pulse Operation  
J.Suzuki et al. (JAERI)

Variable Permanent Magnet

Variable and  
Pulse Operation  
Y.Iwashita et al. (Kyoto Univ.)

#### Equation of Motion in Multiple Magnetic Field

$$\frac{d^2r}{dt^2} = \mp \frac{\mu}{m} \nabla |B|$$

spin parallel  
spin anti-parallel  
as long as  $\omega_L \gg \omega/a$

$$|B| = C_n(x^2 + y^2)^{n/2}$$

- n=1: quadrupole (spin filter)
- n=2: sextupole (focusing lens)
- n=3: octapole
- ...
- n=∞: neutron (mirror) guide

unpolarized neutron → sextupole magnet → spin anti-parallel → spin parallel

Date(2005/08/23) by(H.M.Shimizu) @ Argonne  
page 6
中性子光学素子の開発と応用  
Neutron Optics (NOP)

## Scintillating Neutron Imager

- real-time imaging
- wider dynamic range than imaging plate
- complete set including signal processing, data processing and HV power supply

K.Hirota & S.Sato et al. (RIKEN/KEK)

0.5-0.8mm spatial resolution

Resistance Division Readout PMT's : R2486 (3"-dia.) - R3292(5"-dia.)

Scintillator: ZnS/LiF 0.25mm-thick

Sensitive Area: 50mm dia. (3"-dia. PMT)

Spatial Resolution: 0.5~0.8mm (FWHM)

Detection Efficiency: 30% of <sup>10</sup>He (1-inch, 4-atm.)

Counting Rate: ~a few tens of kcps

Compact data acquisition system

Data transfer through USB2.0

Flatpanel PMT's (2"x2") under development  
spatial resolution < 1mm

中性子光学素子の開発と応用  
Neutron Optics (NOP)

Date(2005/08/23) by(H.M.Shimizu) @ Argonne  
page 7
中性子光学素子の開発と応用  
Neutron Optics (NOP)

## Focusing SANS

J.Suzuki & T.Oku et al. (JAERI)

meas. time = 2 hours

Sample thickness ~ 0.2 mm

quartz cell: 1 μm, 3 μm, 5 μm

SiO<sub>2</sub>: 1 μm, 3 μm, 5 μm

USANS

F-SANS

P-SANS (conventional SANS)

$q_{min}$  is defined as the smallest q where simple subtraction is positive.

Magnetic Focusing SANS lowered  $Q_{min}$  by 1/10 or less compared with conventional pin-hole SANS, in two dimensional imaging.

→ 2-dimensional USANS

Date(2005/08/23) by(H.M.Shimizu) @ Argonne  
page 8
中性子光学素子の開発と応用  
Neutron Optics (NOP)

## Magnetic Small Angle Neutron Scattering

T.Shinohara et al. (RIKEN)

Net vector polarization is zero since neutron spin is polarized along the local magnetic field. The local polarization can be vectorized by adiabatically connecting the multipole field into a solenoid field (or dipole field) to adiabatically transport neutron polarization.

Magnetic Poles of the Superconducting Sextupole Magnet

Solenoid Coil

Field Vector generated by the Solenoid Coil

Field Vectors in the Superconducting Sextupole Magnet

Beam Axis

### magnetism of metal particles

Ni Particles

2D Image of  $|B_z|$

Ni Powder: D=30nm,  $\chi_{vol}=7500$ ,  $\chi_{surf}/\chi_{vol}=0.5$ ,  $L=160nm$

Magnetic field  $H=9G$

Date(2005/08/23) by(H.M.Shimizu) @ Argonne  
page 9
中性子光学素子の開発と応用  
Neutron Optics (NOP)

## Quadrupole Magnetic Spin Filter

Quadrupole

spin-parallel, too large divergence

spin-parallel

spin-antiparallel

neutron absorbing aperture surface

log<sub>10</sub>(I/P)

magnet length [m] ( $\lambda=7\text{Å}$ )

90%

99%

99.9%

99.99%

99.999%

Quadrupole functions as

- (1) spin filter
- (2) collimator (divergence filter)

complete absorbing aperture surface is assumed

$|B| = C_1(x^2 + y^2)^{1/2}$ ,  $C_1 = 166.7 \text{ T/m}$

Date(2005/08/23) by(H.M.Shimizu) @ Argonne  
page 10
中性子光学素子の開発と応用  
Neutron Optics (NOP)

## Magnetic Optics for Spin Echo

**INSE at JAERI**

**Possible Improvement**

Total neutron number can be further increased by employing shorter precession coil. Additional sextupole magnet enhances Q-resolution. Quadrupole spin analyzer enhances analyzing power enabling to pick up tiny spin flip.

Date (2005/08/23) by (H.M.Shimizu) @ Argonne  
page 11  
中性子光学素子の開発と応用  
Neutron Optics (NOP)

## Multipole Spin Filters

**Equation of Motion**

$$d^2\vec{r}/dt^2 = \mp \alpha V |\vec{\beta}|$$

**Extended Halbach Permanent Multipole with NEOMAX**

$P > 0.9999 \Leftrightarrow \Delta P < 10^{-4}$ ,  
for accurate determination of correlation terms in neutron  $\beta$ -decay  
for extracting weak spin-flip processes

Date (2005/08/23) by (H.M.Shimizu) @ Argonne  
page 12  
中性子光学素子の開発と応用  
Neutron Optics (NOP)

## Multipole Spin Filters

**Equation of Motion**

$$d^2\vec{r}/dt^2 = \mp \alpha V |\vec{\beta}|$$

**Extended Halbach Permanent Multipole with NEOMAX**

$P > 0.9999 \Leftrightarrow \Delta P < 10^{-4}$ ,  
for accurate determination of correlation terms in neutron  $\beta$ -decay  
for extracting weak spin-flip processes

Date (2005/08/23) by (H.M.Shimizu) @ Argonne  
page 13  
中性子光学素子の開発と応用  
Neutron Optics (NOP)

## Multipole Spin Filters

**Equation of Motion**

$$d^2\vec{r}/dt^2 = \mp \alpha V |\vec{\beta}|$$

**Extended Halbach Permanent Multipole with NEOMAX**

$P > 0.9999 \Leftrightarrow \Delta P < 10^{-4}$ ,  
for accurate determination of correlation terms in neutron  $\beta$ -decay  
for extracting weak spin-flip processes

Date (2005/08/23) by (H.M.Shimizu) @ Argonne  
page 14  
中性子光学素子の開発と応用  
Neutron Optics (NOP)

## "Use" of Chromatic Abberation

**Energy Sensitive Detector**  
measures energy and polarization combining with spin-flipper sextupole  $\lambda_1 < \lambda_2$

**Cancellation of Gravitational Abberation**  
quadrupole, mixture of quadrupole and sextupole focal plane

**Band Pass Filter**  
sextupole slit

not necessarily magnetic optics but also compound refractive optics

Date (2005/08/23) by (H.M.Shimizu) @ Argonne  
page 15  
中性子光学素子の開発と応用  
Neutron Optics (NOP)

## Transverse Phase Space "Squeezing"

**Liouville's theorem**  
→ 6-dimensional phase volume is conserved.  $(x, p_x, y, p_y, z, p_z)$ .

Sextupole and quadrupole magnetic optics only reshape the beam conserving 2-dimensional projected volumes in  $(x, p_x)$  and  $(y, p_y)$ .

We will be happy if we successfully decrease 4-dimensional projected area  $(x, p_x, y, p_y)$  or 2-dimensional projected areas  $(x, p_x)$  and/or  $(y, p_y)$  by enlarging volume projected on to remaining dimensions.

**Transverse Phase Space "Squeezing"**

Are there any magnetic field to decrease 4-dimensional or 2-dimensional projected phase volume?

Examples were found, but unrealistic for cold neutrons. Realistic solutions may be found for very cold neutrons.

Date (2005/08/23) by (H.M.Shimizu) @ Argonne  
page 16  
中性子光学素子の開発と応用  
Neutron Optics (NOP)

**Refractive optics has chromatic aberrations.**

**Pulsed neutron beam is monochromatic instantaneously.**

**Refractive optics is applicable if we can sweep its strength synchronizing to the neutron TOF.**

Date(2005/08/23) by(H.M.Shimizu) @ Argonne  
page 17  
中性子光学素子の開発と応用  
Neutron Optics (NOP)

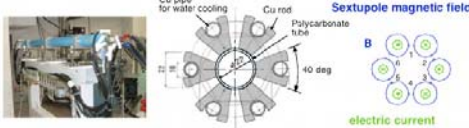
**Variable Magnetic Lens** J.Suzuki et al. (JAERI)

**Pulse Electro-Magnet**



Specifications

- Effective magnet length = 2 m
- Effective bore diameter = 22 mm
- $G = 7,500 \text{ T/m}^2 @ I = 60 \text{ kA}$

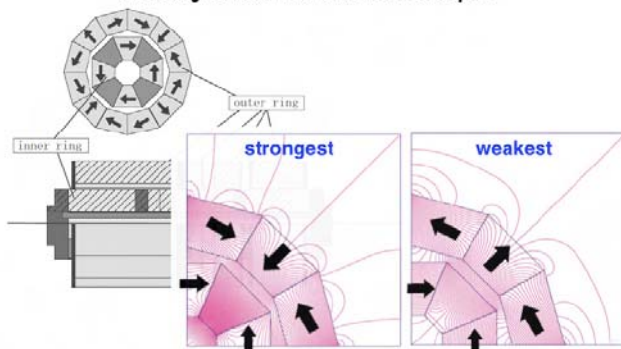


J.Suzuki, Y.Kiyonagi et al., JACRI / Hokkaido Univ.

Date(2005/08/23) by(H.M.Shimizu) @ Argonne  
page 18  
中性子光学素子の開発と応用  
Neutron Optics (NOP)

**Variable Magnetic Lens**

**Rotating Coaxial Permanent Quadrupole**



Inner ring, Outer ring, strongest, weakest

Date(2005/08/23) by(H.M.Shimizu) @ Argonne  
page 19  
中性子光学素子の開発と応用  
Neutron Optics (NOP)

Y.Iwashita et al., Institute for Chemical Research, Kyoto Univ.

**Variable Permanent Quadrupole**  
for Linear Collider Final Focus

$G \sim (60-300) \text{ T m}^{-1}$   $|B| = G \rho (\rho^2 = x^2 + y^2)$

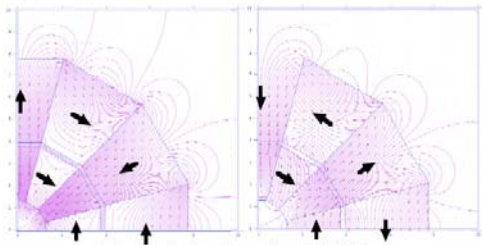


Date(2005/08/23) by(H.M.Shimizu) @ Argonne  
page 20  
中性子光学素子の開発と応用  
Neutron Optics (NOP)

**Variable Permanent Sextupole**  
for Pulsed Neutron Focus

$G \sim (4300-22000) \text{ T m}^{-2}$   $|B| = G \rho^2 / 2 (\rho^2 = x^2 + y^2)$

would be possible in a short R&D period.  $158 \leq \omega \leq 356 \text{ rad/s}$



8.3 revolution/sec for J-PARC.  
remaining issue : heat up due to eddy current

Date(2005/08/23) by(H.M.Shimizu) @ Argonne  
page 21  
中性子光学素子の開発と応用  
Neutron Optics (NOP)

**Enhancing Hydrogen Visibility by Nuclear Polarization**  
for soft-matter researches

Hydrogen nuclei have a large spin-dependent interaction

Coherence is lost through spin-flip processes.

Coherence is maximized when both neutrons and nuclei are polarized in parallel.

→ **Separation of Incoherent Scattering**

Contribution of hydrogen atoms can be extracted by changing nuclear polarization.

→ **Spin Contrast Variation Method**

	spin parallel	spin antiparallel
$^1\text{H}$ 1/2		
$^2\text{H}$ 1		
$^3\text{He}$ 1/2		
$^6\text{Li}$ 1		
$^7\text{Li}$ 3/2		

Date(2005/08/23) by(H.M.Shimizu) @ Argonne  
page 22  
中性子光学素子の開発と応用  
Neutron Optics (NOP)

### Polarizing Hydrogen Nuclei in Sample

**brute-force method**  
 $B=10T$   
 $T < 0.1K$   
 thermal equilibrium

**dynamic nuclear polarization (DNP)**  
 $B=2-5T$   
 $T \leq 1K$   
 paramagnetic center  
 thermal equilibrium → thermal non-equilibrium

**microwave-induced optical nuclear polarization (MIONP)**  
 $B=0.3T$   
 $T \leq 77K$   
 ( $\approx 300K$ )  
 $\pi$ -electron  
 optical excitation → spontaneous spin alignment of triplet state of  $\pi$ -electrons → microwave  
 thermal non-equilibrium

possibility of nuclear spin labelling of hydrogen

M.Minuma et al. (Kyoto Univ.) P=0.4 in bulk at LN<sub>2</sub> temp. and B=3KG H.Sato et al. (RIKEN) S.Muto et al. (KEK)

Date(2005/08/23) by(H.M.Shimizu)@Argonne  
 page 23  
 中性子光学量子の開発と応用 Neutron Optics (NOP)

### Observation of Large Scale Slow Dynamics of Soft-matters

**Structure**  
**Magnetic Focusing SANS**  
 Variable Magnetic Optics  
 Neutron Imager  
 Extension of accessible Q-region of SANS ( $\sim 2$ dim. USANS)  
**Enhancement of Hydrogen Visibility**  
 Sample Nuclear Polarization (DNP and MIONP)  
 Thermal Non-equilibrium Proton Polarization in Sample

**Dynamics**  
**Magnetic Optics for Neutron Spin Echo**  
 Extremely High Neutron Polarization  
 Divergence-Suppressed Beam Delivery  
**Improvement of Q-resolution of NSE by employing additional focusing is under simulation study.**  
**(SANSE: Small Angle Neutron Spin Echo)**

Date(2005/08/23) by(H.M.Shimizu)@Argonne  
 page 24  
 中性子光学量子の開発と応用 Neutron Optics (NOP)

### Observation of Large Scale Slow Dynamics of Soft-matters

**Structure**  
**Magnetic Focusing SANS**  
 Variable Magnetic Optics  
 Neutron Imager  
 Extension of accessible Q-region of SANS ( $\sim 2$ dim. USANS)  
**Enhancement of Hydrogen Visibility**  
**The flexible design becomes possible in VCN region.**  
 Thermal Non-equilibrium Proton Polarization in Sample

**Dynamics**  
**Magnetic Optics for Neutron Spin Echo**  
 Extremely High Neutron Polarization  
 Divergence-Suppressed Beam Delivery  
**Improvement of Q-resolution of NSE by employing additional focusing is under simulation study.**  
**(SANSE: Small Angle Neutron Spin Echo)**

Date(2005/08/23) by(H.M.Shimizu)@Argonne  
 page 25  
 中性子光学量子の開発と応用 Neutron Optics (NOP)

These device studies were initiated using medium- and small-scale neutron sources Electron LINAC at Hokkaido Univ., KENS, IPNS. Their (relatively) flexible beam time allocation is highly preferable for R&D activities.

VCN sources will enable efficient test and evaluation of optical devices with enhanced sensitivities (and hopefully together with flexibilities). They will be play grounds to incubate ideas and skills which would become universally applicable including large-scale neutron sources, and consequently would largely contribute to activate new research fields.

Date(2005/08/23) by(H.M.Shimizu)@Argonne  
 page 26  
 中性子光学量子の開発と応用 Neutron Optics (NOP)

# THE END

Date(2005/08/23) by(H.M.Shimizu)@Argonne  
 page 27  
 中性子光学量子の開発と応用 Neutron Optics (NOP)

Steven M. Bennington

ISIS

## Source Design and Optics on the ISIS Second Target Station



Source Design and Optics on the  
ISIS Second Target Station

S.M. Bennington

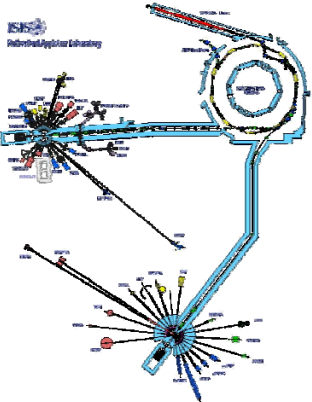


Outline

- ISIS Second Target Station
  - Source Optimisation
  - Composite Moderators
- Elliptical Guides – WISH
- Double Compression - LET



ISIS TS2 – Design Remit



The design remit:  
To optimise the target station  
for long-wavelength neutrons.

- 10Hz (100ms time frame)
- 60μAmps, 48kW

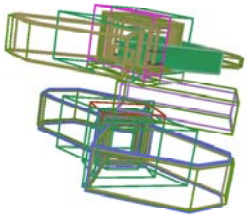


TS2 – Monte Carlo Optimization

- Use pre and post processing of the MCNPX runs to make the optimisation automatic
  - Geometry handlers
  - Optimisation to a Figure of Merit
  - Autor
  - Close

The system v coupled mod

Figure of .



if cluster team



CCLRC TS2 - Design

- Compact design
  - Small target
  - Two wing moderators
- Cold moderators

ISIS

CCLRC TS2 - Target

Target:

- 68mm in diameter x 300 mm long
- Tungsten rod clad in tantalum
- D<sub>2</sub>O cooled

ISIS

CCLRC TS2 - Coupled Moderators

At 48kW we are able to use solid-Methane as moderator

- Cannot cool below 24K due to problems with Wigner energy
- For a simple coupled s-CH<sub>4</sub> moderator peak flux at low energy occurs at 2-3cm width
- There are two strategies to boost the flux
  - Grooves
  - Composite moderators

ISIS

CCLRC TS2 - Composite Moderator

- Hydrogen is transparent below 14meV
- The solid methane “fills-in” below this energy

ISIS

CCLRC TS2 - Composite Moderator

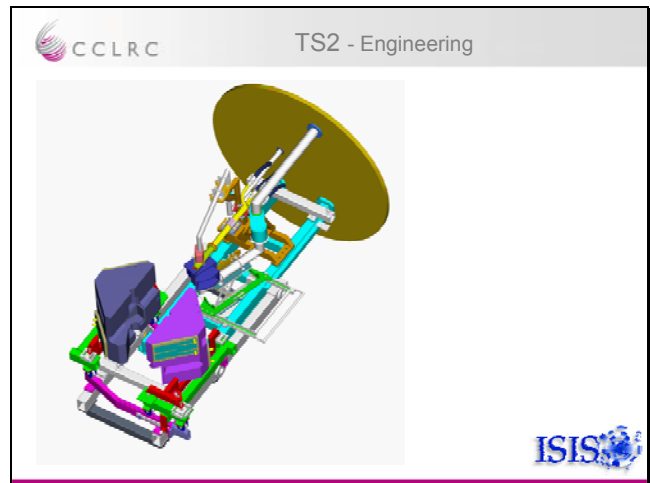
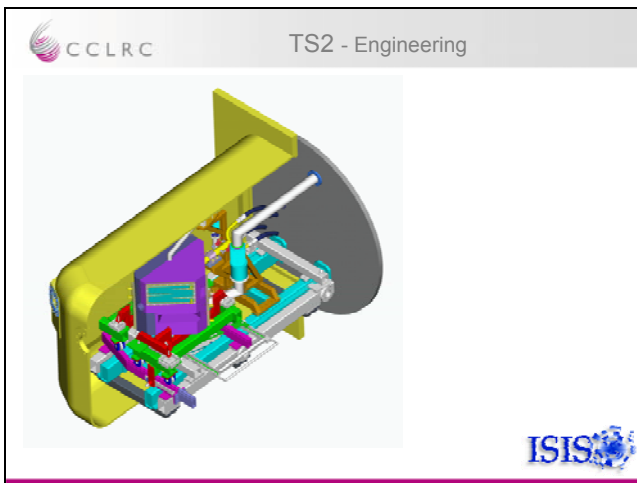
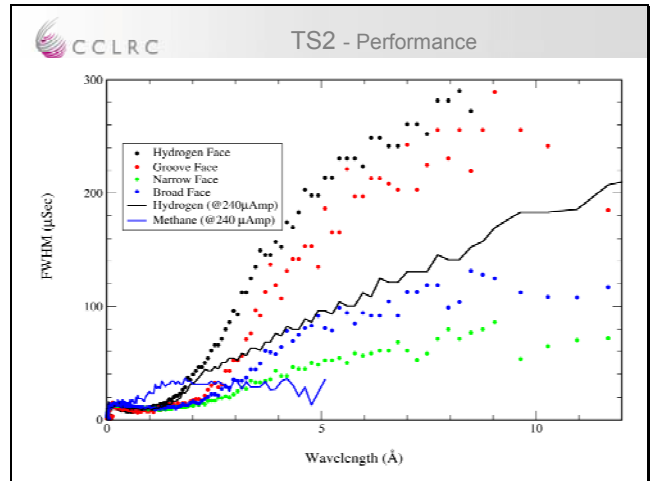
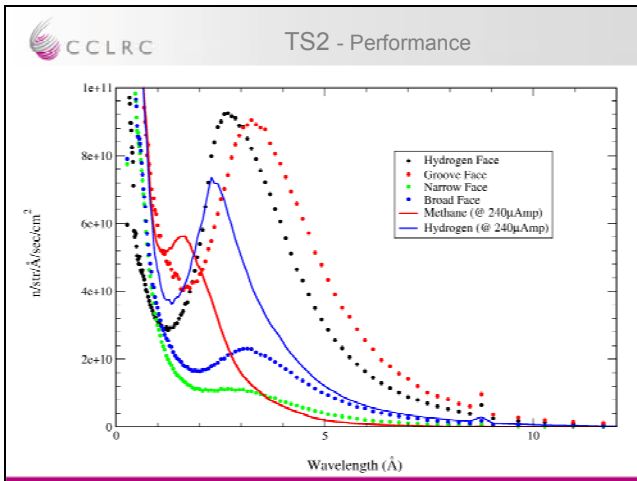
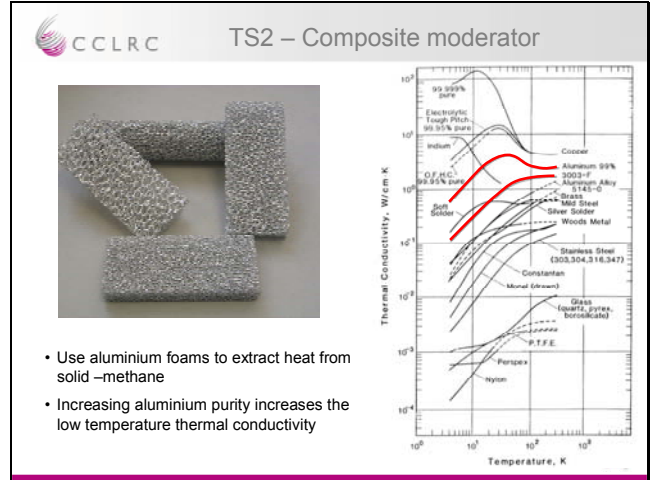
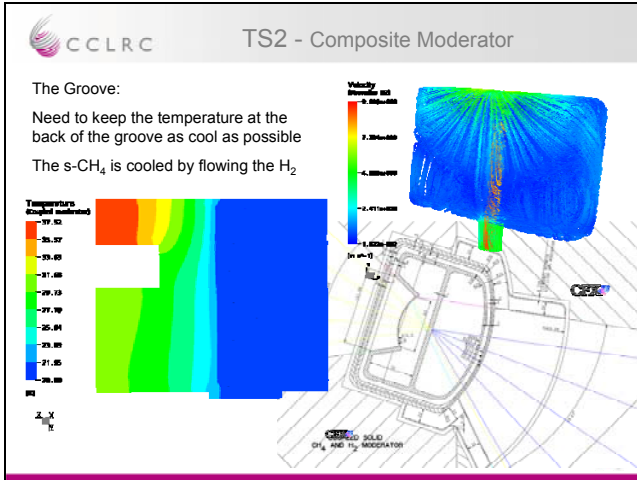
Relative Flux (Energy group 0 - 5 meV)

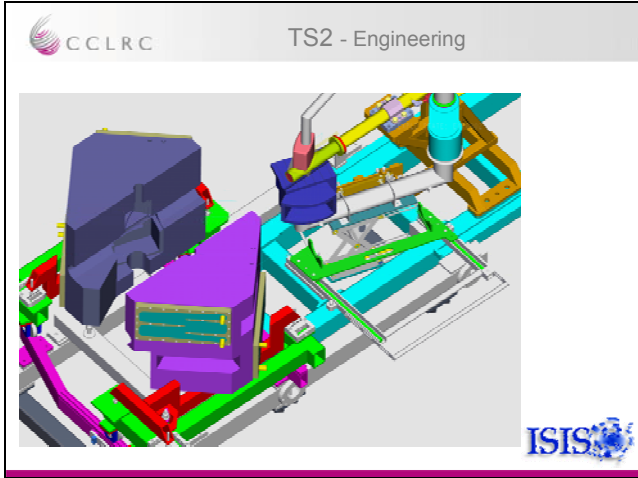
		y (cm)						
		0.0	1.6	3.2	4.8	6.4	8.0	9.6
x (cm)	0.0	0.0	0.464(5)	0.768(4)	<u>1.000(4)</u>	1.197(4)	1.357(4)	1.491(4)
	1.0	1.140(5)	1.618(6)	1.843(5)	1.980(5)	2.075(5)	2.148(5)	
	2.0	1.351(5)	1.738(6)	1.917(5)	2.063(5)	2.144(5)		
	3.0	1.326(5)	1.693(6)	1.896(5)	2.026(5)	2.119(5)		
	4.0	1.285(5)	1.661(6)	1.843(5)	1.984(5)			
	5.0	1.241(5)	1.610(6)	1.823(5)				

ISIS

CCLRC TS2 - Composite Moderator

ISIS





CCLRC Neutron Optics

- WISH – high intensity diffractometer
- LET – Low energy multi-chopper spectrometer

ISIS

CCLRC WISH - Initial Design

50000

Moderator Unpoisoned Decoupled CH<sub>4</sub>

Disk Choppers

Nimonic Chopper

<sup>63</sup>Ni Guide

Monitors

Vertical ballistic funnel m=3

47500

Sample Tank

Collimator

Monitors

Focusing unit

Detector

Beam Stop

Monitor

Details of the focussing sections

m=2	20x13 mm <sup>2</sup>	1250 mm <sup>2</sup>	"weak" focussing
m=2	20x13 mm <sup>2</sup>	1250 mm <sup>2</sup>	"strong" focussing
m=3.4	20x13 mm <sup>2</sup>	1250 mm <sup>2</sup>	10x5 mm <sup>2</sup>

ISIS

CCLRC Supermirrors

Direct view of the moderator :

- Resolution depends on L
- $\Phi \propto \text{solid angle} \propto 1/L^2$
- so the distance is a limiting factor

Using optics :

- Can transport beam up to very large distance .
- However reflectivity drops rapidly in the "supermirror" region

(Measurements from Mirrotron).

- m=1 ,reflectivity about 99%
- above m=1, loose around 10% per extra m.

$\theta_c = 0.0998 \cdot m \cdot \lambda \sim 0.1 m \cdot \lambda$

~ 0.1° at 1 Å

ISIS

CCLRC WISH - Beam transport

- Cold moderator
- Moderator view is 120x120 mm<sup>2</sup>
- Primary flight path is 40.0m

- Long guide with relatively small cross section → most divergent neutron will bounce more than 20 times.
- Using supermirrors is not very efficient in long guide for cold neutrons

n= number of reflections

ISIS

CCLRC WISH – Beam Transport

Phase-space transformation from high divergence-small cross section to low divergence large cross section and back.

$V = \alpha\beta.W.H$  is conserved (at best).  
For a square cross section :  $V = (\text{div})^2.X_s$

ISIS

CCLRC WISH - Elliptical Guide Design

Guide entrance : 1.7 m from Moderator  
Guide exit : 0.5 m before sample  
Guide sections : 0.5 m each – 76 sections in total

ISIS

CCLRC WISH - Elliptical Guide Design

- Guide entrance : 40 x 80 mm
- Guide exit : 22 x 44 mm
- Moderator and sample positioned at ellipse extremes
- 0.5 m sections with 0.5 mm breaks every 1.5 m.

ISIS

CCLRC WISH - Elliptical Guide Design

Intensity (a.u.) vs  $\lambda$  (Å)

- Elliptic m=2
- Tapered m=2-3.6

ISIS

CCLRC WISH - Elliptical Guide Design

Horizontal divergence as a function of wavelength :  
Beam divergence is more homogeneous with elliptical geometry.

Intensity profile at sample position

ISIS

### CCLRC WISH - Elliptical Guide Design

Guide tapering

Elliptical geometry

**ISIS**

### CCLRC WISH - Tuning the Divergence

- Initial design was a guide carousel for the last 2.5m of guide with 3 options.
- but elliptical geometry provide an interesting opportunity to tune the divergence by inserting a set of slits.

**ISIS**

### CCLRC WISH - Results from MC simulations

- Results for horizontal divergence.
- Full simulations including guide breaks and absorbing slits.
- Horizontal divergence is reduced in agreement with predictions.

**ISIS**

### CCLRC WISH - Guide Design

- Should be easy to operate: 5 motorized sets
- Should be less problematic for realignment.
- Simplify the design of the tank area close to sample position
  - fixed geometry
  - fixed collimation
- Each break in the guide is 50mm wide (0.2mm Al windows on both sides).

**ISIS**

### CCLRC WISH - Performance

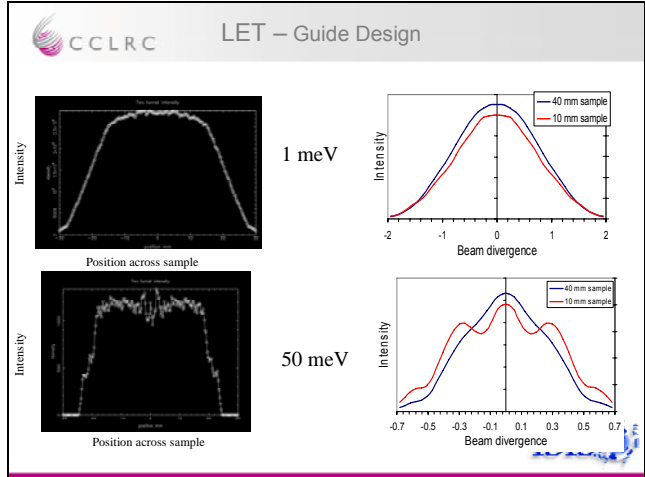
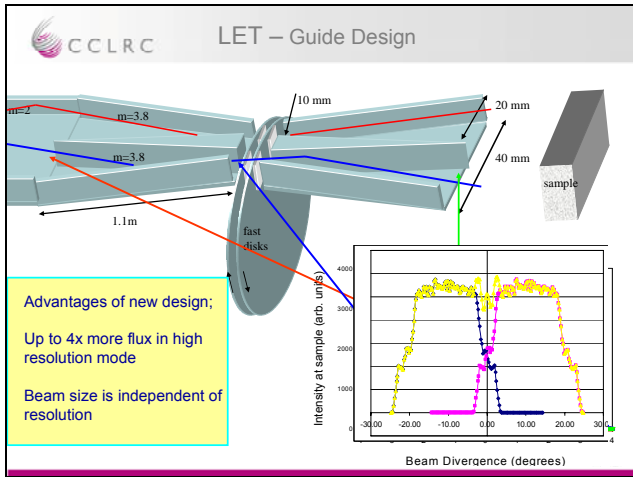
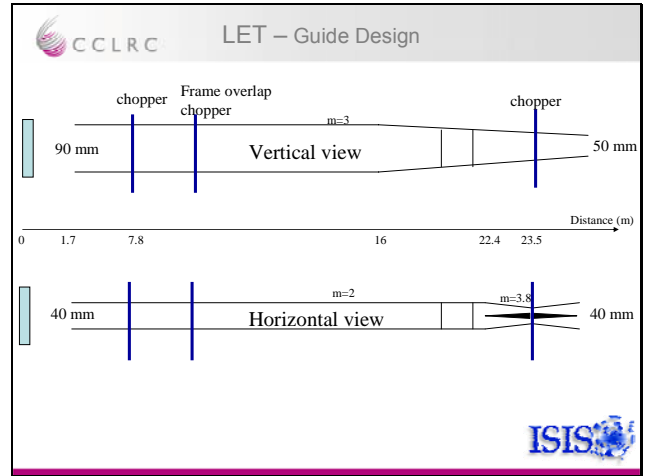
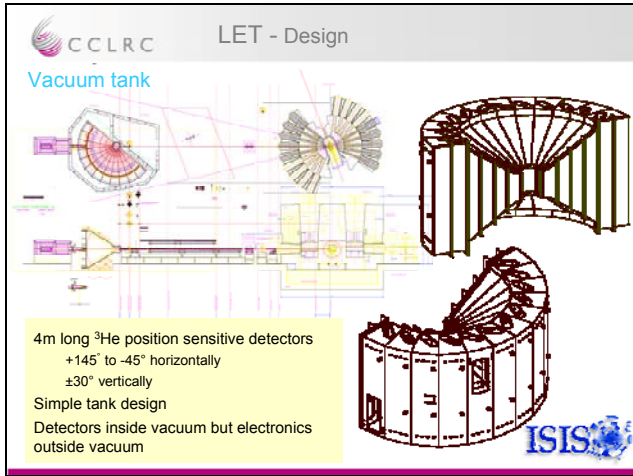
- Integrated flux is  $1.2 \cdot 10^8$  n/cm<sup>2</sup>/s at sample position (50 times GEM).
- Peak flux 200 times GEM at 4 Å in high divergence mode
- Peak flux 20 times GEM at 4 Å with same horizontal divergence

**ISIS**

### CCLRC LET - Specification

Incident energy range	0.5 meV - 80 meV (12-1 Å)
Maximum energy resolution	5 μeV (E=1 meV)
Minimum momentum transfer	$Q_{min} = 0.032 \sqrt{E}$
Maximum momentum transfer	$Q_{max} = 1.32 \sqrt{E}$
Flux at 5 meV(2% resolution)	$5 \times 10^4$ n cm <sup>-2</sup> s <sup>-1</sup>

**ISIS**



Géza Zsigmond

Paul Scherrer Institut

# Numerical Study of Optics and Phase Space Transformation of Ultra Cold Neutrons

Very Cold Neutron Source Workshop, August 22-24, 2005  
Argonne National Laboratory, IPNS

## Numerical Study of Optics and Phase Space Transformation of Ultra Cold Neutrons

G. Zsigmond, P. Allenspach, K.N. Clausen, B. Blau, M. Daum, K. Kirch, A. Pichlmaier  
Paul Scherrer Institut, CH-5232 Villigen PSI, Switzerland



### Outline

#### Motivation of the project:

PST to convert UCN into **monochromatic** CN and VCN

- Optics study to achieve high UCN density and flux from the spallation ultra-cold neutron source at PSI
- High UCN densities in the storage tank system
  - Input flux for a PST from the UCN guide

#### Phase space transformation of ultra-cold neutrons

- What is a PST ?
- Monochromatic cold and very cold neutrons from UCN

#### Predicted PST spectrometer performances

- PST CN-TOF, ballistic and VCN-SE spectrometer

#### Conclusions

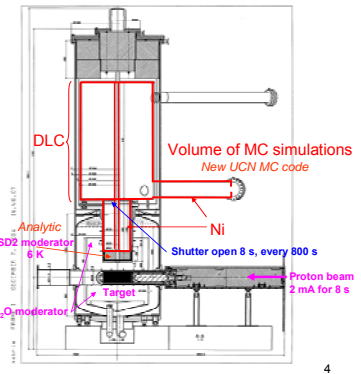
2

Optics study to optimize UCN density and flux from the spallation ultra-cold neutron source at PSI

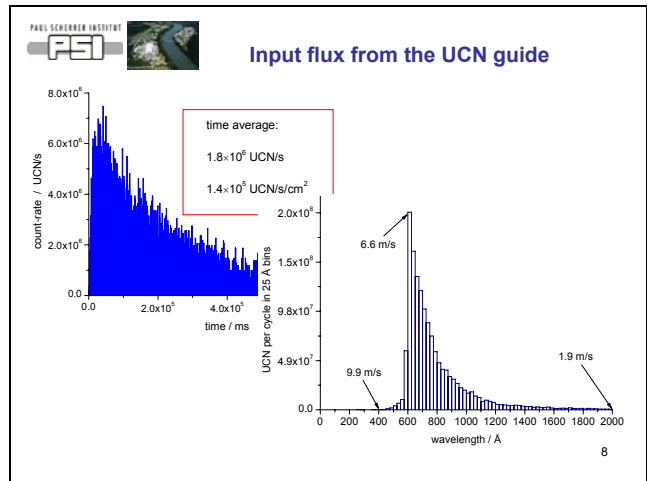
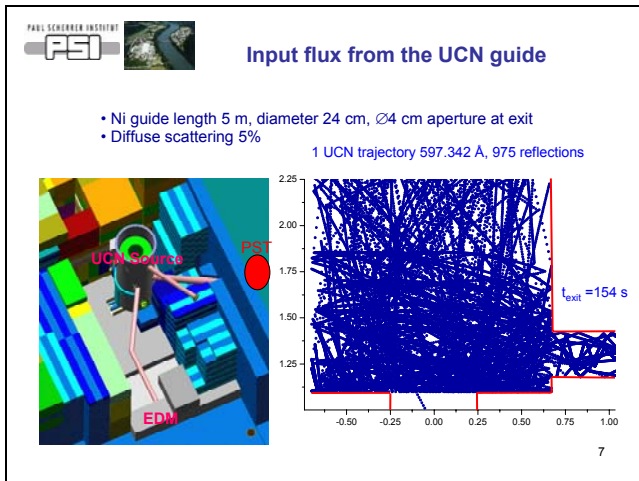
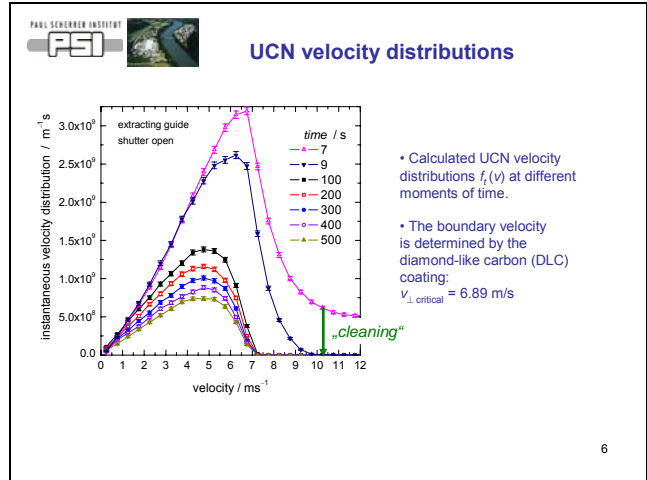
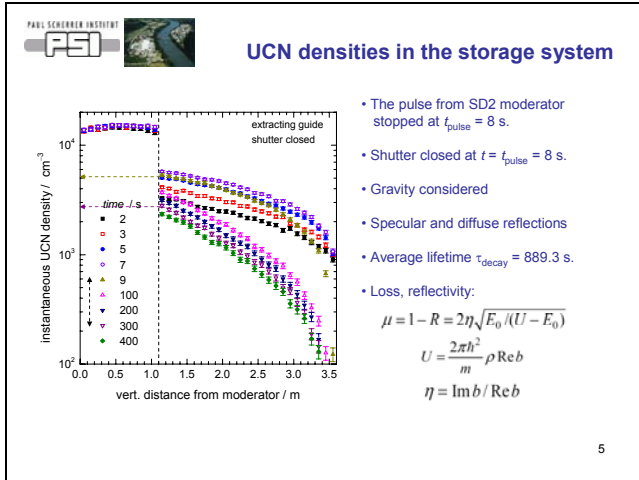
3



### Planned UCN source of PSI

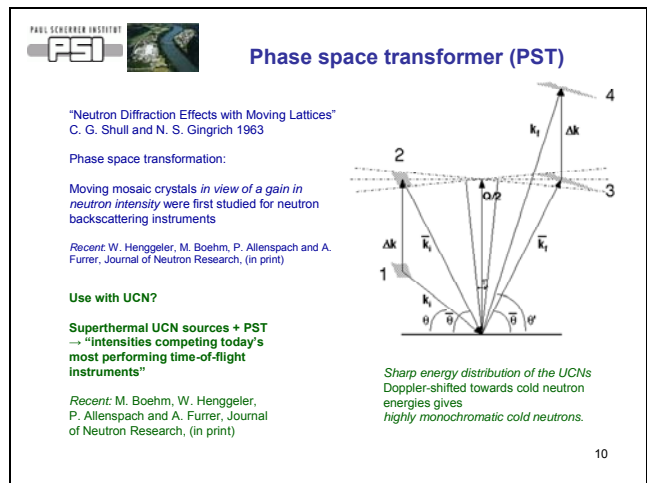


4



### Phase space transformation of ultra-cold neutrons

9



PAUL SCHERRER INSTITUT PSI

### Phase space transformer for UCN

Vacuum chamber

$v_{PST} [\text{m/s}] = 1978.0 / d\text{-spacing} [\text{\AA}] / \cos\alpha$   
working condition

UCN guide

PST crystal

cold neutrons  
 $\lambda = d\text{-spacing}$

Collimator

Analyzer (PST crystal)

Detector

Analyzer arms depending on  $\alpha$  of the PST

Fast rotating arm version ( $v=1$ ) for tests at PF2 ILL

previous fig. simplified to  $k_1 \approx 0$

11

PAUL SCHERRER INSTITUT PSI

### Flux on sample at 0.5 m

PST material	d [Å]	η deg	Freq./N Hz	E meV	2RMS <sub>E</sub> μeV	ΔE/E %	Div.H deg	Div.V deg	Flux/R/N n/s/cm <sup>2</sup>
PG_rot	3.35	3.5	120.82	7.287	68.0	0.94	0.08	0.55	3.7E4
Mica_rot	9.96	2.0	40.64	0.823	22.0	2.3	0.22	0.71	0.8E4
NiTi_rot	30	0.4	13.79	0.090	4.0	4.1	0.57	1.01	2.3E2
NiTi_rot	40	0.5	10.36	0.051	2.0	4.4	0.80	1.13	1.7E2
NiTi_rot	50	1.5	8.3	0.032	2.0	4.8	0.97	1.20	2.3E2
NiTi_rot	100	5.0	4.2	0.009	0.8	8.6	1.42	1.57	1.2E2

Incident energy profile with PG(002)

12

### Predicted PST spectrometer performances

13

PAUL SCHERRER INSTITUT PSI

### Direct geometry TOF spectrometer

Instrument	$\lambda_{\text{incident}}$ Å	Rep. Hz	ΔE μeV	I <sub>on sample</sub> n/cm <sup>2</sup> /s	I <sub>on sample</sub> /ΔE <sup>2</sup>
IN6-ILL	4.1	125	170	$8.9 \times 10^4$	3.1
FOCUS-PSI	3.0	140	300	$3.0 \times 10^4$	0.3
20 μA PSI PST-UCN rot. PG(002)	3.35	120.8	260	$3.7 \times 10^4$	0.5
100 μA PST-UCN rot. PG(002)	3.35	120.8	260	$19 \times 10^4$	2.7
IN5-ILL	10.0	33.3	14.8	$3.1 \times 10^4$	141.5
FOCUS-PSI	10.0	49	30	$0.8 \times 10^4$	8.9
20 μA PSI PST-UCN rot. Mica(002)	9.96	40.4	46	$0.8 \times 10^4$	3.7
100 μA PST-UCN rot. Mica(002)	9.96	40.4	46	$4.0 \times 10^4$	18.7

14

PAUL SCHERRER INSTITUT PSI

### Ballistic reflectometer / spectrometer

$$E_2 = \frac{m_g g L_2}{4 \cos^2 2\theta (\tan 2\theta - \Delta z / L_2)}$$

$L_2$	m	10.0
PSD detect. res. / 2	m	0.001
energy transfer	μeV	0.0
2θ	deg	5.0

PST Input Parameters			PST Output (Simulation)			Resolutions (Analytic)					
d	Width of PST	Speed	$\lambda_1$	$\Delta\lambda_1/\lambda_1$	flux on	$\sigma_0$	$\Delta z$	$E_1$	q	$2\sigma_{\text{det}}$	$\Delta q$
spacing	rocking curve	PST			sample	div. on	vert.	transf	final	resol.	
of PST	at 45° Bragg				(N=100) sample	pos.					
Å	deg	m/s	Å	-	n/s/cm <sup>2</sup>	deg	m	μeV	Å <sup>-1</sup>	μeV	Å <sup>-1</sup>
100	5	27.98	97.9	0.050	5856	1.1	0.57	8.5	0.006	22.62	0.005
206	10	13.58	197.5	0.084	1179	1.3	-0.36	2.1	0.003	1.55	0.003
300	20	9.33	275.2	0.167	850	1.5	-1.52	1.1	0.002	0.56	0.002

15

PAUL SCHERRER INSTITUT PSI

### Ballistic reflectometer / spectrometer

1. Position on detector

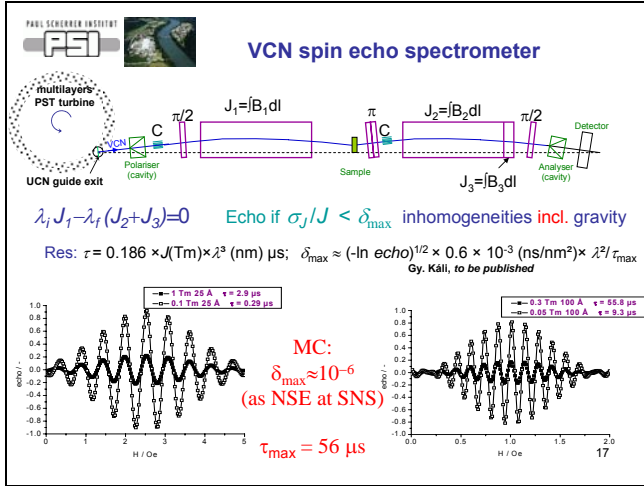
2. Position-to-energy transformation

3. Normalization with  $\Delta E / \Delta z$

MC example

$\lambda = 200 \text{ \AA}$   
 $2\theta = 5^\circ$   
 $L_2 = 10 \text{ m}$

16



PAUL SCHERRER INSTITUT  
PSI

### Conclusions, plans

- Monte Carlo: High UCN densities in the storage tank system
- UCN+PST very effective per proton: 1% yields same flux as SINQ 70%
- Consultations on a **science case** for a PST VCN spectrometer
  - Ballistic Spectrometer
    - $10^3 - 10^4$  VCN/s/cm<sup>2</sup>,  $\Delta\lambda/\lambda \sim 5 - 16\%$
    - $Q_{\min} \sim 0.002 - 0.006 \text{ \AA}^{-1}$ ,  $\Delta E \sim 0.5 - 25 \mu\text{eV}$
  - VCN Spin Echo e.g.  $\lambda = 100 \text{ \AA}$  *best prospects!*
    - $2 \times 10^4$  VCN/s/cm<sup>2</sup> unpolarised,  $\Delta\lambda/\lambda = 20\%$
    - ultra-high resolution  $\tau_{\max} > 55 \mu\text{s} \sim$  time range of XPCS

18

# Roger Pynn

## Los Alamos National Laboratory

### Spin Echo Scattering Angle Measurement with Very Cold Neutrons

#### Spin Echo Scattering Angle Measurement with Very Cold Neutrons

by

Roger Pynn

In collaborations with:

Michael R. Fitzsimmons (LANL), Gian P. Felcher (ANL),  
Helmut Fritzsche (AECL), Marita Gierlings (HMI),  
Janos Major (MPI)

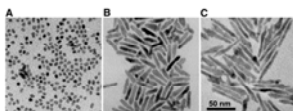
#### Neutron Scattering is Signal-Limited

- There are a limited number of ways to overcome this....
- Spend \$1.5B on a new neutron source
- Use the time-of-flight method
- Use broad wavelength band
  - Doesn't always screw up the resolution – e.g. NSE, SANS, LPSS
- Use an uncollimated or focused beam
  - Often sacrifice resolution in a particular direction – e.g. vertically curved monochromator
  - Beginning to learn how to use NSE to code scattering angles
- Moderate neutrons to lower temperatures
  - Enhances phase space density

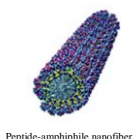
#### Nanoscience & Biology Need Structural Probes for 1-1000 nm



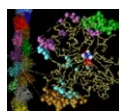
10 nm holes in PMMA



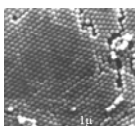
CdSe nanoparticles



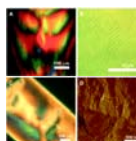
Peptide-amphiphile nanofiber



Actin



Si colloidal crystal



Structures over many length scales in self-assembly of ZnS and cloned viruses



Thin copolymer films

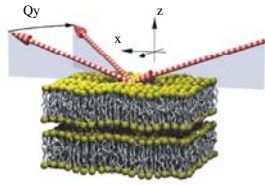
#### Current Limitations of Neutron Scattering for Nanoscience and Biology

- We often want structural and dynamical information over a range of length and time scales simultaneously
  - 1 nm to 1000 nm; psec to  $\mu$ sec (or even msec)
- Difficult to probe lengths much larger than a 100 nm with conventional SANS using  $\lambda \sim 0.6 - 1$  nm
- Many interesting samples are either small or dilute – i.e. they scatter weakly – & the interesting length scales are large
  - Membranes are a good example

Can VCNs help, especially if coupled with SESAME?

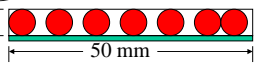
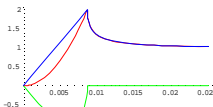
## In Principle, Neutron Reflection can Probe Film Structure (Especially when H/D Substitution is used to Enhance Contrast)

Diffuse scattering along y measures structure & composition fluctuations in the plane of the film



But...diffuse scattering along y is weak and hard to measure with useful resolution, except in very favorable circumstances.....

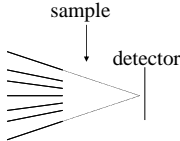
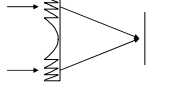
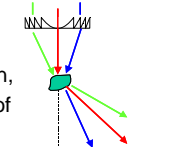
## Scattered Intensity from Thin Films

- Consider 50 nm spheres embedded in a 50 nm thick film 
  - Film volume =  $50 \times 50 \times 50 \times 10^{-6} = 0.125 \text{ mm}^3$
  - Typical SANS sample  $\sim 100 \text{ mm}^3$
  - Surface enhancement factor of 1 to 16 
- $Scattering \sim S(\vec{Q})|T(\vec{k}_i)|^2|T(\vec{k}_f)|^2$
- Even if spheres on surface are 10 x more concentrated than in a typical SANS sample, GISANS is 1 - 3 orders of magnitude less intense than "typical" bulk SANS

## Rock and a Hard Place

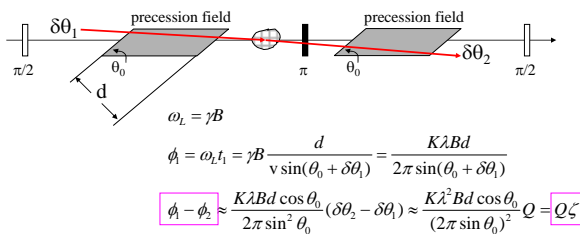
- We need good neutron beam collimation:
  - (a) to measure large length scales accurately
  - (b) to separate scattered and unscattered neutrons (ie achieve  $Q_{min}$ )
 but collimation costs scattered intensity
  - Larger  $\lambda \Rightarrow$  larger  $\theta$  for the same d, i.e. less stringent beam collimation needed
- The samples we care about often scatter very weakly
  - Larger  $\lambda$  does not help directly
- Can we focus neutrons on the sample and still obtain the necessary angular resolution?
  - Beam focusing is easier at large  $\lambda$  because  $f \sim 1/\lambda^2$  for lenses and critical angle scales as  $\lambda$

## Various Schemes

- Collimators converging on detector
  - Increased intensity w/o worse resolution
  - But...needs large sample & SANS from collimator is a problem ( $\lambda$  independent?)
- Refractive or reflective focusing optics
  - No penumbra for main beam & no slit scatter
  - Resolution still depends on detector spot size
  - Easier at large  $\lambda$
- Can we measure  $\theta$  directly for each neutron, without having to define direction of travel of BOTH incident and scattered neutrons?
 

## NSE Angle Coding Illustrated for SANS

- Make the number of spin precessions depend on the neutron's direction of travel instead of (only) its speed.....



with  $K = 0.291 \text{ (Gauss.cm.}\text{\AA)}^{-1}$ .  $\zeta$  is the spin echo length, i.e. the distance probed

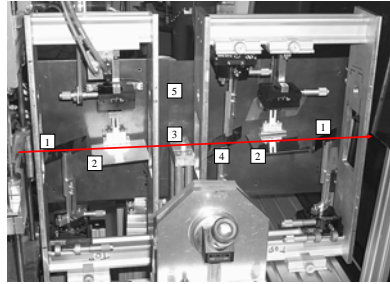
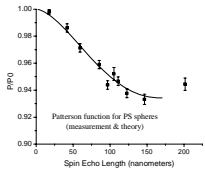
$$P/P_0 = \int_{-\infty}^{\infty} S(Q) \cos(Q\zeta) dQ / \int_{-\infty}^{\infty} S(Q) dQ$$

## How Large is the Spin Echo Length?

Bd (G.cm)	$\lambda$ (Å)	$\theta_0$ (degs)	$\zeta$ (nm)
100	4	20	10
100	4	10	40
100	8	10	150
100	16	10	600
100	22	10	1200

- Note the quadratic dependence of  $\zeta$  on  $\lambda$  and  $1/\sin\theta_0$
- Can probe length scales from 10 – 1000 nm using thin magnetic films as precession fields
  - 100 microns of Permalloy provides 100 G.cm
  - For a  $4\text{\AA} < \lambda < 20\text{\AA}$  band, 100 micron Py foils at  $10^\circ$  give  $40 < \zeta < 1000 \text{ nm}$

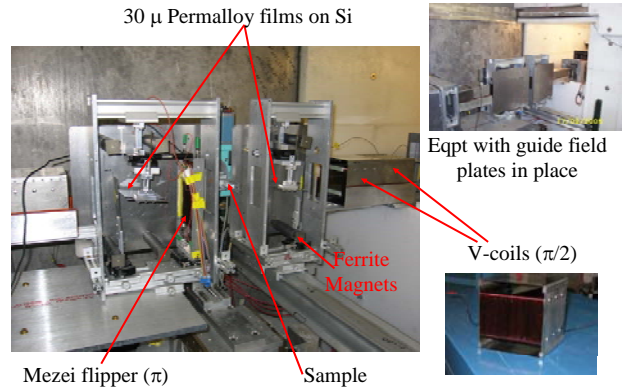
## High Angular Resolution Neutron Scattering using SESAME with Monochromatic Neutrons



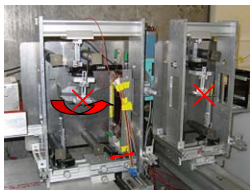
A 200 nm correlation distance was achieved for SANS using Py films tilted at  $2.7^\circ$

- Thin, magnetized  $\text{Ni}_{0.8}\text{Fe}_{0.2}$  films on silicon wafers (labelled 1, 2 & 4) are the principal physical components used.
- Experiment on V-6 reflectometer at HMI using 4.5 Å neutrons. Apparatus is 65 cm long

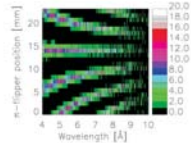
## SESAME at a Pulsed Source on ASTERIX



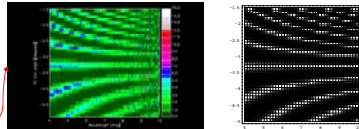
## Obtaining a Spin Echo



Measure flip ratio as a function of flipper position



With  $\pi$  flipper set to echo position, incline 1<sup>st</sup> Py film, then measure flip ratio as a function of 2<sup>nd</sup> film angle

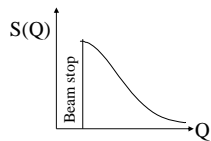


Calculated result allows SEL to be related to lambda

## Effect of using Larger Wavelengths

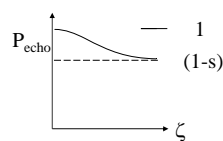
- Large  $\lambda$  band allows access to a large range of length scales
  - Larger dynamic range than conventional SANS, which scales as  $1/\lambda$
- Currently, inclinations of precession films need to be small to reach large spin echo lengths (SEL)
  - Restricts size of sample; increases length of Py in the beam
  - Larger  $\lambda$  resolves this issue
- Current limitation on maximum SEL is thickness variations of the Py precession films
  - Similar to field inhomogeneities in standard spin echo
  - Since precession angle  $\sim \lambda/\sin\theta$  and  $\zeta \sim (\lambda/\sin\theta)^2$ , increasing  $\lambda$  does not allow access to larger SELs for the same precession films

## Comparison of SANS and SESANS



### SANS

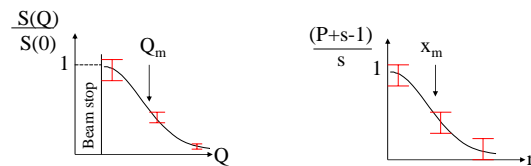
Separates scatt. & unscatt. in space  
Direct measurement of  $S(Q)$   
Small Q scattering lost in beam stop  
Requires tight collimation  
Can use large  $\delta\lambda/\lambda$   
Full azimuthal averaging



### SESANS

Separates scatt. & unscatt. by polarization  
Measure Fourier Transform of  $S(Q)$   
Unscattered beam is also counted  
No restriction on collimation  
Can use large  $\delta\lambda/\lambda$   
Measures in one (Q) direction only

## Gain Factor for SESANS



- Normalize both measurements to unity
  - Error bars decrease with Q for SANS; roughly constant for SESAME
- Calculate measurement times to achieve the same statistical accuracy of the measured signal at  $Q_m$  and  $x_m$ 
  - Get the same answer if we calculate for same accuracy for  $R_g$

## Gain Factor for SESAME

- Times needed to obtain measurements of equal statistical precision are related by (all lengths in nm):

$$Gain = \frac{T_{SANS}}{T_{SESAME}} \approx \frac{s}{6} \frac{P_0}{(P_0 + 1)} \frac{\Omega_{SESAME}}{\Omega_{SANS}} \frac{\Delta\lambda_{SESAME}}{\Delta\lambda_{SANS}} \frac{A_{SESAME}}{A_{SANS}}$$

$$\Omega_{SANS} \approx \lambda^2 / (8\pi R_g)^2 \text{ in order to measure to } Q_{min} \sim 1/(4R_g);$$

$$\Omega_{SESAME} \approx 10^{-3} m^2 \lambda^2 \text{ using a guide that is } m \text{ times nickel}$$

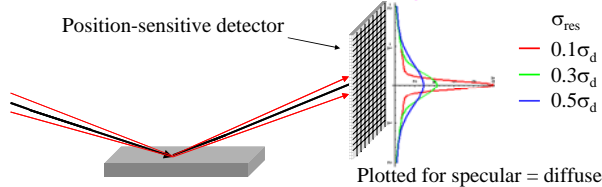
$$Gain \approx 5 \cdot 10^{-2} m^2 s R_g^2 \quad \text{Independent of } \lambda$$

- For 10% scatterer ( $s=0.1$ ) break-even for  $R_g \sim 15$  nm for  $m = 1$
- For larger particles, stronger scatterers, larger samples or larger  $m$ , SESAME gains over conventional SANS

## BUT... Simple SESAME is *not* Good for Weak Scatterers

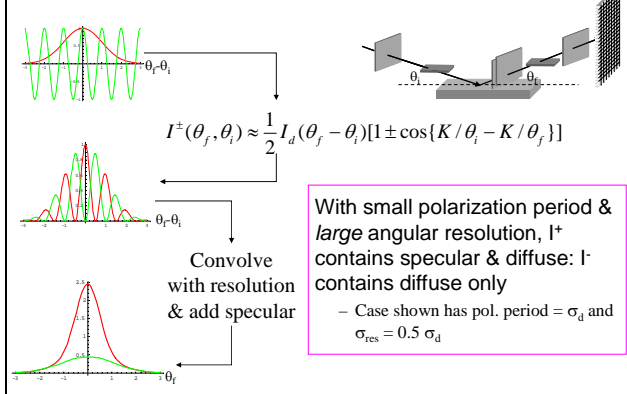
- With simple SESAME – i.e. measurement using a single neutron detector – scattered & unscattered neutrons have different echo polarizations but they overlap on the detector
  - Can avoid this with GISANS by measuring at Yoneda instead of specular
- Hard to discriminate between scattered & unscattered neutrons when the scattering is weak
- The attraction of simple SESAME is that it measures the FT of  $S(Q)$ , but perhaps one should rather think of it as a way to measure scattering angles
  - Every neutron scattered through the same angle has the same echo polarization
  - Neutrons scattered beyond a particular angle are completely depolarized

## An Example from Separation of Specular & Diffuse Scattering



- A similar problem pertains to SANS – how do we separate scattered from non-scattered?
  - Similar to red curve above
  - “Bleeding” of unscattered beam (e.g. due to slit scatter) masks weak SANS (the reason we still use pinholes)
- Conventionally, pinholes allow unscattered beam to be well defined on PSD

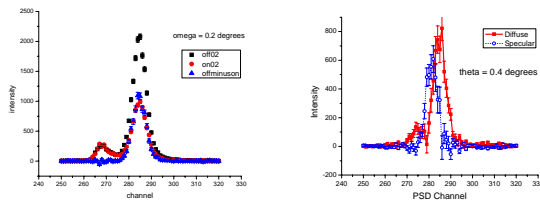
## Separating Specular & Diffuse Scattering with Neutron Spin Echo Angle Coding



With small polarization period & large angular resolution,  $I^+$  contains specular & diffuse:  $I^-$  contains diffuse only

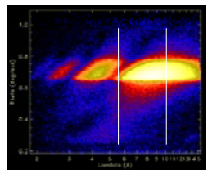
- Case shown has pol. period =  $\sigma_d$  and  $\sigma_{res} = 0.5 \sigma_d$

## Separating Specular & Diffuse Reflection from a Copolymer Film on Silicon



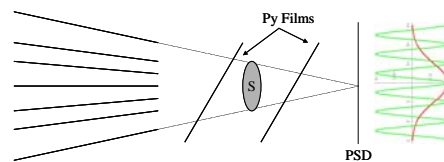
Specular neutron reflection (blue) was separated from diffuse reflection with high fidelity using V6 at HMI (above). Black and red data include “diffuse” scattering.

SPEAR data (right) provide explanation for double peak in diffuse data.



## Combining SESAME & Beam Focusing

- Focused beam increases number of neutrons on sample
  - Will we see polarization fringes?
    - Maybe with converging collimator & not with a lens?
    - May be washed out by spread of main beam (slit scattering, image size etc)?
  - If no fringes....
    - Separate scattered and unscattered neutrons by echo polarization
      - Requires distance to measure scattering angles on PSD
    - Use standard (FT) SESAME but without the main beam (mask detector)
      - Not clear that PSD is useful in this case
      - But .... It might help for weak scattering



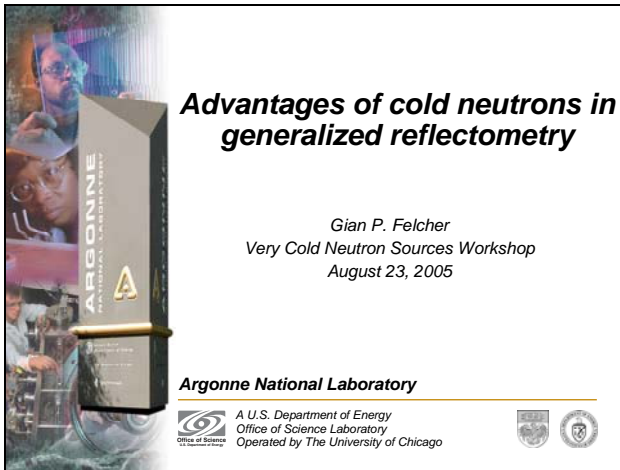
### Points to Note

- NSE does not require highly monochromatic or well-collimated neutron beams
  - Can be used with focused beams; beam polarization usually easier for large  $\lambda$
- NSE provides angular resolution independent of sample size
- NSE apparatus can be short
  - Distance is not used to obtain desired angular resolution & sample size as it is with conventional SANS
  - The length of a pulsed-source instrument can be picked to get the desired wavelength resolution
- The length scale accessible to NSE scales as  $\lambda^2$  rather than as  $\lambda$  as it does for conventional SANS

# Gian Felcher

## Argonne National Laboratory

### Advantages of Cold Neutrons in Generalized Reflectometry



**Advantages of cold neutrons in generalized reflectometry**

Gian P. Felcher  
Very Cold Neutron Sources Workshop  
August 23, 2005

Argonne National Laboratory

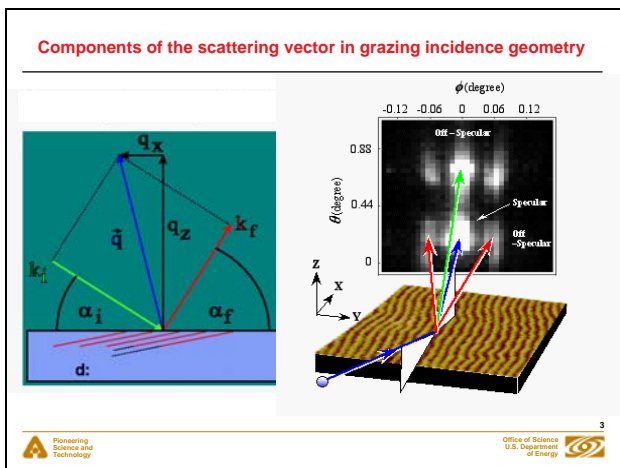
A U.S. Department of Energy  
Office of Science Laboratory  
Operated by The University of Chicago

**Outline**

1. Small angle scattering and spin echo
2. Recent measurements with  $\lambda=5.5 \text{ \AA}$ 
  - In transmission geometry: anodized aluminum
  - In reflection geometry: polystyrene droplets on silicon
3. Advantages of longer wavelengths

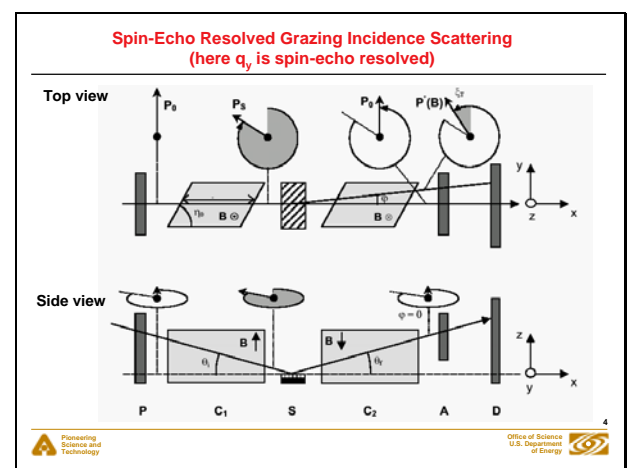
2

**Components of the scattering vector in grazing incidence geometry**

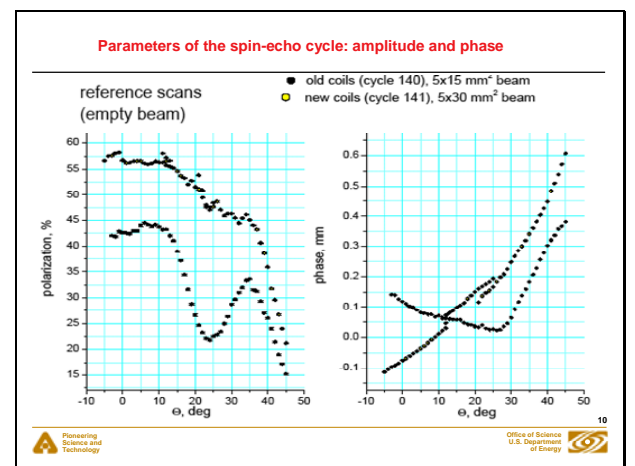
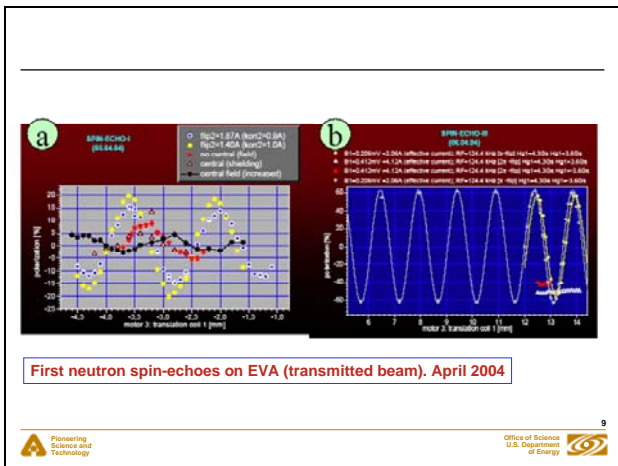
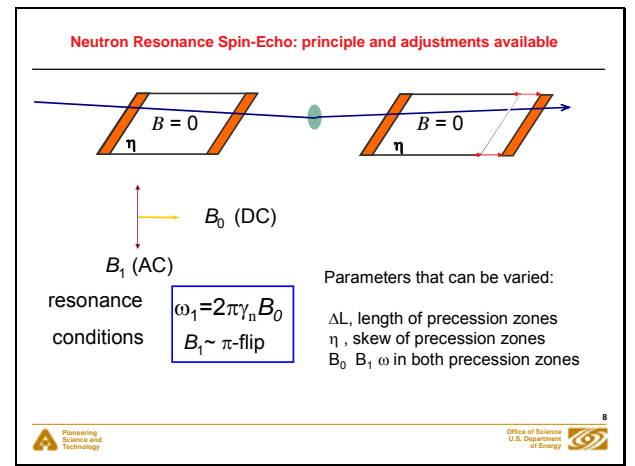
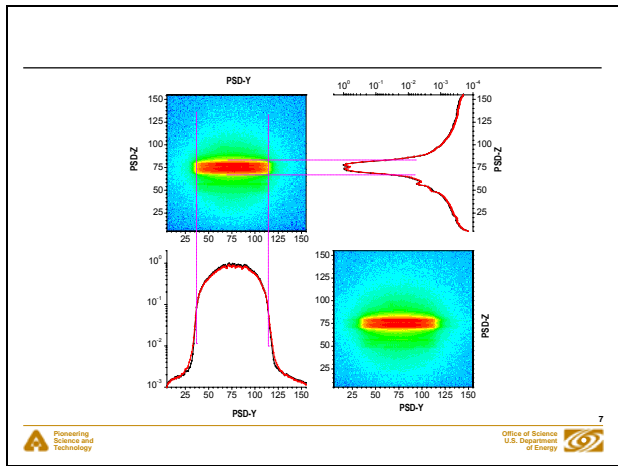
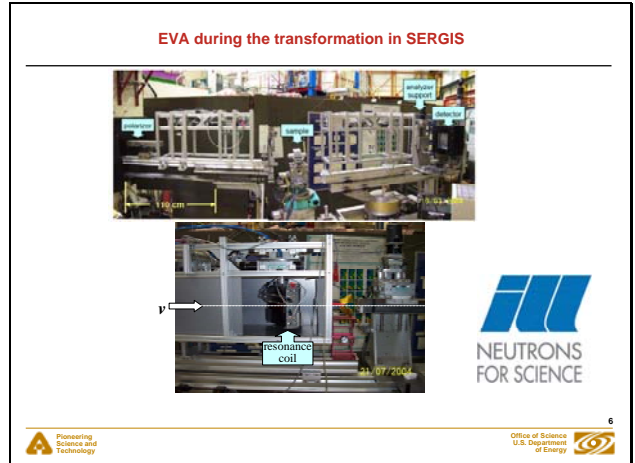
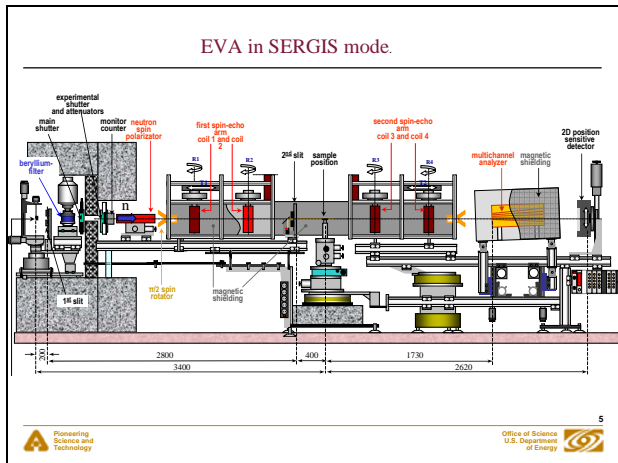


3

**Spin-Echo Resolved Grazing Incidence Scattering (here  $q_z$  is spin-echo resolved)**



4



### Encoding the scattering angle

Neutron spin phase  
After both precession zones  
(one before, one after the sample)

$$\xi_1 - \xi_2 \approx \frac{2\pi\gamma_n B d \cdot \cot \eta_0 \sin \varphi}{v}$$

$$= \left\{ \frac{\gamma_n B d \lambda \cdot \cot \eta_0}{v} \right\} \left( \frac{2\pi \sin \varphi}{\lambda} \right)$$

$$\approx \{\text{spin-echo-length}\} \cdot q_x$$

$\lambda$  (neutron wavelength) 5.5 Å  
 $v$  (neutron velocity) 720 m/s  
 $\eta$  (tilt of precession coil) 45°  
 $B$  (magnetic field in leg) 310G  
 $D$  (length of precession leg) 50 cm  
Spin echo length 3500Å

The intensity measured at the detector  
after the analyzer  
is modulated by  $\cos(\xi_1 - \xi_2)$



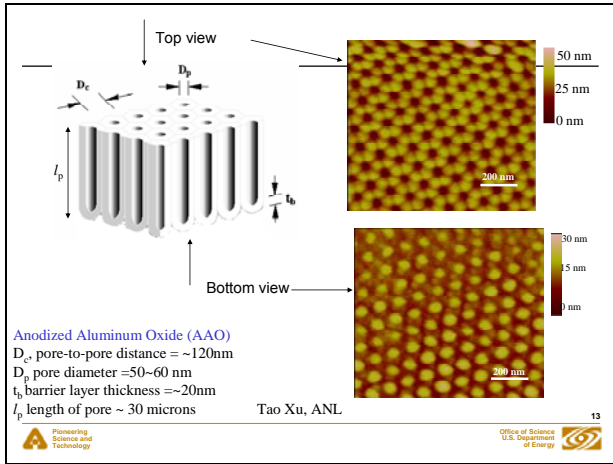
11

### Capabilities of EVA in 2005

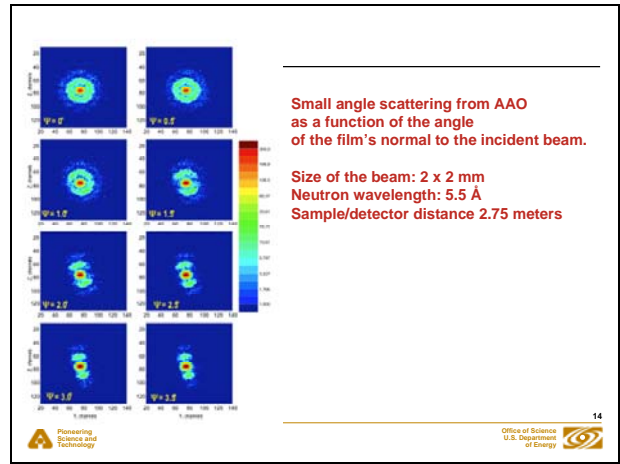
- Beam size 50x5mm
- Wave numbers covered from  $1 \cdot 10^{-3}$  to  $4 \cdot 10^{-2}$  Å<sup>-1</sup>
- 5.5 Å monochromatized neutron beam
- Max. spin-echo length 4500Å
- Fourier transformed result, large length scales, **interparticle structure factor** are emphasized



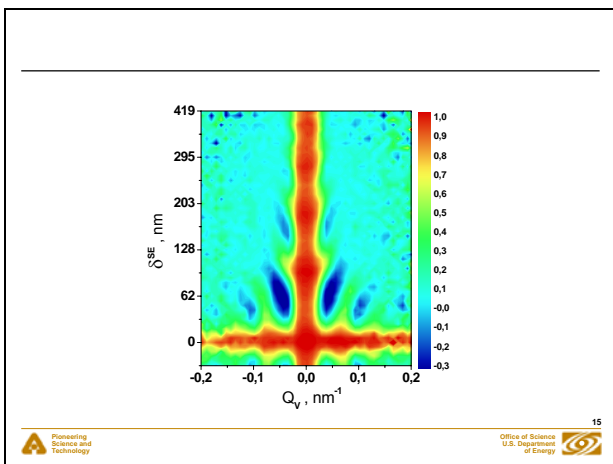
12



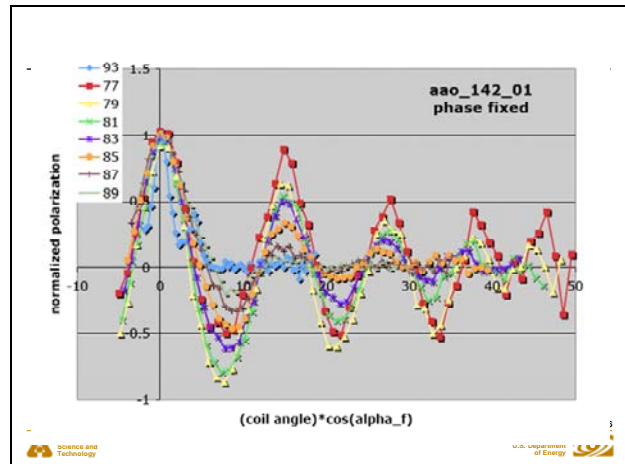
13



14



15



16

Droplets of polystyrene on a silicon surface (10nm high, 550 nm lattice)

**The issues**

Dewetting at the surface versus segregation in the bulk

Thickness dependence

Kinetics

Microphase separation

**The observations**

Real space: AFM, SIMS

Reciprocal space: GISAXS, GISANS

*What remains to be understood?*

*Is there a role for SERGIS?*

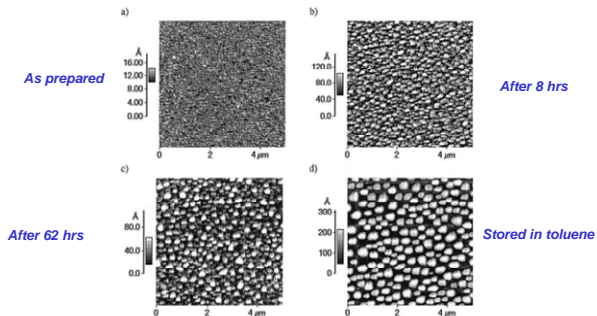


Pioneering Science and Technology

Office of Science U.S. Department of Energy

17

**Polymer blend: dPS-PpMS: effect of annealing at 160 C**  
Initial thickness ~35 Å (1/3 of gyration radius)

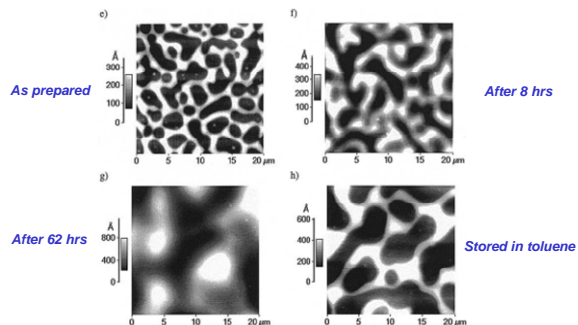


Pioneering Science and Technology

Office of Science U.S. Department of Energy

18

**Polymer blend: dPS-PpMS: effect of annealing at 160 C**  
Initial thickness ~ 2700 Å (26 times the gyration radius)



Pioneering Science and Technology

Office of Science U.S. Department of Energy

19

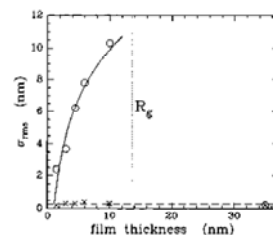


Figure 4. Root mean square surface roughness  $R_{rms}$  plotted as a function of the initially prepared film thickness  $I$ . Values calculated from small scan areas are plotted with crosses; ones from large scan areas, with circles. The symbol size pictures the error bar of the experimental data. The solid line is a model fit as explained in the text.



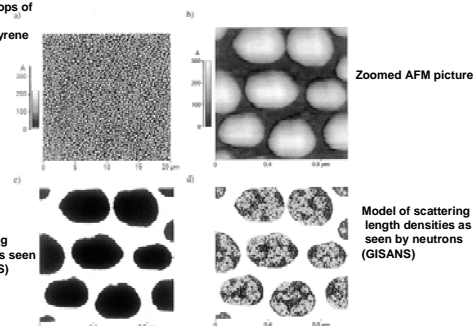
Pioneering Science and Technology

Office of Science U.S. Department of Energy

20

**Dewetting of polymer-blend films from silicon**  
A comparative study of P. Müller-Buschbaum et al., Physica B283,53 (2000)

AFM picture of drops of d-polystyrene/polyparamethylstyrene on silicon



Model of scattering length densities as seen by X-rays (GISAXS)

Model of scattering length densities as seen by neutrons (GISANS)



Pioneering Science and Technology

Office of Science U.S. Department of Energy

21

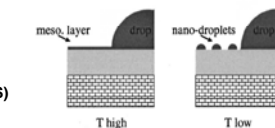
**3 length scales**

Samples studied

• Homopolymer Deuterated poly-styrene (PS) (157kg/mol)

• Blend: Deuterated poly-styrene (PS) and protonated poly-(paramethyl styrene) (pMS) (157kg/mol)

• Diblock copolymer of PS and pMS (230 kg/mol 0.47 PS fraction)

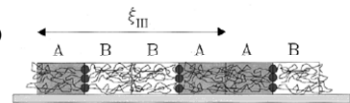


Length scales

I. Droplet Spacing (600nm)

II. Nano droplets ??

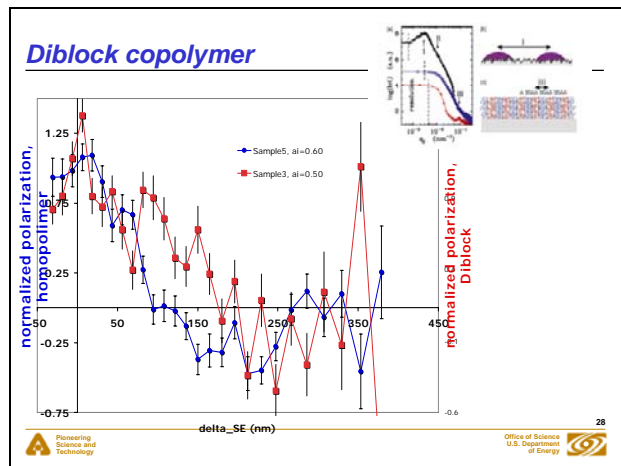
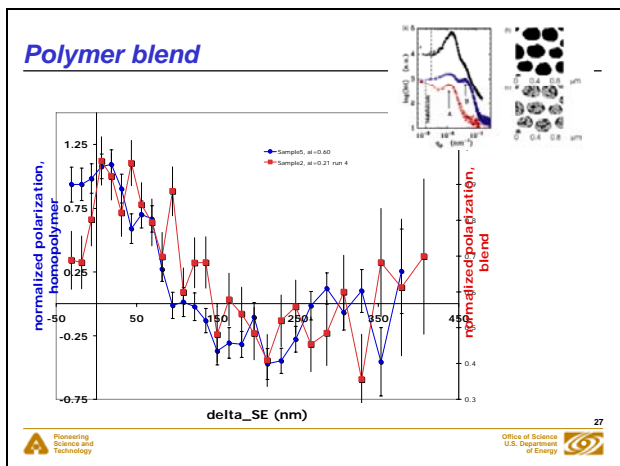
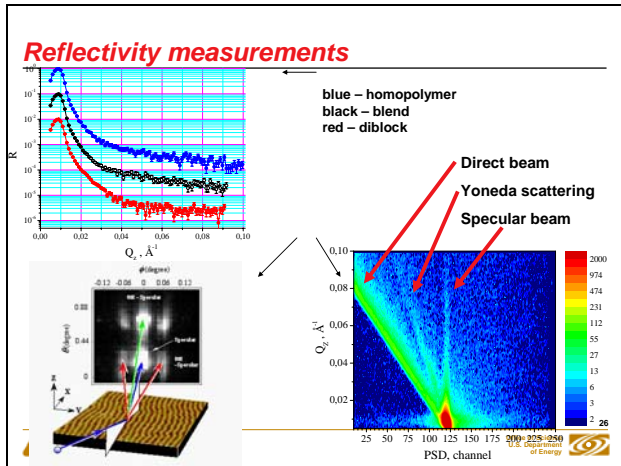
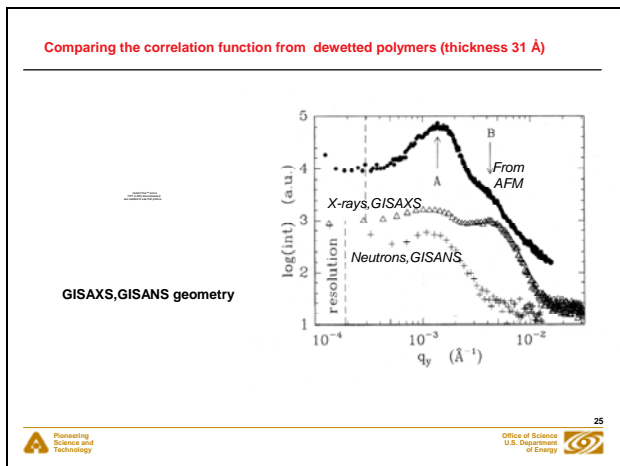
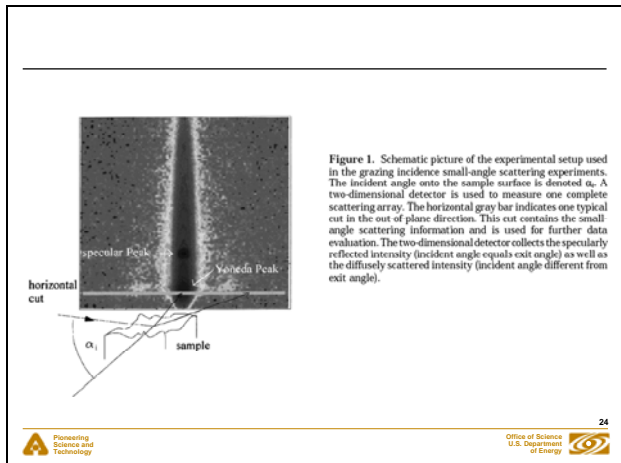
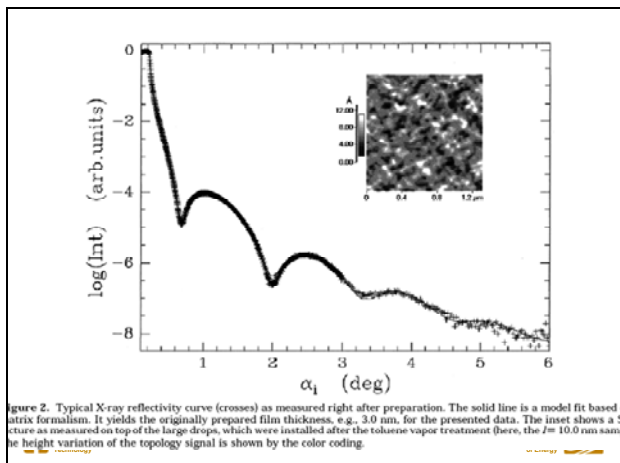
III. Micro phase separation



Pioneering Science and Technology

Office of Science U.S. Department of Energy

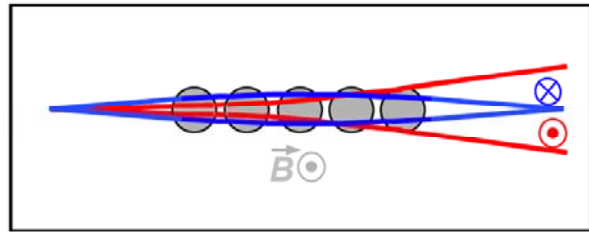
22



## Technical conclusion, prospects

- Crucial to have **large detector area**, to avoid truncation of scattering
- Search for the best spin handling device is **not over yet**:
  - single crystal ferrites?
  - ferromagnetic thin films?
  - adiabatic/non adiabatic neutron spin  $\pi$  and  $\pi/2$  turners?
  - Polarized He<sup>3</sup> analyzer?
- **Advantages of a longer wavelength (20 Å):**
  - Along x (scattering mode) better angular resolution
  - Along y (spin echo mode) neutrons can be magnetically focused.

## The basic idea A magnetic multiple refractive lens



## A close-up of the device



## How it works

- The energy of a neutron in matter or a magnetic field

$$E = -\boldsymbol{\mu} \cdot \mathbf{B} + \frac{2\pi\hbar^2}{m} \rho b$$

- The corresponding index of refraction:

$$n = \sqrt{1 - \frac{E}{E_0}} \cong 1 + \frac{m\lambda^2}{h^2} \boldsymbol{\mu} \cdot \mathbf{B} - \frac{\lambda^2}{2\pi} \rho b \cong 1 - \frac{\epsilon}{2}$$

- As a function of spin:

$$n \cong 1 \mp \frac{m\lambda^2}{h^2} \mu |B|$$

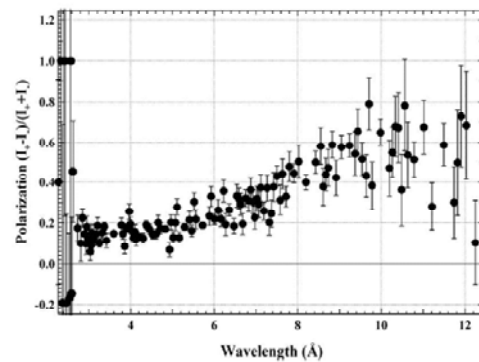
- The focal length:

$$\frac{1}{f} = \pm N \frac{2}{r} \left( \frac{n}{n_0} - 1 \right)$$

## A first test

- 200 high field toroidal magnets (OD ½", ID ¼") were arranged in contact with each other in two parallel rows with their cylinder and magnetic axes coaligned.
- A mild steel U-bar provided support and the return field.
- The polarizing effect of the low-field cores was measured using the POSY1 polarized-beam neutron reflectometer at IPNS.

## The polarization effect



---

**Have collaborated to the SERGIS development:**

Argonne National Laboratory:

*P. Falus, G. Felcher, K. Littrell, S. te Velthuis*

Los Alamos National Laboratory

*M. Fitzsimmons, R. Pynn*

Max Planck Institut für Metallforschung, Stuttgart

*H. Dosch, M. Dridi, R. Maier, J. Major, M. Metzger,*

*A. Vorobiev, M. Wahl*

Institut Laue Langevin

*R. Gähler, S. Klimko*

From other institutions:

*K. Habicht, HMI Berlin*

*T. Keller, MPI für Festkörperforschung, Stuttgart*

*Th. Rekveldt, IRI Delft*



Researching  
Science and  
Technology



Office of Science  
U.S. Department  
of Energy

35